Hydrodynamics and the quantum butterfly effect in black holes and large N quantum field theories

Scopelliti, V.

Hydrodynamics and the quantum butterfly effect in black holes and large N quantum field theories

Proefschrift

ter verkrijging van
de graad van Doctor aan de Universiteit Leiden,
op gezag van Rector Magnificus prof. mr. C.J.J.M. Stolker,
volgens besluit van het College voor Promoties
te verdedigen op Woensdag 9 Oktober 2019
klokke 16:15 uur

door

Vincenzo Scopelliti

geboren te Messina (Italië) in 1991

Promotor:	Prof. dr. K. E. Schalm
Promotiecommissie:	Dr. D. Bagrets (University of Cologne) Dr. M. Blake (Massachusetts Institute of Technology) Prof. dr. E. R. Eliel Prof. dr. J. W. van Holten Prof. dr. ir. W. van Saarloos

Casimir PhD series, Delft-Leiden 2019-27
ISBN 978-90-8593-410-3
An electronic version of this thesis can be found
at https://openaccess.leidenuniv.nl

The research presented in this thesis was supported in part by a VICI award of the Netherlands Organization for Scientific Research (NWO) and by the Netherlands Organization for Scientific Research/Ministry of Science and Education (NWO/OCW).

Cover: the front cover represents Poseidon, the Greek god who rules the sea and the water, as represented on a Greek vase (ca. 480 - 460 BCE) by the Aegisthus Painter. The vase is now part of the collection of the Yale University Art Gallery, New Haven, CT, USA. In front of Poseidon, a representation of a black hole, the most chaotic object in nature, is displayed, surrounded by Hawking radiation. The relation between quantum chaos and hydrodynamics is the main focus of this thesis. On the back cover, one sees a photo of a wood-inlay work by Giovan Francesco Capoferri, dated 1524, in the Basilica di Santa Maria Maggiore in Bergamo, Italy, with the title: *Magnum chaos*. The black hole on the front of the cover is a modification of this work.
The original pictures of the wood-inlay and the vase are in the public domain and can be respectively found at: https://upload.wikimedia.org/wikipedia/commons/7/79/Lotto_Capoferri_Magnum_Chaos.jpg
and
https://artgallery.yale.edu/collections/objects/25657.

To my family

Contents

1 Introduction **1**
- 1.1 Classical thermalization . . . 2
- 1.2 Quantum thermalization . . . 3
- 1.3 Information scrambling and out-of-time ordered correlators (OTOC) . . . 5
- 1.4 Quantum systems without quasiparticles . . . 9
- 1.5 Holographic duality . . . 10
- 1.6 A hydrodynamical refresh . . . 13
- 1.7 Hydrodynamic transport coefficients at weak coupling and in holography . . . 15
- 1.8 Quantum chaos and hydrodynamics . . . 17
- 1.9 Summary of results . . . 18
- 1.10 This Thesis . . . 22
  - 1.10.1 Chapter 2 . . . 22
  - 1.10.2 Chapter 3 . . . 22
  - 1.10.3 Chapter 4 . . . 23
  - 1.10.4 Chapter 5 . . . 23

2 Quantum chaos in diluted weakly coupled field theories **25**
- 2.1 Introduction . . . 25
- 2.2 Boltzmann transport and chaos from a gross energy exchange kinetic equation . . . 27
- 2.3 A derivation of the gross exchange kinetic equation from the OTOC . . . 30
- 2.4 Results and discussion . . . 34
- 2.A Diagrammatic expansion of $|\mathcal{T}_{12\to 34}|^2$ in the theory of $N\times N$ Hermitian matrix scalars . . . 38

3 Towards the Quantum Critical Point **45**
- 3.1 Introduction . . . 45
- 3.2 Hydrodynamic transport at weak coupling and scrambling: formal similarities . . . 47
  - 3.2.1 Relevant correlation function for transport in the hydrodynamic regime . . . 48

3.2.2 Decoupling of the OTOC in the extended Schwinger-Keldysh formalism . . . 50
3.2.3 Decoupling of the OTOC BSE: ϕ^4 matrix model example . . . 56
3.3 Kinetic theory of many-body chaos . . . 59
3.3.1 Quick review of the Boltzmann equation . . . 60
3.3.2 From the BSE to the quantum Boltzmann equation 63
3.3.3 The Quantum Boltzmann equation for many-body chaos . . . 65
3.4 Bosonic $O(N)$ vector model at the quantum critical regime 67
3.4.1 Transport in the O(N) vector model with the 2PI formalism . . . 71
3.4.2 Kinetic theory analysis . . . 78
3.4.3 Towards the bosonic Quantum Critical Point . . . 83
3.5 Gross-Neveu model at the quantum critical point . . . 84
3.5.1 Brief review of many-body chaos in GN . . . 85
3.5.2 Hydrodynamic transport in GN model . . . 86
3.5.3 The kernel in the helicity basis . . . 92
3.5.4 The physics behind the analytic continuation . . . 95
3.5.5 Kinetic theory analysis . . . 98
3.5.6 Towards the fermionic Quantum Critical Point . . 101
3.6 Conclusion . . . 102
3.A Notation for fermions . . . 102
3.B Some identities . . . 103
3.C Imaginary part of the self energy in the GN model . . . 105
3.D Pinching-poles approximation . . . 106
3.E Analytic continuation . . . 108
3.F Consistency of the result for the $N \times N$ matrix model . . 111
3.G From the BSE to the kinetic equation in the ϕ^4 matrix model 112

4 Black Hole scrambling from hydrodynamics 117
4.1 Introduction . . . 117
4.2 Scrambling and hydrodynamical transport . . . 119
4.3 Shock waves from linearized gravitational perturbations . 120
4.4 Hydrodynamics and the sound mode . . . 123
4.5 Discussion . . . 124

5 Regulator dependence of the OTOC and kinetic theory at rescue 127
5.1 Introduction . . . 127

5.2 A two-parameter family of extended Schwinger-Keldysh contours . . . 130
5.2.1 The α-contour . . . 133
5.2.2 OTOCS and physical observables in SK formalism 135
5.3 Contour dependence of the Lyapunov spectrum in a weakly coupled Φ^4 theory . . . 137
5.3.1 The contour dependence regulates the IR . . . 144
5.3.2 Kinetic theory interpretation of the α-deformed OTOC 145
5.4 Contour dependence of the Lyapunov exponent in the SYK model . . . 148
5.4.1 Study of the OTOC in SYK in the strongly coupled limit: conformal limit analysis . . . 151
5.4.2 Study of the OTOC in SYK in the limit of large interaction order . . . 152
5.5 The Lyapunov spectrum and the Loschmidt echo . . . 155
5.5.1 Loschmidt echo . . . 156
5.6 Conclusion . . . 160
5.A Numerical calculation in matrix model . . . 162

Bibliography **165**

Samenvatting **195**

Summary **199**

Curriculum Vitæ **203**

List of publications **205**

Acknowledgements **207**

1 Introduction

How does a closed quantum system thermalize? And why do black holes emit thermal radiation? Over the last decades, these two seemingly unrelated questions have attracted the attention of researchers in physics with backgrounds as different as condensed matter, quantum information, statistical mechanics and high-energy physicists. The reason behind this renewed interest is the idea that an underlying unknown mechanism might explain several puzzles that are still open problems in these fields, starting from the black hole information paradox, to the properties of cold atomic systems, till the very basic foundations of quantum statistical mechanics. It all relates to an essential feature of quantum mechanics: the role and the dynamics of quantum information. Since quantum mechanics is unitary, the information must be preserved. Nonetheless, experiments on closed quantum systems and theoretical predictions on black hole dynamics indicate that these systems have a thermal behaviour. Regardless of the unitary time evolution, quantum information seems to be degraded, dissipated. How to reconcile these contradictions is one of the most exciting challenges of today's physics. Beyond the purely theoretical appeal, the solution of these questions may heavily affect the near future technologies in light of the recent progresses towards building a quantum computer.

The dynamics of quantum information has recently been recast in terms of the information spreading in a quantum system. This information scrambling has some properties that reminds one of quantum chaos and is often referred to as the quantum butterfly effect. Whether these two concepts are indistinguishable or not is an open question we are not going to directly address in this thesis, but we believe it deserves caution.

In this thesis we try to understand the microscopic origin of scrambling in two opposite limits: weakly coupled field theories and strongly coupled field theories with holographic duals. By doing so, we push forward a very fascinating idea, namely that this microscopic quantum butterfly effect leaves imprints in the late-time physics, by affecting transport properties of the hydrodynamical excitations of the system. This could provide new techniques to study scrambling and shed some light on the above-mentioned problems.

As required by the object of investigation, this thesis contains topics

from different fields within physics. For this reason, in this chapter we try to provide the basic elements to enable the reader to understand the motivations that led our research. In the following two sections, we review the concepts of classical and quantum thermalization. In section 1.3 we present a recently proposed observable to study scrambling. We conclude this chapter by summarizing the results of this thesis and by giving an overview to the following chapters.

1.1 Classical thermalization

When we focus on a closed classical system, for example a gas of particles, we know that after some time the velocities of the particles will be described by the Maxwell-Boltzmann distribution, even though they were randomized at the very beginning. This property, the fact that everywhere in the box the distribution function is the same, can be considered as a definition of classical thermalization. Classical systems reach this state in a dynamical way. Because of the nonlinear, and hence chaotic, equations of motion, each particle starts to explore the full phase space manifold allowed by energy conservation. This *ergodization* of the motion is such that, after some time, particles with different velocities will likely have a velocity very close to the center of the Boltzmann distribution.[1] Therefore it is clear that, in classical physics, one of the main drivers to ergodicity and so to thermalization is *chaos*[2]. A convenient definition of classical chaos is an extreme sensitivity to the initial conditions. Given two trajectories on the phase space which are very close to each other at a given time, they will quickly depart from each other with a rate set by the Lyapunov exponent

$$\lambda_{\mathrm{L}} = \lim_{t\to\infty,\delta\mathbf{X}_0\to\mathbf{0}} \frac{1}{t}\mathrm{Log}\left(\frac{|\delta\mathbf{X}(t)|}{|\delta\mathbf{X}(0)|}\right). \tag{1.1}$$

This property of dynamical systems has been brought to the general public under the suggestive name of butterfly effect, which is nowadays used also in the scientific community.

[1] During the time evolution, a finite size system eventually returns arbitrarily close to its initial state. This property, representing the statement of the Poincaré recurrence theorem [1], does not represent a problem for thermalization since the recurrence time is exponentially long in the system size. Moreover, statistical mechanics allows for atypical configuration as far as they have exponentially small probability.

[2] The connection between chaotic dynamics and ergodization is still an open problem. While chaotic systems are ergodic, the opposite does not necessarily have to be true.

1.2 Quantum thermalization

The dynamical thermalization, occurring in classical mechanics, cannot be extended in a simple way to quantum mechanics, because this means that a pure initial state would evolve into a mixed state (thermal), in contrast with the unitarity of the time evolution. Nevertheless, we expect the out-of-equilibrium dynamics of closed quantum systems to drive it into a state whose properties are very similar to what we would naively define as a thermal state: a stationary value of macroscopic quantities and stability over a wide range of initial conditions. This expectation is driven not only by physical intuition, but also by numerical results on isolated quantum systems [2].[3] One definition of thermalization involves the expectation value of the observable and can be stated as follows. Let's consider a closed quantum system driven out-of-equilibrium and let it evolve in time. If the system was initially prepared in a state with a well defined mean energy and, during the evolution, the expectation value of the observable can be well approximated by the microcanonical expression, we can consider the system as having thermalized [3] . Given an initial state $\phi = \sum_n c_n |n\rangle$ and the observable $\mathcal{O}$, the expectation value evolves with time as follows

$$\langle \phi(t)|\mathcal{O}|\phi(t)\rangle = \sum_n |c_n|^2 \mathcal{O}_{nn} + \sum_{n,n\neq m} c_m^* c_n e^{i(E_m - E_n)t} \mathcal{O}_{mn}. \tag{1.2}$$

Requiring that this correlation function, after some thermalization time τ_t, matches a microcanonical result is a highly non trivial constraint. A first reason is that the time independent part of (1.2), $|c_n|^2 \mathcal{O}_{nn}$, should match the microcanonical result. Furthermore, we should also impose the second term to vanish. At first sight, the latter requirement might seem very easy to satisfy, as in long time limit the second term averages to zero. But clearly it is very important to estimate the time scale at which it starts to hold. This is related to the spacing of the energy levels, a property which discerns whether a system possesses quasiparticle excitations or not. Indeed, the high energy spectrum of a generic many-body system is characterised by a level spacing exponentially suppressed in the system size[4]. The low energy spectrum, instead, changes. If a system has quasiparticle excitations, the

[3] A comprehensive list of the literature on the numerical studies can be found in [3].

[4] This can be easily seen for a quasiparticle system by considering a simple model of metal (with quasiparticles) with N sites. The energy of the system is described by $E = \sum_{\alpha=1}^{N} \epsilon_\alpha n_\alpha + ...$, where ϵ_α are the single particle energies and $n_\alpha = 0, 1$ the occupation numbers. As there are 2^N many-body levels, the spacing is proportional to 2^{-N}. This property holds also for systems without quasiparticle excitations [4].

single-particle level spacing behaves like $1/N$. But in a system without quasiparticles, the spacing is still exponentially suppressed in N.

This implies that the time at which the second term of (1.2) starts to vanish, proportional to the inverse level spacing $t^* \sim (E_n - E_m)^{-1}$, in a many body system can be exponentially long. Moreover the study of thermalization highly depends on the nature of excitations in the system, since in absence of quasiparticles even the analysis of the low energy sector of the spectrum can be non trivial.

A step forward in understanding the quantum thermalization was the work of Deutsch [5], who used Random Matrix Theory (RMT) to show that, for a random Hamiltonian, the first term of (1.2) indeed coincides with the microcanonical result. RMT, though, is a crude approximation since it washes away all the state dependence of the result, for example the energy of the state (which is crucial in the microcanonical description). These results are equivalent to the infinite temperature limit [3, 5].

The more refined explanation for the thermal expectation value of a local observable is provided by the Eigenstate Thermalization Hypothesis, conjectured by Srednicki in a series of seminal papers [6, 7]. For quantum systems that thermalize, the Hypothesis states that the spectrum of the Hamiltonian H is such that the expectation value of a local observable over the eigenstates n and m of H is of the following form[5]

$$\langle m|\mathcal{O}|n\rangle = \mathcal{O}(\bar{E})\delta_{mn} + e^{-S(\bar{E})/2} f_{\mathcal{O}}(\bar{E},\omega) R_{mn}. \tag{1.3}$$

In the above equation, $\bar{E}$ is the average energy of the states n and m, $\bar{E} = \frac{E_n+E_m}{2}$, and ω the difference, $\omega = E_m - E_n$. Moreover, $\mathcal{O}(\bar{E})$ and $f_{\mathcal{O}}(\bar{E},\omega)$ are smooth functions of the arguments and $\mathcal{O}(\bar{E})$ corresponds to the microcanonical expectation value at energy $\bar{E}$ of the operator $\mathcal{O}$. R_{mn} are random numbers with zero mean and unit variance and $S(\bar{E})$ is the microcanonical entropy.

Despite the successes of the ETH ansatz in describing the thermal behaviour of the correlation functions of local operators, there are still many open questions. In quantum mechanics a pivotal role is played by quantum information, which also in this case seems to be crucial [3]. Nevertheless, what ETH is not able to describe is the dynamics behind thermalization. Thanks to the collective effort of the last decade, we now understand that, under time evolution, the information spreads and

[5] The ETH can be formulated also in terms of operators which are not strictly local, but still subextensive with respect to the number of degrees of freedom, as in [8]. This allows to study ETH also in intrinsically non local systems, as for example SYK model.

delocalizes (it *scrambles*) over the system, becoming inaccessible to local experimental measurements which locally only probe an effectively thermal state.

This can be considered one of the qualitative explanations behind ETH and justifies the use of local operators. In more clear terms, it is important to understand the dynamical process that underlies the ETH ansatz. By drawing an analogy with the classical case, this might be connected to some mechanism that naively could be defined quantum chaos. Furthermore, as we see from equation (1.3), checking thermalization with the ETH ansatz requires the knowledge of the spectrum and the eigenstate of the system, which in a many-body systems is remarkably hard to compute.

The problems listed in the previous paragraphs raise the question whether it is possible to study the dynamics of quantum thermalization using some new observables or new techniques. In the coming section, we will review the out-of-time correlation function (OTOC), which has recently attracted lots of interested in the study of quantum chaos. Afterwards we will discuss a seemingly exotic idea, representing one of the main drives for this thesis, which is to understand quantum chaos by looking at properties of the late-time physics encoded in the hydrodynamical excitations.

1.3 Information scrambling and out-of-time ordered correlators (OTOC)

In the previous section we reviewed some essential features of the ETH and stressed how it seems to release the tension between thermalization and the unitary evolution of quantum mechanics. We can think of it as a precise understanding of thermalization in energy space, but it would be interesting to see what it means in the position space and in time. The way the community understands quantum thermalization nowadays is highly connected to the concept of local operators. When we perform an experimental measurement, in many cases we are probing the system locally, and we have no access to the degrees of freedom in regions far from the probe. This operation corresponds to tracing those degrees of freedom out, giving rise to the thermal spectrum. Clearly, if the information in a quantum system was not subjected to dynamics, *i.e.* it stayed localized, it would be easily detected in an experiment and we would not see thermalization. Our understanding of quantum thermalization strongly indicates that in quantum systems information has a dynamics and, consequently, it spreads over the degrees of freedom of the whole

system. This process is called information scrambling, and has acquired an essential role in the studies of Black Hole information paradox, quantum thermalization and quantum information theory.

In order to probe the information scrambling, a so-called out-of-time correlations function (OTOC) has been put forward. This 4-point function was first introduced in the context of superconductivity by Larkin and Ovchinnikov [9] . There, this correlation function was not put in relation with quantum chaos but it was shown to measure the difference between the classical and the quantum results. Only subsequently the connection with quantum chaos arose [10–16]; since then, this correlation function has appeared in the context of black holes physics and the Sachdev-Ye-Kitaev (SYK) model [17] [10, 18] and there has been a big effort to create experimental protocols to measure it [19–29]. Moreover, several techniques were used to compute it either numerically or analytically [10, 11, 14, 30–49] and its connections with operator growth were studied in [31, 32, 38, 50–54]

The OTOC is defined as follows: given two operators V and W, opportunely normalized, it is

$$C(\mathbf{x},t) = \langle [V(\mathbf{x},t),W(0)]^\dagger [V(\mathbf{x},t),W(0)]\rangle. \tag{1.4}$$

We can understand the information scrambling in terms of the time evolution of an operator, in this case V, initially located at the position $\mathbf{x}$. As a consequence of time evolution, this operator will start spreading over the system. The spreading of the operator can be easily visualized in a spin chain where V at time zero is a single site spin operator [55]. In the Heisenberg picture, the time evolution can be written in terms of nested commutators of the operator V with the full Hamiltonian H and, because of these commutators, the time evolution will contain spin operators of other sites.

We can probe the spreading by considering the commutator with an operator inserted in $\mathbf{0}$, for example with $[V(\mathbf{x},t),W(0)]$. At time zero the commutator vanishes because of causality. However, with time evolution the operator $V(\mathbf{x},t)$ will become more and more delocalized, and at some time t^* its front will hit the insertion $W(0)$, developing a non trivial value of the commutator. This simple picture would suggest the following

$$C'(\mathbf{x},t) = \langle [V(\mathbf{x},t),W(0)]\rangle \tag{1.5}$$

as a good observable for operator spreading. Such correlation function corresponds to the retarded (advanced) Green's function for t positive (negative). Unfortunately, the time ordered 2-point correlation functions,

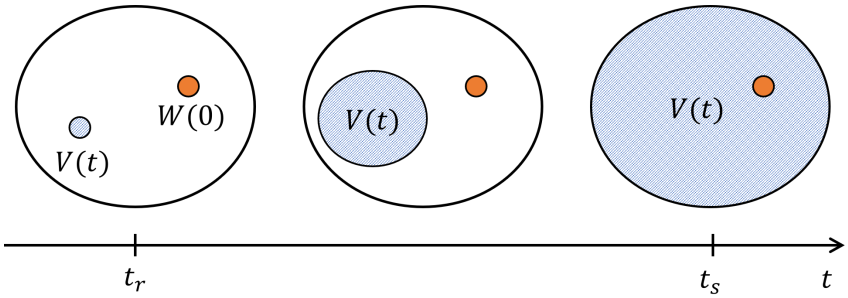

Figure 1.1: Representation of operator spreading. Figure taken from [56].

computed on a thermal state, decay very quickly and they are too constrained to carry information about scrambling. In order to extract such information, (1.4) turns up to be a fruitful choice.

If we focus on hermitian operators W and V, (1.4) can be rewritten as

$$C(\mathbf{x},t) = 2 - 2\,\mathrm{Re}F(\mathbf{x},t) \tag{1.6}$$

where

$$F(\mathbf{x},t) = \langle V(\mathbf{x},t)W(0)V(\mathbf{x},t)W(0)\rangle. \tag{1.7}$$

The latter expression represents the out-of-time order contribution to $C(\mathbf{x},t)$ and it contains all the physics about scrambling. The time dependence of this correlation function for chaotic system can be parametrized as

$$F(\mathbf{x},t) = 1 - \epsilon\, e^{\lambda_{\mathrm{L}}(t-g(\mathbf{x}))} \tag{1.8}$$

where λ_{L} is conjectured to be the highest Lyapunov exponent of the system, ϵ is a small term inversely proportional to the local number of degrees of freedom and $g(\mathbf{x})$ is a function that represents the spatial profile. For many large N field theories, $g(\mathbf{x})$ has a linear behaviour $g(\mathbf{x}) = \frac{|\mathbf{x}|}{v_{\mathrm{B}}}$, where v_{B} is the speed at which the front depicted in Fig. (1.1) moves and it is called the *butterfly velocity*.

On a thermal state, the OTOC is often defined as follows

$$C(\mathbf{x},t) = -\langle \rho[V(\mathbf{x},t),W(0)]^\dagger[V(\mathbf{x},t),W(0)]\rangle, \tag{1.9}$$

ρ being the thermal density matrix. A slightly different definition involves a symmetric insertion of the density matrix in the correlation function

$$C^{\mathrm{S}}(\mathbf{x},t) = -\langle \rho^{1/2}[V(\mathbf{x},t),W(0)]^\dagger\rho^{1/2}[V(\mathbf{x},t),W(0)]\rangle. \tag{1.10}$$

That (1.9) and (1.10) might have different properties is a topic that has not been considered in the last few years and will be discussed in chapter 5. With this configuration, the out-of-time ordered function acquires a new fundamental property. Under mild hypotheses, such as analyticity of correlation functions and unitarity of time evolution, Maldacena, Shenker and Stanford proved in [16] that, if the correlation function (1.10) presents an exponential growth regime, the Lyapunov exponent satisfies the following upper bound

$$\lambda_{\mathrm{L}} \leq \frac{2\pi \mathrm{k_B} T}{\hbar}. \tag{1.11}$$

The bound is saturated by systems which have a gravitational dual; this proves the *fast scrambling conjecture*, introduced in [11], which states that Black Holes are the fastest scramblers in nature. Nevertheless it is not known yet whether the saturation of the bound represents a sufficient condition for a theory to have a holographic dual. The right hand side of (1.11) is intimately connected to the nature of black holes and, in particular, to their event horizon. It can be shown [12, 14, 15] that, in a theory with a holographic dual, the OTOC corresponds to the effect on the geometry of few particles moving from the boundary towards the bulk. Once in the proximity of the event horizon, the energy of the particle, in the local frame, will be highly boosted, creating a shock wave along the horizon. The Lyapunov exponent is a measure of such a boost, which for any Black Hole results in the value $\frac{2\pi \mathrm{k_B} T}{\hbar}$.

The bound (1.11) appears like a fundamental property of quantum mechanics, and its possible interpretations and consequences are very fascinating. For the moment, we can rewrite the bound (1.11) in terms of the Lyapunov time $\tau_{\mathrm{L}} = 1/\lambda_{\mathrm{L}}$

$$\tau_{\mathrm{L}} \geq \frac{1}{2\pi} \frac{\hbar}{\mathrm{k_B} T}. \tag{1.12}$$

In this form it will soon be clear why the bound has been intensively studied in the last years, and it has to do with transport in strongly coupled systems without quasiparticles. This is one of the main open problems of today's physics, both from the theoretical and experimental point of view and in the next section we will try to highlight its connection with the above mentioned bound.

1.4 Quantum systems without quasiparticles

In this section we take an apparent departure from the topics of the previous pages, which hopefully will be soon clear to the reader. Our current understanding of transport in ordinary metals is provided by the Landau theory of Fermi liquids [57], which is built on the concept of quasiparticles. There, the relevant excitations are long lived and have a pivotal property: the energy of a state made of quasiparticles is simply the sum of their energies. These quasiparticles have the same quantum numbers as electrons, and interact with each other. When the system is perturbed, the interactions restore thermal equilibrium after a local equilibration time, which we indicate with τ_e. If the system is gapless, τ_e has a temperature dependence that, in the $T \to 0$ limit, goes as $\tau_e \sim 1/T^2$. In the presence of a gap Δ, instead, the equilibration time is even longer and scales as $\tau_e \sim e^{\Delta/T}$. Despite its success, there are still materials which Landau theory is not able to describe, such as cuprates, heavy fermions, ruthenates, pnictides, vanadium dioxide, fullerenes and organics. The electrons in these materials are strongly correlated and present a linear in T resistivity in a wide region of their phase space [58, 59]. The resistivity scaling suggests that the local equilibration time is exceptionally short and scales as $\tau_e \sim 1/T$. The surprising feature of this scaling is that, besides being very robust against disorder, it is present in systems with very different microscopic details. It seems thus that some universal mechanisms underlies the physics in this regime. This mechanism has been named Planckian dissipation [60–62] and states that strongly coupled systems without quasiparticles are the fastest in thermalizing. Furthermore their local equilibration time saturates the lower "dimensional analysis" bound

$$\tau_e \geq C \frac{\hbar}{k_B T}, \tag{1.13}$$

where C is some temperature independent constant of order one. More recently, measurements on thermal diffusivities [63] showed Planckian dissipation in YBCO samples.

The similarities between (1.12) and (1.13) might be interpreted as the existence of a connection among the Lyapunov time and the local equilibration time. Moreover, in this light, it was proposed by Blake [64, 65] that charge and thermal diffusivities of critical systems could be expressed as

$$D_{\mathrm{C/T}} \propto v_{\mathrm{B}}^2 \tau_L, \tag{1.14}$$

where the identity holds up to a numerical prefactor. This proposal was tested in several systems [66] but soon it became evident that the

connection with charge diffusion was not as robust as thermal diffusion. The latter connectio is quite robust. Indeed in [67–69] it was shown that, in the infrared, the thermal diffusivity of a generic strongly coupled system with holographic dual satisfies relation (1.14) regardless of charge density, periodic potential strength, or magnetic field. Those results were obtained by using the holographic duality, which we are going to quickly review in the following section.

1.5 Holographic duality

Since its discovery in 1997 by Maldacena [70], AdS/CFT has profoundly changed the way we look at gravity and strongly coupled field theories. In this section we will try to give a very general overview on the topic, mainly focusing on the aspects that are necessary to understand some of the results of this thesis, and the reason why we have tried to address certain questions.[6]

The idea of holography can be traced back to two important results. In 1974, 't Hooft realized that $SU(N_c)$ gauge theories greatly simplify in the large N_c limit, keeping the 't Hooft coupling $\lambda = g^2_{YM} N_c$ fixed [75]. In this limit, organized as a perturbative expansion in λ, the leading contribution is given by planar diagrams. In the same work, t'Hooft noticed that this expansion could be connected to a string theory path integral. On a completely different perspective, the work of Bekenstein on black holes thermodynamics [76] showed that the entropy of a Black Hole depends on its surface, and not on its volume. This indicates that in a gravitational theory gravitational degrees of freedom rearrange the information on a surface of codimension one, making possible (in principle) a description of $d+1$ dimensional gravity in terms of a field theory defined in d dimensions [77, 78].

AdS/CFT is an exact realization of this idea. In its most essential definition, the AdS/CFT correspondence is a duality between a conformal large N supersymmetric Yang-Mills theory (Large N SYM) defined in d dimensions and a classical gravitational theory defined on a $d+1$ spacetime with a negative cosmological constant, namely Anti-de-Sitter. Its origins lies in string theory, where large N SYM is equivalent to string theory in AdS. It is a strong-weak duality, *i.e.* it relates a strongly coupled theory to a weakly coupled one. This means that it allows to quantitatively

[6] For a review on the topic, see [71]. Applications to condensed matter physics are reviewed in the following books [72–74].

understand properties of strongly coupled field theories by studying classic gravitational dynamics.

Bekenstein's argument gives a hint about the holographic nature of gravity, but a natural question to ask is what does this extra dimension correspond to from the QFT point of view. Given a QFT defined on a d dimensional spacetime, we know since Wilson [79] that the theory changes according to the energy (or spacetime) scale μ we focus on. The way the theory changes by varying this scale is described by the Renormalization Group (RG) equation

$$\mu \frac{dg(\mu)}{d\mu} = \beta(g(\mu)), \tag{1.15}$$

where $g(\mu)$ schematically represent the coupling constants of the theory. A remarkable fact of equation (1.15) describing the renormalization group flow is that it is local in the energy scale. This might seem a minor aspect but has strong implications, specially in AdS/CFT. In holography, the renormalization scale not only becomes dynamical, but also geometrical. Its dynamics is governed by the Einstein action with a negative cosmological constant $-2\Lambda = \frac{d(d-1)}{L^2}$

$$S = \frac{1}{2\kappa^2} \int d^{d+1}x\sqrt{-g} \left(R + \frac{d(d-1)}{L^2} \right), \tag{1.16}$$

with $\kappa = 8\pi G_N$ and G_N the Newton's constant and L is the AdS radius. The zero temperature solution in vacuum is described by the metric

$$ds^2 = \left(\frac{L}{z}\right)^2 (\eta_{\mu\nu} dx^\mu dx^\nu + dz^2), \tag{1.17}$$

where $\mu, \nu = 0, ..., d-1$. The direction z can be considered as a renormalization group scale and the excitation of the theory are rearranged along z according to their wavelength, as represented in Fig. (1.2). We see that motion in $z \to \lambda z$ precisely can be accounted for by scaling $x \to \lambda x$.

On a more quantitative ground, the holographic correspondence can be stated in terms of an identity of two partition functions, called the GKPW rule [81, 82]

$$\langle e^{\int d^d x \sum_i J_i(x)\mathcal{O}_i(x)} \rangle_{\text{QFT}} = \int \mathcal{D}g\mathcal{D}\phi_i \, e^{iS_{bulk}[g,\phi_i(x,z)]|_{\phi(x,z=0)=J(x)}}. \tag{1.18}$$

The left hand side of the equality is the partition function of a QFT deformed by a source J. The right hand side corresponds to the gravitational partition function, dominated by the saddle point value, where

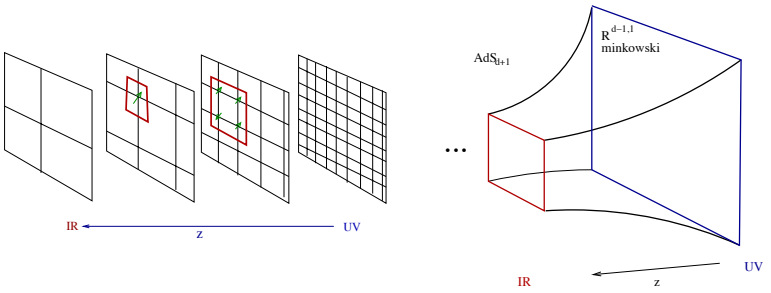

Figure 1.2: The emerging dimension in the AdS/CFT correspondence can be though of as a renormalization scale. The excitations of the dual field theory are rearranged over the boundary according to their wavelenghts: the long wavelenght, low energy dynamics of the dual theory is captured by events in the bulk. Short distance, high energy excitations are described by the gravitational degrees of freedom close to the boundary. The duality rearranges the excitation. Figure taken from [80].

the boundary value (at $z \to 0$) of the field ϕ is set by J, the value of the source of its dual operator $\mathcal{O}$. Including this fundamental identity, the duality can be summarized in terms of a dictionary, where quantities of the two theories are related. Some of the entries of the dictionary are presented in the tabular below. The order used to list them is not casual since the connection between the gravitational dynamics in the bulk and stress tensor properties in the boundary will be the essential motivation to pursue the results of chapter 4 that connect quantum chaos to the energy-energy correlation function.

Another feature of gravity that holography incorporates naturally that deserves attention for this thesis is the fluid/gravity correspondence [83]. This states that the spacetime dynamics, on a AdS background, can be mapped into the dynamics of a fluid living on the *boundary*. Since the long wavelength of the fluid is described by hydrodynamics and, in the AdS/CFT correspondence, the IR of the boundary theory is described by the bulk gravitational degrees of freedom, the fluid/gravity correspondence connects the hydrodynamic behaviour of the fluid living on the boundary with the gravitational perturbation of the event horizon. After a perturbation, Einstein's equations reproduce hydrodynamical equations and allow to compute the conductivities of the fluid [83, 84]. This does not imply that the event horizon is purely hydrodynamical, because very far from equilibrium the hydrodynamic approximation is not valid. Nevertheless, Black Holes have the surprising feature that they hydrodynamize very quickly.

The idea of a connection between the dynamics of black hole horizons and the Navier-Stokes equations of hydrodynamics dates back to the 80's when Thorne, Price and MacDonald formulated the so-called membrane paradigm [85]. They realized that, for an external observer, the behaviour of black holes would resemble the behaviour of a fluid membrane, *surrounding their event horizon*, with well-defined properties as viscosity and conductivity.

Boundary (Operators)	**Bulk (fields)**
stress-energy tensor T_{ab}	metric field $g_{\mu\nu}$
global current J^a	Maxwell field A_a
scalar operator $\mathcal{O}$	scalar field ϕ
conformal dimension of the operator	mass of the field
source of the operator	boundary value of the field
VEV of the operator	boundary value of radial momentum of the field
global symmetry	local symmetry
temperature of the field theory	Black Hole temperature
phase transition	Black Hole instability

1.6 A hydrodynamical refresh

When focusing on the long-wavelength and late-time description of a given system, often the result is a very old theory, whose origins go back to the early works of Euler and Bernoulli in the XVIII century: hydrodynamics. Even though it is a very old theory, there are still many properties that are not understood, like turbulence for example, and in the last years we have witnessed a revival of interest about its applications. In the present-day view, hydrodynamics is an effective field theory that is conventionally formulated in terms of equations of motion. The action formulation has recently been addressed in[7] [87–98] and, as often happens going from the equations of motion to the action, it has revealed new symmetries and constraints. The equations of motions of (relativistic) hydrodynamics are simply the conservation laws of the systems; for example, if there are no more conserved currents than the stress energy tensor, the EOMs are

$$\partial_\mu T^{\mu\nu} = 0. \tag{1.19}$$

[7] For review on the topic see [86] and references therein.

As stated, this does not represent a well-posed problem in $d \geq 2$ since there are $d(d+1)/2$ degrees of freedom and d equations of motion[8]. A crucial step in deriving the hydrodynamical equation is the hypothesis of *local thermal equilibrium*, which reduces sensibly the number of degrees of freedom. When the system is perturbed at long wavelength, it is possible to consider as dynamical variable the temperature $T(\mathbf{x})$ as a function of space and time, and the velocity four vector $u^\mu(\mathbf{x})$, subject to the normalization condition $u^\mu u_\mu = -1$. This choice makes the problem well posed, since there are d unknowns and d equations of motion. As typical for effective field theories, the stress-energy tensor can be written in terms of a gradient expansion in spatial derivatives and as a function of the dynamical variables. At zero-th order the expansion gives

$$T^{\mu\nu}(x) = \epsilon\, u^\mu u^\nu + p\, \mathrm{P}^{\mu\nu}, \tag{1.20}$$

where ϵ is the energy density, p the pressure density and with $\mathrm{P}^{\mu\nu} = u^\mu u^\nu + g^{\mu\nu}$ we have indicated the projectors along the direction transverse to the four-velocity u^μ. In this order, the hydrodynamical equations do not present any dissipation, as can be easily shown [99]. Entropy production appears in first order, with the introduction of the dissipation tensor and transport coefficients

$$T^{\mu\nu}(x) = \epsilon\, u^\mu u^\nu + p\, \mathrm{P}^{\mu\nu} - \sigma^{\mu\nu}. \tag{1.21}$$

The dissipation component of the stress energy tensor can be generally parametrized as follows

$$\sigma^{\mu\nu} = \mathrm{P}^{\mu\alpha}\mathrm{P}^{\nu\beta}\left[\eta\left(\partial_\alpha u_\beta + \partial_\beta u_\alpha - \frac{2}{3} g_{\alpha\beta}\partial_\rho u^\rho\right) + \zeta g_{\alpha\beta}\partial_\rho u^\rho\right], \tag{1.22}$$

the coefficients η and ζ being respectively the shear and the bulk viscosity. The form (1.22) of the dissipation tensor is not unique, but is chosen in such a way to affect only the spatial component of the stress-energy tensor T^{ij}.

The analytical structure of the hydrodynamical correlators, namely the location of the poles, can be extracted from the normal modes of the linearised hydrodynamical equations, *i.e.* by looking at solutions of the form $e^{-i\omega t + i\mathbf{k}\cdot\mathbf{x}}$. For example, let's restrict the analysis to the stress-energy tensor, and choose a frame where the spatial momentum is aligned with the z direction, $\mathbf{k} = (0, 0, k)$. It is possible to show that the stress energy

[8] In CFT, the case $d = 2$ is well defined since there is an extra constraint on the stress energy tensor which has to be traceless.

tensor has two physically different hydrodynamical modes, the shear and the sound modes [99]. The components T^{0i} and T^{zi}, with $i = (x, y)$, satisfy the following linearised hydrodynamic equation

$$\partial_t T^{0i} = -\frac{\eta}{\epsilon + p}\partial_z^2 T^{0i}, \tag{1.23}$$

which can be immediately recognized as a diffusion equation. Indeed by looking for a solution of the form $e^{-i\omega t+ikz}$ we get

$$\omega(k) = -i\frac{\eta}{\epsilon + p}k^2, \tag{1.24}$$

with diffusion constant $D_s = \frac{\eta}{\epsilon+p}$. Besides shear modes, there are also propagating sound modes, represented by simultaneous excitations of T^{00}, T^{0z} and T^{zz}. After diagonalizing a system of coupled hydrodynamic equations, the condition these modes have to satisfy is the following [100]

$$\omega(k) = v_s k - \frac{i}{2}\left(\frac{4}{3}\eta + \zeta\right)\frac{k^2}{\epsilon + p}, \tag{1.25}$$

where $v_s = \sqrt{\frac{\partial p}{\partial \epsilon}}$ is the speed of sound.

1.7 Hydrodynamic transport coefficients at weak coupling and in holography

The late-time and long-scale physics of a generic classical or a quantum many-body system is governed by the long-lived quantities, which are nothing but the conserved currents. Their conservation laws become the equation of motion and the theory is called hydrodynamics, which indeed is nothing but the dynamics of the conserved quantities. This in turn expresses the universality of its prediction, which heavily rely on symmetries arguments. Although it has a high degree of universality, the hydrodynamic prediction is intimately connected to the underlying microscopic physics via some of the coefficients of this expansion: the transport coefficients like viscosities and diffusivities. Given a Lagrangian the computation of these coefficients represents a challenge even at weak coupling, since they often manifest a nonanalytic dependence on the coupling parameters. Traditionally, for high-energy applications like QCD or relativistic QFTs in $3 + 1$ dimensions, the main tool has been to solve the Boltzmann equation [101–108]. Another approach, based on quantum field theory, can be found in [109, 110].

Another way to compute transport coefficients, more used in low-energy many-body physics condensed matter, makes use of the Kubo formulae for specific correlation functions, like the following ones for shear viscosity η or electrical conductivity σ [111]

$$\eta = \frac{\beta}{20} \lim_{p^0,\mathbf{p}\to 0} \int d^4x e^{ip\cdot x} \langle T_{ij}(x) T^{ij}(0)\rangle, \tag{1.26}$$

$$\sigma = \frac{\beta}{6} \lim_{p^0,\mathbf{p}\to 0} \int d^4x e^{ip\cdot x} \langle J_i(x) J^{i}(0)\rangle, \tag{1.27}$$

where T_{ij} is the traceless stress-energy tensor, J_i is the $U(1)$ current and the sum over repeated indices is intended. In the weakly coupled regime, the formulae (1.26) and (1.27) might suggest that, by simply performing loops expansion of the correlation function in the integral, we could get the proper perturbative results for the shear viscosity. Unfortunately, this expansion is not reliable due to the appearance of infrared singularities [112], and a full resummation of a series of diagrams is required [101]. This becomes an even more challenging task when relativistic gauge theories are considered. The pioneering computation of the shear viscosity for a scalar field with ϕ^4 interaction

$$\mathcal{L} = \frac{1}{2}(\partial_\mu \phi)^2 - \frac{1}{2} m^2 \phi^2 - \frac{\lambda}{4!}\phi^4, \tag{1.28}$$

was performed in [101, 112]. There, by using a finite temperature optical theorem, Jeon derived the cutting rules at finite temperature and then showed that an infinite set of ladder diagrams had to be resummed in order to obtain the correct leading order result. Since then, several works addressed this question for more complicated field theories and using different techniques, such as the real time close time-path contour (CTP) [113, 114] and the Imaginary Time Formalism (ITF) [115] of thermal field theory. Within the latter approach, a non perturbative resummation provided by the two-Particle-Irreducible (2PI) formalism was introduced in the computation of transport quantities in [116, 117] .

In this thesis we will extensively make use of those techniques, developed to compute the Kubo formulae, to evaluate the following correlation function

$$iG_{\mathrm{R}}(x,p|y,q) = \theta(x^0 - y^0)\langle[\rho(x,p),\rho(y,q)]\rangle \tag{1.29}$$

where we have defined the Wigner transport of the bilocal density operator

$$\begin{aligned}\rho(x,p) &= \int_y e^{-ipy}\,\mathrm{Tr}\left[\phi(x-y/2)\phi(x+y/2)\right] \\ &= \int_k e^{ikx}\,\mathrm{Tr}\left[\phi(p+k/2)\phi(p-k/2)\right], \end{aligned} \tag{1.30}$$

and the trace is taken over the internal indices of the field ϕ.

While in a weakly coupled QFT the computation of correlation functions which appear in the Kubo formulae is very involved, in strongly coupled field theories with holographic dual things simplify remarkably. By using the dictionary, it is possible to show that the stress-energy tensor two-point functions can be extracted by a perturbative gravity computation in the bulk. This allows an exact numerical solution and, in the hydrodynamic limit, an analytical solution [99, 100, 118–120]. We will use these techniques in chapter 4 to derive one of the most important results of this thesis.

1.8 Quantum chaos and hydrodynamics

In the previous sections we have briefly reviewed the conundrum represented by the thermalization of a closed quantum system. We have also given the qualitative understanding on how this thermal behaviour emerges, namely because of the scrambling of quantum information. Nevertheless, several questions have no satisfactory answer yet. We still lack a comprehensive dynamical understanding of how this information-scrambling happens. Moreover, we don't know whether scrambling and quantum chaos are the same phenomenon. We believe that these are essential questions to address, especially in light of the fast scrambling conjecture. The latter is likely to be a fundamental result, able to classify different states of matter. Unfortunately, it does not explain the mechanisms that determine whether a system can be close to saturation of the bound or not.

On general grounds, we know that, for relativistic theories, the mechanisms underlying the way a system (nearly) out-of-equilibrium reaches the thermal state leaves clear imprints in the analytic structure of the conserved currents-correlation functions [121, 122]. Since the dynamics of conserved currents is by definition hydrodynamics, it seems reasonable to try to understand many-body chaos by looking for signatures in the analytical structure of hydrodynamic excitations.

There is further evidence in support of this idea. As already mentioned, the scrambling properties of strongly coupled theories with holographic duals at finite temperature are set by the gravitational dynamics in the

bulk. By using the membrane paradigm, we can imagine that this involves the correlation functions of the stress-energy tensor, which very quickly assume a form dictated by hydrodynamics.

Furthermore, some insights come from the study of the Sachdev-Ye-Kitaev (SYK) model. This is a $(0+1)$ theory of fermions with quartic all-to-all interaction, and Lagrangian (in the case of Majorana fermions)

$$H = -\sum_{ijkl} J_{ijkl}\, \chi^i \chi^j \chi^k \chi^l. \tag{1.31}$$

This model saturates the bound on chaos and is supposed to have a gravity dual. In the infrared limit, it exhibits a $SL(2,\mathbb{R})$ symmetry, which is reminiscent of the AdS_2 geometry. In [123], Jensen wrote a hydrodynamic effective field theory which is maximally chaotic and captures some features of the AdS_2 geometry. The fact that the IR physics of the SYK model can be captured by a hydrodynamical mode which is also maximally chaotic should be considered as further evidence that, at least for (nearly) maximally chaotic systems, hydrodynamics carries some information about scrambling.

1.9 Summary of results

In this thesis we address some of the questions raised so far. In the first part, we try to understand what is the dynamics of scrambling, or of quantum chaos. We tackle this problem for weakly coupled quantum field theories (or large N) and we draw an analogy with the quantum Boltzmann equation (QBE). Even though the QBE relies on the concept of quasiparticles, in 1997 Damle and Sachdev showed [124] that the QBE can be used also to study conductivities and transport properties above the two-dimensional superfluid-insulator quantum critical point. This means that, by carefully controlling the QBE, it can give predictions about excitations of systems in the absence of quasiparticles. The QBE can be generally written in the form

$$(\partial_t + \mathbf{v}\cdot\nabla) f(t,\mathbf{x},\mathbf{p}) = -\mathcal{L}[f] \tag{1.32}$$

where $\mathcal{L}$ is the linearized collision integral, which clearly encodes all the relevant information about the physics.

The starting point of our results is that, while the QBE is usually extracted from two-point functions [125–127], it is possible to obtain the linearized QBE in a clean way from the 4-point function (1.29). As we

explain with (hopefully sufficient) detail in chapter 2, the conceptual advantage is the immediate matching of the QFT expressions with their kinetic theory counterparts. In this approach, the operator $(\partial_t + \mathbf{v}\cdot\nabla) + \mathcal{L}$, which defines the QBE, is fully encoded in the analytical structure of this 4-point Greens function[9]. Indeed such correlation function $f(\omega, p, q)$, in the spatially homogeneous case, satisfies the following Bethe-Salpeter equation (BSE)

$$-i\omega\, f(\omega,p) = \delta(p_0^2 - E_{\mathbf{p}}^2)\left(1 + \int_l \hat{R}^{\text{transp}}(p,l) f(\omega,l)\right). \tag{1.33}$$

where $f(\omega,p) = \int_q f(\omega,p,q)$. Once on-shell, the kernel $\hat{R}^{\text{transp}}$ reproduces exactly the collision operator $\hat{C}$, determining the matching of the QFT result with the Boltzmann equation. Moreover, all the information about the relaxation times, eventual branch cuts and hydrodynamic modes are intrinsically hidden in $\hat{R}$, as the correlation function is formally obtained by inverting (1.33)

$$f(\omega,p) = \frac{\mathcal{I}_p}{-i\omega - \int_l \hat{R}^{\text{transp}}(p,l)}. \tag{1.34}$$

Focusing on the OTOC, $f'(t,\mathbf{x})$, at weak coupling the computation requires a resummation of *ladder* diagrams and it is also performed by a Bethe-Salpeter equation (BSE). This BSE can be recast into the following integro-differential equation

$$-i\omega\, f'(\omega,p) = \delta(p_0^2 - E_{\mathbf{p}}^2)\left(1 + \int_l \hat{R}^{\text{OTOC}}(p,l) C(\omega,l)\right). \tag{1.35}$$

$f'(\omega,p)$ being the Fourier transform in p and Laplace transform in ω of the OTOC. Clearly, since in the late time regime ($\omega \to 0$ limit) the OTOC has the form $f'(t) \propto e^{\lambda_L t}$, the spectrum of the integral operator $\hat{R}'(p,l)$ contains all the informations about ergodicity, *i.e.* the Lyapunov spectrum is given by its positive eigenvalues.

In order to understand the scrambling dynamics, we can dissect the OTOC-BSE. The way we have phrased it highlights it on purpose, but the surprising result is that the OTOC-BSE is also a kinetic equation of the form

$$(\partial_t + \mathbf{v}\cdot\nabla) f'(t,\mathbf{x},\mathbf{p}) = -\mathcal{L}'[f'] \tag{1.36}$$

[9] This can be considered as the analogue of what happens in hydrodynamics. There, as reviewed in section 1.6, the universality of the equation of motions is translated in the universal form of the pole structure.

where the collision integral is nearly the same as (1.32). Instead of measuring the net number of collisions, as the standard QBE, it counts the gross number of collisions. This is to say that the terms appearing in $\mathcal{L}$ and $\mathcal{L}'$ are the same, with one of the signs flipped. We showed this results for ϕ^4 matrix model (chapter 2), (bosonic) $O(N)$ vector model in $(2+1)$ dimensions and the Gross-Neveu model in $(2+1)$ dimensions (chapter 3) . Moreover, we also show that the linearised kinetic operator, $\hat{R}^{\text{transp}}(p,l)$, is analytically related to the kernel of the BSE of the OTOC, $\hat{R}^{\text{OTOC}}(p,l)$, as follows

$$\hat{R}^{\text{OTOC}}(p,l) = \sinh(\beta p_0/2)^{-1}\, \hat{R}^{\text{transp}}(p,l)\, \sinh(\beta l_0/2). \tag{1.37}$$

It is tempting to read the previous expression as a new fluctuation dissipation relation:

$$C(\omega,p) = \sinh(\beta p_0/2) f(\omega,p), \tag{1.38}$$

which would suggest that the OTOC can be obtained as analytical continuation of the hydrodynamic correlation function governing transport. However, in this thesis we will not succumb to this temptation and we will postpone this question to future work. Another reason why we wrote (1.37) in this form is that it makes clear that the relation is nothing but a similarity transformation, which preserves the spectrum and other properties. Nevertheless we warn the incautious reader that, both in (1.35) and (1.37), there are delta functions which project out some eigenvalues. Indeed we know that unitarity forbids eigenvalues with positive imaginary part for the collision integral of the (standard) Boltzmann equation.

We now comment about the consequences of (1.37). Since, as we have argued before, the full physics of scrambling is encoded in $\hat{R}^{\text{OTOC}}(p,l)$ and most of the hydrodynamical transport physics is encoded in $\hat{R}^{\text{transp}}(p,l)$, this relation has a profound meaning and should be considered as a starting point for any further attempt to find imprints of ergodicity in the hydrodynamic spectrum. Moreover, we stress that (1.37) not only holds for the ϕ^4 model (chapter 2), but also for models which describe the physics above a QCP (chapter 3), where there are no quasiparticle excitations.[10] Therefore this seems to be a quite general result for weakly coupled systems, or large N QFTs. We have repeatedly hinted the suggestive similarities between transport computations and scrambling computations. At infinite coupling and for theories with gravitational dual, the idea that quantum chaos constrains transport is indeed true and it is realized in

[10] For fermions, we prove in chapter 3 that (1.37) is modified by replacing sinh → cosh.

the phenomenon discovered in chapter 4 of this thesis (based on [128]), and later termed *pole-skipping* [56]. In section 1.3, we sketched the classification of the hydrodynamical modes and we showed that the energy-energy correlation function contains sound modes, whose perturbative dispersion relation is given by (1.25). Let us define the following point in the analytically continued (ω, k) plane

$$k_c = i\frac{\lambda_L}{v_B}, \qquad \omega_c = \omega(k_c) = i\lambda_L, \tag{1.39}$$

where $\lambda_L = 2\pi T$ and v_B is the butterfly velocity, defined in the previous pages. Pole-skipping is the statement that the fully resummed hydrodynamic series (1.25), after the analytic continuation $\omega \to i\omega$ and $k \to ik$, passes through the point (ω_c, k_c). Since the dispersion relation (1.25) parametrizes the pole structure of the energy-energy two-point function, this implies that this correlator has the form

$$G_R^{EE}(\omega, k) = \frac{b(\omega, k)}{a(\omega, k)} \tag{1.40}$$

and $a(\omega_c, k_c) = 0$. Moreover, (2) at the point (ω_c, k_c) also the residue vanishes,

$$b(\omega_c, k_c) = 0. \tag{1.41}$$

This implicates that the pole in the correlator $G_R^{EE}(\omega, k)$ disappears. This phenomenon has been later understood in terms of an effective field theory [56] as the fact that both ergodicity and hydrodynamics are governed by the same mode, which survives at late time. The robustness of such modes is due to the exsistence of a new symmetry (a shift symmetry) of the effective action. Whether this is a feature of systems saturating the bound on chaos is still an open problem. Furthermore, we now know that mathematically pole-skipping, as described in holographic systems, is a manifestation of a degeneracy of Einstein equation [129]. Recently, it was also proven that this phenomenon is present not only for energy density correlators [130] but persists also away from infinite coupling [131]. New constraints on thermal correlators (in holographic systems) coming from pole-skipping (although not immediately relatable to chaos) have been recently discovered in [132].

What happens going towards the weak-coupling limit, and so departing from the bound, it is still unknown.

1.10 This Thesis

1.10.1 Chapter 2

We first write a Boltzmann-like equation for the gross energy exchange in a bosonic system. We do this by modifying the collision integral in order to take into account the gross number of interactions between particles instead of the net number of interaction, which corresponds to the standard Boltzmann equation. After that, we show how this kinetic equation matches the BSE satisfied by the OTOC. We then review how to compute the out-of-time ordered correlation function in quantum field theory. This can be done by using the Schwinger-Keldysh (SK) formalism over the closed time path (CTP) contour . After analyzing the properties of this modified SK contour, we show that the computation of the OTOC is remarkably simplified. We explicitly use this framework to compute the OTOC in a $N \times N$ matrix ϕ^4 bosonic theory, without taking any large N limit.

1.10.2 Chapter 3

In this chapter, we focus our attention to the interplay between chaos and hydrodynamics in systems close to the quantum critical point (QCP). In the quantum critical regime, there is no quasiparticle interpretation, but it was shown that many transport properties can be inferred by analytically extending the result in the symmetric phase to the quantum critical phase. This chapter is mainly based on [133]. To understand these questions, we make an extensive use of some results regarding transport obtained in the imaginary time formalism (ITF) and we use the two-particle-irreducible effective action. We first analyze the bosonic $O(N)$ vector model, and we study the 4-point correlation function which is relevant for transport in the hydrodynamic limit. This computation generalizes at small external frequency some previous results by Aarts et Martinez [134, 135] which were obtained at strict zero frequency. This allows us to compare the equations governing transport with the BSE for the OTOC, which was obtained by Chowdhury and Swingle in [136]. Again, the mapping between the two results holds and confirms our conjectured connection between chaos and hydrodynamics. By going into the kinetic theory limit, we observe that indeed the OTOC is nothing but a gross energy exchange kinetic equation. In the second part of this chapter, we address a similar analysys to a system in a fermionic quantum critical regime, namely the $2 + 1$ the Gross-Neveu model. Here we first use the 2PI formalism to

compute the 4-point function relevant to transport and then we compare it with the OTOC computation performed in [137]. This case, in a even more clear way, shows how transport and chaos are described by the same BSE equation but correspond to two different boundary conditions. Such difference, in turn, determines the sign flip of the kinetic equation for chaos with respect to the QBE. We explicitly show how the linearized Boltzmann equations emerge from a QFT computation of a time ordered 4-point function. By inspecting these results, it is straightforward to see that indeed the kinetic theory for gross particle exchange reproduces the BSE for the out-of-time correlation function.

1.10.3 Chapter 4

In this chapter we investigate the connection between quantum chaos and hydrodynamics in theories with a holographic dual. These theories are strongly coupled large N theories, and the out-of-time order correlation function can be computed by means of the AdS/CFT correspondence. This result was obtained some years ago by Shenker and Stanford in [12], who showed that the Lyapunov exponent can be extracted by studying a shockwave geometry in the bulk. We show that this shockwave computation can be understood in terms of a sound-wave excitation of the bulk geometry. Since these excitations have a physical interpretation as hydrodynamical energy-energy correlation functions of the dual boundary theory, we prove that for holographic theories the Lyapunov exponent and the butterfly velocity characterize the response to an highly out-of-equilibrium perturbation. We moreover identify the imprinting of quantum chaos in the analytical properties of the energy-energy correlation function which is now known as *pole-skipping*.

1.10.4 Chapter 5

In this last chapter we address an important question regarding the out-of-time correlation function. We try to understand whether this correlation function is independent of the way it gets regularised on the thermal circle. This should have been one of the first questions to ask because of the high interest of the community in this *observable*. Over the last years, several authors have computed this correlation function using a particular regularization, claiming a regularization independence of the result. Drawing a comparison, it would be like computing a correlation function in a gauge theory without verifying it is gauge independent. Based on the results obtained in [138], we show both in weak and strongly

coupled theories that the OTOC strongly depend on the regularization. For the weak-coupling analysis we use the ϕ^4 bosonic theory, while for the strong coupling limit we focus on the SYK model. We explain why this correlation function depends on the contour and we explain why most of the investigations by other authors have overlooked this. This result gives rise to the question of which of the correlation functions is physically sensible. By using the kinetic theory results of the previous chapters, we show that the only meaningful OTOC is the symmetrical one (separated by half the thermal circle), which corresponds to a gross energy exchange. All the other OTOCs correspond to kinetic equations which give too much weight to either the *gain* or the *loss* terms in the collision integral. This results indeed shows that the only meaningful OTOC (in QFT) is the one for which a bound on the Lyapunov exponent has been proven.

2 Quantum chaos in diluted weakly coupled field theories

For perturbative scalar field theories, the late-time-limit of the out-of-time-ordered correlation function that measures (quantum) chaos is shown to be equal to a Boltzmann-type kinetic equation that measures the total gross (instead of net) particle exchange between phase space cells, weighted by a function of energy. This derivation gives a concrete form to numerous attempts to derive chaotic many-body dynamics from ad hoc kinetic equations. A period of exponential growth in the total gross exchange determines the Lyapunov exponent of the chaotic system. Physically, the exponential growth is a front propagating into an unstable state in phase space. As in conventional Boltzmann transport, which follows from the dynamics of the net particle number density exchange, the kernel of this kinetic integral equation for chaos is also set by the 2-to-2 scattering rate. This provides a mathematically precise statement of the known fact that in dilute weakly coupled gases, transport and scrambling (or ergodicity) are controlled by the same physics.[1]

2.1 Introduction

The weakly interacting dilute gas is one of the pillars of physics. It provides a canonical example for the statistical foundation of thermodynamics and its kinetic description—the Boltzmann equation—allows for a computation of the collective transport properties from collisions of the microscopic constituents. Historically, this provided the breakthrough evidence in favor of the molecular theory of matter. A crucial point in Boltzmann's kinetic theory is the assumption of *molecular chaos* whereby all $n > 2$ quasi-particle correlations are irrelevant due to diluteness and the validity of ensemble averaging, i.e. ergodicity [127, 139–146]. However, finding a precise quantitative probe of this underlying chaotic behavior in many-body systems has been a notoriously difficult problem. In the past,

[1] The contents of this chapter have been published in S. Grozdanov, K. E. Schalm and V. Scopelliti, Phys.Rev. E **99** (2019) no.1, 012206.

phenomenological approaches positing a Boltzmann-like kinetic equation (see e.g. [147]) have reproduced numerically computed properties of chaos, such as the Lyapunov exponents, but a fundamental origin supporting this approach is lacking.

A measure of chaos applicable to both weakly coupled (kinetic) and strongly coupled quantum systems (without quasi-particles) is a period of exponential growth of a thermal out-of-time-ordered correlator (OTOC):

$$C(t) = \theta(t) \langle [\hat{W}(t), \hat{V}(0)]^\dagger [\hat{W}(t), \hat{V}(0)] \rangle_\beta \,, \tag{2.1}$$

where $W(t)$ and $V(0)$ are generic operators and $\beta = 1/T$. For example, choosing $W(t) = q(t)$, $V(0) = p(0) \equiv -i\hbar \frac{\partial}{\partial q(0)}$ one immediately sees that $C(t)$ probes the dependence on initial conditions—and, hence, if this dependence displays exponential growth, chaos. This OTOC was first put forth in studies of quantum electron transport in weakly disordered materials [148–150], which noted that in quantum systems the regime of classical exponential growth cuts off at the so-called Ehrenfest time, and of late, it has been used to detect exponential growth of perturbations characteristic of chaos in strongly coupled quantum systems [12, 15, 16, 151]. This has led in turn to a reconsideration of this OTOC in weakly coupled field theories [136, 152–157]. A strong impetus for this renewed interest has been a possible connection between chaotic behavior and transport, in particular, late-time diffusion (see e.g. recent [66, 128, 158–160]). Many weakly coupled studies have indeed found such a connection. Intuitively, this should not be a surprise. In weakly coupled particle-like theories, chaotic short-time behavior is clearly set by successive uncorrelated 2-to-2 scatterings, but the dilute molecular chaos assumption in Boltzmann's kinetic theory shows that 2-to-2 scattering also determines the late-time diffusive transport coefficients. A mathematically precise relation, however, between chaos and transport in dilute perturbative systems did not exist.

In this chapter, we will provide this relation. We will show that a direct analogue of the conventional Boltzmann transport equation, but where one traces the total gross exchange between phase space cells weighted by an energy factor, rather than net particle number density, computes the late-time behavior of chaos in terms of the exponential growth of the OTOC of a bosonic system before the Ehrenfest time. The resemblance between the OTOC computation and kinetic equations was already noted in [152], although with a different interpretation. Our result is explicit in the physical meaning of the kinetic equation for chaos and makes particularly clear the relation between chaos and transport in dilute weakly coupled theories, as the kernel in both cases is the 2-to-2 scattering cross-section,

even though transport is a relaxational process and chaos an exponentially divergent one. This OTOC-derived gross exchange equation shares many of the salient features of the earlier postulated chaos-determining kinetic equations [147, 161], explaining post facto why they obtained the correct result.

2.2 Boltzmann transport and chaos from a gross energy exchange kinetic equation

To exhibit the essence of the statement that chaos-driven ergodicity follows from a gross exchange equation analogous to the Boltzmann equation, we first construct this equation from first principles and show how it captures the exponential growth of microscopic energy-weighted exchanges due to inter-particle collisions. Then, in the next section, we derive this statement from the late-time limit of the OTOC in perturbative quantum field theory.

Consider the linearized Boltzmann equation for the time dependence of the change of particle number density per unit of phase space: $\delta n(t,\mathbf{p}) = n(t,\mathbf{p}) - n(E_{\mathbf{p}})$, where $n(\mathbf{p})$ is the equilibrium Bose-Einstein distribution $n(\mathbf{p}) = 1/(e^{\beta E(\mathbf{p})} - 1)$ that depends on the energy $E(\mathbf{p})$.[2] In terms of the one-particle distribution function, $f(t,\mathbf{p}) = \frac{\delta n(t,\mathbf{p})}{n(\mathbf{p})(1+n(\mathbf{p}))}$, the linearized Boltzmann equation is a homogeneous evolution equation for $f(t,\mathbf{p})$ (see e.g. [162–164]):[3]

$$\partial_t f(t,\mathbf{p}) = -\int_{\mathbf{l}} \mathcal{L}(\mathbf{p},\mathbf{l}) f(t,\mathbf{l}), \tag{2.2}$$

where the kernel of the collision integral

$$\mathcal{L}(\mathbf{p},\mathbf{l}) \equiv -\left[R^{\wedge}(\mathbf{p},\mathbf{l}) - R^{\vee}(\mathbf{p},\mathbf{l})\right] \tag{2.3}$$

measures the difference between the rates of scattering into the phase-space cell and scattering out the phase space cell. The factor

$$R^{\wedge}(\mathbf{p},\mathbf{l}) = \frac{1}{n(\mathbf{p})(1+n(\mathbf{p}))} \int_{\mathbf{p}_2,\mathbf{p}_3,\mathbf{p}_4} d\Sigma(\mathbf{p},\mathbf{p}_2|\mathbf{p}_3,\mathbf{p}_4) \times \left(\delta(\mathbf{p}_3-\mathbf{l}) + \delta(\mathbf{p}_4-\mathbf{l})\right), \tag{2.4}$$

[2] For simplicity, we assume spatial homogeneity of the gas with the energy $E(\mathbf{p})$ and think of all quantities as averaged over space, e.g. $n(t,\mathbf{p}) = \int d\mathbf{x}\, n(t,\mathbf{x},\mathbf{p})$.

[3] In relativistic theories $\int_{\mathbf{p}} \equiv \int \frac{d^3p}{(2\pi)^3} \frac{1}{2E(\mathbf{p})}$ and $\int_p \equiv \int \frac{d^4p}{(2\pi)^4}$. For a non-relativistic system, $\int_{\mathbf{p}} \equiv \int \frac{d^3p}{(2\pi)^3}$, and similarly, $\int_{\mathbf{x}} \equiv \int d^3x$ and $\int_x \equiv \int d^4x$.

counts increases of the local density by one unit. The factor

$$R^{\vee}(\mathbf{p},\mathbf{l}) = \frac{1}{n(\mathbf{p})(1+n(\mathbf{p}))} \int\limits_{\mathbf{p}_2,\mathbf{p}_3,\mathbf{p}_4} d\Sigma(\mathbf{p},\mathbf{p}_2|\mathbf{p}_3,\mathbf{p}_4) \times \left(\delta(\mathbf{p}-\mathbf{l}) + \delta(\mathbf{p}_2-\mathbf{l})\right), \tag{2.5}$$

counts decreases of the number density by one unit. Here,

$$\begin{aligned} d\Sigma(\mathbf{p},\mathbf{p}_2|\mathbf{p}_3,\mathbf{p}_4) = n(\mathbf{p})\, n(\mathbf{p}_2)\, \frac{1}{2} |\mathcal{T}_{pp_2\to p_3p_4}|^2 \\ \times (1+n(\mathbf{p}_3))(1+n(\mathbf{p}_4)) \\ \times (2\pi)^4 \delta^4(p+p_2-p_3-p_4) \end{aligned} \tag{2.6}$$

with $|\mathcal{T}_{pp_2\to p_3p_4}|^2$ the transition amplitude squared. By defining an inner product

$$\langle\phi|\psi\rangle = \int_{\mathbf{p}} n(\mathbf{p})(1+n(\mathbf{p}))\phi^*(\mathbf{p})\psi(\mathbf{p})\,, \tag{2.7}$$

one can use the symmetries of the cross-section $d\Sigma(\mathbf{p}_1,\mathbf{p}_2|\mathbf{p}_3,\mathbf{p}_4) = d\Sigma(\mathbf{p}_2,\mathbf{p}_1|\mathbf{p}_3,\mathbf{p}_4) = d\Sigma(\mathbf{p}_3,\mathbf{p}_4|\mathbf{p}_1,\mathbf{p}_2) = d\Sigma(\mathbf{p}_1,\mathbf{p}_2|\mathbf{p}_4,\mathbf{p}_3)$ to show that the operator $\mathcal{L}(\mathbf{p},\mathbf{l})$ is not only Hermitian on this inner product, but also positive semidefinite—all its eigenvalues are real and $\xi_n \geq 0$. Hence, the solutions to the Boltzmann equation are purely relaxational:

$$f(\mathbf{p},t) = \sum_n A_n e^{-\xi_n t}\phi_n(\mathbf{p}), \tag{2.8}$$

where $\sum_n$ formally stands for either a sum over discrete values or an integral over a continuum (see e.g. [162–165]). Moreover, every $\xi = 0$ eigenvalue is associated with a symmetry and has an associated conserved quantity—a collisional invariant.

Let us instead trace the total gross exchange, rather than the net flux, by changing the sign of the outflow $R^{\vee}(\mathbf{p},\mathbf{l})$ in the kernel of the integral $\mathcal{L}(\mathbf{p},\mathbf{l})$. A distribution function that follows from Eq. (5.4) with the kernel $\mathcal{L}_{\text{total}}(\mathbf{p},\mathbf{l}) = -\left[R^{\wedge}(\mathbf{p},\mathbf{l}) + R^{\vee}(\mathbf{p},\mathbf{l})\right]$ counts additively the total in- and out-flow of particles from a number density inside a unit of phase space. However, this over-counts because the loss rate $R^{\vee}(\mathbf{p},\mathbf{l})$ consists of a drag (self-energy) term, $2\Gamma_{\mathbf{p}}$, caused by the thermal environment — the term proportional to $\delta(\mathbf{p}-\mathbf{l})$ in Eq. (3.57) — in addition to a true loss rate term, $R^{\vee_T}(\mathbf{p},\mathbf{l}) = R^{\vee}(\mathbf{p},\mathbf{l}) - 2\Gamma_{\mathbf{p}}\delta(\mathbf{p}-\mathbf{l})$. Only $R^{\vee_T}$ changes the number of particles in $f(t,\mathbf{p})$ due to deviations coming from $f(t,\mathbf{p}\neq\mathbf{l})$.

Accounting for this, and changing only the sign of the true outflow, we arrive at a gross exchange equation

$$\partial_t f_{\text{gross}}(t,\mathbf{p}) = \int_{\mathbf{l}} \left[R^{\wedge}(\mathbf{p},\mathbf{l}) + R^{\vee}(\mathbf{p},\mathbf{l}) - 4\Gamma_{\mathbf{p}}\delta(\mathbf{p}-\mathbf{l})\right] f_{\text{gross}}(t,\mathbf{l})\,. \tag{2.9}$$

The central result of this chapter is that tracking the time-evolution of this gross exchange—weighted additionally by an odd function $\mathcal{E}(E)$ of the energy E to be specified below—is a microscopic kinetic measure of chaos (or scrambling). It is thus quantified by the distribution $f_{EX} \equiv \mathcal{E}(E) f_{\text{gross}}$ and governed by

$$\partial_t f_{EX}(t,\mathbf{p}) = \int_{\mathbf{l}} \frac{\mathcal{E}[E_{\mathbf{p}}]}{\mathcal{E}[E_{\mathbf{l}}]} \left[R^{\wedge}(\mathbf{p},\mathbf{l}) + R^{\vee}(\mathbf{p},\mathbf{l}) - 4\Gamma_{\mathbf{p}}\delta(\mathbf{p}-\mathbf{l})\right] f_{EX}(t,\mathbf{l})\,. \tag{2.10}$$

Specifically, Eq. (2.10) can be derived from the late-time behavior of the OTOC of local field operators in perturbative relativistic scalar quantum field theories. The OTOC selects a specific functional $\mathcal{E}(E)$, such that in the limit of high temperature, $\mathcal{E}(E) \to 1/E$. The distribution f_{EX} can grow exponentially and indefinitely because the Hermitian operator

$$\mathcal{L}_{EX}(\mathbf{p},\mathbf{l}) = -\frac{E_{\mathbf{l}}}{E_{\mathbf{p}}}\left(R^{\wedge}(\mathbf{p},\mathbf{l}) + R^{\vee}(\mathbf{p},\mathbf{l}) - 4\Gamma_{\mathbf{p}}\delta(\mathbf{p}-\mathbf{l})\right) \tag{2.11}$$

is no longer positive semi-definite. It permits a set of negative eigenvalues, $\xi_m < 0$, which characterize the exponential growth in the amount of gross energy exchanged inside the system. This exponential evolution persists to $t \to \infty$ [156], so ξ_m specify a subset of all Lyapunov exponents λ_L of the many-body system, with $\lambda_{L,m} = -\xi_m$ by definition. Finally, since choosing a different odd $\mathcal{E}(E)$ results in a similarity transformation of the kernel, the spectrum of f_{OTOC} equals the spectrum of f_{EX}.

The above construction tremendously simplifies the computation of the Lyapunov exponents for weakly interacting dilute systems. Beyond providing a physically intuitive picture of chaos, it reduces the calculation of Lyapunov exponents to a calculation of $|\mathcal{T}_{pp_2\to p_3p_4}|^2$, which is entirely determined by particle scattering. For example, in a theory of $N \times N$ Hermitian massive scalars Φ_{ab},

$$\mathcal{L} = \text{tr}\left(\frac{1}{2}\left(\partial_t\Phi\right)^2 - \frac{1}{2}(\nabla\Phi)^2 - \frac{m^2}{2}\Phi^2 - \frac{1}{4!}g^2\Phi^4\right), \tag{2.12}$$

for which the transition probability appropriately traced over external states equals

$$|\mathcal{T}_{12\to 34}|^2 = \frac{1}{6} g^4 \left(N^2+5\right). \tag{2.13}$$

Eq. (2.10) directly computes the Lyapunov exponents (see Fig. 2.1). In the $\beta \to 0$ limit, the leading exponent becomes

$$\lambda_L \simeq \frac{0.025 T^2}{48m} \frac{1}{2} |\mathcal{T}_{12\to 34}|^2 \simeq \frac{0.025}{4} \frac{g^4 (N^2+5) T^2}{144m}. \tag{2.14}$$

In the large N limit, Eq. (5.47) recovers the explicit OTOC result of [152] after correcting a factor of a 1/4 miscount (see Appendix 2.A).

2.3 A derivation of the gross exchange kinetic equation from the OTOC

To set the stage, we first show how the linearized Boltzmann equation (5.4) arises in quantum field theory, using the theory in Eq. (2.12) as an example. The derivation is closely related to the Kadanoff-Baym quantum kinetic equations [144, 166]. It builds on similar derivations in [101, 126, 167]. A complementary approach to the derivation here, which is closer in spirit to the Kadanoff–Baym derivation, but makes the physics less transparent, is the generalized OTOC contour quantum kinetic equation of [153].

The one-particle distribution function $f(t, \mathbf{x}, \mathbf{p})$ follows from the Wigner transform of the bilocal operator

$$\begin{aligned} \rho(x,p) &= \int_y e^{-ip\cdot y} \operatorname{Tr}\left[\Phi(x+y/2)\Phi(x-y/2)\right] \\ &= \int_k e^{ikx} \operatorname{Tr}\left[\Phi(p+k/2)\Phi(p-k/2)\right]. \end{aligned} \tag{2.15}$$

When the momentum is taken to be on shell, the Wigner function $\rho(x,p)$ becomes proportional to the relativistic one-particle operator-valued distribution function $\rho(x, \mathbf{p}, E_{\mathbf{p}}) = n(x, \mathbf{p})$ [144]. The expectation value of the scalar density is then $\langle \rho \rangle_\beta$.

We now consider the linearized Boltzmann equation as a dynamical equation for fluctuations $\delta\rho(x,p) = n(\mathbf{p})(1+n(\mathbf{p}))f(x,p)$ in the bilocal density operator:

$$\left[\partial_{x^0} \delta(x-y)\delta(p-q) + \mathcal{L}(x,p|y,q)\right] \delta\rho(y,q) = 0. \tag{2.16}$$

If the fluctuations are small, and the assumption of molecular chaos holds, the central limit theorem implies that the two point function of the fluctuations in the bilocal density is the Green's function for the linearized Boltzmann operator

$$\begin{aligned} iG_R^{\rho\rho}(x,p|y,q) &= \theta(x^0-y^0)\langle[\delta\rho(x,p),\delta\rho(y,q)]\rangle \\ &= \left[\partial_{x^0}\delta(x-y)\delta(p-q)+\mathcal{L}(x,p|y,q)\right]^{-1}. \end{aligned} \tag{2.17}$$

Because the linearized Boltzmann equation is causal and purely relaxational, the two-point function in (5.80) is retarded. This implies that it is possible to extract the collision integral of the linearized Boltzmann equation directly from the analytic structure of the retarded Green's function $G_R^{\rho\rho}(x,p|y,q)$. As a result, the eigenvalues of the Boltzmann equation ξ_n are also the locations of the poles of $G_R^{\rho\rho}$. This establishes a direct connection between weakly coupled quantum field theory and quantum kinetic theory. From the definition of $\rho(k,p)$, Eq. (5.80) can be expressed in terms of the connected[4] Schwinger-Keldysh (SK) four-point functions (see Ref. [168]) of the microscopic fields $G_R^{\rho\rho}(k,p;\ell,q) = -G_{1111}^{\Phi^2\Phi^2} + G_{1122}^{\Phi^2\Phi^2}$, where

$$\begin{aligned} G_{1122}^{\Phi^2\Phi^2} &= i\,\langle \mathrm{Tr}\,[\Phi_1(p+k/2)\Phi_1(-p+k/2)] \\ &\quad\times\ \mathrm{Tr}\,[\Phi_2(q+\ell/2)\Phi_2(-q+\ell/2)]\rangle_{SK}\,, \end{aligned} \tag{2.18}$$

and similarly for $G_{1111}^{\Phi^2\Phi^2}$. Here, $\Phi_{1,2}$ denote the doubled fields on the forward and backward contours of the SK path integral, respectively. In translationally invariant systems, $\ell = -k$. It is convenient to introduce the Keldysh basis, $\Phi_a = \Phi_1 - \Phi_2$ and $\Phi_r = \frac{1}{2}(\Phi_1+\Phi_2)$. Then $G_R^{\rho\rho}$ is a linear combination of 16 four-point functions $G_{\alpha_1\alpha_2\alpha_3\alpha_4} = i2^{n_{r_{\alpha_i}}}\langle\Phi_{\alpha_1}\Phi_{\alpha_2}\Phi_{\alpha_3}\Phi_{\alpha_4}\rangle$ with $\alpha_i = \{a,r\}$ and $n_{r_{\alpha_i}}$ counting the number of α_i indices equal to r. In the limit of small frequency and momenta, $\omega \equiv k^0 \to 0$ and $\mathbf{k}\to 0$, however, it is only a single one of these four-point functions that contributes to the final expression [133, 168, 169]:

$$\begin{aligned} \lim_{k\to 0} G_R^{\rho\rho}(p,q|k) &= -\lim_{k\to 0}\frac{\beta k^0}{2}\mathcal{N}(p^0)G^*_{aarr}(p,q|k) \\ &= -\lim_{k\to 0}\frac{\beta k^0}{4}\mathcal{N}(p^0)\mathcal{N}(q^0)\,\langle f(p,k)f(q,-k)\rangle\,, \end{aligned} \tag{2.19}$$

where $\mathcal{N}(p^0) = n(p^0)\left(1+n(p^0)\right)$. The exact four-point function $G^*_{aarr}(p,q|k)$ obeys a system of Bethe-Salpeter equations (BSEs) that nevertheless still

[4] The disconnected part gives a product of the equilibrium one-point functions $\langle\rho\rangle_\beta$.

couples all 16 $G_{\alpha_1\alpha_2\alpha_3\alpha_4}$. However, it turns out that in the limit of small ω and $\mathbf{k}$, G^*_{aarr} decouples and is governed by a single BSE [133, 168]:

$$G^*_{aarr}(p,q|k) = \Delta_{ra}(p+k)\Delta_{ar}(p)\Big[i(2\pi)^4\delta^4(p-q)N^2 - \int_l R^{\text{transp}}(p,l)G^*_{aarr}(l,q|k)\Big], \tag{2.20}$$

where $\Delta_{\alpha_1\alpha_2} = -i\,2^{n_{r\alpha_i}}\langle\Phi_{\alpha_1}\Phi_{\alpha_2}\rangle$ is the Schwinger-Keldysh two-point function and $R^{\text{transp}}(p,\ell) = d\Sigma_{p\to l}/\mathcal{N}(p^0)$, with $d\Sigma_{p\to l}$ the transition probability of an off-shell particle with energy-momentum $(p^0,\mathbf{p})$ scattering of the thermal bath to an off-shell particle with energy-momentum $(l^0,\mathbf{l})$.[5] Defining $G^*_{aarr}(p|k) = \int_q G^*_{aarr}(p,q|k)$, Eq. (2.20) reduces to

$$G^*_{aarr}(p|k) = \Delta_{ra}(p+k)\Delta_{ar}(p)\Big[iN^2 - \int_l R^{\text{transp}}(p,l)G^*_{aarr}(l|k)\Big]. \tag{2.21}$$

The product $\Delta_{ra}(p+k)\Delta_{ar}(p)$ has four poles with imaginary parts $\pm i\Gamma_{\mathbf{p}}$. However, as $k\to 0$, only a contribution from two poles remains. This pinching pole approximation, ubiquitous in the study of hydrodynamic transport coefficients and spectra of finite temperature quantum field theories [101, 168], gives

$$G^*_{aarr}(p|k) = \frac{\pi}{E_{\mathbf{p}}}\frac{\delta(p_0^2-E_{\mathbf{p}}^2)}{-i\omega+2\Gamma_{\mathbf{p}}}\Big[iN^2 - \int_l R^{\text{transp}}(p,l)G^*_{aarr}(l|k)\Big]. \tag{2.22}$$

To find the solution of the integral equation (2.22), we make the ansatz whereby $G^*_{aarr}(p|k)$ is supported on-shell:

$$G^*_{aarr}(p|k) = \delta(p_0^2-E_{\mathbf{p}}^2)G^{ff}(\mathbf{p}|k). \tag{2.23}$$

Hence,

$$(-i\omega+2\Gamma_{\mathbf{p}})G^{ff}(\mathbf{p}|k) = \frac{i\pi N^2}{E_{\mathbf{p}}} - \int_{\mathbf{l}}\frac{1}{2E_{\mathbf{p}}} \times\left[R^{\text{transp}}(\mathbf{p},E_{\mathbf{p}}|\ell,E_\ell) + R^{\text{transp}}(\mathbf{p},E_{\mathbf{p}}|\ell,-E_\ell)\right]G^{ff}(\mathbf{l}|k)\,. \tag{2.24}$$

[5] $R^{\text{transp}}(p,\ell) = -\frac{\sinh(\beta p^0/2)}{\sinh(\beta\ell^0/2)}R(l-p)$ where $R(l-p)$ is the rung function computed in [152]. Note that the $R(l-p)$ in [152] is not the same as $R^\wedge$ or $R^\vee$ used here.

It can be shown that [6]

$$\frac{1}{2E_{\mathbf{p}}} R^{\text{transp}}(\mathbf{p}, E_{\mathbf{p}}|\ell, E_\ell) = -R^{\wedge}(\mathbf{p}, \mathbf{l}) \tag{2.25}$$

and [101, 133, 168]

$$\frac{1}{2E_{\mathbf{p}}} R^{\text{transp}}(\mathbf{p}, E_{\mathbf{p}}|\mathbf{l}, -E_{\mathbf{l}}) = R^{\vee}(\mathbf{p}, \mathbf{l}) - 2\Gamma_{\mathbf{p}}\delta(\mathbf{p}-\mathbf{l})\,. \tag{2.26}$$

Thus, Eq. (2.24) is solved by

$$G^{ff}(\mathbf{p}|k) = \frac{i\pi N^2}{E_{\mathbf{p}}} \frac{1}{-i\omega - \int_{\mathbf{l}} [R^{\wedge}(\mathbf{p}, \mathbf{k}) - R^{\vee}(\mathbf{p}, \mathbf{k})]}\,. \tag{2.27}$$

Hence, the spectrum of $G^{ff}(\mathbf{p}|k^0 = \omega, \mathbf{k} = 0)$ equals the spectrum of the one-particle distribution $f(t, \mathbf{p})$ determined by the linearized Boltzmann equation (5.4).

The derivation of the kinetic equation (2.10) for quantum chaos from the OTOC now follows from an analogous line of arguments. The OTOC,

$$\begin{aligned} C(t) = &- i \int_k e^{-ikt} \int_{p,q} \Big\langle [\Phi_{ab}(p+k), \Phi^\dagger_{a'b'}(-q-k)] \\ &\times [\Phi^\dagger_{ab}(-p), \Phi_{a'b'}(q)] \Big\rangle\,, \end{aligned} \tag{2.28}$$

is a four-point function, which, as shown in [152], also obeys a BSE in the limit of $\omega \to 0$. Indicating with $\mathcal{G}_{OTOC}(p, q|k, p+q-k)$ the term inside the integrals in Eq. (5.79), i.e. $C(t) \equiv \int_k e^{-ikt} \int_{p,q} \mathcal{G}_{OTOC}(p, q|k, p+q-k)$, we define

$$\widetilde{\mathcal{G}}(p|k) = \int_q \mathcal{G}_{OTOC}(p, q|k, p+q-k)\,. \tag{2.29}$$

The correlator $\widetilde{\mathcal{G}}(p|k)$ then obeys the following integral equation:

$$\begin{aligned} \widetilde{\mathcal{G}}(p|k) = \frac{\pi}{E_{\mathbf{p}}} \frac{\delta(p_0^2 - E_{\mathbf{p}}^2)}{-i\omega + 2\Gamma_{\mathbf{p}}} \Big[& iN^2 \\ & - \int \frac{d^4\ell}{(2\pi)^4} \frac{\sinh(\beta\ell_0/2)}{\sinh(\beta p_0/2)} R^{\text{transp}} \widetilde{\mathcal{G}}(\ell|k) \Big]. \end{aligned} \tag{2.30}$$

[6] See Appendix 3.G in next chapter.

Eq. (2.30) agrees with the result found in [152], even though it is expressed here with different notation. The advantage of writing $\widetilde{\mathcal{G}}(p|k)$ as in (2.30) is that it makes transparent the similarities between $\widetilde{\mathcal{G}}(p|k)$ and $G^*_{aarr}(p|k)$ from Eq. (2.22), which governs transport. A priori, there is no reason to expect $\widetilde{\mathcal{G}}(p|k)$ and $G^*_{aarr}(p|k)$ to be related. Nevertheless, by comparing (2.22) with (2.30), it is clear that in this calculation, the only difference between the two BSE equations is the factor $\frac{\sinh(\beta\ell_0/2)}{\sinh(\beta p_0/2)}$ appearing in the measure of the kernel of (2.30). As we will see in Section 2.4, this factor is crucial for the fact that, while related, the spectra of $G^*_{aarr}(p|k)$ and $\widetilde{\mathcal{G}}(p|k)$ are distinct: the spectrum of $G^*_{aarr}(p|k)$ only possesses relaxational modes while $\widetilde{\mathcal{G}}(p|k)$ exhibits exponentially growing modes which can be associated with many-body quantum chaos.

To find a solution of Eq. (2.30), as in the case of Eq. (2.22), we again introduce an on-shell ansatz $\widetilde{\mathcal{G}}(p|k) = \delta(p_0^2 - E_{\mathbf{p}}^2)G^{\mathrm{ff}}(\mathbf{p}|k)$. This gives

$$(-i\omega + 2\Gamma_{\mathbf{p}})G^{\mathrm{ff}}(\mathbf{p}|k) = \frac{i\pi N^2}{E_{\mathbf{p}}} - \int_{\mathbf{l}} \frac{\sinh(\beta E_{\mathbf{l}}/2)}{\sinh(\beta E_{\mathbf{p}}/2)} \frac{1}{2E_{\mathbf{p}}} \times \left(R^{\mathrm{transp}}(\mathbf{p}, E_{\mathbf{p}}|\mathbf{l}, E_{\mathbf{l}}) - R^{\mathrm{transp}}(\mathbf{p}, E_{\mathbf{p}}|\mathbf{l}, -E_{\mathbf{l}})\right) G^{\mathrm{ff}}(\mathbf{l}|k), \tag{2.31}$$

where one of the signs in front of $\mathcal{K}$ is now reversed due to the fact that factor $\frac{\sinh(\beta\ell_0/2)}{\sinh(\beta p_0/2)}$ in the measure is an odd function of energy. Thus, the spectrum of $G^{\mathrm{ff}}(\mathbf{l}|k)$, and hence, of the OTOC, equals the spectrum of the following kinetic equation

$$\partial_t f_{OTOC}(t, \mathbf{p}) = \int_{\mathbf{l}} \frac{\sinh(\beta E_{\mathbf{l}}/2)}{\sinh(\beta E_{\mathbf{p}}/2)} \times \left[R^{\wedge}(\mathbf{p}, \mathbf{l}) + R^{\vee}(\mathbf{p}, \mathbf{l}) - 4\Gamma_{\mathbf{p}}\delta(\mathbf{p} - \mathbf{l})\right] f_{OTOC}(t, \mathbf{l}), \tag{2.32}$$

which precisely matches with the kinetic equation for the OTOC put forward in Eq. (2.10), with $\mathcal{E}(E_{\mathbf{p}}) = 1/\sinh(\beta E_{\mathbf{p}}/2)$, or $\lim_{\beta\to 0} \mathcal{E}(E_{\mathbf{p}})/\mathcal{E}(E_{\mathbf{l}}) = E_{\mathbf{l}}/E_{\mathbf{p}}$. As noted there, this spectrum of Eq. (2.10) is in fact independent of $\mathcal{E}(E)$ as long as the function $\mathcal{E}$ is odd.

2.4 Results and discussion

In addition to greatly simplifying the computation of chaotic behavior in dilute weakly interacting systems and providing a physical picture for the meaning of many-body chaos, the gross energy exchange kinetic equation recasting of the OTOC makes it conspicuously clear how in such

systems scrambling (or ergodicity) and transport are governed by the same physics [128]. The kernel of the kinetic equation in both cases is the 2-to-2 scattering cross-section. Nevertheless, the equations for f_{OTOC}, or equivalently, f_{EX}, and f are subtly different, which allows for the crucial qualitative difference: a chaotic, Lyapunov-type divergent growth of f_{EX} versus damped relaxation of f. Their spectra at $\mathbf{k} = 0$ and small ω are presented in Figure 2.1. As already noted below Eq. (2.30), the two *off-shell* late-time BSEs (2.22) and (2.30) are the same upon performing the following identification:

$$\widetilde{\mathcal{G}}(p|k) = G^{*}_{aarr}(p|k)/\sinh(\beta p^0/2). \tag{2.33}$$

The most general solution to this BSE thus includes the information about chaos and transport. However, the divergent modes (in time) of the OTOC are projected out by the on-shell condition and thus do not contribute to the correlators that compute transport. For example, the shear viscosity η can be inferred from the following retarded correlator (see e.g. [101]):

$$\langle T^{xy}(k), T^{xy}(-k)\rangle_R = \int_{p,q} p_x p_y q_x q_y \, G_R^{\rho\rho}(k|p,q)\,, \tag{2.34}$$

where $k = (\omega, 0, 0, k_z)$. The integrals over p and q, together with the on-shell condition, project out the odd modes in p^0 which govern chaos, and transport is only sensitive to the even, stable modes [170].

The fact that, when off shell, the BSEs (2.22) and (2.30) can be mapped onto each other is by itself a highly non-trivial result which opens several questions. In particular, this observation seems to indicate that in some cases, the information about scrambling and ergodicity, which has so far been believed to be accessible only by studying a modified, extended SK contour and OTOCs, can instead be addressed by a suitable analysis of the analytic properties of correlation functions on the standard SK contour. How our result implies such new analytical properties, remains to be discovered. We remark, however, that studies in (holographic) strongly coupled theories uncovered precisely this type of a relation between hydrodynamic transport at an analytically continued imaginary momentum and chaos. In particular, as we discovered in [128], chaos is encoded in a vanishing residue ("pole-skipping") of the retarded energy density two-point function, which tightly constrains the behavior of the dispersion relation of longitudinal (sound) hydrodynamic excitations. The same imprint of chaos on properties of transport was later also observed in a proposed effective (hydrodynamic) field theory of chaos [56]. Despite the fact that it is at present unknown how general pole-skipping is and whether

other related analytic signatures of chaos in observables that characterize transport exist, it may be possible that properties of many-body quantum chaos in dilute weakly coupled theories are also uncoverable from transport, as in strongly coupled theories [128]. We defer these questions to future works.

The kinetic equation for many-body chaos, that we have derived here, also gives concrete form to past attempts to do so, which were based on a phenomenological ansatz that one should count additively the number of collisions [147, 161]. In essence, that is also what our gross exchange equation does. The exponential divergence can thus be understood as a front propagation into unstable states [172]. This analogy was already noted in [153] who derived a kinetic equation for chaos from the Dyson equation for the 4×4 matrix of the four-contour SK Green's functions. By our arguments above that relate the poles of the OTOC to a dynamical equation for f_{OTOC}, the resulting equations in [153] should contain a decoupled subsector that is equivalent to the kinetic equation derived here.

Finally, we wish to note that the small parameter that sets the Ehrenfest time and controls the regime of exponential growth in the OTOC in all these systems is the perturbative small 't Hooft coupling $\lambda = g^2 N$. The BSE from which the kinetic equation is derived is formally equivalent to a differential equation of the type

$$\left(\frac{d}{dt} - g^4 N^2 L \right) f = N^2 \,. \tag{2.35}$$

This is solved by

$$f = -\frac{1}{g^4 L} + c_0 \, e^{g^4 N^2 L t} . \tag{2.36}$$

The Ehrenfest (or scrambling) time, where the exponential becomes of order of the constant term, is therefore

$$t_{scr} = \frac{1}{g^4 N^2 L} \ln(1/g^4 L c_0) . \tag{2.37}$$

For small g^2, this can be an appreciable timescale for any value of N, and there is no need for a large N number of species.

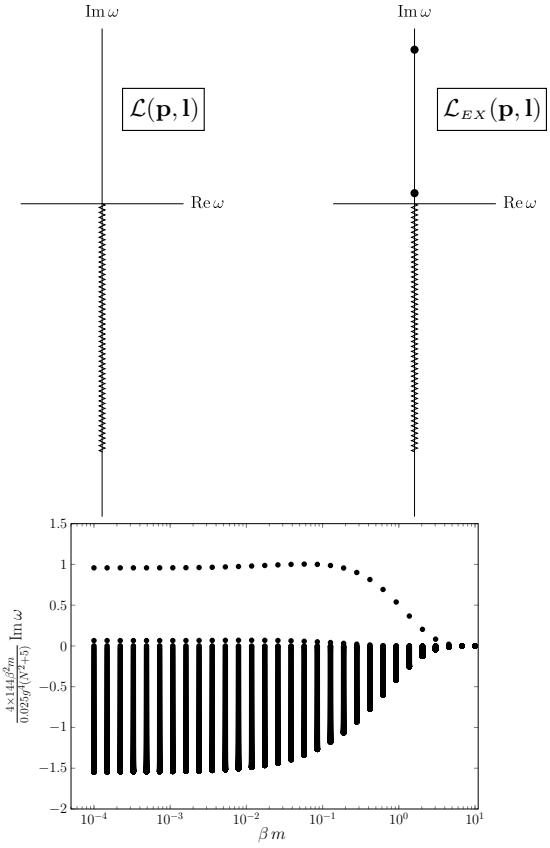

Figure 2.1: The spectra of the kernel $\mathcal{L}(\mathbf{p},\mathbf{l})$ for the linearized Boltzmann equation (and also of $\langle T^{xy}(k_z), T^{xy}(-k_z)\rangle_R$, cf. Eq. (2.34)) (top left) and of the kernel $\mathcal{L}_{EX}(\mathbf{p},\mathbf{l})$ for the kinetic equation for the OTOC (top right) are plotted over the complex ω plane and in the limit of $\beta m \to 0$. In the lower half of the complex ω plane, there is a dense sequence of numerically obtained poles. In both spectra, these poles are believed to be the signature of a branch cut. See [170] and also [121, 122, 165, 171]. In the upper half of the complex ω plane, only the kernel $\mathcal{L}_{EX}(\mathbf{p},\mathbf{l})$ has distinct poles which are identified with the Lyapunov exponents, as explained below equation (2.11). The dependence of these two Lyapunov exponents and the branch cuts on βm is depicted in the inlay (bottom). For large values of βm, the Lyapunov exponents decay exponentially. The plots are obtained by diagonalizing the kernels of the integral equations (2.20) and (2.32) after a discretization with $N = 1000$ grid points on the domain $p \in [m/N, N \times m]$. The discretization is not uniform. This is done in order for the diagonalization to appropriately account for the contributions of both the soft momenta and collinear momenta $\mathbf{p} \approx \mathbf{l}$, which are not negligible even when both $\mathbf{p}$ and $\mathbf{l}$ are large [101, 133]. The finite size of the branch cuts, i.e. its end point for large $\mathrm{Im}(\omega)$, is related to finite domain of the discretization procedure.

2.A Diagrammatic expansion of $|\mathcal{T}_{12\to34}|^2$ in the theory of $N \times N$ Hermitian matrix scalars

Here, we present the diagrammatic expansion and the relevant combinatorial factors for each of the diagrams that enter into the 2-to-2 transition amplitude $|\mathcal{T}_{12\to34}|$ in the theory of $N \times N$ Hermitian matrix scalars (9). The square of the 2-to-2 transition amplitude, $|\mathcal{T}_{12\to34}|^2$, is the square of the amputated connected four-point function. At lowest non-trivial order:

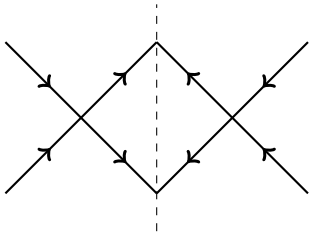

For $N = 1$ the theory is just scalar ϕ^4 theory and the answer is straightforward: $|\mathcal{T}_{12\to34}|^2 = g^4$.

For $N > 1$ theory, the actual amplitude we wish to compute is additionally traced over the external indices, since,

$$C(t) = -i \int_k e^{-ikt} \int_{p,q} \Big\langle [\Phi_{ab}(p+k), \Phi^\dagger_{a'b'}(-q-k)] \times [\Phi^\dagger_{ab}(-p), \Phi_{a'b'}(q)] \Big\rangle \,, \tag{2.38}$$

The way that the matrix indices need to be contracted is across the cut. An easy way to see this from the free non-interacting result: $C(t)_{g^2=0} = G_R^{ab,cd} G_{cd,ab;R}$. Graphically,

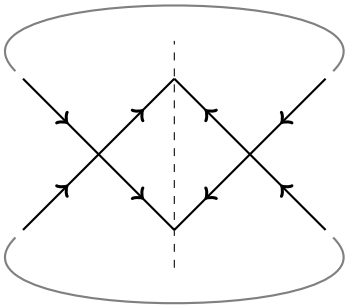

Above the arrows denote momentum-flow. We are interested in the way the weight changes as a function of N.

To find this answer, we use that Hermitian matrices span the adjoint of $U(N)$. Following 't Hooft, one can then use double line notation in terms of fundamental N-"charges". Using this double line notation, the vertex equals.

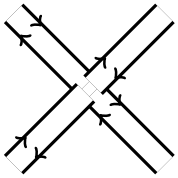

One needs to connect the two vertices across the cut, and then contract, i.e. trace over the external indices, in all possible ways. We will do so step-wise.

Consider first the transition probability. Connecting the first leg across the cut is unambiguous, i.e., each possible choice gives the same answer:

$|\mathcal{T}_{12\to34}|^2 =$ 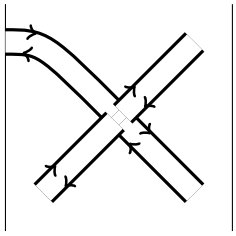

Contracting the next line, however, gives rise to in-equivalent possibilities, each with the same weight w. They are

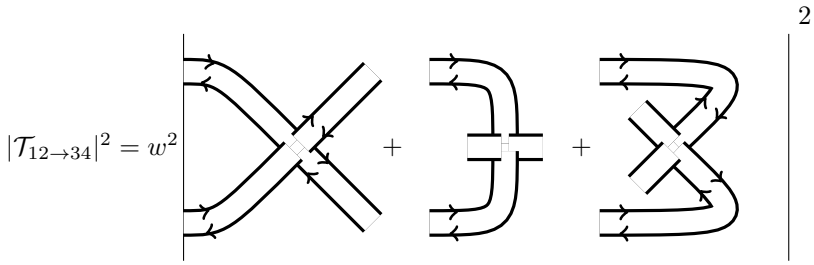

Now, multiplying out the various combinations, each of the six independent combinations can be contracted in two ways over the external indices. As a result, we obtain the following set of twelve independent diagrams.

Diagram 1 with weight N^4 and multiplicity 1:

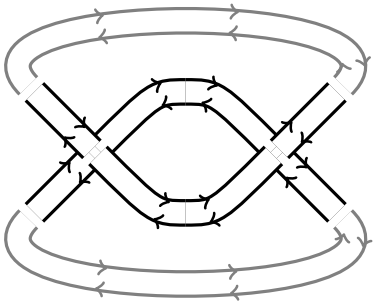

Diagram 2 with weight N^2 and multiplicity 1:

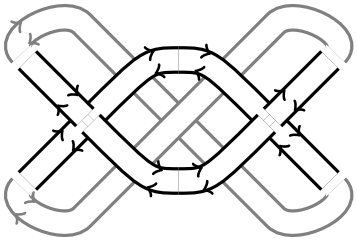

Diagram 3 with weight N^2 and multiplicity 2 (a crossterm diagram):

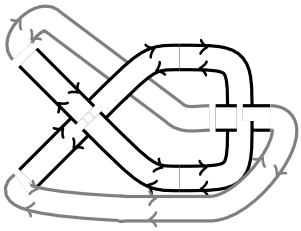

Diagram 4 with weight N^2 and multiplicity 2 (a crossterm diagram). It equals Diagram 3 mirrored across the horizontal axis:

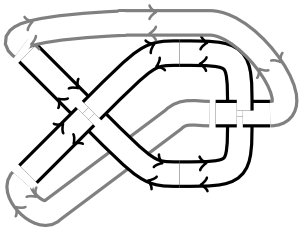

Diagram 5 with weight N^2 and multiplicity 2 (a crossterm diagram):

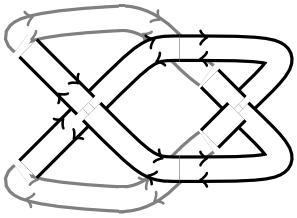

Diagram 6 with weight N^2 and multiplicity 2 (a crossterm diagram):

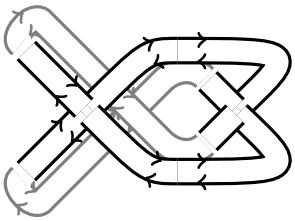

Diagram 7 with weight N^4 and multiplicity 1:

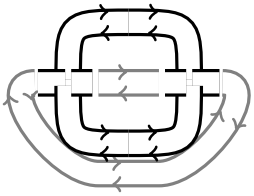

Diagram 8 with weight N^2 and multiplicity 1:

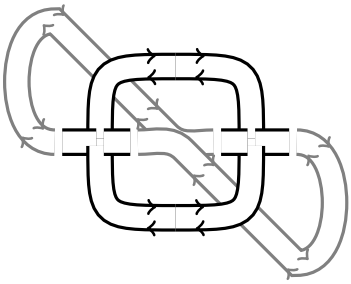

Diagram 9 with weight N^2 and multiplicity 2 (a crossterm diagram):

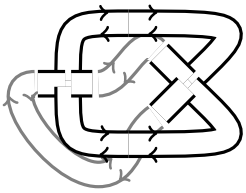

Diagram 10 with weight N^2 and multiplicity 2 (a crossterm diagram). It equals Diagram 9 mirrored across the horizontal axis:

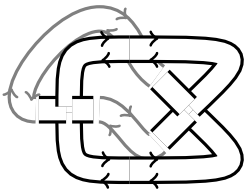

Diagram 11 with weight N^4 and multiplicity 1:

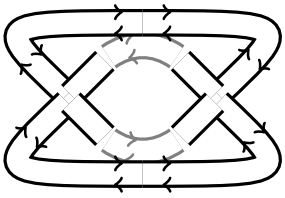

Diagram 12 with weight N^2 and multiplicity 1:

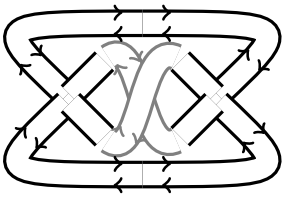

In total, we thus have three diagrams with weights N^4, each with multiplicity 1. Moreover, we have nine diagrams with weights N^2, three of which have multiplicity 1, and six have multiplicity 2. This gives us a total relative weight of

$$\text{weight} = 3N^4 + 15N^2\,. \tag{2.39}$$

The transition probability therefore equals

$$\frac{1}{N^2}\mathrm{Tr}\,|\mathcal{T}_{12\to34}|^2 = w^2(3N^2+15)\,. \tag{2.40}$$

By demanding that this expression reproduces the result for $N=1$ (the theory of a single real scalar field), we find $w^2 = g^4/18$. The total transition probability is therefore

$$\frac{1}{N^2}\mathrm{Tr}\,|\mathcal{T}_{12\to34}|^2 = \frac{g^4}{6}(N^2+5)\,, \tag{2.41}$$

which we used in the kinetic theory prediction, i.e. in Eq. (10), to give us the leading Lyapunov exponent λ_L.

3 Towards the Quantum Critical Point

In weakly coupled or large N QFTs, we show the existence of an analytical relation between the *off-shell* out-of-time ordered correlation function (OTOC) and the correlation function which determines hydrodynamic transport. We explicitly exhibit such relation for a ϕ^4 matrix model and for systems close to a quantum critical point (QCP), respectively the bosonic $O(N)$ vector model and the Gross-Neveu model in $(2+1)$ dimensions. This result opens a new and precise direction to understand how information is scrambled in QFTs and which imprints this leaves on the physics of the long-lived excitations governed by hydrodynamics. A Boltzmann-like interpretation of many-body quantum chaos readily follows from this result, showing that also in the quantum critical regime many-body chaos can be understood as the counting of a gross (energy) exchange.

3.1 Introduction

Traditionally the QBE is obtained from the statistical two-point function [125–127],. The starting point of our results is that it is possible to obtain the linearized QBE in a very clean way from a 4-point function.

This 4-point function must also be resummed; this resummation is expressed in terms of a BSE which, in the spatial homogeneous case and long time limit ($\omega \to 0$), reads

$$-i\omega\, f(\omega,p) = \delta(p_0^2 - E_{\mathbf{p}}^2)\left(1 + \int_l \hat{R}^{\text{transp}}(p,l) f(\omega,l)\right). \tag{3.1}$$

where $f(\omega,p) = \int_q f(\omega,p,q)$. Once on-shell, the kernel $\hat{R}^{\text{transp}}$ reproduces exactly the collision operator $\hat{C}$. All the information about the relaxation times, eventual branch cuts and hydrodynamic and non hydrodynamical modes are intrinsically hidden in $\hat{R}^{\text{transp}}$.

The similarity of this equation with the BSE for chaos,

$$-i\omega\, C(\omega,p) = \delta(p_0^2 - E_{\mathbf{p}}^2)\left(1 + \int_l \hat{R}^{\mathrm{OTOC}}(p,l)C(\omega,l)\right), \tag{3.2}$$

is *not* coincidental. We can now summarize the most important results of this chapter. We show that, for a broad class of theories, ϕ^4 matrix model, (bosonic) vector model in $(2+1)$ dimension and the Gross-Neveu model in $(2+1)$ dimensions (for fermions), the linearised kinetic operator, $\hat{R}^{\mathrm{transp}}(p,l)$, is analytically related to the kernel of the BSE of the OTOC (3.31), $\hat{R}^{\mathrm{OTOC}}(p,l)$, as follows

$$\hat{R}^{\mathrm{OTOC}}(p,l) = \sinh(\beta p_0/2)^{-1}\, \hat{R}^{\mathrm{transp}}(p,l)\sinh(\beta l_0/2) \qquad \text{bosons,} \tag{3.3}$$

$$\hat{R}^{\mathrm{OTOC}}(p,l) = \cosh(\beta p_0/2)^{-1}\, \hat{R}^{\mathrm{transp}}(p,l)\cosh(\beta l_0/2) \qquad \text{fermions.} \tag{3.4}$$

This form in which we wrote (3.3) moreover makes clear that the relation is nothing but a similarity transformation which naively preserves the spectrum and other properties, even though the OTOC should have exponentially growing modes while the QBE only relaxing ones. The correct eigenvalues for either chaos or Boltzmann transport are only obtained after a *projection* out of some eigenvectors.

For the QBE, these precisely project out the growing modes whereas the OTOC contains the complementary spectrum. As our models are sufficiently generic, we are confident to put forward that this holds for all perturbative QFTs.

This is the significant finding we wish to present. Naively, the full physics of scrambling is encoded in $\hat{R}^{\mathrm{OTOC}}(p,l)$ and most of the hydrodynamical transport physics is encoded in $\hat{R}^{\mathrm{transp}}(p,l)$, but in truth they are literally the same. This relation has a profound meaning and should be considered as a starting point for any further attempt to find imprints of ergodicity in the hydrodynamic spectrum. Moreover, as we show in the present chapter, (3.3) not only holds for the ϕ^4 model, but also for models which describe the physics above a QCP, where there are no quasiparticle excitations. Therefore this is a quite general result for weakly coupled systems or systems studied in the large N limit.

Our presentation of the results (3.3) starts in section 3.2, where we show some formal similarities between the out-of-time ordered correlation function and the correlation function which defines transport. Those similarities can be summarized in two fundamental properties:

1 using the real time formalism, with a doubling of fields, by performing

the Keldysh rotation of the fields, only one of the 2^4 correlation functions contributes to the late time limit;

2 the BSE a priori couples all different 2^4 Keldysh components of the correlation function; in the late time limit a single 4-point function decouples and the BSE can be written in closed form.

For the case of transport, those results were shown in a series of papers first by Jeon [101], then in real time formalism by Wang and Heinz [113, 114] and later in the imaginary time formalism by Valle Basagoiti [115]. In section 3.2.2 we prove (1) for the OTOC, and in section 3.2.3 (2). In each case we only do so for $N \times N$ matrix scalar ϕ^4 field theory, but the results clearly extend to the other models.

In section 3.3 we review the derivation of the quantum Boltzmann equation. We summarize what the complementary solution is and argue that this other kinetic equation is a kinetic equation for chaos. In the following sections, we will give the full background for the connection between scrambling and transport. We show how this works for a bosonic $O(N)$ vector model in $2+1$ dimensions and for the Gross-Neveu model in $(2+1)$ dimension, respectively in section 3.4 and 3.5. Moreover we show that the relations (3.3) hold even in the proximity of the QCP. We do this by computing in both systems the BSE for transport and comparing the results with the studies of the OTOC performed in [136, 137].

At the end of sections 3.4 and 3.5 we derive from the BSE the kinetic theory equations both from chaos and transport. We prove that, in both cases, they agree with the kinetic equations for quantum chaos agree stated in section 3.3. Moreover, we show that the OTOC can be obtain from the transport BSE simply by a different choice of boundary conditions (and vice versa).

3.2 Hydrodynamic transport at weak coupling and scrambling: formal similarities

In this section we show some formal similarities ((1) and (2) in the above discussion) between the out-of-time-order correlation function and the late time limit of the density-density correlation functions, which are used to describe transport.

3.2.1 Relevant correlation function for transport in the hydrodynamic regime

The Wigner transform of the scalar density operator

$$\rho(x,p) = \int d^4y e^{-ipy} \phi\left(x + \frac{y}{2}\right) \phi\left(x - \frac{y}{2}\right), \tag{3.5}$$

corresponds to the quantum field theory analogue of the single particle distribution function which appears in the Boltzmann equation. Obviously $\int dp\, \rho(x,p) = \phi^2(x)$. If we write the Fourier transform of (3.5) with respect to the coordinate x, we see that

$$\rho(k,p) = \phi(p + k/2)\phi(-p + k/2). \tag{3.6}$$

Generally, all currents can be constructed out of this bilocal density operator. Consider for instance the contribution $\partial_i\phi\partial_j\phi$ that appears in the spatial components of the stress-energy tensor operator

$$\mathcal{F}[\partial_i\phi\partial_j\phi](k) = \int d^4p\, (p+k)_i\, \phi(p+k)\, p_j\phi(-p); \tag{3.7}$$

this can be written in terms of the Wigner transform defined above,

$$\begin{aligned}\mathcal{F}[\partial_i\phi\partial_j\phi](k) &= \int d^4p\, (p+k)_i\, p_j\, \rho(k, p+k/2) \\ &= \int d^4p\, (p+k/2)_i\, (p-k/2)_j\, \rho(k,p).\end{aligned} \tag{3.8}$$

This shows that, for $i \neq j$ we can express the stress energy tensor as

$$T^{ij}(k) = \int d^4p\, (p+k/2)^i\, (p-k/2)^j\, \rho(k,p). \tag{3.9}$$

In QFT, correlation functions can be obtained as variations of the path integral with respect to external sources. Such variation provides a well defined time ordering. When studying out-of-equilibrium physics, a convenient technique is given by the Schwinger-Keldysh path integral [173–176], which doubles the time branch and involves both time-ordered and anti time-ordered contributions (see Fig. 3.1 for the finite temperature case).

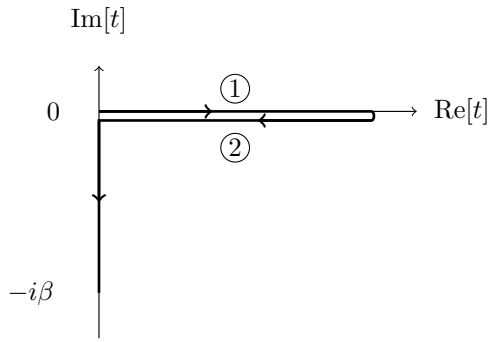

Figure 3.1: The Schwinger-Keldysh time contour includes two real time branches that are respectively labelled as 1 and 2. Correlation functions on this contour are always contour-ordered as shown by the arrows. Operators inserted in the branch 1 are time-ordered, while operators inserted in branch 2 are anti time-ordered.

By construction, the retarded Green's function of the stress energy tensor $G_R^{ij,lm}(x,y)$ is

$$G_R^{ij,lm}(x,y) = G_{11}^{ij,lm}(x,y) - G_{12}^{ij,lm}(x,y), \tag{3.10}$$

where the subscripts $1,2$ label the time branch where the stress-energy tensor is inserted. In Fourier transform, (3.10) is

$$G_R^{ij,lm}(k,-k) = G_{11}^{ij,lm}(k,-k) - G_{12}^{ij,lm}(k,-k). \tag{3.11}$$

We can now easily show that the retarded Green's function of the non-diagonal component of the stress-energy tensor is related to the retarded Green's function of the operator (3.5). By using (3.9), we have

$$\begin{aligned} -iG_R^{ij,lm}(k,-k) &= \langle T_1^{ij}(k) T_1^{lm}(-k)\rangle - \langle T_2^{lm}(-k) T_1^{ij}(k)\rangle \\ &= \int d^4p d^4q \, (p+k/2)_i \, (p-k/2)_j \, (q-k/2)_l \, (q+k/2)_m \\ &\quad \times \left(\langle \rho_1(k,p)\rho_1(-k,q)\rangle - \langle \rho_2(-k,q)\rho_1(k,p)\rangle\right), \end{aligned} \tag{3.12}$$

with $i \neq j$ and $m \neq n$. We remind the reader that the correlation functions are always contour-ordered along the Keldysh contour, this explains the ordering $T_2^{lm}(-k)T_1^{ij}(k)$ in the expectation value. We can recast (3.12) in the more readable form

$$\begin{aligned} G_R^{T^{ij},T^{lm}}(k,-k) = \int d^4p d^4q \, (p+k/2)_i \, (p-k/2)_j \, (q-k/2)_l \, (q+k/2)_m \\ \times \; G_R^{\rho\rho}(k|p,q). \end{aligned}$$

The Kubo formula for shear viscosity involves the correlation functions of the shear channel components of the stress-energy tensor. For this reason, we choose the external momentum in the z direction, $k = (k_0, 0, 0, k_z)$, and $i = l = x$ and $j = m = y$

$$G_R^{ij,lm}(k,-k) = \int d^4p d^4q \, p_x p_y q_x q_y \, G_R^{\rho\rho}(k|p,q). \tag{3.13}$$

By definition (indicating with $\mathcal{T}_{SK}$ the contour ordering)

$$\begin{aligned} iG_R^{\rho\rho}(k|p,q) &= \langle \mathcal{T}_{SK}\,[\phi_1(p+k)\phi_1(-p)\phi_1(-q-k)\phi_1(q)]\rangle \\ &\quad - \langle \mathcal{T}_{SK}\,[\phi_1(p+k)\phi_1(-p)\phi_2(-q-k)\phi_2(q)]\rangle \\ &= -i(G_{1111}(p+k,-p,-q-k,q) - G_{1122}(p+k,-p,-q-k,q)). \end{aligned} \tag{3.14}$$

The previous expression states that the $G_R^{\rho\rho}(k|p,q)$ corresponds to the difference of two 4-point functions. In order to simplify (3.14), we can try to perform a Keldysh rotation,

$$\phi_r = \frac{\phi_1 + \phi_2}{2}, \;\; \phi_a = \phi_1 - \phi_2, \tag{3.15}$$

to basis where $G_{\mathrm{R}} = G_{ra}$ and $G_{\mathrm{A}} = G_{ar}$. After such rotation, the right-hand-side of (3.14) contains the linear combination of $2^4 = 16$ correlation functions.

However, in the limit of vanishing $\omega = k_0$ and $\mathbf{k} = (0, 0, k_z)$, Wang and Heinz showed in [113] that, for any bosonic field theory, the following holds

$$\begin{aligned} &G_{1111}(p+k,-p,-q-k,q) - G_{1122}(p+k,-p,-q-k,q) \\ &\overset{\omega\to 0}{\approx} \frac{1}{4}(N_{\mathbf{q}+\mathbf{k}} - N_{\mathbf{q}})G_{rraa}(p,q|k) = \frac{1}{4}(N_{\mathbf{p}} - N_{\mathbf{p}+\mathbf{k}})G^*_{aarr}(p,q|k). \end{aligned} \tag{3.16}$$

In the long time limit in which we are interested, the retarded 2-point function of the bilocal density operator, written in terms of fundamental fields in the Keldysh basis, $G_R^{\rho\rho}(k|p,q)$, thus assumes the simple form:

$$\begin{aligned} G_R^{\rho\rho}(k|p,q) &= \frac{1}{4}(N_{\mathbf{q}} - N_{\mathbf{q}+\mathbf{k}})G_{rraa}(p,q|k) \\ &= \frac{1}{4}(N_{\mathbf{p}+\mathbf{k}} - N_{\mathbf{p}})G^*_{aarr}(p,q|k). \end{aligned} \tag{3.17}$$

3.2.2 Decoupling of the OTOC in the extended Schwinger-Keldysh formalism

In this section we show how a similar simplification applies to the OTOC by using an extended version of the real time formalism of QFT. Considering

an hermitian operator O, we will focus on the following out-of time correlation function

$$C(t,\mathbf{x}) = \langle \rho^{1/2}[O(t,\mathbf{x}),O(0,\mathbf{0}))]\rho^{1/2}[O(t,\mathbf{x}),O(0,\mathbf{0}))]\rangle. \tag{3.18}$$

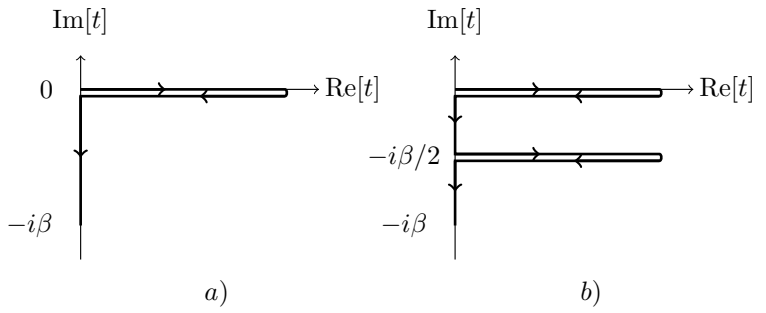

Figure 3.2: The different time contours. *a*) is the standard time contour in Schwinger Keldysh; *b*) is the extended contour necessary to compute the OTOC.

By expanding the commutators in (3.18), a new type of contribution appears besides the two-time ordered terms. The two terms are

$$-\langle \rho^{1/2}O(t,\mathbf{x})O(0,\mathbf{0}))\rho^{1/2}O(t,\mathbf{x})O(0,\mathbf{0}))\rangle - [(t,\mathbf{x}) \leftrightarrow (0,\mathbf{0})]. \tag{3.19}$$

In order to include these new terms, the contour of the path integral depicted in Fig. 3.1 has to be modified as shown in Fig. 3.2 *b*), by adding another time fold.

To preserve the ordering in the out-of-time correlation function,

$$\begin{aligned} C(x,y,w,z) =& \langle [O(x),O(y)][O(w),O(z)]\rangle = \langle O(x)O(y)O(w)O(z)\rangle \\ &+ \langle O(y)O(x)O(z)O(w)\rangle - \langle O(y)O(x)O(w)O(z)\rangle \\ &- \langle O(x)O(y)O(z)O(w)\rangle, \end{aligned} \tag{3.20}$$

we need to insert the operators in the correct branch. Labelling the 4 branches of the modified contour as in Fig. 3.3,

then (3.20) can be rewritten as

$$\begin{aligned} C(x,y,w,z) =& C^{4321}(x,y,w,z) + C^{3412}(x,y,w,z) - C^{3421}(x,y,w,z) \\ &- C^{4312}(x,y,w,z). \end{aligned} \tag{3.21}$$

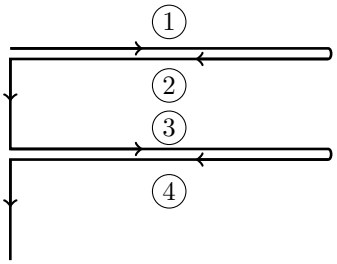

Figure 3.3: The insertions on the extended Keldysh contour can be labelled with an index $i = 1, ..., 4$.

In the last line, we have used the fact that, in the Schwinger-Keldysh formalism, correlation functions are contour-ordered. This means that the operator inserted in branch 4 will always appear on the most left side of the correlator. For example, as shown in fig. 3.4,

$$\begin{aligned} C^{3412}(x,y,w,z) &\equiv \langle \mathcal{T}_{SK}[O_3(x)O_4(y)O_1(w)O_2(z)]\rangle \\ &= \langle O(y)O(x)O(z)O(w)\rangle. \end{aligned} \tag{3.22}$$

Now we can perform the standard Keldysh rotation pairwise in the space of the operators, namely independently rotating the fields in the first and second time-fold,

$$O_r = \frac{O_1 + O_2}{2}, \;\; O_a = O_1 - O_2; \tag{3.23}$$

$$O_R = \frac{O_3 + O_4}{2}, \;\; O_A = O_3 - O_4. \tag{3.24}$$

Subscripts (a, r) are the Keldysh indices of the first time fold and (A, R) of the second time-fold. The basis change is implemented by the following block-diagonal matrix

$$\widetilde{Q} = \begin{pmatrix} Q & 0 \\ 0 & Q \end{pmatrix}, \; Q^{i\alpha} = \begin{pmatrix} 1 & -1/2 \\ 1 & -1/2 \end{pmatrix}. \tag{3.25}$$

Then, the commutator-squared (3.21) can be expressed as follows

$$\begin{aligned} C(x,y,w,z) = (Q^{4\alpha}Q^{3\beta} - Q^{3\alpha}Q^{4\beta})(Q^{2\gamma}Q^{1\delta} - Q^{1\gamma}Q^{2\delta}) \\ \times C^{\alpha\beta\gamma\delta}(x,y,w,z). \end{aligned} \tag{3.26}$$

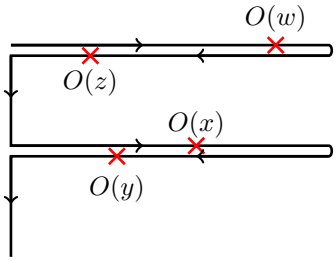

Figure 3.4: The evaluation of correlation functions is such that the insertions on the extended Keldysh contour are always contour ordered in the SK path integral.

Clearly, because of the block-diagonal structure of the $\widetilde{Q}$ matrix, the only non vanishing contribution is for $(\alpha,\beta) = \{(A,R),(R,A)\}$ and $(\gamma,\delta) = \{(a,r),(r,a)\}$. So

$$\begin{aligned} 4C(x,y,w,z) =& C^{RAra}(x,y,w,z) + C^{ARar}(x,y,w,z) - C^{RAar}(x,y,w,z) \\ & - C^{ARra}(x,y,w,z) \\ =& C^{RrAa}(x,w,y,z) + C^{AaRr}(x,w,y,z) - C^{RaAr}(x,w,y,z) \\ & - C^{ArRa}(x,w,y,z). \end{aligned} \tag{3.27}$$

So far we studied the correlator square with arbitrary insertions (x,y,w,z). The commutator-squared is defined by the choice $w = x$ and $y = z = 0$. For this choice, rotating back to the old basis, it is possible to show that, for any t, it holds [1]

$$C^{RaAr}(x,x,0,0) = C^{ArRa}(x,x,0,0) = 0. \tag{3.28}$$

The previous results remarkably simplifies the form of the commutator-squared

$$4C(x,0,x,0) = C^{RrAa}(x,x,0,0) + C^{AaRr}(x,x,0,0). \tag{3.29}$$

Equation (3.29) makes clear that the OTOC can in general be split into two channels, according to the sign of the time argument. Indeed it is possible to show that

$$\begin{aligned} C^{RrAa}(x,x,0,0) &= \theta(x^0) C^{RrAa}(x,x,0,0), \\ C^{AaRr}(x,x,0,0) &= \theta(-x^0) C^{AaRr}(x,x,0,0). \end{aligned}$$

[1] This result is reminiscent of the fact that the product of the advanced and the retarded Greens functions with the same time argument is zero

If we are interested in the late time regime of the OTOC, with $t > 0$, we can simply focus on the $C^{RrAa}(x, x, 0, 0)$. Consequently we can restrict our analysis to $f(x) \equiv C^{RrAa}(x, x, 0, 0)$ and

$$\begin{aligned} f(k) &= \int_x e^{ikx} f(x) \equiv \int_x e^{ikx} C^{RrAa}(x, x, 0, 0) \\ &= \int_{x,p_1,p_2,p_3,p_4} e^{i(k-p_1-p_2)x} C^{RrAa}(p_1, p_2, p_3, p_4)(2\pi)^4 \delta^4(p_1 + p_2 + p_3 + p_4) \\ &= \int_{pq} C^{RrAa}(p + k, -p, -q - k, q). \end{aligned} \tag{3.30}$$

Thus the computation of OTOC reduces to the study of the 4-point function on a modified SK contour

$$f(k) = \int_{pq} C^{RrAa}(p, q|k), \tag{3.31}$$

where, for brevity, we indicated $(p, q|k) = (p+k, -p, -q-k, q)$. Comparing (3.31) with (3.17), we observe that the commutator square resembles an analytical continuation of the $G_R^{\rho\rho}(k|p, q)$ in the long time limit. Let us also observe that, by consistently reshuffling the momenta and the SK indices in the integral, we obtain

$$f(k) = \int_{pq} C^{RrAa}(p, q|k) = \int_{pq} C^{AaRr}(p, q| - k). \tag{3.32}$$

We will use (3.32) as a consistency check for our results.

In order to compute (3.31), we shall need some further knowledge of the structure of the Green's functions in this extended SK path integral. We first define the correlation functions in this extended SK contour as follows

$$G_{a_1 \ldots a_n}(x_1, .., x_n) = (-i)^{n-1} \langle \mathcal{T}_{SK}[O(x_1)_{a_1} ... O(x_n)_{a_n}] \rangle \tag{3.33}$$

where the index a_i runs over the time brannches, $a_1 = 1, ..., 4$. After performing the rotation to the Keldysh basis, the correlation functions read

$$G_{\alpha_1 \ldots \alpha_n}(x_1, .., x_n) = (-i)^{n-1} 2^{n_r - 1} 2^{n_R - 1} \langle \mathcal{T}_{SK}[O(x_1)_{\alpha_1} ... O(x_n)_{\alpha_n}] \rangle,$$

and n_r and n_R count respectively the the r and R indices among $\{\alpha_i\}$.

We now specialize to the bosonic case. It can be shown that

$$\begin{aligned}
&G_{ra}(k) = G_{RA}(k),\\
&G_{Ra}(k) = G_{Ra}(k) = 0,\\
&G_{ar}(k) = G_{AR}(k),\\
&G_{rR}(k) = \frac{1}{2}e^{\beta k^0/2}(N(k^0)-1)\left[G_{ra}(k) - G_{ar}(k)\right],\\
&G_{Rr}(k) = \frac{1}{2}e^{-\beta k^0/2}(N(k^0)+1)\left[G_{ra}(k) - G_{ar}(k)\right],
\end{aligned}$$

with $N(k^0) = 1 + 2n_B(k^0)$, $n_B(k^0)$ being the Bose-Einstein distribution function $n_B(k^0) = \frac{1}{e^{\beta k^0}-1}$. Moreover, since $e^{\beta k^0/2}(N(k^0)-1) = e^{-\beta k^0/2}(N(k^0)+1)$, the (rR) and (Rr) components are all same

$$\begin{aligned}
&G_{rR}(k) = G_{Rr}(k),\\
&G_{rR}(-k) = G_{Rr}(k) = G_{rR}(k).
\end{aligned}$$

In this extended Keldysh basis, the set of Green's functions can be summarized as follows

$$G = \left(\begin{array}{c|c} G_{\alpha\beta} & G_1 \\ \hline G_2 & G_{\alpha\beta} \end{array}\right), \tag{3.34}$$

with

$$G_{\alpha\beta} = \begin{pmatrix} G_{rr} & G_{ra} \\ G_{ar} & G_{aa} \end{pmatrix}, \quad G_1 = \begin{pmatrix} G_{rR} & 0 \\ 0 & 0 \end{pmatrix}, \quad G_2 = \begin{pmatrix} G_{Rr} & 0 \\ 0 & 0 \end{pmatrix}. \tag{3.35}$$

Furthermore, many properties in this contour are remnant of the canonical SK path integral. By using that any n-point function with only a indices vanishes in standard SK, it is easy to see that any n-point functions with at least an index A (a), but without a R (r), vanishes. An example of this statement is the following

$$\begin{aligned}
&G^{AA\alpha_3\alpha_4}(x,y,w,z) = G^{A\alpha_3 A\alpha_4}(x,y,w,z) = G^{A\alpha_3\alpha_4 A}(x,y,w,z) \\
&= G^{\alpha_3 AA\alpha_4}(x,y,w,z) = G^{\alpha_3 A\alpha_4 A}(x,y,w,z) = G^{\alpha_3\alpha_4 AA}(x,y,w,z) = 0,
\end{aligned} \tag{3.36}$$

if $(\alpha_3, \alpha_4) \in \{a, r\}$.

3.2.3 Decoupling of the OTOC BSE: ϕ^4 matrix model example

The framework presented in the previous section is valid for any bosonic theory and can be easily generalized to the fermionic case. We shall stay with the bosonic theory, however. We will now show that the BSE that determines the exact expression for $G^{RrAa}(p,q|k)$ (3.31) remains a closed equation in the late time limit, decoupling from all the other Green's functions. We will specialize to the case of $N \times N$ Hermitian massive scalars Φ_{ab}, with a Φ^4 interaction in $(3+1)$ dimensions. The Lagrangian we are considering is

$$\mathcal{L} = \mathrm{tr}\left(\frac{1}{2}(\partial\Phi)^2 - \frac{1}{2}(\nabla\Phi)^2 - \frac{m^2}{2}\Phi^2 - \frac{g^2}{4!}\Phi^4\right). \tag{3.37}$$

We are interested in the the following class of 4-point functions

$$G^{\alpha_1\alpha_2\alpha_3\alpha_4}(p,q|k) = i2^{n_r-1}\langle \mathcal{T}_{SK}[\phi^{ab}_{\alpha_1}(p+k)\phi^{ba}_{\alpha_2}(-p)\phi^{a'b'}_{\alpha_3}(-q-k)\phi^{b'a'}_{\alpha_4}(q)]\rangle. \tag{3.38}$$

This correlation function satisfies the following Bethe-Salpeter equation

$$\begin{aligned} G^{\alpha_1\alpha_2\alpha_3\alpha_4}(p,q|k) &= iG^{\alpha_1\alpha_3}(p+k)G^{\alpha_2\alpha_4}(-p)(2\pi)^4\delta^4(p-q) \\ &\quad - \frac{1}{2}G^{\alpha_1\beta_1}(p+k)G^{\alpha_2\gamma_1}(-p)\int_l K_{\beta_1\gamma_1\beta_4\gamma_4}(p,l|k)G^{\beta_4\gamma_4\alpha_3\alpha_4}(l,q|k) \end{aligned} \tag{3.39}$$

where the indices run on $\alpha = \{a, r\}$. (3.39) represents a nested set of equations which couples all the 2^4 correlation function. In order to compute hydrodynamical transport coefficients, as shear viscosity η, only G^{rraa} and its complex conjugate are needed. In the hydrodynamical limit, $\mathbf{k} \to 0$ and $k^0 = \omega \to 0$, this coupled system of BSE also considerably simplifies and the relevant components, G_{rraa} and G^*_{rraa}, decouple [114, 168]. In this limit, a crucial role is played by the *pinching-poles* approximation, which we discuss in Appendix 3.D. Building on the results for a purely scalar field [113, 169], for *any* values of N the BSE reads [44]

$$\begin{aligned} G^{aarr}(p,q|k) =& G^{ar}(p+k)G^{ar}(-p) \\ &\times\left[i(2\pi)^4\delta^4(p-q) - \int_l R^{\mathrm{transp}}(p,l)\, G^{aarr}(l,q|k)\right] \end{aligned} \tag{3.40}$$

where the kernel is

$$R^{\mathrm{transp}}(p,l) = -\frac{g^4}{2}\frac{N^2+5}{6}\frac{1+n(l_0)}{1+n(p_0)}\int_l n(s_0)(1+n(s_0-l_0+p_0))\rho(s)\rho(s-l+p). \tag{3.41}$$

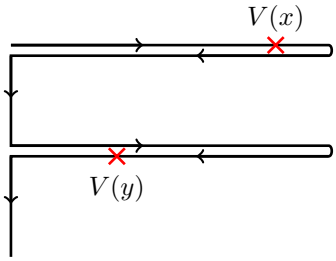

Figure 3.5: In the computation of the OTOC, each vertex insertion (V) can be inserted in one of the 4 time branches. The insertions in the same fold is already taken into account by using the dressed Green's functions on the rails. The new contribution comes from the insertions in the different folds.

The factor in front of the kernel is the two-to-two particle scattering amplitude $\frac{1}{2}|\mathcal{T}_{2\to 2}|^2 = \frac{g^4}{2}\frac{N^2+5}{6}$, which indeed reduce to the standard $|\mathcal{T}_{2\to 2}|^2 = g^4$ for the single scalar case ($N = 1$). If we are interested in computing the OTOC, the BSE (3.39) does not change form. We simply take the indices in 2-fold contour $\alpha = \{a, r, A, R\}$ and we need to evaluate the expression for the kernel $K_{\beta_1\gamma_1\beta_4\gamma_4}$.

$$K_{\alpha_1\beta_1\alpha_4\beta_4}(p,l|k) = \frac{N^2+5}{6}\lambda_{\alpha_1\alpha_2\alpha_3\alpha_4}\lambda_{\beta_1\beta_2\beta_3\beta_4}\int_s G_{\beta_2\alpha_2}(s)G_{\beta_3\alpha_3}(s-l+p), \tag{3.42}$$

with

$$\lambda_{\alpha_1\alpha_2\alpha_3\alpha_4} = g^2\frac{1-(-1)^{n_a}}{4}. \tag{3.43}$$

Each vertex can be inserted in only 2 of the 4 branches (either $1,2$ or $3,4$). This means that the indices $\{\alpha_1,\alpha_2,\alpha_3,\alpha_4\}$ need to be either $\{A,R\}$ or $\{a,r\}$, as for example shown in fig. 3.5.

Now let's specialise the BSE to the commutator squared (3.31). The BSE becomes

$$\begin{aligned} G^{RrAa}(p,q|k) &= iG^{RA}(p+k)G^{ra}(-p)(2\pi)^4\delta^4(p-q)+ \\ &- \frac{1}{2}G^{R\alpha_1}(p+k)G^{r\beta_1}(-p)\int_l K_{\alpha_1\beta_1\alpha_4\beta_4}(p,l|k)C^{\alpha_4\beta_4Aa}(l,q|k), \end{aligned} \tag{3.44}$$

which simplifies with the use of the relations (3.36),

$$G^{RrAa}(p,q|k) = iG^{RA}(p+k)G^{ra}(-p)(2\pi)^4\delta^4(p-q) - \frac{1}{2}G^{R\alpha_1}(p+k)G^{r\beta_1}(-p) \times \int_l \left(K_{\alpha_1\beta_1 Rr}(p,l|k)C^{RrAa}(l,q|k) + K_{\alpha_1\beta_1 rR}(p,l|k)C^{rRAa}(l,q|k)\right). \tag{3.45}$$

Focusing on first term in (3.45), the possible choices for the indices are $\alpha_1 \in \{A,R,r\}$ and $\beta_1 \in \{a,r,R\}$ since, expanding the product $G^{R\alpha_1}G^{r\beta_1}$, few terms vanish due to the identities $G^{Ra} = G^{rA} = 0$. Moreover, from the definition of the kernel (3.42), $K_{\alpha_1\beta_1\alpha_4\beta_4} = 0$ if α_1 and α_4 or β_1 and β_4 belong to different time folds. This reduces the combinations to $\alpha_1 \in \{A,R\}$ and $\beta_1 \in \{a,r\}$. By using $K_{RrRr} = K_{RaRr} = K_{ArRr} = 0$, we can furthermore simplify the first term in (3.45)

$$G^{R\alpha_1}(p+k)G^{r\beta_1}(-p)\int_l K_{\alpha_1\beta_1 Rr}(p,l|k)C^{RrAa}(l,q|k) = G^{RA}(p+k)G^{ra}(-p)\int_l K_{AaRr}(p,l|k)C^{RrAa}(l,q|k). \tag{3.46}$$

In a similar manner, it is possible to show that the second term in (3.45) vanishes

$$G^{R\alpha_1}(p+k)G^{r\beta_1}(-p)\int_l K_{\alpha_1\beta_1 rR}(p,l|k)C^{rRAa}(l,q|k) = G^{Rr}(p+k)G^{rR}(-p)\int_l K_{rRrR}(p,l|k)C^{RrAa}(l,q|k) = 0. \tag{3.47}$$

This means that the BSE for the OTOC is the following

$$G^{RrAa}(p,q|k) = G^{RA}(p+k)G^{ra}(-p)\left(i(2\pi)^4\delta^4(p-q) - \frac{1}{2}\int_l K_{AaRr}(p,l|k)C^{RrAa}(l,q|k)\right). \tag{3.48}$$

Thus, the kernel of the BSE is simply given by the product of Wightman

functions connecting the two time folds

$$K_{AaRr}(p,l|k) = \frac{1}{4}g^4\frac{N^2+5}{6}\int_s G_{Rr}(s)G_{Rr}(s-l+p)$$
$$= g^4\frac{N^2+5}{6}e^{\beta(l^0-p^0)/2}\int_s n(s_0)(1+n(s_0-l_0+p_0))\rho(s)\rho(s-l+p). \tag{3.49}$$

The BSE of the commutator squared eventually reads

$$G^{RrAa}(p,q|k) = G^{RA}(p+k)G^{ra}(-p)\Bigg(i(2\pi)^4\delta^4(p-q) - \int_l R^{\mathrm{OTOC}}(p,l)C^{RrAa}(l,q|k)\Bigg) \tag{3.50}$$

and

$$R^{\mathrm{OTOC}}(p,l) = g^4\frac{N^2+5}{12}e^{\beta(l^0-p^0)/2} \times \int_s n(s_0)(1+n(s_0-l_0+p_0))\rho(s)\rho(s-l+p). \tag{3.51}$$

Our derivation of the G^{RrAa}, which is summarized by equations (3.50) and (3.51), is valid for any N, even $N = 1$. Similarly to the case of transport, the BSE for the commutator squared decoupled, even though a priori the RHS of the BSE couples all the 4^4 4-point functions. By comparing (3.40) and (3.41) with (3.50) and (3.51), we can easily see that

$$R^{\mathrm{OTOC}}(p,l) = \frac{\sinh(\beta l_0/2)}{\sinh(\beta p_0/2)}R^{\mathrm{transp}}(p,l). \tag{3.52}$$

We observe that the term $e^{\beta(l^0-p^0)/2}$ is remnant of the regularization, as it comes from $e^{\sigma(l^0-p^0)}$, σ being the time width of the extended SK path integral. For an analysis of the consequences of the regularization dependence of the OTOC, we refer to chapter 5.

3.3 Kinetic theory of many-body chaos

In the previous section we have shown that, although a priori very different, once the late time limit is taken the commutator squared and the retarded

Green's function of the bilocal density field have many properties in common. In this section we make this connection more precise, within the quantum Boltzmann equation framework.

The BSE for the correlation function of the bilocal density operator is the QFT analogue of the Boltzmann equation. It was already noted in the literature that the collision integral entered the form of the BSE [101, 110, 126] and that it can be used to compute transport coefficients through Kubo relations. We reviewed this above. We now show that the BSE not only contains the collisional integral, but by appropriately retaining the first order in the external frequency, the BSE is nothing but the Fourier transform of the Boltzmann equation. This result, which is by itself of interest, acquires more appeal in light of the findings of the previous sections, namely the connection between the BSE that defines the OTOC and the BSE of the bilocal density operator. This thus allows us to derive the kinetic equation for many-body chaos which reproduces exactly the computation of the OTOC, and thus the Lyapunov spectrum. This kinetic equation shows that the OTOC, so the scrambling of information in a system, computes some gross (energy) exchange in contrast to net number exchange for transport.

In the subsequent sections we shall show that, since the relation holds also in the quantum critical limit of both bosonic and fermionic states, our kinetic equation unequivocally implies that, even in this critical regime, energy dynamics plays a crucial role in the information scrambling.

3.3.1 Quick review of the Boltzmann equation

The Boltzmann equation governs the time evolution of the single-particle distribution function $f(\mathbf{p}, \mathbf{r}, t)$. In terms of the change of particle number density per unit of phase space: $\delta n(t, \mathbf{p}) = n(t, \mathbf{p}) - n(E_{\mathbf{p}})$, the distribution function can be expressed as

$$f(t, \mathbf{p}) = \frac{\delta n(t, \mathbf{p})}{(1 + n(\mathbf{p}))n(\mathbf{p})} \tag{3.53}$$

where $n(\mathbf{p})$ is the equilibrium Bose-Einstein distribution $n(\mathbf{p}) = 1/(e^{\beta E(\mathbf{p})} - 1)$ which depends on the energy of the *on-shell* particle $E(\mathbf{p})$. Here we restrict the analysis to the spatially homogeneous case and consider all quantities as space-averaged (e.g. $n(t, \mathbf{p}) = \int d\mathbf{x}\, n(t, \mathbf{x}, \mathbf{p})$). Moreover we focus only on the contribution given by the two-to-two scattering to the dynamics of the phase-space. Higher order contributions require to go beyond the uncrossed ladder approximation, and we will not consider

this case. The linearized Boltzmann equation is a homogeneous evolution equation for $f(t,\mathbf{p})$ (see e.g. [162–164]):[2]

$$\partial_t f(t,\mathbf{p}) = -\int_{\mathbf{l}} \mathcal{L}(\mathbf{p},\mathbf{l}) f(t,\mathbf{l}), \tag{3.54}$$

where the kernel of the collision integral

$$\mathcal{L}(\mathbf{p},\mathbf{l}) \equiv -\left[R^{\wedge}(\mathbf{p},\mathbf{l}) - R^{\vee}(\mathbf{p},\mathbf{l})\right] \tag{3.55}$$

measures the difference between the rates of scattering into the phase-space cell and scattering out the phase space cell. The term $R^{\wedge}$ takes into account the increases of the local density by scattering with a thermal excitation and it reads

$$R^{\wedge}(\mathbf{p},\mathbf{l}) = \frac{1}{n(\mathbf{p})(1+n(\mathbf{p}))} \int_{\mathbf{p}_2,\mathbf{p}_3,\mathbf{p}_4} d\Sigma(\mathbf{p},\mathbf{p}_2|\mathbf{p}_3,\mathbf{p}_4)\left(\delta(\mathbf{p}_3-\mathbf{l})+\delta(\mathbf{p}_4-\mathbf{l})\right). \tag{3.56}$$

The factor $R^{\vee}(\mathbf{p},\mathbf{l})$, instead, involves the loss of the density in the phase cell occurred by the annihilation into the thermal bath or scattering from the bath into the same cell

$$R^{\vee}(\mathbf{p},\mathbf{l}) = \frac{1}{n(\mathbf{p})(1+n(\mathbf{p}))} \int_{\mathbf{p}_2,\mathbf{p}_3,\mathbf{p}_4} d\Sigma(\mathbf{p},\mathbf{p}_2|\mathbf{p}_3,\mathbf{p}_4)\left(\delta(\mathbf{p}-\mathbf{l})+\delta(\mathbf{p}_2-\mathbf{l})\right). \tag{3.57}$$

Here, the infinitesimal cross section is weighted with the phase space contribution given by the equilibrium distribution function ((n_B) for initial states and $(1+n_B)$ for final states)

$$d\Sigma(\mathbf{p},\mathbf{p}_2|\mathbf{p}_3,\mathbf{p}_4) = \frac{1}{2}|\mathcal{T}_{pp_2\to p_3p_4}|^2\, n(\mathbf{p})\, n(\mathbf{p}_2)\,(1+n(\mathbf{p}_3))(1+n(\mathbf{p}_4)) \times (2\pi)^4\delta^4(p+p_2-p_3-p_4) \tag{3.58}$$

and $|\mathcal{T}_{pp_2\to p_3p_4}|^2$ the two-to-two transition amplitude squared. Some of the spectral properties of the Boltzmann equation can be studied by introducing the following inner product

$$\langle\psi'|\psi\rangle = \int_{\mathbf{p}} n(\mathbf{p})(1+n(\mathbf{p}))\psi'^{*}(\mathbf{p})\psi(\mathbf{p}). \tag{3.59}$$

[2] To make the formula easier to read, we indicate with $\int_p \equiv \int \frac{d^4p}{(2\pi)^4}$ and $\int_{\mathbf{p}} \equiv \int \frac{d^3p}{(2\pi)^3}\frac{1}{2E(\mathbf{p})}$ for relativistic theories. For a non-relativistic system, $\int_{\mathbf{p}} \equiv \int \frac{d^3p}{(2\pi)^3}$. Similarly, $\int_x \equiv \int d^4x$ and $\int_{\mathbf{x}} \equiv \int d^3x$.

By using the symmetries of the cross-section

$$\begin{aligned} d\Sigma(\mathbf{p}_1,\mathbf{p}_2|\mathbf{p}_3,\mathbf{p}_4) &= d\Sigma(\mathbf{p}_2,\mathbf{p}_1|\mathbf{p}_3,\mathbf{p}_4) = d\Sigma(\mathbf{p}_3,\mathbf{p}_4|\mathbf{p}_1,\mathbf{p}_2) \\ &= d\Sigma(\mathbf{p}_1,\mathbf{p}_2|\mathbf{p}_4,\mathbf{p}_3) \end{aligned} \tag{3.60}$$

it is possible to show that the operator $\mathcal{L}(\mathbf{p},\mathbf{l})$ is not only Hermitian on this inner product, but also positive semidefinite. This in turn means that all its eigenvalues are real and $\xi_n \geq 0$ and that the solutions to the Boltzmann equation are purely relaxational:

$$f(\mathbf{p},t) = \sum_n A_n e^{-\xi_n t}\phi_n(\mathbf{p}). \tag{3.61}$$

In the previous equation we have formally indicated with $\sum_n$ either a sum over discrete values or an integral over a continuum (see e.g. [162–165]). Another remarkable property of the spectrum is that every $\xi = 0$ eigenvalue corresponds to a symmetry and hence an associated conserved quantity (a collisional invariant). For the bosonic/fermionic field theory, the kinetic equation thus takes the form

$$\begin{aligned} \partial_t f(\mathbf{p},t) = &+ \frac{1}{1\pm n_{B/F}(\mathbf{p})}\int_{\mathbf{l},\mathbf{p_2},\mathbf{p_4}} \frac{(2\pi)^4\delta^4(\mathbf{p}^{\mathrm{os}}+\mathbf{p_2}^{\mathrm{os}}-\mathbf{l}^{\mathrm{os}}-\mathbf{p_4}^{\mathrm{os}})|\mathcal{T}|^2}{2E_{\mathbf{p}}} \\ &\times n_{B/F}(E_{\mathbf{p_2}})(1\pm n_{B/F}(E_{\mathbf{l}}))(1\pm n_{B/F}(E_{\mathbf{4}}))f(\mathbf{l},t) \\ &- \frac{1/2}{1\pm n_{B/F}(\mathbf{p})}\int_{\mathbf{l},\mathbf{p_2},\mathbf{p_4}} \frac{(2\pi)^4\delta^4(\mathbf{p}^{\mathrm{os}}+\mathbf{l}^{\mathrm{os}}-\mathbf{p_2}^{\mathrm{os}}-\mathbf{p_4}^{\mathrm{os}})|\mathcal{T}|^2}{2E_{\mathbf{p}}} \\ &\times n_{B/F}(E_{\mathbf{l}})(1\pm n_{B/F}(E_{\mathbf{p_2}}))(1\pm n_{B/F}(E_{\mathbf{4}}))f(\mathbf{l},t) \\ &- \frac{1/2}{1\pm n_{B/F}(\mathbf{p})}\int_{\mathbf{l},\mathbf{p_2},\mathbf{p_4}} \frac{(2\pi)^4\delta^4(\mathbf{p}^{\mathrm{os}}+\mathbf{l}^{\mathrm{os}}-\mathbf{p_2}^{\mathrm{os}}-\mathbf{p_4}^{\mathrm{os}})|\mathcal{T}|^2}{2E_{\mathbf{p}}} \\ &\times n_{B/F}(E_{\mathbf{l}})(1\pm n_{B/F}(E_{\mathbf{p_2}}))(1\pm n_{B/F}(E_{\mathbf{4}}))f(\mathbf{p},t). \end{aligned} \tag{3.62}$$

where we denoted with $\mathbf{p}^{\mathrm{os}} = (E_{\mathbf{p}},\mathbf{p})$ the *on-shell* momenta and

$$\begin{aligned} \delta^4(\mathbf{p}^{\mathrm{os}}+\mathbf{p_2}^{\mathrm{os}}-\mathbf{l}^{\mathrm{os}}-\mathbf{p_4}^{\mathrm{os}}) = &\,\delta^3(\mathbf{p}^{\mathrm{os}}+\mathbf{p_2}^{\mathrm{os}}-\mathbf{l}^{\mathrm{os}}-\mathbf{p_4}^{\mathrm{os}}) \\ &\times\delta(E_{\mathbf{p}}+E_{\mathbf{p_2}}-E_{\mathbf{l}}-E_{\mathbf{p_4}}). \end{aligned}$$

The first line corresponds to the *gain* term $R^{\wedge}(\mathbf{p},\mathbf{l})$,

$$\begin{aligned} R^{\wedge}(\mathbf{p},\mathbf{l}) = &+ \frac{1}{1\pm n_{B/F}(\mathbf{p})}\int_{\mathbf{p_2},\mathbf{p_4}} \frac{(2\pi)^4\delta^4(\mathbf{p}^{\mathrm{os}}+\mathbf{p_2}^{\mathrm{os}}-\mathbf{l}^{\mathrm{os}}-\mathbf{p_4}^{\mathrm{os}})|\mathcal{T}|^2}{4E_{\mathbf{p}}E_{\mathbf{l}}} \\ &\times n_{B/F}(E_{\mathbf{p_2}})(1\pm n_{B/F}(E_{\mathbf{l}}))(1\pm n_{B/F}(E_{\mathbf{4}})), \end{aligned} \tag{3.63}$$

while the second and third line correspond to the *loss* term $R^{\vee}(\mathbf{p},\mathbf{l})$

$$\begin{aligned} R^{\vee}(\mathbf{p},\mathbf{l}) =& \frac{1/2}{1\pm n_{B/F}(\mathbf{p})}\int_{\mathbf{p}_2,\mathbf{p}_4}\frac{(2\pi)^4\delta^4(\mathbf{p}^{\rm os}+\mathbf{l}^{\rm os}-\mathbf{p_2}^{\rm os}-\mathbf{p_4}^{\rm os})|\mathcal{T}|^2}{4E_{\mathbf{p}}E_{\mathbf{l}}} \\ &\times n_{B/F}(E_{\mathbf{l}})(1\pm n_{B/F}(E_{\mathbf{p_2}}))(1\pm n_{B/F}(E_{\mathbf{4}})) \\ &+\frac{1/2}{1\pm n_{B/F}(\mathbf{p})}\int_{\mathbf{p}_2,\mathbf{p}_4}\frac{(2\pi)^4\delta^4(\mathbf{p}^{\rm os}+\mathbf{l}^{\rm os}-\mathbf{p_2}^{\rm os}-\mathbf{p_4}^{\rm os})|\mathcal{T}|^2}{4E_{\mathbf{p}}E_{\mathbf{l}}} \\ &\times n_{B/F}(E_{\mathbf{l}})(1\pm n_{B/F}(E_{\mathbf{p_2}}))(1\pm n_{B/F}(E_{\mathbf{4}})). \end{aligned} \tag{3.64}$$

Moreover, we will see that the second term in $R^{\vee}$ is proportional the imaginary part of the self energy $2\,\Gamma_{\mathbf{p}}$.

3.3.2 From the BSE to the quantum Boltzmann equation

We now show how the quantum Boltzmann equation (3.62) can be derived from the BSE. For the sake of clarity, we first focus on the theory of $N\times N$ Hermitian matrix scalars. We then prove this results for the case of the bosonic $O(N)$ vector model (section 3.4) and the Gross-Neveu model (section 3.5). We start with the BSE for the 4-point Green's function $G^{*}_{aarr}(p+k,p)$ which, up to some thermal factor, coincides with $G^{\rho\rho}_{\rm R}(p+k,p)$ as stated in (3.17). In the long wavelength and late time limit, $k=(\omega,\mathbf{0})$ and $\omega\to 0$, this correlation function satisfies the following BSE [44, 113]

$$G^{*}_{aarr}(p+k,p)=G_{\rm R}(p+k)G_{\rm A}(p)\left[iN^2-\int_l R^{\rm transp}(p,l)G^{*}_{aarr}(l+k,l)\right], \tag{3.65}$$

where $G_{\rm R/A}$ are respectively the retarded/advanced Green's function and $R^{\rm transp}$ is the kernel of the BSE. Because of the long time limit, the product $G_{\rm R}(p+k)G_{\rm A}(p)$ suffers of the *pinching-pole* singularity, and can be approximated as follows [3]

$$G_{\rm R}(p+k)G_{\rm A}(p)=\frac{\pi}{E_{\mathbf{p}}}\frac{\delta(p_0^2-E_{\mathbf{p}}^2)}{-i\omega+2\Gamma_{\mathbf{p}}}. \tag{3.66}$$

The BSE has thus the form

$$G^{*}_{aarr}(p+k,p)=\frac{\pi}{E_{\mathbf{p}}}\frac{\delta(p_0^2-E_{\mathbf{p}}^2)}{-i\omega+2\Gamma_{\mathbf{p}}}\left[iN^2-\int_l R^{\rm transp}(p,l)G^{*}_{aarr}(l+k,l)\right]. \tag{3.67}$$

[3] For a discussion about the *pinching-pole* singularity, see Appendix 3.D.

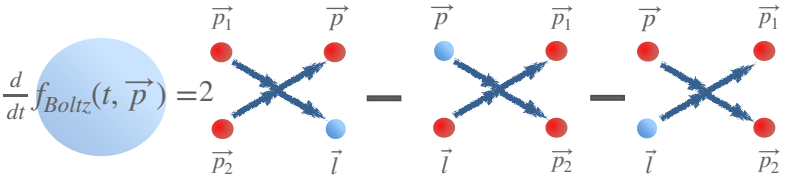

Figure 3.6: Pictorial representation of the linearised Boltzmann equation. The blue halo indicates the out of equilibrium distribution function, while the red the equilibrium distribution function.

In order to find the solution, we can pose an ansatz. We realize that the choice can be narrowed down to two different classes. They are

$$G^*_{aarr}(p+k,p) = G_1(\omega,\mathbf{p})\delta(p_0 - E_\mathbf{p}) \pm G_2(\omega,\mathbf{p})\delta(p_0 + E_\mathbf{p}). \tag{3.68}$$

Let's focus on the ansatz with plus,

$$G^*_{aarr}(p+k,p) = G_1(\omega,\mathbf{p})\delta(p_0 - E_\mathbf{p}) + G_2(\omega,\mathbf{p})\delta(p_0 + E_\mathbf{p}). \tag{3.69}$$

We now show that this choice of ansatz for G^*_{aarr} is correct, since it projects the solution into the physical subspace of relaxing modes described by the quantum Boltzmann equation. Substituting (3.69) into the BSE, we arrive to the following system of equations

$$(-i\omega + 2\Gamma_\mathbf{p})G_1(\mathbf{p},\omega) = \frac{\pi}{2E^2_\mathbf{p}} iN^2 - \int \frac{d\mathbf{l}}{(2\pi)^3}\frac{1}{4E_\mathbf{p}E_\mathbf{l}} \tag{3.70}$$
$$(R^{\text{transp}}(\mathbf{p},E_\mathbf{p}|\mathbf{l},E_\mathbf{l})G_1(\mathbf{l},\omega) + R^{\text{transp}}(\mathbf{p},E_\mathbf{p}|\mathbf{l},-E_\mathbf{l})G_2(\mathbf{l},\omega)),$$
$$(-i\omega + 2\Gamma_\mathbf{p})G_2(\mathbf{p},\omega) = \frac{\pi}{2E^2_\mathbf{p}} iN^2 - \int \frac{d\mathbf{l}}{(2\pi)^3}\frac{1}{4E_\mathbf{p}E_\mathbf{l}} \tag{3.71}$$
$$(R^{\text{transp}}(\mathbf{p},-E_\mathbf{p}|\mathbf{l},E_\mathbf{l})G_1(\mathbf{l},\omega) + R^{\text{transp}}(\mathbf{p},-E_\mathbf{p}|\mathbf{l},-E_\mathbf{l})G_2(\mathbf{l},\omega)).$$

By using the symmetries of the kernel,

$$R^{\text{transp}}(\mathbf{p},-E_\mathbf{p}|\mathbf{l},E_\mathbf{l}) = R^{\text{transp}}(\mathbf{p},E_\mathbf{p}|\mathbf{l},-E_\mathbf{l}), \tag{3.72}$$

we can define the variables $G^\pm(\mathbf{p},\omega) = G_1(\mathbf{p},\omega) \pm G_2(\mathbf{p},\omega)$ which satisfy the following equations

$$(-i\omega + 2\Gamma_\mathbf{p})G^\pm(\mathbf{p},\omega) + \int \frac{d\mathbf{l}}{(2\pi)^3}\frac{1}{4E_\mathbf{p}E_\mathbf{l}} \tag{3.73}$$
$$(R^{\text{transp}}(\mathbf{p},E_\mathbf{p}|\mathbf{l},E_\mathbf{l}) + R^{\text{transp}}(\mathbf{p},E_\mathbf{p}|\mathbf{l},-E_\mathbf{l}))G^\pm(\mathbf{l},\omega) = \frac{\pi}{2E^2_\mathbf{p}} iN^2(1\pm 1).$$

The physical correlation function G^*_{aarr} corresponds to the solution G^+. Indeed, as we show in Appendix 3.G for the case of $N \times N$ hermitian matrix field (and in the following sections for the $O(N)$ vector model and the GN model), the terms appearing in the *on-shell* BSE kernel of G^+ can be identified with the *gain* and *loss* terms of the collision integral of the Boltzmann equation

$$R^{\wedge}(\mathbf{p},\mathbf{l}) = \frac{1}{4E_{\mathbf{p}}E_{\mathbf{l}}} R^{\text{transp}}(\mathbf{p}, E_{\mathbf{p}}|\mathbf{l}, E_{\mathbf{l}}), \tag{3.74}$$

$$R^{\vee}(\mathbf{p},\mathbf{l}) = \frac{1}{4E_{\mathbf{p}}E_{\mathbf{l}}} R^{\text{transp}}(\mathbf{p}, E_{\mathbf{p}}|\mathbf{l}, -E_{\mathbf{l}}) + 2(2\pi)^3\delta^3(\mathbf{p}-\mathbf{l})\Gamma_{\mathbf{p}}. \tag{3.75}$$

Thus, by comparing (3.74) and (3.75) to (3.73), G^+ can be formally solved as

$$G^+(\mathbf{p},\omega) = \left[\frac{1}{-i\omega + \mathcal{L}(\mathbf{p},\mathbf{l})}\right] \frac{\pi}{E^2_{\mathbf{p}}} iN^2, \tag{3.76}$$

the operator $\mathcal{L}(\mathbf{p},\mathbf{l})$ being the collision integral of the Boltzmann equation (3.55)

$$\mathcal{L}(\mathbf{p},\mathbf{l}) = -(R^{\wedge}(\mathbf{p},\mathbf{l}) - R^{\vee}(\mathbf{p},\mathbf{l})), \tag{3.77}$$

as depicted in fig. 3.6. This equation, in the strict $\omega = 0$ limit, equals the equation used in [101] to find the shear viscosity. Its spectrum is negative definite and gives the relaxation times of the theory. This proves our statement that the quantum Boltzmann equation can be derived from the BSE of the retarded Green's function of the bilocal density operator $G^{\rho\rho}_{\text{R}}$. Moreover, from (3.76), we can deduce that the poles/branch cuts of $G^{\rho\rho}_{\text{R}}$ corresponds to the relaxation times/branch cuts of the theory we can be easily addressed in this framework.

3.3.3 The Quantum Boltzmann equation for many-body chaos

In the previous section we have shown that, starting from the BSE for $G^{\rho\rho}_{\text{R}}$, the solution is found by an appropriate choice of ansatz (plus in (3.68)) and it reproduces the quantum Boltzmann equation. We now want to study the physics of the other solution of the *same* BSE, corresponding to the minus in the ansatz (3.68). We show that the latter exactly reproduces the commutator squared correlation function.

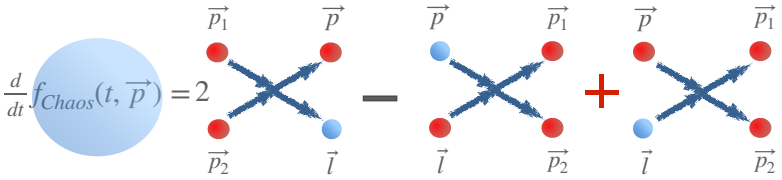

Figure 3.7: Pictorial representation of kinetic equation for the OTOC. The blue halo indicates the out of equilibrium distribution function, while the red the equilibrium distribution function.

By choosing a minus in (3.68), we obtain the following system of equation

$$(-i\omega + 2\Gamma_{\mathbf{p}})G_1(\mathbf{p},\omega) = \frac{\pi}{2E_{\mathbf{p}}^2} iN^2 - \int \frac{d\mathbf{l}}{(2\pi)^3}\frac{1}{4E_{\mathbf{p}}E_{\mathbf{l}}} \tag{3.78}$$
$$(R^{\text{transp}}(\mathbf{p}, E_{\mathbf{p}}|\mathbf{l}, E_{\mathbf{l}})G_1(\mathbf{l},\omega) - R^{\text{transp}}(\mathbf{p}, E_{\mathbf{p}}|\mathbf{l}, -E_{\mathbf{l}})G_2(\mathbf{l},\omega)),$$
$$(-i\omega + 2\Gamma_{\mathbf{p}})G_2(\mathbf{p},\omega) = -\frac{\pi}{2E_{\mathbf{p}}^2} iN^2 - \int \frac{d\mathbf{l}}{(2\pi)^3}\frac{1}{4E_{\mathbf{p}}E_{\mathbf{l}}} \tag{3.79}$$
$$(-R^{\text{transp}}(\mathbf{p}, -E_{\mathbf{p}}|\mathbf{l}, E_{\mathbf{l}})G_1(\mathbf{l},\omega) + R^{\text{transp}}(\mathbf{p}, -E_{\mathbf{p}}|\mathbf{l}, -E_{\mathbf{l}})G_2(\mathbf{l},\omega)).$$

As before, we can define $G_{\pm}(\mathbf{p},\omega) = G_1(\mathbf{p},\omega) \pm G_2(\mathbf{p},\omega)$ which satisfy

$$(-i\omega + 2\Gamma_{\mathbf{p}})G^{\pm}(\mathbf{p},\omega) + \int \frac{d\mathbf{l}}{(2\pi)^3}\frac{1}{4E_{\mathbf{p}}E_{\mathbf{l}}} \tag{3.80}$$
$$\times (R^{\text{transp}}(\mathbf{p}, E_{\mathbf{p}}|\mathbf{l}, E_{\mathbf{l}}) - R^{\text{transp}}(\mathbf{p}, E_{\mathbf{p}}|\mathbf{l}, -E_{\mathbf{l}}))G^{\pm}(\mathbf{l},\omega) = \frac{\pi}{2E_{\mathbf{p}}^2} iN^2(1 \mp 1).$$

Since the commutator squared has an inhomogeneous term, the physical out-of-time correlation function $f(t,\mathbf{p})$ corresponds to the solution G^-. It can be formally written as

$$G^-(\mathbf{p},\omega) = \left[\frac{1}{-i\omega + \mathcal{L}'(\mathbf{p},\mathbf{l})}\right]\frac{\pi}{E_{\mathbf{p}}^2} iN^2. \tag{3.81}$$

In order to find the Lyapunov exponent(s), one usually study the poles of G^-. The operator $\mathcal{L}'(\mathbf{p},\mathbf{l})$ is

$$\mathcal{L}'(\mathbf{p},\mathbf{l}) = \int \frac{d\mathbf{l}}{(2\pi)^3}\frac{1}{4E_{\mathbf{p}}E_{\mathbf{l}}} \tag{3.82}$$
$$(R^{\text{transp}}(\mathbf{p}, E_{\mathbf{p}}|\mathbf{l}, E_{\mathbf{l}}) - R^{\text{transp}}(\mathbf{p}, E_{\mathbf{p}}|\mathbf{l}, -E_{\mathbf{l}}))f(\mathbf{l}) - 2\Gamma_{\mathbf{p}}\, f(\mathbf{p}).$$

By using the same results of the previous section, (3.74) and (3.75), we can now give a clear interpretation to the physics captured by the Lyapunov exponent, which are the eigenvalue of the linearized collision integral $\mathcal{L}'$,

$$\mathcal{L}'(\mathbf{p},\mathbf{l}) = -(R^{\wedge}(\mathbf{p},\mathbf{l}) + R^{\vee}(\mathbf{p},\mathbf{l}) - 4(2\pi)^3\delta^3(\mathbf{p}-\mathbf{l})\Gamma_{\mathbf{p}}), \tag{3.83}$$

depicted in fig. 3.7. Compared to the previous result for transport (3.77), here the kernel contains a sign difference which encodes the microscopic dynamics of scrambling, *i.e.* the OTOC counts the gross number of collision compared to the the net energy in the collision tracked by the standard quantum Boltzmann equation.

In order to understand the generality of our results, in the next sections we will focus on systems close to a quantum critical point, where the effects of entanglement and long range interaction becomes more important.

3.4 Bosonic $O(N)$ vector model at the quantum critical regime

In this section we provide further detailed evidences in support of our findings. We will show that our results even extend into the quantum critical regime. We focus on vector models with N components real fields ϕ_a in $(2+1)$ dimensions. Provided with a $O(N)$ symmetry, these theories have a quantum phase transition (QPT) at zero temperature [61], between the disordered phase with vanishing vacuum expectation value , $\langle\phi_a\rangle = 0$, and the order symmetry breaking phase $\langle\phi_a\rangle \neq 0$. They capture the relevant long wavelength degrees of freedom of many physical systems, such as the superfluid to bosonic Mott insulator transition [177] (realised for $N = 2$) and the paramagnet to Heisenberg antiferromagnet ($N = 3$) [17, 178, 179]. Although on both sides of the QCP the system is described by quasiparticle excitations, the finite temperature regime directly above the QPT diagram, often referred to as quantum critical regime, does not have such excitations. This observation might lead the reader to think that the kinetic theory developed in the previous section does not apply, since the pillar of kinetic theory is indeed the existence of quasiparticles.

This objection is too quick. Firstly, we stress that our results concerns hydrodynamical correlation functions. The kinetic theory limit can be considered as providing a microscopic picture of the physics underlying the curious relation between hydrodynamical transport correlation functions and out-of-time correlation functions, but this connection needs not to be limited to this case. Secondly and more concretely, in their seminal

paper [124], Damle and Sachdev showed that one can use kinetic theory approaches in the quantum critical regime, despite the fact that there are no quasiparticle excitations. If we are interested in the dc conductivities, $\omega = 0$, at the quantum critical point, where by definition $T = 0$, there are two opposite limit that could be considered: the $T = 0, \omega \to 0$ *coherent* and *collisionless* regime, and the $\omega = 0, T \to 0$ *incoherent*, *collision-dominated* and *hydrodynamic* regime. They showed that the coherent regime does not yield the correct response, since the process considered are not relevant for the physical properties of the QCP. Instead, it is the hydrodynamic collision-dominated regime that provides the correct description of the dc conductivities and of transport. Moreover, such properties can be obtained by means of the Boltzmann equation, in a regime with quasiparticles and by continuity must hold in the non quasiparticle regime as well. As it is a collision-dominated regime, the collision integral plays the major role.

Now we can turn to our findings. In a recent paper [136], Chowdhury and Swingle studied scrambling in these theories, focusing particularly on the region of the phase diagram above the QCP. We will now review some of their findings and explain how they fit in the framework we have introduced in this chapter and [44]. The Lagrangian of the theory is

$$\mathcal{L} = \frac{1}{2}(\partial\phi_a)^2 - \frac{v}{2N}\left(\phi_a^2 - \frac{N}{g}\right)^2, \tag{3.84}$$

where $v > 0$ is the self interaction coupling strength and and $g > 0$. In the strong coupling limit, corresponding to $v \to \infty$, the 2+1 dimensional theory is a conformal QFT. By introducing an Hubbard-Stratonovich field, $\lambda(t, \mathbf{x})$, to decouple the quartic term , the action becomes

$$\mathcal{L} = \frac{1}{2}(\partial\phi_a)^2 + \frac{\lambda(t,\mathbf{x})}{2\sqrt{N}}\left(\phi_a^2 - \frac{N}{g}\right) + \frac{\lambda(t,\mathbf{x})^2}{8v}. \tag{3.85}$$

In order to probe the onset of chaos, the authors studied the squared commutator

$$C(t,\mathbf{x}) = -\frac{1}{N^2}\sum_{a,b}\mathrm{Tr}\left[\rho^{1/2}[\phi_a(t,\mathbf{x}),\phi_b]\rho^{1/2}[\phi_a(t,\mathbf{x}),\phi_b]\right]. \tag{3.86}$$

The retarded and Wightman correlation functions involving the ϕ fields are

$$\begin{aligned} G_{\mathrm{R}}(t,\mathbf{x})\delta_{ab} &= -i\theta(t)\langle[\phi_a(t,\mathbf{x}),\phi_b]\rangle = -i\theta(t)\mathrm{Tr}\left(\rho[\phi_a(t,\mathbf{x}),\phi_b]\right), \\ G_W^{\beta/2}(t,\mathbf{x})\delta_{ab} &= \mathrm{Tr}\left(\rho^{1/2}\phi_a(t,\mathbf{x})\rho^{1/2}\phi_b(0)\right), \\ G_W(t,\mathbf{x})\delta_{ab} &= \mathrm{Tr}\left(\rho\phi_a(t,\mathbf{x})\phi_b(0)\right). \end{aligned}$$

The spectral function of the ϕ field, as usual related to the imaginary part of the retarded correlator, in the large N limit is

$$\rho(\omega, \mathbf{k}) = -2\mathrm{Im}[G_{\mathrm{R}}(\omega, \mathbf{k})] = \frac{\pi}{E_{\mathbf{k}}}(\delta(\omega - E_{\mathbf{k}}) - \delta(\omega + E_{\mathbf{k}})), \tag{3.87}$$

with $E_{\mathbf{k}})^2 = \mathbf{k}^2 + \mu^2$, μ being the thermal mass. The Wightman function is also intimately related to the spectral function, as follows

$$G_W(\omega, \mathbf{k}) = \frac{\rho(\omega, \mathbf{k})}{2\sinh(\beta\omega/2)}. \tag{3.88}$$

The Hubbard-Stratonovich field Green's functions in Euclidean time, which we will refer to with a λ subscript, in momentum space reads

$$G_\lambda(i\omega_n, \mathbf{k}) = \frac{1}{-1/4v - \Pi(i\omega_n, \mathbf{k})}. \tag{3.89}$$

and $\Pi(i\omega_n, \mathbf{k})$ is the one loop ϕ_i bubble in Euclidean time. The retarded Green's function can be obtained by analytic continuation of the Euclidean one, $G_{R,\lambda}(\omega, \mathbf{k}) = -G_{E,\lambda}(i\omega_n \to \omega + i\epsilon, \mathbf{k})$. $\Pi_{\mathrm{R}}(\omega, \mathbf{k})$ is obtained by the standard analytic continuation

$$\Pi_{\mathrm{R}}(\omega, \mathbf{k}) = \Pi(i\omega_n \to \omega + i0^+, \mathbf{k}), \tag{3.90}$$

with

$$\Pi(i\omega_n, \mathbf{k}) = \frac{1}{2}\sum\!\!\!\!\!\!\int_{\nu_m, \mathbf{k}} G(i\omega_n + i\nu_m)G(i\omega_n). \tag{3.91}$$

The Wightman function is

$$G^{\beta/2}_{W,\lambda}(\omega, \mathbf{k}) = \frac{\rho_\lambda(\omega, \mathbf{k})}{2\sinh(\beta\omega/2)} = e^{-\frac{\beta\omega}{2}} G^{21}_{W,\lambda}(\omega, \mathbf{k}), \tag{3.92}$$

where

$$G^{21}_{W,\lambda}(\omega, \mathbf{k}) = (1 + n(\omega))\rho_\lambda(\omega, \mathbf{k}). \tag{3.93}$$

To study the quantum critical regime, we will have to take the strong coupling limit, $v \to \infty$, in which the expression for the retarded Green's function of the Hubbard-Stratonovich field simplifies

$$G_{\mathrm{R},\lambda}(\omega, \mathbf{k}) = \frac{1}{\Pi_{\mathrm{R}}(\omega, \mathbf{k})}, \tag{3.94}$$

and the spectral density of the Hubbard-Stratonovich field can be approximated as

$$\rho_\lambda(\omega, \mathbf{k}) = -2\,\mathrm{Im}\left[\frac{1}{\Pi_{\mathrm{R}}(\omega, \mathbf{k})}\right] = \frac{2\,\mathrm{Im}\left[\Pi_{\mathrm{R}}\right]}{\mathrm{Im}\left[\Pi_{\mathrm{R}}\right]^2 + \mathrm{Re}\left[\Pi_{\mathrm{R}}\right]^2}. \tag{3.95}$$

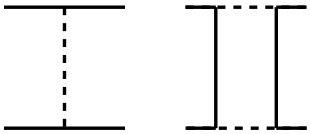

Figure 3.8: The contributions to the kernel of the OTOC. *a*) corresponds to $G_{W,\lambda}$ while *b*) corresponds to G_{eff} in (3.96).

The derivation of the Bethe-Salpeter equation for C (3.86) is given in [136] and the result is

$$C(\omega,p) = G_{\mathrm{R}}(k-p)G_{\mathrm{R}}(p)\left[1+\int_l R^{\mathrm{OTOC}}(p,l)C(\omega,l)\right], \tag{3.96}$$

whose kernel is given by the Wightman propagator of the auxiliary field and by

$$R^{\mathrm{OTOC}}(p,l) = \frac{1}{N}(G^{\beta/2}_{W,\lambda}(l-p) + G_{eff}(l,p)), \tag{3.97}$$

$$G_{eff}(l,p) = \int_{l'} G^{\beta/2}_{W}(l'-p)G^{\beta/2}_{W}(l-l')G^{\lambda}_{A}(l')G^{\lambda}_{R}(l'). \tag{3.98}$$

Similarly to the matrix model (3.66), in the low frequency limit $k=(\omega,\mathbf{0})$ and $\omega\to 0$, the product $G_{\mathrm{R}}(k-p)G_{\mathrm{R}}(p)$ can be approximated with [136]

$$G_{\mathrm{R}}(k-p)G_{\mathrm{R}}(p) \approx_{\omega\to 0} \frac{\pi}{E_{\mathbf{p}}}\frac{\delta(p_0^2-E_{\mathbf{p}}^2)}{(-i\omega+2\Gamma_{\mathbf{p}})}, \tag{3.99}$$

so the BSE (3.96) reads

$$(-i\omega+2\Gamma_{\mathbf{p}})C(p|\omega) = \frac{\pi}{E_{\mathbf{p}}}\delta(p_0^2-E_{\mathbf{p}}^2)\int\frac{d^3l}{(2\pi)^3}R^{\mathrm{OTOC}}(p,l)C(l|\omega). \tag{3.100}$$

By evaluating the delta function, (3.100) becomes

$$\begin{aligned}&(-i\omega+2\Gamma_{\mathbf{p}})C(\omega,\mathbf{p}) \\ &\quad-\int_{\mathbf{l}}\frac{1}{4E_{\mathbf{p}}E_{\mathbf{l}}}(R^{\mathrm{OTOC}}(E_{\mathbf{p}},\mathbf{p}|E_{\mathbf{l}},\mathbf{l}) + R^{\mathrm{OTOC}}(E_{\mathbf{p}},\mathbf{p}|-E_{\mathbf{l}},\mathbf{l})))C(\omega,\mathbf{l}) = \frac{\pi}{2E_{\mathbf{p}}^2}\end{aligned} \tag{3.101}$$

3.4.1 Transport in the O(N) vector model with the 2PI formalism

By computing the transport in this model we will show that , also in this case, there exists a mapping between the kernels of the OTOC and the kernels of transport,

$$R^{OTOC}(p,l) = \frac{\sinh(\beta l^0/2)}{\sinh(\beta p^0/2)} R^{\text{transp}}(p,l), \tag{3.102}$$

and that the interpretation of scrambling in terms of the kinetic theory equation depicted in fig. 3.7 holds also in the region above the quantum critical point.

Besides the methods we have already mentioned, *i.e.* the use of the finite temperature optical theorem by Jeon, and the more compact use of Schwinger-Keldysh formalism by Heinz and Wang, there is another way to approach the problem and it is by means of the two-particle irreducible $2PI$ effective action. The advantage of using this effective action is that, at the first non trivial truncation in the large N, or in weak coupling, it automatically provides the proper resummation of the relevant diagrams [117, 134, 180]. Moreover it can be proved that, in presence of gauge fields, the result obtained does not depend on the gauge fixing term and respects the Ward identities [116, 181]. In the present chapter we will focus only on a self-interacting spin-0 and spin-1/2 fields, but this formalism allows quite easily a generalization to gauge theories. We will use this method here.

In this section we will closely follow [134], though with the Lagrangian (3.84) in $(2+1)$ dimensions. The effective action in the bosonic case can be parametrized as follows [182]

$$\Gamma[G] = \frac{i}{2}\text{Tr}\ln G^{-1} + \frac{i}{2}\text{Tr}\, G_0^{-1}(G - G_0) + \Gamma_2[G], \tag{3.103}$$

where the 2PI part $\Gamma_2[G]$ can be expanded in $1/N$. For the model considered, (3.84), the expansion is [182]

$$\Gamma_2[G] = \Gamma_2[G]^{LO} + \Gamma_2[G]^{NLO} + ... \tag{3.104}$$

where the leading and the next to the leading order terms are depicted in

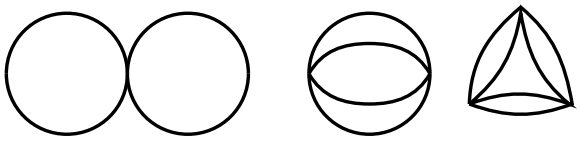

a) *b)*

Figure 3.9: The contributions to the 2PI effective action in the $1/N$ expansion. *a)* is the leading order contribution in $1/N$ and *b)* the next-to-the leading order.

fig. 3.9 and corresponds to the terms

$$\Gamma_2[G]^{LO} = -\frac{v}{2N}\int_x G_{mm}(x,x)G_{nn}(x,x) \tag{3.105}$$

$$\Gamma_2[G]^{NLO} = \frac{i}{2}\mathrm{Tr}\left[-\frac{4iv}{N}\Pi - \left(\frac{4iv}{N}\Pi\right)^2 - \left(\frac{4iv}{N}\Pi\right)^3 - ...\right] = \frac{i}{2}\mathrm{Tr}\ln\mathbf{B}. \tag{3.106}$$

In (3.106) the bubble diagram $\Pi(x,y)$, depicted in 3.10, is

$$\Pi(x,y) = \frac{1}{2}G_{ab}(x,y)G_{ab}(x,y), \tag{3.107}$$

and we defined the auxiliary bilocal field $\mathbf{B}(x,y)$ as follows

$$\mathbf{B}(x,y) = \delta_{\mathcal{C}}(x-y) + \frac{4iv}{N}\,\Pi(x,y). \tag{3.108}$$

The inverse of $\mathbf{B}(x,y)$ has a very intuitive physical meaning: by defining

$$D(x,y) = -\frac{2iv}{N}\,\mathbf{B}(x,y)^{-1} \tag{3.109}$$

and using the identity $\int_y \mathbf{B}(x,y)\mathbf{B}(y,z)^{-1} = \delta_{\mathcal{C}}(x-z)$, we readily obtain that the correlator D,which we will now refer to as auxiliary field, satisfies the following equation, depicted in fig. 3.11,

$$D(x,y) = \frac{4iv}{N}\left(\delta(x-y) - \int_z \Pi(x,z)D(z,y)\right). \tag{3.110}$$

From the effective action (3.104) and the corresponding large N expansion (3.105), we can obtain the integral equation for the truncated 4-point

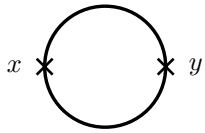

Figure 3.10: The bubble diagram $\Pi(x, y)$ contributions to the 2PI effective action in the $1/N$ expansion.

function

$$\Gamma^{(4)}_{ab;cd}(x, y; x', y') = \Lambda_{ab;cd}(x, y; x', y') + \frac{1}{2}\int_{ww'zz'} \Lambda_{ab;ef}(x, y; w, z) G_{ee'}(w, w') G_{ff'}(z, z') \Gamma^{(4)}_{e'f';cd}(w', z'; x', y') \tag{3.111}$$

The previous expression is quite general and can be used both in Imaginary Time Formalism (ITF) and in the Closed Time Path (CTP) formalism, without any restriction on the number of time folds. So, by properly adding the indices that parametrize the SK contour, the previous equation gives the BSE for any time-ordered or out-of-time ordered correlation function in the large N expansion for a bosonic theory. By imposing the extremization of the effective action (3.173), we obtain the Schwinger-Dyson equation

$$G^{-1}_{ab}(x, y) = G^{-1}_{0,ab}(x, y) - \Sigma_{ab}(x, y), \tag{3.112}$$

with the free propagator being

$$G^{-1}_{0,ab}(x, y) = -\delta_{ab}(\Box_x + 4v^2/g^2)\delta^4(x - y). \tag{3.113}$$

The self-energies are defined as functional derivatives of the 2PI effective action (3.104) with respect to the bilocal field G_{ab}

$$\Sigma_{ab}(x, y) = 2i\frac{\delta\Gamma_2[G]}{\delta G_{ab}(x, y)}, \tag{3.114}$$

and the kernels of the (3.111) can be obtained by a further functional derivative with respect to G

$$\Lambda_{ab;cd}(x, y; x', y') = \frac{\delta\Sigma_{ab}(x, y)}{\delta G_{cd}(x', y')}. \tag{3.115}$$

Figure 3.11: The diagrammatic recursive expression of the propagator $D(x, y)$ (3.110).

Up to this point, the expressions are still in real time and the BSE for the amputated 4-point function (3.111) is very lengthy and contains several terms. Nevertheless, since we are interested in the late time physics, most of these terms are negligible. This statement is the equivalent to the pinching pole approximation. In order to use it, it is convenient to move into momentum space and use the Matsubara formalisms, for which an analogue of the pinching pole approximation was derived in [115]. In momentum space, the correlation function is

$$G(i\omega_n, \mathbf{p}) = \frac{1}{\omega_n^2 + \mathbf{p}^2 + 4\frac{v^2}{g^2} + \Sigma(i\omega_n, \mathbf{p})}. \tag{3.116}$$

The self energy contributions are computed using (3.114) and read

$$\Sigma^{LO}(i\omega_n, \mathbf{p}) = 2v \sum\!\!\!\!\!\!\int_{\nu_m, \mathbf{k}} G(i\nu_m, \mathbf{k}) \tag{3.117}$$

$$\Sigma^{NLO}(i\omega_n, \mathbf{p}) = -\sum\!\!\!\!\!\!\int_{\nu_m, \mathbf{k}} G(i\omega_n + i\nu_m, \mathbf{p} + \mathbf{k}) D(i\nu_n, \mathbf{k}). \tag{3.118}$$

The correlation function D is obtained by inverting the (3.110), choosing the Matsubara contour and going into momentum space

$$D(i\omega_n, \mathbf{p}) = \frac{1}{-\frac{N}{4v} - \Pi(i\omega_n, \mathbf{p})}. \tag{3.119}$$

Finally, the bubble diagram is

$$\Pi(i\omega_n, \mathbf{p}) = \frac{N}{2} \sum\!\!\!\!\!\!\int_{\nu_m, \mathbf{k}} G(i\omega_n + i\nu_m, \mathbf{p} + \mathbf{k}) G(i\nu_m, \mathbf{k}). \tag{3.120}$$

From now on we will use the following convention: with capital case momenta we indicate momenta in imaginary time formalism, $P = (i\omega_n, \mathbf{p})$, where $\omega_n = 2\pi n T$ is the Matsubara frequency. With lower case, instead, we indicate momenta after the analytic continuation to Lorentzian signature.

The amputated 4-point function is related to 3-point vertex function by the following identity

$$\Gamma_{ab}(P+Q,P) = 2\delta_{ab} + \sum_{n'} \int_{\mathbf{l}} G(L+Q)G(L)\Gamma^{(4)}_{cc,ab}(L,P;Q) \tag{3.121}$$

By inserting the BSE for the $\Gamma^{(4)}_{cc,ab}$ into the previous expression, we obtain a BSE for the 3-point vertex

$$\Gamma_{ab}(P+Q,P) = 2\delta_{ab} + \frac{1}{2}\sum_{n'} \int_{\mathbf{l}} G(L+Q)\Gamma_{cd}(L+Q,L)G(L)\Lambda_{cd;ab}. \tag{3.122}$$

Parametrizing the vertex as

$$\Gamma_{ab}(P+Q,P) = 2\delta_{ab}\Gamma(P+Q,P) \tag{3.123}$$

we can thus derive the BSE for the diagonal part $\Gamma(P+Q,P)$ by simply substituting the previous expression in (3.122) and contracting with δ_{ab}

$$\Gamma(P+Q,P) = 1 + \frac{1}{2N}\sum_{n'} \int_{\mathbf{l}} G(L+Q)\Gamma(L+Q,L)G(L)\Lambda_{cc;aa}(L,P;Q). \tag{3.124}$$

By means of (3.115), the leading and next-to-leading order contribution to the kernel of the integral equation are

$$\begin{aligned}\Lambda_{cd;ab}(L,P;Q) = &-\frac{4v}{N}\delta_{ab}\delta_{cd} + (\delta_{ac}\delta_{bd} + \delta_{ad}\delta_{bc})D(L-P) \\ &+ 2\delta_{ab}\delta_{cd}D(R)D(R+Q)G(L-R)G(R-P),\end{aligned}$$

whose diagonal parts, depicted in fig. 3.12, are

$$\Lambda^{LO}_{cc;aa}(L,P;Q) = -4vN,$$
$$\Lambda^{NLO}_{cc;aa}(L,P;Q) = 2ND(L-P) + 2N^2 D(R)D(R+Q)G(L-R)G(R-P).$$

First, in order to compare with the results of [136], we observe that it is convenient to take the N dependence out of D in (3.119) and of the bubble loop in (3.120), $D \to D/N$ and $\Pi \to N\Pi$. The correlation functions of the auxiliary field D are identical to the correlation functions of the Hubbard-Stratonovich field λ of the Lagrangian (3.85), as can be see by comparing (3.89) and (3.91) with (3.119) and (3.120)

$$D(i\omega_n, \mathbf{p}) = G_\lambda(i\omega_n, \mathbf{p}). \tag{3.125}$$

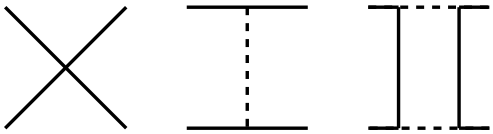

Figure 3.12: The contributions to the kernel of the 4-point function in the 2PI formalism. *a)* corresponds to $\Lambda^{LO}_{cc;aa}(L,P;Q)$, while *b)* and *c)* to the two terms in $\Lambda^{NLO}_{cc;aa}(L,P;Q)$. As we will show, *a)* will be subleading with respect to *b)* and *c)* after the analytic continuation to real frequencies.

Moreover, we include the factor of $1/2$ in front of the kernels (3.124) and we have

$$\begin{aligned}\Lambda^{LO}(L,P;Q) \equiv \frac{1}{2}\Lambda^{LO}_{cc;aa}(L,P;Q) =& -2vN,\\ \Lambda^{NLO}(L,P;Q) \equiv \frac{1}{2}\Lambda^{NLO}_{cc;aa}(L,P;Q) =& G_\lambda(L-P)\\ &+ G_\lambda(R)G_\lambda(R+Q)G(L-R)G(R-P).\end{aligned}$$

The BSE for the 3-point vertex has thus the form

$$\Gamma(P+Q,P) = 1+\frac{1}{N}\sum_{n'}\int_{\mathbf{l}} G(L+Q)\Gamma(L+Q,L)G(L)\left[\Lambda^{LO}+\Lambda^{NLO}(L,P;Q)\right]. \tag{3.126}$$

Now, we multiply the bare vertex Γ with the propagators in the loop, as depicted in fig 3.13, which in Euclidean is

$$\begin{aligned}\int_p \tilde{G}(p+q,p) &= \sum\!\!\!\!\!\!\int_{p_n,\mathbf{p}} \tilde{G}(ip_n+i\nu_{n'},ip_n)|_{i\nu_{n'}\to q_0+i0^+}\\ &= \sum\!\!\!\!\!\!\int_{p_n,\mathbf{p}} G(ip_n+i\nu_{n'})\Gamma(ip_n+i\nu_{n'},ip_n)G(ip_n)|_{i\nu_{n'}\to q_0+i0^+}.\end{aligned} \tag{3.127}$$

This function satisfies the following BSE, which can be obtained from (3.126),

$$\begin{aligned}\tilde{G}(P+Q,P) =& G(P+Q)G(P)\\ &\left[1+\frac{1}{N}\sum_{n'}\int_{\mathbf{l}}\tilde{G}(L+Q,L)\left[\Lambda^{LO}+\Lambda^{NLO}(L,P;Q)\right]\right].\end{aligned} \tag{3.128}$$

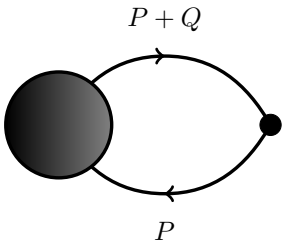

Figure 3.13: Diagrammatic representation of the full correlator $\tilde{G}$ as a function of the vertex 3-point function $\Gamma(P+Q,P)$.

This integral equation is still expressed in imaginary time and it has to be analytically continued after performing the Matsubara sum. Following the techniques developped in [115, 183], and described in Appendix 3.E, we obtain the following result

$$\tilde{G}(p+q,p) = G_R(p+q)G_A(p) \left[1+\frac{1}{N}\int_l (n(l_0-p_0)-n(l_0))\Lambda^{NLO}(l,p)\tilde{G}(l+q,l)\right], \tag{3.129}$$

where

$$\Lambda^{NLO}(l,p) = \rho_\lambda(l-p) + \int_s (n(p_0-s_0)-n(l_0-s_0))\rho(p-s)\rho(l-s) \times G_{R,\lambda}(s)G_{A,\lambda}(s). \tag{3.130}$$

A closer look to the (3.129) shows that the leading order rung, $\Lambda^{LO}_{cc;aa}$, does not contribute to the BSE in real time. This is because the $\Lambda^{LO}_{cc;aa}$ does not contain any *pinching-pole* singularity and it is subleading with respect to $\Lambda^{NLO}_{cc;aa}$. As shown in appendix 3.B, massaging the product $(n(l_0-p_0)-n(l_0))\Lambda^{NLO}(l,p)$ gives a kernel

$$(n(l_0-p_0)-n(l_0))\Lambda^{NLO}(l,p) = \frac{n_B(l_0)}{n_B(p_0)} \times \left[G^{21}_\lambda(l-p) + \int_s G_{12}(p-s)G_{21}(l-s)G_{R,\lambda}(s)G_{A,\lambda}(s)\right]. \tag{3.131}$$

Thus the BSE for transport is

$$\tilde{G}(p+q,p) = G_R(p+q)G_A(p)\left[1+\int_l R^{\text{transp}}(l,p)\tilde{G}(l+q,l)\right], \tag{3.132}$$

with

$$R^{\text{transp}}(p,l) = \frac{1}{N}\frac{n_B(l_0)}{n_B(p_0)} \times \left[G^{21}_{\lambda}(l-p) + \int_s G_{12}(p-s)G_{21}(l-s)G_{R,\lambda}(s)G_{A,\lambda}(s)\right]. \tag{3.133}$$

Now we want to compare it with the kernel of the OTOC (3.97). By using (3.92) and

$$G^{\beta/2}(l-p) = e^{-\beta(l_0-p_0)/2}G^{21}_W(l-p) = e^{\beta(l_0-p_0)/2}G^{12}_W(l-p), \tag{3.134}$$

we obtain that the kernel R^{transp} and the kernel $R^{\text{OTOC}}(l,p)$ are related by the simple relation

$$R^{\text{OTOC}}(l,p) = \frac{\sinh(\beta l_0/2)}{\sinh(\beta p_0/2)}R^{\text{transp}}(l,p), \tag{3.135}$$

which proves our claim. Substituting the previous relation into the on-shell BSE for chaos, we obtain the following equation

$$(-i\omega + 2\Gamma_{\mathbf{p}})C(\omega,\mathbf{p}) - \int_{\mathbf{l}}\frac{\sinh(\beta E_{\mathbf{l}}/2)}{\sinh(\beta E_{\mathbf{l}}/2)}\frac{1}{4E_{\mathbf{p}}E_{\mathbf{l}}} \times (R^{\text{transp}}(E_{\mathbf{p}},\mathbf{p}|E_{\mathbf{l}},\mathbf{l}) - R^{\text{transp}}(E_{\mathbf{p}},\mathbf{p}|-E_{\mathbf{l}},\mathbf{l})))C(\omega,\mathbf{l}) = \frac{\pi}{2E^2_{\mathbf{p}}} \tag{3.136}$$

Similarly to section 3.3.2, we can find the following solution for the BSE for $\tilde{G}(p+q,p)$ (3.132)

$$(-i\omega + 2\Gamma_{\mathbf{p}})\tilde{G}(\omega,\mathbf{p}) - \int_{\mathbf{l}}\frac{1}{4E_{\mathbf{p}}E_{\mathbf{l}}} \times (R^{\text{transp}}(E_{\mathbf{p}},\mathbf{p}|E_{\mathbf{l}},\mathbf{l}) + R^{\text{transp}}(E_{\mathbf{p}},\mathbf{p}|-E_{\mathbf{l}},\mathbf{l})))\tilde{G}(\omega,\mathbf{l}) = \frac{\pi}{2E^2_{\mathbf{p}}}. \tag{3.137}$$

In the next section we explore the kinetic theory limit of both BSEs.

3.4.2 Kinetic theory analysis

In this section we show how the different the sign in (3.136) and (3.137) corresponds to a different counting in the collision integral of the kinetic equation, as depicted respectively in fig. 3.7 and fig. 3.6. We write the kernel (3.130) as follows

$$\Lambda^{NLO}(r,p) = \rho_\lambda(r-p) + \int_l (n(l^0) - n(r^0-p^0+l^0))\rho(l)\rho(r-p+l)|G_{\lambda,R}(p-l)|^2. \tag{3.138}$$

The imaginary part of the bosonic self-energy is given by (3.120) after performing the Matsubara sum and taking the analytical continuation to obtain the retarded bubble

$$\mathrm{Im}\Pi_R(r-p) = -\frac{1}{4}\int_L (n(l^0) - n(r^0 - p^0 + l^0))\rho(l)\rho(r-p+l). \quad (3.139)$$

Since

$$\rho_\lambda(p) = -2\,\mathrm{Im}\Pi_{R,\lambda}(p)|G_{\lambda,R}(p)|^2, \quad (3.140)$$

by inserting $\int_{L'} \delta^3(r+l-l'-p)$, (3.138) becomes

$$\Lambda^{NLO}(r,p) = \frac{1}{2}\int_{l,l'} (n(l^0) - n(l'^0))\rho(l)\rho(l')[|G_{\lambda,R}(r-p)|^2 + |G_{\lambda,R}(r-l')|^2 + |G_{\lambda,R}(r+l)|^2]. \quad (3.141)$$

We recognize the term inside parenthesis as the (*off-shell*) scattering amplitude for the process $(r,l) \to (p,l')$, as depicted in fig. 3.14

$$|\mathcal{T}_{(r,l)\to(p,l')}|^2 = \frac{1}{N}(|G_{\lambda,R}(r-p)|^2 + |G_{\lambda,R}(r-l')|^2 + |G_{\lambda,R}(r+l)|^2), \quad (3.142)$$

and we can rewrite the kernel as

$$\Lambda^{NLO}(r,p) = \frac{N}{2}\int_{l,l'} (n(l^0) - n(l'^0))\rho(l)\rho(l')|\mathcal{T}_{(r,l)\to(p,l')}|^2. \quad (3.143)$$

Now we express the kernel of the *on-shell* BSE for chaos (3.136) and transport (3.137) gain and loss processes. Thus we focus on

$$\frac{1}{4E_{\mathbf{p}}E_{\mathbf{l}}}(R^{\mathrm{transp}}(E_{\mathbf{p}},\mathbf{p}|E_{\mathbf{l}},\mathbf{l}) \pm R^{\mathrm{transp}}(E_{\mathbf{p}},\mathbf{p}|-E_{\mathbf{l}},\mathbf{l}))). \quad (3.144)$$

Using the definition of R^{transp} (3.133) we obtain

$$\begin{aligned}
&\int_{\mathbf{r},\mathbf{l},\mathbf{l}'} \frac{1}{2E_{\mathbf{p}}}(n(E_{\mathbf{r}}-E_{\mathbf{p}}) - n(E_{\mathbf{r}}))(n(E_{\mathbf{l}}) - n(E_{\mathbf{l}'}))\delta(E_{\mathbf{r}}+E_{\mathbf{l}}-E_{\mathbf{p}}-E_{\mathbf{l}'}) \\
&\qquad \times \frac{1}{N}(|G_{\lambda,R}(E_{\mathbf{r}}-E_{\mathbf{p}})|^2 + |G_{\lambda,R}(E_{\mathbf{r}}-E_{\mathbf{l}'})|^2 + |G_{\lambda,R}(E_{\mathbf{r}}+E_{\mathbf{l}})|^2) \\
\mp \frac{1}{2}&\int_{\mathbf{r},\mathbf{l},\mathbf{l}'} \frac{1}{2E_{\mathbf{p}}}(n(E_{\mathbf{r}}+E_{\mathbf{p}}) - n(E_{\mathbf{r}}))(n(E_{\mathbf{l}}) - n(-E_{\mathbf{l}'}))\delta(E_{\mathbf{l}}+E_{\mathbf{l}'}-E_{\mathbf{p}}-E_{\mathbf{r}}) \\
&\qquad \times \frac{1}{N}(|G_{\lambda,R}(E_{\mathbf{r}}+E_{\mathbf{p}})|^2 + |G_{\lambda,R}(E_{\mathbf{r}}-E_{\mathbf{l}'})|^2 + |G_{\lambda,R}(E_{\mathbf{r}}-E_{\mathbf{l}})|^2).
\end{aligned} \quad (3.145)$$

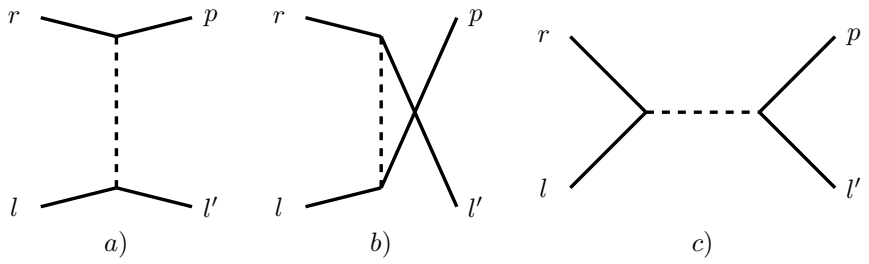

Figure 3.14: The contributions to the kernel of the kinetic equation of the creation of a particle with momentum p, first line in eq. (3.147).

By using the identities satisfied by the Bose-Einstein distribution function and listed in Appendix 3.B, we can rewrite the previous expression as follows

$$\begin{aligned}
&\frac{1}{1+n(E_{\mathbf{p}})}\int_{\mathbf{r},\mathbf{l},\mathbf{l}'}\frac{1}{2E_{\mathbf{p}}}n(E_{\mathbf{l}'})(1+n(E_{\mathbf{r}}))(1+n(E_{\mathbf{l}}))\delta(E_{\mathbf{r}}+E_{\mathbf{l}}-E_{\mathbf{p}}-E_{\mathbf{l}'})\\
&\qquad\times\frac{1}{N}(|G_{\lambda,R}(E_{\mathbf{r}}-E_{\mathbf{p}})|^2+|G_{\lambda,R}(E_{\mathbf{r}}-E_{\mathbf{l}'})|^2+|G_{\lambda,R}(E_{\mathbf{r}}+E_{\mathbf{l}})|^2)+\\
&\mp\frac{1/2}{1+n(E_{\mathbf{p}})}\int_{\mathbf{r},\mathbf{l},\mathbf{l}'}\frac{1}{2E_{\mathbf{p}}}n(E_{\mathbf{r}})(1+n(E_{\mathbf{l}}))(1+n(E_{\mathbf{l}'}))\delta(E_{\mathbf{l}}+E_{\mathbf{l}'}-E_{\mathbf{p}}-E_{\mathbf{r}})\\
&\qquad\times\frac{1}{N}(|G_{\lambda,R}(E_{\mathbf{r}}-E_{\mathbf{l}})|^2+|G_{\lambda,R}(E_{\mathbf{r}}-E_{\mathbf{l}'})|^2+|G_{\lambda,R}(E_{\mathbf{r}}+E_{\mathbf{p}})|^2).
\end{aligned}\tag{3.146}$$

By comparison with (3.62), it is clear that the first two lines of (3.146) correspond to R^{gain}, while the third and fourth lines of (3.146) are identical to the second line of (3.62).

$$\begin{aligned}
&\frac{1}{1+n(E_{\mathbf{p}})}\int_{\mathbf{r},\mathbf{l},\mathbf{l}'}\frac{1}{2E_{\mathbf{p}}}n(E_{\mathbf{l}'})(1+n(E_{\mathbf{r}}))(1+n(E_{\mathbf{l}}))\delta(E_{\mathbf{r}}+E_{\mathbf{l}}-E_{\mathbf{p}}-E_{\mathbf{l}'})\\
&\qquad\qquad|\mathcal{T}_{(r,l)\to(p,l')}|^2\\
&\pm\frac{1/2}{1+n(E_{\mathbf{p}})}\int_{\mathbf{r},\mathbf{l},\mathbf{l}'}\frac{1}{2E_{\mathbf{p}}}n(E_{\mathbf{r}})(1+n(E_{\mathbf{l}}))(1+n(E_{\mathbf{l}'}))\delta(E_{\mathbf{l}}+E_{\mathbf{l}'}-E_{\mathbf{p}}-E_{\mathbf{r}})\\
&\qquad\qquad|\mathcal{T}_{(r,p)\to(l,l')}|^2.
\end{aligned}\tag{3.147}$$

In order to complete the analysis of the BSE, we need to understand the $2\Gamma_{\mathbf{p}}$ contribution in (3.136) and (3.137). To do so, since $\Gamma_{\mathbf{p}}=$

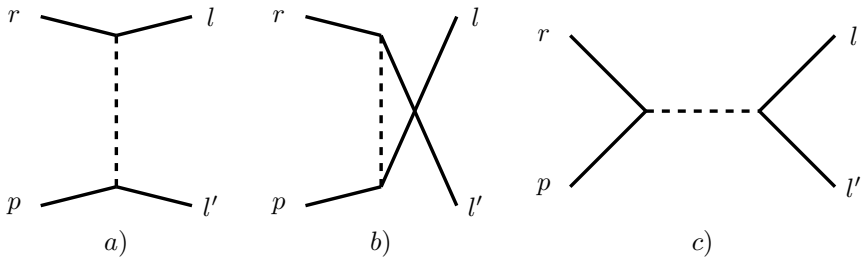

Figure 3.15: The contributions to the kernel of the kinetic equation of the annihilation of a particle with momentum p, last line in eq. (3.147).

$-\mathrm{Im}\Sigma^{NLO}(E_{\mathbf{p}},\mathbf{p})/E_{\mathbf{p}}$, we start by inspecting $\mathrm{Im}\Sigma^{NLO}(E_{\mathbf{p}},\mathbf{p})$

$$\mathrm{Im}\,\Sigma^{NLO}(P)=\frac{1}{2}\int_R \rho(R)\rho_\lambda(R-P)(n(r^0)-n(r^0-p^0)). \tag{3.148}$$

By means of (3.140), expanding $\mathrm{Im}\,\Pi_R$ with (3.139) and retaining only the kinematically allowed terms, we arrive to

$$\begin{aligned}\mathrm{Im}\Sigma^{NLO}(E_{\mathbf{p}},\mathbf{p})=\frac{1}{4}\int_{\mathbf{l},\mathbf{l}',\mathbf{r}} \\ \Big[(n(E_{\mathbf{l}})-n(E_{\mathbf{l}'}))(n(E_{\mathbf{r}})-n(E_{\mathbf{r}}-E_{\mathbf{p}}))|D_R(E_{\mathbf{r}}-E_{\mathbf{p}},\mathbf{r}-\mathbf{p})|^2 \\ \times\delta(E_{\mathbf{r}}+E_{\mathbf{l}}-E_{\mathbf{p}}-E_{\mathbf{l}'}) \\ +(n(E_{\mathbf{l}})-n(-E_{\mathbf{l}'}))(n(-E_{\mathbf{r}})-n(-E_{\mathbf{r}}-E_{\mathbf{p}}))|D_R(E_{\mathbf{r}}+E_{\mathbf{p}},\mathbf{r}+\mathbf{p})|^2 \\ \times\delta(E_{\mathbf{r}}+E_{\mathbf{p}}-E_{\mathbf{l}}-E_{\mathbf{l}'}) \\ +(n(-E_{\mathbf{l}})-n(-E_{\mathbf{l}'}))(n(E_{\mathbf{r}})-n(E_{\mathbf{r}}-E_{\mathbf{p}}))|D_R(E_{\mathbf{r}}-E_{\mathbf{p}},\mathbf{r}-\mathbf{p})|^2 \\ \times\delta(E_{\mathbf{r}}+E_{\mathbf{l}'}-E_{\mathbf{p}}-E_{\mathbf{l}})\Big].\end{aligned} \tag{3.149}$$

We can now use the properties of the Bose-Einstein distribution function

listed in Appendix 3.B. Thus,

$$\begin{aligned}\mathrm{Im}\Sigma^{NLO}(E_{\mathbf{p}},\mathbf{p}) = \frac{1}{4}\int_{\mathbf{l},\mathbf{l}',\mathbf{r}} \\ \Bigg[-\frac{1}{1+n(E_{\mathbf{p}})} n(E_{\mathbf{l}'})(1+n(E_{\mathbf{r}}))(1+n(E_{\mathbf{l}}))|D_R(E_{\mathbf{r}}-E_{\mathbf{p}},\mathbf{r}-\mathbf{p})|^2 \\ \times \delta(E_{\mathbf{r}}+E_{\mathbf{l}}-E_{\mathbf{p}}-E_{\mathbf{l}'}) \\ -\frac{1}{1+n(E_{\mathbf{p}})} n(E_{\mathbf{r}})(1+n(E_{\mathbf{l}}))(1+n(E_{\mathbf{l}'}))|D_R(E_{\mathbf{r}}+E_{\mathbf{p}},\mathbf{r}+\mathbf{p})|^2 \\ \times \delta(E_{\mathbf{r}}+E_{\mathbf{p}}-E_{\mathbf{l}}-E_{\mathbf{l}'}) \\ -\frac{1}{1+n(E_{\mathbf{p}})} n(E_{\mathbf{l}})(1+n(E_{\mathbf{r}}))(1+n(E_{\mathbf{l}'}))|D_R(E_{\mathbf{r}}-E_{\mathbf{p}},\mathbf{r}-\mathbf{p})|^2 \\ \times \delta(E_{\mathbf{r}}+E_{\mathbf{l}'}-E_{\mathbf{p}}-E_{\mathbf{l}}) \Bigg].\end{aligned} \tag{3.150}$$

Finally, by properly relabelling the integration variables, we recognize the expression

$$\begin{aligned}\mathrm{Im}\Sigma^{NLO}(E_{\mathbf{p}},\mathbf{p}) = \\ -\frac{1/4}{1+n(E_{\mathbf{p}})}\int_{\mathbf{r},\mathbf{l},\mathbf{l}'} n(E_{\mathbf{r}})(1+n(E_{\mathbf{l}}))(1+n(E_{\mathbf{l}'}))\delta(E_{\mathbf{l}}+E_{\mathbf{l}'}-E_{\mathbf{p}}-E_{\mathbf{r}}) \\ \times (|D_{\mathrm{R}}(E_{\mathbf{r}}-E_{\mathbf{l}})|^2+|D_{\mathrm{R}}(E_{\mathbf{r}}-E_{\mathbf{l}'})|^2+|D_{\mathrm{R}}(E_{\mathbf{r}}+E_{\mathbf{p}})|^2).\end{aligned} \tag{3.151}$$

The thermal width is

$$\begin{aligned}2\Gamma_{\mathbf{p}} = \frac{1/2}{1+n(E_{\mathbf{p}})}\int_{\mathbf{r},\mathbf{l},\mathbf{l}'} \frac{1}{2E_{\mathbf{p}}} n(E_{\mathbf{r}})(1+n(E_{\mathbf{l}}))(1+n(E_{\mathbf{l}'})) \\ \delta(E_{\mathbf{l}}+E_{\mathbf{l}'}-E_{\mathbf{p}}-E_{\mathbf{r}}) \times (|D_{\mathrm{R}}(E_{\mathbf{r}}-E_{\mathbf{l}})|^2+|D_{\mathrm{R}}(E_{\mathbf{r}}-E_{\mathbf{l}'})|^2+ \\ |D_{\mathrm{R}}(E_{\mathbf{r}}+E_{\mathbf{p}})|^2).\end{aligned} \tag{3.152}$$

Thus, also for the bosonic $O(N)$ vector model we have identified the gain and loss contribution in the kernel of the BSE

$$R^{\wedge}(\mathbf{p},\mathbf{l}) = \frac{1}{4E_{\mathbf{p}}E_{\mathbf{l}}} R^{\mathrm{transp}}(\mathbf{p},E_{\mathbf{p}}|\mathbf{l},E_{\mathbf{l}}), \tag{3.153}$$

$$R^{\vee}(\mathbf{p},\mathbf{l}) = -\frac{1}{4E_{\mathbf{p}}E_{\mathbf{l}}} R^{\mathrm{transp}}(\mathbf{p},E_{\mathbf{p}}|\mathbf{l},-E_{\mathbf{l}}) + 2(2\pi)^2\delta^2(\mathbf{p}-\mathbf{l})\Gamma_{\mathbf{p}} \tag{3.154}$$

We can now rewrite the BSE for transport (3.137) and chaos (3.136) as kinetic equation with the following collision integrals

$$-i\omega\,\tilde{G}(\omega,\mathbf{p}) = \int_{\mathbf{l}} (R^{\wedge}(\mathbf{p},\mathbf{l}) - R^{\vee}(\mathbf{p},\mathbf{l}))\,\tilde{G}(\omega,\mathbf{l}), \tag{3.155}$$

$$-i\omega\,C(\omega,\mathbf{p}) = \int_{\mathbf{l}} (R^{\wedge}(\mathbf{p},\mathbf{l}) + R^{\vee}(\mathbf{p},\mathbf{l}) - 4(2\pi)^2\delta^2(\mathbf{p}-\mathbf{l})\Gamma_{\mathbf{p}})C(\omega,\mathbf{l}) \tag{3.156}$$

3.4.3 Towards the bosonic Quantum Critical Point

In the previous sections we showed that also in the $O(N)$ model scrambling and transport are related at the level of Green's function. From this, it is possible to derive the kinetic theory interpretation of scrambling as in equation (3.156). The derivation of these identities merely rely on two hypothesis: the large N limit and the hydrodynamic limit. Consequently, our results hold as far as these hypothesis are satisfied. As mentioned in the introduction, close to the QCP transport can be studied by analytically continuing the hydrodynamic computation, performed outside the quantum critical regime, into the quantum critical regime. In the $O(N)$ model, this regime is obtained in the strong coupling limit ($v \to \infty$) of the Lagrangian (3.84),

$$\mathcal{L} = \frac{1}{2}(\partial\phi_a)^2 - \frac{v}{2N}\left(\phi_a^2 - \frac{N}{g}\right)^2, \tag{3.157}$$

at the value of the critical coupling g_c. This value can be obtained by imposing that the thermal mass vanishes, and equals to [136]

$$\frac{1}{g_c} = \frac{\Lambda}{4\pi}, \tag{3.158}$$

Λ being the physical cutoff. In the quantum critical region, away from zero temperature, the thermal mass becomes $\mu^2 \approx 0.962T$ [136]. The only changes in the BSE, both for transport and chaos, are thus the value of the thermal mass in the *on-shell* condition, $E_{\mathbf{p}} = \mathbf{p}^2 + \mu^2$ and the expression of the Hubbard-Stratonovich propagator, which enters the transition amplitude squared:

$$D(i\omega_n,\mathbf{k}) = \frac{1}{-1/4v - \Pi(i\omega_n,\mathbf{k})} \overset{v\to\infty}{=} -\frac{1}{\Pi(i\omega_n,\mathbf{k})}. \tag{3.159}$$

This completes our proof that, also in the proximity of a bosonic quantum critical point, scrambling can be microscopically understood in terms of counting the gross (energy) exchange.

3.5 Gross-Neveu model at the quantum critical point

Having discussed the case of bosonic quantum critical point in the previous section, we now turn our attention to fermionic quantum critical points. Although the great successes of the bosonic $O(N)$ vector model to capture critical phenomena within the Landau-Ginsburg-Wilson paradigm, whose critical regime can be described entirely in terms of fluctuations of a bosonic order parameter, it is nowadays clear that this does not cover all possible scenarios. Over the last years, it became evident that a plethora of interesting phenomena involve massless fermionic excitations at low energies coupled to vectorial [184–186], real [187, 188] or complex [189–195] order parameters. Those systems are described by fermionic quantum critical points which the bosonic $O(N)$ vector model fails to capture. In this context, a main role is played by the Gross-Neveu model (GN) [196] and the Gross-Neveu-Yukawa model (GNY) [197]. Specifically, here we study the Gross-Neveu model in $(2+1)$ dimension with N flavours of Dirac fermions. The Lagrangian is, in Euclidean time,

$$\mathcal{L}_{GN} = \psi^\dagger_{i,\alpha}(\partial_\tau - i\boldsymbol{\sigma}\cdot\boldsymbol{\nabla})_{\alpha\beta}\psi_{i,\beta} - \frac{g}{4N}(\psi^\dagger_{i,\alpha}\sigma^z_{\alpha\beta}\psi_{i,\beta})^2 \tag{3.160}$$

where we indicated with Latin letters the flavours indices, with Greek letters the spin indices and ψ_i is a two-component Dirac spinor. We also assume the summation over repeated indices. Moreover the Pauli matrices are defined as usual $\boldsymbol{\sigma} = (\sigma^x, \sigma^y)$. This action is symmetric under $x \to -x$ and $\psi_i \to i\sigma^x\psi_i$. This model has a quantum phase transition separating the Dirac semimetal phase and the gapped insulator with broken Z_2 symmetry. By introducing a Hubbard-Stratonovich field ϕ to decouple the quartic interaction,

$$\mathcal{L}_{GN} = \psi_i^{\dagger\,\alpha}(\partial_\tau - i\sigma\cdot\nabla)_\alpha^{\ \beta}\psi_{i,\beta} + \frac{1}{g}\phi^2 + \frac{1}{\sqrt{N}}\phi\,(\psi^\dagger\sigma^z\psi), \tag{3.161}$$

the action stays symmetric under $x \to -x$, $\psi_i \to i\sigma^x\psi_i$ and $\phi \to -\phi$. The expectation value of the field ϕ is thus the order parameter of the spontaneous Z_2 symmetry breaking. As the Z_2 symmetry can be related to the inversion symmetry of a honeycomb lattice, it captures the physics of graphene, graphene-like materials [198, 199] and cold atoms in optical lattice [200–202]. A related theory is the Gross-Neveu-Yukawa (GNY) model, whose matter content is represented by massless Dirac fermions

and a massive Φ^4 boson, minimally coupled with Lagrangian

$$\mathcal{L}_{GNY} = \psi^\dagger_{i,\alpha}(\partial_\tau - i\sigma\cdot\nabla)_{\alpha\beta}\psi_{i,\beta} + \frac{1}{2}(\partial\phi)^2 + \frac{1}{2}(\nabla\Phi)^2 + \frac{m^2}{2}\Phi^2 + \frac{\lambda}{4!N}\Phi^4 + \frac{u}{\sqrt{N}}\Phi\,\psi^\dagger_{i,\alpha}\sigma^z_{\alpha\beta}\psi_{i,\beta}. \tag{3.162}$$

The GNY model describes also other symmetry classes, as chiral Heisenberg and chiral XY universality classes [203, 204]. Assuming small λ and as far as we focus on the long wavelength and low energy (compared to the mass m) degrees of freedom, we can integrate out the boson in (3.162). The result is (3.161) with the identification $g = \sqrt{2}u/m$. The low-energy, long wavelength limit of the GNY model thus coincide with the GN model [203] and the results of this section apply to all classes of systems previously mentioned.

3.5.1 Brief review of many-body chaos in GN

By means of the introduction of a scalar field to decouple the interaction in (3.161), the Lagrangian can be expressed as (3.161). The properties of many-body chaos for the GN model in $2+1$ dimensions, in the Lagrangian form of (3.161), were investigated in [137]. There, the authors computed the OTOC in the large N limit,

$$f^\beta_\alpha(t) = \frac{1}{N^2}\sum_{ij,\gamma}\int d^2x \times \mathrm{Tr}\left[\rho^{1/2}\{\psi_{i\alpha}(t,\mathbf{x}), \psi^{\dagger\,\gamma}_j(0,\mathbf{0})\}\rho^{1/2}\{\psi_{j\gamma}(0,\mathbf{0}), \psi^{\dagger\,\beta}_i(t,\mathbf{x}),\}\right], \tag{3.163}$$

by deriving an integro-differential equation (BSE),

$$f_\alpha{}^\beta(\nu;\omega,\mathbf{p}) = \frac{1}{N}S_R(\omega+\nu,\mathbf{p})_\alpha{}^\gamma S_A(\omega,\mathbf{p})_\delta{}^\beta \times\left[\delta^\delta_\gamma + \int_{\omega',\mathbf{r}}\Lambda^{OTOC}(\nu;\omega,\mathbf{p},\omega',\mathbf{r})^{\delta\gamma'}_{\gamma\delta'} f_{\gamma'}{}^{\delta'}(\nu;\omega',\mathbf{r})\right]. \tag{3.164}$$

The kernel of the BSE is

$$\Lambda^{OTOC}(r,p)^{\delta\gamma'}_{\gamma\delta'} = (\sigma^z)^{\gamma'}_\gamma(\sigma^z)^\delta_{\delta'}D_W^{\beta/2}(p-r) + \int_l(\sigma^z\,S_W^{\beta/2}(p-l)\sigma^z)^\delta_\gamma\,(\sigma^z\,S_W^{\beta/2}(r-l)\sigma^z)^{\gamma'}_{\delta'}\,D^R(l+q)D^A(l), \tag{3.165}$$

where the retarded Greens function of the fermion and the boson are respectively[4]

$$S_R(t,\mathbf{x})^{\beta}_{\alpha}\delta_{ij} = -i\theta(t)\langle\rho\{\psi_{i\alpha}(t,\mathbf{x}),\psi_j^{\dagger\,\beta}\}\rangle, \tag{3.166}$$

$$D_R(t,\mathbf{x}) = -i\theta(t)\langle\rho[\phi(t,\mathbf{x}),\phi]\rangle, \tag{3.167}$$

and the Wightman functions are computed with insertion separated by half of the thermal circle

$$S_W(t,\mathbf{x})^{\beta}_{\alpha}\delta_{ij} = -i\langle\sqrt{\rho}\,\psi_{i\alpha}(t,\mathbf{x})\,\sqrt{\rho}\psi_j^{\dagger\,\beta}\rangle, \tag{3.168}$$

$$D_W(t,\mathbf{x}) = -i\langle\sqrt{\rho}\,\phi(t,\mathbf{x})\sqrt{\rho}\,\phi\rangle. \tag{3.169}$$

In momentum space, the Wightman functions can be expressed in terms of the spectral function

$$S_W(\omega,\mathbf{p})^{\beta}_{\alpha}\delta_{ij} = \frac{\rho^{\beta}_{\alpha}(\omega,\mathbf{p})}{2\cosh(\beta\omega/2)}, \tag{3.170}$$

$$D_W(\omega,\mathbf{p}) = \frac{\rho_D(\omega,\mathbf{p})}{2\sinh(\beta\omega/2)}, \tag{3.171}$$

which satisfy $\rho(\omega,\mathbf{p}) = -2\mathrm{Im}G_R(\omega,\mathbf{p})$ and $\rho_D(\omega,\mathbf{p}) = -2\mathrm{Im}D_R(\omega,\mathbf{p})$.

3.5.2 Hydrodynamic transport in GN model

In this section we use the 2PI formalism to derive the transport equation for the GN model in $2+1$ dimensions to compare with the OTOC. The effective action for the original GN Lagrangian

$$\mathcal{L}_{GN} = \psi^{\dagger}_{i,\alpha}(\partial_\tau - i\sigma\cdot\nabla)_{\alpha\beta}\psi_{i,\beta} - \frac{g}{4N}(\psi^{\dagger}_{i,\alpha}\sigma^{z}_{\alpha\beta}\psi_{i,\beta})^2 \tag{3.172}$$

can be parametrized as follows [115, 182]

$$\Gamma[S] = -i\mathrm{Tr}\ln S^{-1} - i\mathrm{Tr}\ln S_0^{-1}(S - S_0) + \Gamma_2[S], \tag{3.173}$$

S_0 being the free propagator in the Euclidean time and S the full dressed 2-point function, satisfying

$$S^{-1} = S_0^{-1} - \Sigma. \tag{3.174}$$

In (3.173), $\Gamma_2[S]$ includes the contribution of all the amputated 2-particle irreducible diagrams (2PI) with exact propagators on the internal lines.

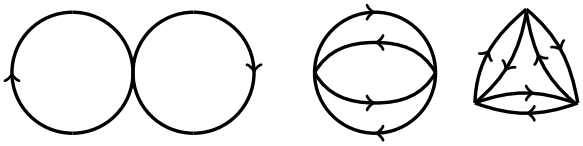

Figure 3.16: The contributions to the 2PI effective action in the $1/N$ expansion. *a*) is the leading order contribution Γ^{LO} and *b*) the first terms in the series of next-to-the leading order Γ^{NLO}.

In the 2PI formalism, the self energies can be derived as functional derivative of the 2PI effective action

$$\Sigma_{ij|\alpha\beta}(x,y) \equiv -i\frac{\delta\Gamma_2[S]}{\delta S_{ji|\beta\alpha}(y,x)}. \tag{3.175}$$

In the following, unless differently specified, we will use a condensed notation, using Latin letters both flavour, spin and space-time indices. This simplifies the previous expression as

$$\Sigma_{ij} = -i\frac{\delta\Gamma_2[S]}{\delta S_{ji}}. \tag{3.176}$$

The 4-point vertex function is defined as the amputated connected 4-point function and satisfies the following functional equation

$$\Gamma^{(4)}_{ij,kl} = \Lambda_{ij,kl} - \Lambda_{ij,ef}S^{ff'}S^{e'e}\Gamma^{(4)}_{f'e',kl}, \tag{3.177}$$

in which the kernel is by definition the functional derivative of the self energy with respect to the bilocal field S

$$\Lambda_{ij,kl} \equiv i\frac{\delta^2\Gamma_2[S]}{\delta S_{ji}\delta S_{lk}} = -\frac{\delta\Sigma_{kl}}{\delta S_{ji}}. \tag{3.178}$$

Now, following [182], we perform the large N expansion of the effective action considering the leading and the next-to-leading order, which diagrammatically are expressed in fig. 3.16

[4]For a review on the convention for fermions at finite temperature, see the Appendix 3.A.

Figure 3.17: The diagrammatic recursive expression of the propagator $D(x, y)$.

$$\Gamma_2^{LO}[S] = \frac{g}{4N}\int_x \mathrm{Tr}[\sigma^z S(x,x)\sigma^z S(x,x)], \tag{3.179}$$

$$\Gamma_2^{NLO}[S] = \frac{i}{2}\mathrm{Tr}\ln\mathcal{B}, \tag{3.180}$$

and

$$\mathcal{B}(x,y) = \delta_{\mathcal{C}}(x-y) - \frac{ig}{2N}\Pi(x,y), \tag{3.181}$$

$$\Pi(x,y) = -\mathrm{Tr}[S(x,y)\sigma^z S(y,x)\sigma^z] = -S(x,y)_{ab|\alpha\beta}\,\sigma^z_{\beta\gamma}\,S(y,x)_{ba|\gamma\delta}\,\sigma^z_{\delta\alpha}. \tag{3.182}$$

In the last line we have explicited the indices to stress the structure of the Hilbert space we are considering and we note that the functional derivative of the bubble diagram satifies

$$\frac{\delta\Pi(x',y')}{\delta S_{lk|\beta\alpha}(y,x)} = -2\delta(x'-y)\delta(y'-x)(\sigma^z_{\alpha\gamma}\,S(x,y)_{kl|\gamma\delta}\,\sigma^z_{\delta\beta}). \tag{3.183}$$

Let's now compute the leading and next-to-the leading order contribution to the self-energies (for the sake of clarity we will write the indices in the intermediate steps)

$$\Sigma^{LO}_{kl|\gamma\delta}(x',y') = -i\frac{\delta\Gamma_2^{LO}[S]}{\delta S_{lk|\delta\gamma}(y',x')} = -i\frac{g}{2N}\delta(x'-y')(\sigma^z\,S(x',y')_{kl}\,\sigma^z)_{\gamma\delta}, \tag{3.184}$$

$$\begin{aligned}\Sigma^{NLO}_{kl|\gamma\delta}(x',y') &= -i\frac{\delta\Gamma_2^{NLO}[S]}{\delta S_{lk|\delta\gamma}(y',x')} = \frac{-ig}{4N}\int_{w,z}\mathcal{B}^{-1}(z,w)\frac{\delta\Pi(w,z)}{\delta S_{lk|\delta\gamma}(y',x')}\\ &= \frac{ig}{2N}\mathcal{B}^{-1}(x',y')(\sigma^z\,S(x',y')_{kl}\,\sigma^z)_{\gamma\delta}\\ &= D(x',y')(\sigma^z\,S(x',y')_{kl}\,\sigma^z)_{\gamma\delta},\end{aligned} \tag{3.185}$$

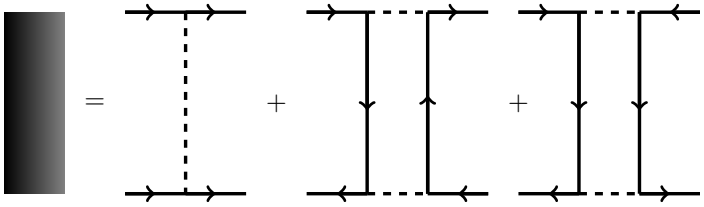

Figure 3.18: Diagrammatic representation of the kernel Λ^{NLO} computed in (3.188).

where we have defined $D(x',y') = \frac{ig}{2N}\mathcal{B}^{-1}(x',y')$. Inserting (3.181) into the identity $\mathcal{B}^{-1}\mathcal{B} = 1$, we obtain an integral equation for $D(x,y)$, depicted in fig. 3.17

$$D(x,y) = \frac{ig}{2N}\left[\delta_{\mathcal{C}}(x-y) + \int_z \Pi(x,z)D(z,y)\right]. \tag{3.186}$$

This two-point function is an effective description of the polarization bubble and, as we will see, corresponds to the propagator of an Hubbard-Stratonovich field introduced to linearise the quadratic interaction in the action. Now we compute the kernel using (3.178). The leading order contribution is simply

$$\begin{aligned}\Lambda^{LO}_{ij;kl|\alpha\beta;\gamma\delta}(x,y;x',y') &= i\frac{\delta\Sigma^{LO}_{kl|\gamma\delta}(x',y')}{\delta S_{ji|\beta\alpha}(y,x)} \\ &= \frac{g}{2N}\delta_{kj}\delta_{li}\delta(x'-y')\delta(x'-y)\delta(y'-x)(\sigma^z)_{\gamma\beta}(\sigma^z)_{\alpha\delta}.\end{aligned} \tag{3.187}$$

Similarly to the bosonic $O(N)$ case, this will not affect the final BSE after the Matsubara sum. Going to the NLO term,

$$\begin{aligned}&\Lambda^{NLO}_{ij;kl|\alpha\beta;\gamma\delta}(x,y;x',y') = i\frac{\delta\Sigma^{NLO}_{kl|\gamma\delta}(x',y')}{\delta S_{ji|\beta\alpha}(y,x)} \\ &= \delta_{kj}\delta_{li}\delta(x'-y)\delta(y'-x)(\sigma^z)_{\gamma\beta}(\sigma^z)_{\alpha\delta}D(x',y') - \int_{w'z'}\delta(w'-y)\delta(z'-x) \\ &\quad (D(x',w')D(z',y') + D(y',w')D(z',x'))(\sigma^z\, S(x,y)_{ij}\,\sigma^z)_{\alpha\beta}(\sigma^z\, S(x',y')_{kl}\,\sigma^z)_{\gamma\delta} \\ &= \delta_{kj}\delta_{li}\delta(x'-y)\delta(y'-x)(\sigma^z)_{\gamma\beta}(\sigma^z)_{\alpha\delta}D(x',y') \\ &\quad - 2(\sigma^z\, S(x,y)_{ij}\,\sigma^z)_{\alpha\beta}(\sigma^z\, S(x',y')_{kl}\,\sigma^z)_{\gamma\delta}\, D(x',y)D(x,y').\end{aligned} \tag{3.188}$$

We now go to momentum space and we observe that the the 4-point function $\Gamma^{(4)}_{kl,ij}(R,P;Q)$ is related to the 3-point vertex $\Gamma_{ij}(P+Q,P)$, as shown in fig. 3.19.

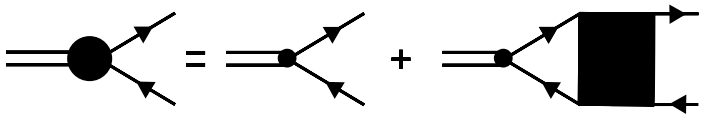

Figure 3.19: Representation of the relation among the 3-vertex and the amputated 4-point connected Green's function.

Since more convenient, we will focus on the latter

$$\Gamma_{ij}(P+Q,P) = \Gamma^0_{ij}(\mathbf{p}) - \sum\!\!\!\!\!\!\int_R S(R+Q)\Gamma^0(\mathbf{r})_{kl}S(R)\Gamma^{(4)}_{kl,ij}(R,P;Q) \quad (3.189)$$

where $\Gamma^0_{ij}(\mathbf{p})$ is the coupling between the fermionic fields and the external operator. For instance, in the shear viscosity the operator is the stress energy and we have $\Gamma^0_{ij}(\mathbf{p}) = \frac{1}{2}(\sigma^i p^j + \sigma^j p^i - \delta^{ij}\sigma\cdot\mathbf{p})$. If we want to focus on the density operator, defined as (3.6)

$$\rho(x,p) = \int_y e^{-ipy}\mathrm{Tr}(\psi(x-y/2)\bar{\psi}(x+y/2)) = \int_k e^{ikx}\mathrm{Tr}(\psi(p+k/2)\bar{\psi}(p-k/2)), \quad (3.190)$$

such insertion is just δ_{ij}. From now on we will focus on the latter. As shown in fig. 3.20, this vertex satisfies the following integral equation

$$\Gamma_{ij}(P+Q,P) = \Gamma^0_{ij}(\mathbf{p}) - \sum\!\!\!\!\!\!\int_R S(R+Q)\Gamma(R+Q,R)S(R)\Lambda_{kl,ij}(R,P;Q) \quad (3.191)$$

The previous equation is written in imaginary time. To obtain the real time value, a sum over Matsubara frequencies is required, which corresponds to the proper choice of the analytical continuation. It can be shown by induction that, because of the form of the BSE, $\Gamma_{ij}(P+Q,P)$ has branch cuts both in $\mathrm{Im}(p_0) = 0$ and $\mathrm{Im}(p_0+q^0) = 0$. An analysis similar to the previous section on the $O(N)$ model can be carried out. Also in this case, in the long time limit corresponding to $q_0 \to 0$, the pinching pole approximation selects only one analytic continuation of the vertex in the imaginary time formalism, which corresponds to $i(p_0+q_0) \to p_0+q_0+i0$ and $ip_0 \to p_0 - i0$. Consequently, the shear viscosity which is obtained by the resummed skeleton diagram we have focused on but with a different insertion $\Gamma^{(0)ij}$

$$G_{\pi\pi}(Q) = -\sum\!\!\!\!\!\!\int_P \mathrm{Tr}(S(P+Q)\Gamma_{ij}(P+Q,P)S(P)\Gamma^{(0)ij}(\mathbf{p})). \quad (3.192)$$

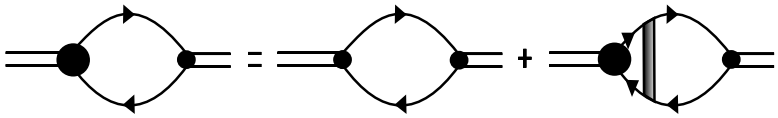

Figure 3.20: BSE for the 3-point vertex function.

In the limit of vanishing external momentum, it is given by

$$\lim_{q_0,\mathbf{q}\to 0} G_{\pi\pi}(q_0,\mathbf{q}) = -\lim_{q_0,\mathbf{q}\to 0}\int_p \mathrm{Tr}(S_R(p+q)\Gamma_{ij}(p_0+q_0+i0,p_0-i0)S_A(p)\Gamma^{(0)ij}(\mathbf{p})), \tag{3.193}$$

and the shear viscosity is determined by

$$\eta = \frac{1}{20}\lim_{q_0,\mathbf{q}\to 0}\frac{\partial}{\partial q^0}\mathrm{Re}G_{\pi\pi}(q_0,\mathbf{0}) \tag{3.194}$$

Now, let's go back to the evaluation of the density-density correlation function and define the vertex as

$$\tilde{\Gamma}^{\beta}_{\alpha}(p+q,p) = S_R(p+q)^{\gamma}_{\alpha}\Gamma^{\delta}_{\gamma}(p_0+q_0+i0,p_0-i0)S_A(p)^{\beta}_{\delta}. \tag{3.195}$$

The BSE for the (3.195), after the analytical continuation we discussed above is

$$\tilde{\Gamma}^{\beta}_{\alpha}(p+q,p) = S_R(p+q)^{\gamma}_{\alpha}S_A(p)^{\beta}_{\delta}\left[\delta^{\delta}_{\gamma} + \int_r \tilde{\Lambda}(r,p)^{\delta\gamma'}_{\gamma\delta'}\tilde{\Gamma}(r+q,r)^{\delta'}_{\gamma'}\right] \tag{3.196}$$

where the analytically continued kernel reads

$$\begin{aligned}\tilde{\Lambda}(r,p)^{\delta\gamma'}_{\gamma\delta'} = (n_B(r^0-p^0)+n_F(r^0))\Bigg[&(\sigma^z)^{\gamma'}_{\gamma}(\sigma^z)^{\delta}_{\delta'}\rho_B(r-p) \\ &+ 2\int_l (n_F(p^0-l^0)-n_F(r^0-l^0))(\sigma^z\,\rho_F(p-l)\sigma^z)^{\delta}_{\gamma} \\ &\times(\sigma^z\,\rho_F(r-l)\sigma^z)^{\gamma'}_{\delta'}D^R(l+q)D^A(l)\Bigg].\end{aligned} \tag{3.197}$$

This result is similar to the kernel of the BSE for the shear viscosity obtained in [181] for $q=0$ for the large N_f QCD. The main difference, besides the dimensionality, can be reduced to the presence of vector boson in QCD, while here the boson is simply a scalar. This suggests that the analysis performed in this section can be extended to the case of QCD in

the large N_f limit. After some algebra, and using the identities written in Appendix 3.B, we arrive to the final expression

$$\tilde{\Gamma}^{\beta}_{\alpha}(p+q,p) = S_R(p+q)^{\gamma}_{\alpha} S_A(p)^{\beta}_{\delta} \left[\delta^{\delta}_{\gamma} + \int_r \tilde{\Lambda}(r,p)^{\delta\gamma'}_{\gamma\delta'} \tilde{\Gamma}(r+q,r)^{\delta'}_{\gamma'}\right], \quad (3.198)$$

where the kernel is

$$\tilde{\Lambda}(r,p)^{\delta\gamma'}_{\gamma\delta'} = (\sigma^z)^{\gamma'}_{\gamma}(\sigma^z)^{\delta}_{\delta'} D_W(p-r) + \int_l (\sigma^z S_W(p-l)\sigma^z)^{\delta}_{\gamma} (\sigma^z S_W(r-l)\sigma^z)^{\gamma'}_{\delta'} D^R(l+q) D^A(l).$$

We now proceed by showing the relation between the BSE for transport and the BSE for scrambling. If we express the Wightman functions D_W and S_W in terms of the symmetrized ones, after some simplification we find

$$\tilde{\Gamma}^{\beta}_{\alpha}(p+q,p) = S_R(p+q)^{\gamma}_{\alpha} S_A(p)^{\beta}_{\delta} \left[\delta^{\delta}_{\gamma} + \int_r \frac{\cosh(\beta \mathrm{p}^0/2)}{\cosh(\beta \mathrm{r}^0/2)} \Lambda^{OTOC}(r,p)^{\delta\gamma'}_{\gamma\delta'} \tilde{\Gamma}(r+q,r)^{\delta'}_{\gamma'}\right], \quad (3.199)$$

$$\Gamma^{\beta}_{OTOC,\alpha}(p+q,p) = S_R(p+q)^{\gamma}_{\alpha} S_A(p)^{\beta}_{\delta} \left[\delta^{\delta}_{\gamma} + \int_r \Lambda^{OTOC}(r,p)^{\delta\gamma'}_{\gamma\delta'} \Gamma^{\delta'}_{OTOC,\gamma'}(r+q,r)\right] \quad (3.200)$$

where $\Lambda^{OTOC}(r,p)$ is the kernel of the BSE for OTOC in the Gross-Neveu model (3.165) derived in [137]

$$\Lambda^{OTOC}(r,p)^{\delta\gamma'}_{\gamma\delta'} = (\sigma^z)^{\gamma'}_{\gamma}(\sigma^z)^{\delta}_{\delta'} D^{\beta/2}_W(p-r) + \int_l (\sigma^z S^{\beta/2}_W(p-l)\sigma^z)^{\delta}_{\gamma} (\sigma^z S^{\beta/2}_W(r-l)\sigma^z)^{\gamma'}_{\delta'} D^R(l+q) D^A(l).$$

This proves our claim that relates the kernel of the BSE of the OTOC to the kernel of the BSE of the bilocal density operator.

3.5.3 The kernel in the helicity basis

Now, lets' try to understand the physics behind the factor $\frac{\cosh(\beta \mathrm{p}^0/2)}{\cosh(\beta \mathrm{r}^0/2)}$ for the fermionic case. In the bosonic case, the factor $\frac{\sinh(\beta \mathrm{p}^0/2)}{\sinh(\beta \mathrm{r}^0/2)}$ automatically provided the natural weighting for the ansatz (and the consequent sign flip in the kernel). The fermion case it is slightly more elaborate, since this factor is even with respect to the momenta p_0 and l_0.

In this section we show which are the proper ansätze that give the correct solutions respectively for the case of transport and chaos. For this we need to rewrite the kernel (3.197) in a way that allows us to interpret the physics

$$\tilde{\Lambda}(r,p)^{\delta\gamma'}_{\gamma\delta'} = (n_B(r^0-p^0)+n_F(r^0))\Bigg[(\sigma^z)^{\gamma'}_{\gamma}(\sigma^z)^{\delta}_{\delta'}\rho_B(r-p) + 2\int_{L,L'}(n_F(l^0)-n_F(l'^0))(\sigma^z\,\rho_F(l)\sigma^z)^{\delta}_{\gamma}\,(\sigma^z\,\rho_F(l')\sigma^z)^{\gamma'}_{\delta'}|D^R(p-l)|^2\Bigg]. \tag{3.201}$$

The fermionic spectral density, which is

$$\rho_F(p^0,\mathbf{p}) = \frac{\not{p}\pi}{|\mathbf{p}|}(\delta(p^0-|\mathbf{p}|)-\delta(p^0+|\mathbf{p}|)) = \not{p}\rho(p^0,\mathbf{p}), \tag{3.202}$$

can be written in the helicity basis as follows

$$\rho_F(l^0,\mathbf{l}) = 2\pi\sum_a \mathcal{P}_a(\mathbf{l})\delta(l^0-a|\mathbf{l}|), \tag{3.203}$$

where we introduced the projector into the helicity basis

$$\mathcal{P}_a(\mathbf{k}) = \frac{1+a\sigma\cdot\hat{\mathbf{k}}}{2}. \tag{3.204}$$

Substituting this in the second line of the expression of (3.201), with the additional substitution

$$(\sigma^z\,\rho_F(l)\sigma^z)^{\delta}_{\gamma} = 2\pi\sum_a(\sigma^z\mathcal{P}_a(\mathbf{l})\sigma^z)^{\delta}_{\gamma}\delta(l^0-a|\mathbf{l}|), \tag{3.205}$$

allows us to rewrite the kernel as

$$\tilde{\Lambda}(r,p)^{\delta\gamma'}_{\gamma\delta'} = (n_B(r^0-p^0)+n_F(r^0))\Bigg[(\sigma^z)^{\gamma'}_{\gamma}(\sigma^z)^{\delta}_{\delta'}\rho_B(r-p) \tag{3.206}$$

$$+2\sum_{a,b}\int_{l,l'}(n_F(l^0)-n_F(l'^0))\,(\sigma^z\mathcal{P}_b(\mathbf{l})\sigma^z)^{\delta}_{\gamma}(\sigma^z\mathcal{P}_a(\mathbf{l}')\sigma^z)^{\gamma'}_{\delta'}$$

$$(2\pi)^2\delta(l'^0-a|\mathbf{l}'|)\delta(l^0-b|\mathbf{l}|)|D^R(p-l)|^2\Bigg]. \tag{3.207}$$

Similarly as before, the spectral function of the auxiliary field, ρ_B, encodes the fermionic bubble diagram and can be rewritten as

$$\rho_B(r-p) = -2\,|D_R(r-p)|^2\,\mathrm{Im}\Pi_R(r-p). \tag{3.208}$$

In order to find the expression for the imaginary part of the bosonic self energy $\mathrm{Im}\Pi_R(p)$, we can use formula (3.182) in Fourier space and perform the Matsubara sum, which is done in Appendix 3.C. After analytically continuing to obtain the retarded contribution, we can take the imaginary part and the expression reads

$$\mathrm{Im}\Pi_R(p) = -\frac{1}{2}\sum_{a,b}\int_{\mathbf{l}} K_{ab}(\mathbf{l},\mathbf{l}+\mathbf{p})\,(n_F(a|\mathbf{l}|) - n_F(b|\mathbf{l}+\mathbf{p}|)) \\ (2\pi)\delta(p^0 + a|\mathbf{l}| - b|\mathbf{l}+\mathbf{p}|), \tag{3.209}$$

where we have defined the following quantity

$$K_{ab}(\mathbf{p},\mathbf{l}) = \mathrm{Tr}[\sigma^z P_a(\mathbf{p})\sigma^z P_b(\mathbf{l})] = \frac{1-ab\,\hat{p}\cdot\hat{l}}{2} \tag{3.210}$$

and use it to simplify the expression of the $\mathrm{Im}\Pi_R(r-p)$ by introducing the momentum $\mathbf{l}'$ and imposing the energy conservation:

$$\begin{aligned}\mathrm{Im}\Pi_R(r-p) &= -\frac{1}{2}\sum_{a,b}\int_{\mathbf{l}} K_{ab}(\mathbf{l},\mathbf{l}+\mathbf{r}-\mathbf{p})\,(n_F(a|\mathbf{L}|) - n_F(b|\mathbf{l}+\mathbf{r}-\mathbf{p}|)) \\ &\qquad \times (2\pi)\delta(r^0 - p^0 + a|\mathbf{l}| - b|\mathbf{l}+\mathbf{r}-\mathbf{p}|) \\ &= -\frac{1}{2}\sum_{a,b}\int_{\mathbf{l},\mathbf{l}'} K_{ab}(\mathbf{l},\mathbf{l}')\,(n_F(a|\mathbf{l}|) - n_F(b|\mathbf{l}'|))(2\pi)^2 \\ &\qquad \delta^2(\mathbf{l}'+\mathbf{p}-\mathbf{r}-\mathbf{l}) \times (2\pi)\delta(r^0 - p^0 + a|\mathbf{l}| - b|\mathbf{l}'|).\end{aligned} \tag{3.211}$$

We can now write the kernel (3.207) as

$$\begin{aligned}\tilde{\Lambda}(r,p)^{\delta\gamma'}_{\gamma\delta'} &= (n_B(r^0-p^0) + n_F(r^0))\sum_{a,b}\int_{l,l'}(n_F(l^0) - n_F(l'^0)) \\ &\times \delta(l^0 - a|\mathbf{l}|)\delta(l'^0 - b|\mathbf{l}'|)(2\pi)^3\delta^3(r+l-p-l')\Big((\sigma^z)^{\gamma'}_{\gamma}(\sigma^z)^{\delta}_{\delta'}K_{ab}(\mathbf{l},\mathbf{l}') \\ &\times |D^R(r-p)|^2 + 2(\sigma^z\mathcal{P}_b(\mathbf{l})\sigma^z)^{\delta}_{\gamma}(\sigma^z\mathcal{P}_a(\mathbf{l}')\sigma^z)^{\gamma'}_{\delta'}|D^R(p-l)|^2\Big),\end{aligned}$$

which, by relabelling the momenta l and l', can be rewritten in terms of the s, t and u-channels

$$\tilde{\Lambda}(r,p)^{\delta\gamma'}_{\gamma\delta'} = (n_B(r^0-p^0)+n_F(r^0))\sum_{c,d}\int_{l,l'}(n_F(l^0)-n_F(l'^0)) \tag{3.212}$$

$$\times\,\delta(l^0-c|\mathbf{l}|)\delta(l'^0-d|\mathbf{l}'|)(2\pi)^3\delta^3(r+l-p-l')$$

$$\times\Bigg((\sigma^z)^{\gamma'}_{\gamma}(\sigma^z)^{\delta}_{\delta'}K_{cd}(\mathbf{l},\mathbf{l}')|D^R(r-p)|^2+(\sigma^z\mathcal{P}_c(\mathbf{l})\sigma^z)^{\delta}_{\gamma}(\sigma^z\mathcal{P}_d(\mathbf{l}')\sigma^z)^{\gamma'}_{\delta'}$$

$$\times|D^R(r-l')|^2+(\sigma^z\mathcal{P}_d(\mathbf{l}')\sigma^z)^{\delta}_{\gamma}(\sigma^z\mathcal{P}_c(\mathbf{l})\sigma^z)^{\gamma'}_{\delta'}|D^R(r+l)|^2\Bigg). \tag{3.213}$$

We have massaged the kernel in a way that it is easy to project into helical basis. This is a convenient way to analyze both the *on-shell* BSEs, which we do in the next section.

3.5.4 The physics behind the analytic continuation

To recapitulate, in the previous section we saw that the off-shell BSE for transport are, up to a similarity transformation, the same

$$\Gamma^{\beta}_{OTOC,\alpha}(p+q,p) = S_R(p+q)^{\gamma}_{\alpha}S_A(p)^{\beta}_{\delta}\Bigg[\delta^{\delta}_{\gamma}+\int_r\frac{\cosh(\beta r_0/2)}{\cosh(\beta p_0/2)} \tag{3.214}$$

$$\times\,\Lambda(r,p)^{\delta\gamma'}_{\gamma\delta'}\,\Gamma^{\delta'}_{OTOC,\gamma'}(r+q,r)\Bigg],$$

$$\Gamma^{\beta}_{\alpha}(p+q,p) = S_R(p+q)^{\gamma}_{\alpha}S_A(p)^{\beta}_{\delta}\Bigg[\delta^{\delta}_{\gamma}+\int_r\Lambda(r,p)^{\delta\gamma'}_{\gamma\delta'}\,\Gamma^{\delta'}_{\gamma'}(r+q,r)\Bigg],$$

with a kernel that can be expressed as (3.212). Now we want to explicitly take the late time limit, $q_0\to 0$, and project both the BSEs (3.214) into the helical basis. To do so, we observe that the product of retarded and advanced Green's function in the pinching pole approximation can be written as [137]

$$S_R(p+q)^{\gamma}_{\alpha}S_A(p)^{\beta}_{\delta}\approx 2\pi\sum_a\mathcal{P}_a(\mathbf{p})^{\gamma}_{\alpha}\mathcal{P}_a(\mathbf{p})^{\beta}_{\delta}\frac{\delta(p^0-a|\mathbf{p}|)}{-iq^0+2\Gamma_{\mathbf{p},a}}. \tag{3.215}$$

Since the homogeneous equation is defined with momentum p on-shell, an obvious ansatz is,

$$\Gamma^{\beta}_{\alpha}(p+q,p) = \sum_{a} f_a(q^0, p_0, \mathbf{p}) \mathcal{P}_a(\mathbf{p})^{\beta}_{\alpha} \delta(p^0 - a\mathbf{p}). \tag{3.216}$$

This will turn out to be the solution that describes chaos. Substituting into Equation (3.214), one has

$$\begin{aligned}\sum_{a} f_a(q^0, p_0, \mathbf{p}) \mathcal{P}_a(\mathbf{p})^{\beta}_{\alpha} \delta(p^0 - a\mathbf{p}) = 2\pi \sum_{a} \mathcal{P}_a(\mathbf{p})^{\gamma}_{\alpha} \mathcal{P}_a(\mathbf{p})^{\beta}_{\delta} \frac{\delta(p^0 - a|\mathbf{p}|)}{-iq^0 + 2\Gamma_{\mathbf{p},a}} \\ \times \left[\delta^{\delta}_{\gamma} + \int_r \frac{\cosh(\beta r_0/2)}{\cosh(\beta r_0/2)} \Lambda(r,p)^{\delta\gamma'}_{\gamma\delta'} \right. \\ \left. \times \sum_{b} f_b(q^0, r_0, \mathbf{r}) \mathcal{P}_b(\mathbf{r})^{\delta'}_{\gamma'} \delta(r^0 - b\mathbf{r}) \right].\end{aligned} \tag{3.217}$$

We now study the a component of the above BSE and trace over the spin indices α, β

$$\begin{aligned}f_a(q^0, p_0, \mathbf{p}) \delta(p^0 - a\mathbf{p}) = 2\pi \frac{\delta(p^0 - a|\mathbf{p}|)}{-iq^0 + 2\Gamma_{\mathbf{p},a}} + \frac{\delta(p^0 - a|\mathbf{p}|)}{-iq^0 + 2\Gamma_{\mathbf{p},a}} \\ \times \int_r \frac{\cosh(\beta \mathbf{r}/2)}{\cosh(\beta \mathbf{p}/2)} \mathcal{P}_a(\mathbf{p})^{\gamma}_{\alpha} \mathcal{P}_a(\mathbf{p})^{\beta}_{\delta} \Lambda(r,p)^{\delta\gamma'}_{\gamma\delta'} \mathcal{P}_b(\mathbf{r})^{\delta'}_{\gamma'} \\ \sum_{b} f_b(q^0, r_0, \mathbf{r}) \delta(r^0 - b\mathbf{r}).\end{aligned} \tag{3.218}$$

We can define the effective kernel as $\Lambda_{ab}(r,p) = \mathcal{P}_a(\mathbf{p})^{\gamma}_{\alpha} \mathcal{P}_a(\mathbf{p})^{\alpha}_{\delta} \Lambda(r,p)^{\delta\gamma'}_{\gamma\delta'} \mathcal{P}_b(\mathbf{r})^{\delta'}_{\gamma'}$,

$$\begin{aligned}\Lambda_{ab}(r,p) = (n_B(r^0 - p^0) + n_F(r^0)) \sum_{c,d} \int_{l,l'} (n_F(l^0) - n_F(l'^0)) \delta(l^0 - c|\mathbf{l}|) \\ \times \delta(l'^0 - d|\mathbf{l}'|)(2\pi)^3 \delta^3(r + l - p - l') \\ \times \Big(K_{ab}(\mathbf{p}, \mathbf{r}) K_{cd}(\mathbf{l}, \mathbf{l}') |D^R(r-p)|^2 + K_{ac}(\mathbf{p}, \mathbf{l}) K_{bd}(\mathbf{r}, \mathbf{l}') |D^R(r-l')|^2 \\ + K_{bc}(\mathbf{r}, \mathbf{l}) K_{ad}(\mathbf{p}, \mathbf{l}) |D^R(r+l)|^2 \Big).\end{aligned} \tag{3.219}$$

In (3.219), momenta p and r are not on shell yet. We can use (3.219) to rewrite (3.218)

$$-iq^0 f_a(q^0, a\mathbf{p}, \mathbf{p}) = 2\pi + \sum_b \int_{\mathbf{r}} \frac{\cosh(\beta \mathbf{r}/2)}{\cosh(\beta \mathbf{p}/2)} \times \left(\Lambda_{ab}(\mathbf{r}, \mathbf{p}) - 2\Gamma_{\mathbf{r},a} (2\pi)^2 \delta^2(\mathbf{p} - \mathbf{r}) \delta_{ab} \right) f_b(q^0, b\mathbf{r}, \mathbf{r}), \tag{3.220}$$

having defined $\Lambda_{ab}(\mathbf{r}, \mathbf{p}) = \Lambda_{ab}(b|\mathbf{r}|, \mathbf{r}, a|\mathbf{p}|, \mathbf{p})$. By means of (3.219), it is easy to check the following properties of the kernel

$$\begin{aligned} \Lambda_{++}(\mathbf{r}, \mathbf{p}) &= \Lambda_{--}(\mathbf{r}, \mathbf{p}), \\ \Lambda_{-+}(\mathbf{r}, \mathbf{p}) &= \Lambda_{+-}(\mathbf{r}, \mathbf{p}), \end{aligned} \tag{3.221}$$

which are again consequences of the particle-hole symmetry. We observe that, at this stage, the ratios $\frac{\cosh(\beta \mathbf{r}/2)}{\cosh(\beta \mathbf{p}/2)}$ represents a similarity transformation, so it can be neglected since it does not affect the spectrum. Because of this, from now on we will drop this factor.

Before we show that (3.220) is the chaos BSE, we now consider another possible ansatz, which we will see is correct one for transport, that corresponds to (3.216) with the choice

$$f_a(q^0, p_0, \mathbf{p}) = a \tilde{f}_a(q^0, p_0, \mathbf{p}), \tag{3.222}$$

where the a labels the helicity. This leads to the following BSE (after multiplying for a and using $a^2 = 1$)

$$-iq^0 \tilde{f}_a(q^0, a\mathbf{p}, \mathbf{p}) = 2\pi a \sum_b \int_{\mathbf{r}} \left(ab \Lambda_{ab}(b\mathbf{r}, \mathbf{r}, a\mathbf{p}, \mathbf{p}) - 2\Gamma_{\mathbf{r},a} (2\pi)^2 \delta(\mathbf{p} - \mathbf{r}) \delta_{ab} \right) \tilde{f}_b(q^0, b\mathbf{r}, \mathbf{r}). \tag{3.223}$$

In the previous equation, the factor ab plays the analogous role of the factor $\frac{\sinh(\beta r_0/2)}{\sinh(\beta p_0/2)}$ for the bosonic case. We now prove the statement that (3.223) leads to the Boltzmann equation, while the other reproduces the OTOC. As before, the difference in the kernel is simply given by a different counting of the contribution of scattering processes, as shown in the cartoon in fig.

3.6 and 3.7. We start by expanding and using the identities

$$\begin{aligned}
-iq^0 f_+(q^0,\mathbf{p}) =& 2\pi \\
&+ \int_{\mathbf{r}} \Lambda_{++} f_+(q^0,\mathbf{r}) + \Lambda_{+-} f_-(q^0,\mathbf{r}) - 2\Gamma_{\mathbf{r}}(2\pi)^2\delta^2(\mathbf{p}-\mathbf{r}) f_+(q^0,\mathbf{r}), \\
-iq^0 f_-(q^0,\mathbf{p}) =& 2\pi \\
&+ \int_{\mathbf{r}} \Lambda_{+-} f_+(q^0,\mathbf{r}) + \Lambda_{++} f_-(q^0,\mathbf{r}) - 2\Gamma_{\mathbf{r}}(2\pi)^2\delta^2(\mathbf{p}-\mathbf{r}) f_-(q^0,\mathbf{r})
\end{aligned}$$

The sum $f(q^0,\mathbf{p}) = f_+(q^0,\mathbf{p}) + f_-(q^0,\mathbf{p})$ satisfies

$$-iq^0 f(q^0,\mathbf{p}) - \int_{\mathbf{r}} \left(\Lambda_{++} + \Lambda_{+-} - 2\Gamma_{\mathbf{r}}(2\pi)^2\delta^2(\mathbf{p}-\mathbf{r}) \right) f(q^0,\mathbf{r}) = 4\pi. \tag{3.224}$$

The eigenvalue of this integral equation correspond to the Lyapunov exponent of the theory. To derive the transport relaxation time, instead, we have

$$\begin{aligned}
-iq^0 \tilde{f}_+(q^0,\mathbf{p}) &= \int_{\mathbf{r}} \Lambda_{++} \tilde{f}_+(q^0,\mathbf{r}) - \Lambda_{+-} \tilde{f}_-(q^0,\mathbf{r}) - 2\Gamma_{\mathbf{r}}(2\pi)^2\delta^2(\mathbf{p}-\mathbf{r}) \tilde{f}_+(q^0,\mathbf{r}), \\
-iq^0 \tilde{f}_-(q^0,\mathbf{p}) &= \int_{\mathbf{r}} -\Lambda_{+-} \tilde{f}_+(q^0,\mathbf{r}) + \Lambda_{++} \tilde{f}_-(q^0,\mathbf{r}) - 2\Gamma_{\mathbf{r}}(2\pi)^2\delta^2(\mathbf{p}-\mathbf{r}) \tilde{f}_-(q^0,\mathbf{r}).
\end{aligned}$$

The sum $\tilde{f}(q^0,\mathbf{p}) = \tilde{f}_+(q^0,\mathbf{p}) + \tilde{f}_-(q^0,\mathbf{p})$ satisfies

$$-iq^0 \tilde{f}(q^0,\mathbf{p}) = \int_{\mathbf{r}} \left(\Lambda_{++} - \Lambda_{+-} - 2\Gamma_{\mathbf{r}}(2\pi)^2\delta^2(\mathbf{p}-\mathbf{r}) \right) \tilde{f}(q^0,\mathbf{r}). \tag{3.225}$$

The eigenvalues of this integral equation corresponds to the relaxation times of the theory, *i.e.* the integral operator is nothing but the collision integral of the Boltzmann equation. We now can continue with the interpretation of the ansatz (3.216) and (3.222) in terms of kinetic equations.

3.5.5 Kinetic theory analysis

We want to show that, using the notation of the previous sections,

$$\begin{aligned}
R^{\wedge}(\mathbf{p},\mathbf{r}) &= \Lambda_{++}(\mathbf{p},\mathbf{r}), \\
R^{\vee}(\mathbf{p},\mathbf{r}) &= \Lambda_{+-}(\mathbf{p},\mathbf{r}) + 2\Gamma_{\mathbf{r}}(2\pi)^2\delta^2(\mathbf{p}-\mathbf{r}).
\end{aligned} \tag{3.226}$$

The first line is straightforward to verify. Indeed, using the identity (valid for $a|\mathbf{p}| + d|\mathbf{l}'| = c|\mathbf{l}| + b|\mathbf{r}|$)

$$(n_B(b|\mathbf{r}| - a|\mathbf{p}|) + n_F(b|\mathbf{r}|))(n_F(c|\mathbf{l}|) - n_F(d|\mathbf{l}'|)) = \frac{1 - n_F(b|\mathbf{r}|)}{1 - n_F(a|\mathbf{p}|)} \times n_F(d|\mathbf{l}'|)(1 - n_F(c|\mathbf{l}|)).$$

For $a = b = +$,

$$\Lambda_{++} = + \frac{1}{1 - n_F(\mathbf{p})} \sum_{cd} \int_{\mathbf{r},\mathbf{l},\mathbf{p}_4} (2\pi)^3 \delta(\mathbf{p} + \mathbf{l}' - \mathbf{r} - \mathbf{l}) \delta(E_{\mathbf{p}} + cE_{\mathbf{l}} - E_{\mathbf{r}} - dE_{\mathbf{l}'}) n_F(dE_{\mathbf{l}'})(1 - n_F(E_{\mathbf{r}}))(1 - n_F(cE_{\mathbf{l}}))|\mathcal{T}^{\mathbf{r},\mathbf{l}\to\mathbf{p},\mathbf{l}'}_{bcad}|^2. \tag{3.227}$$

In the previous expressions we defined the scattering amplitude, depicted in Fig. 3.21

$$\left|\mathcal{T}^{(\mathbf{r},\mathbf{l})\to(\mathbf{p},\mathbf{l}')}_{bcad}\right|^2 = K_{ab}(\mathbf{p},\mathbf{r}) K_{cd}(\mathbf{l},\mathbf{l}') |D_R(b|\mathbf{r}| - a|\mathbf{p}|, \mathbf{r} - \mathbf{p})|^2 + K_{ac}(\mathbf{p},\mathbf{l}) K_{bd}(\mathbf{r},\mathbf{l}') \times |D_R(b|\mathbf{r}| - d|\mathbf{l}'|, \mathbf{r} - \mathbf{l}')|^2 + K_{ad}(\mathbf{p},\mathbf{l}') K_{bc}(\mathbf{r},\mathbf{l}) \times |D_R(b|\mathbf{r}| + c|\mathbf{l}|, \mathbf{r} + \mathbf{l})|^2 \tag{3.228}$$

For $a = +$, $b = -$, the kernel provides the contribution to a different scattering process, depicted in fig. 3.22, when the particle with momentum p from the thermal bath is annihilated,

$$\Lambda_{+-} = + \frac{1/2}{1 - n_F(\mathbf{p})} \sum_{cd} \int_{\mathbf{r},\mathbf{p}_2,\mathbf{p}_4} (2\pi)^3 \delta(\mathbf{p} + \mathbf{r} - \mathbf{l} - \mathbf{l}') \delta(E_{\mathbf{p}} + E_{\mathbf{r}} - cE_{\mathbf{l}} - dE_{\mathbf{l}'}) n_F(E_{\mathbf{r}})(1 - n_F(cE_{\mathbf{l}}))(1 - n_F(dE_{\mathbf{l}'}))|\mathcal{T}^{\mathbf{r},\mathbf{p}\to\mathbf{l},\mathbf{l}'}_{-+cd}|^2. \tag{3.229}$$

To conclude, we need to rewrite the expression of $2\Gamma_{\mathbf{p}}$,

$$\Gamma_{\mathbf{p},a} = \frac{1}{2N} \sum_b \int_{\mathbf{r}} [n(b|\mathbf{r}| - a|\mathbf{p}|) + n_F(b|\mathbf{r}|)] K_{ab}(\mathbf{p},\mathbf{r}) \rho_D(b|\mathbf{r}| - a|\mathbf{p}|, \mathbf{r} - \mathbf{p}) \tag{3.230}$$

which satisfies $\Gamma_{\mathbf{p},+} = \Gamma_{\mathbf{p},-}$, as a consequence of the particle-hole symmetry.

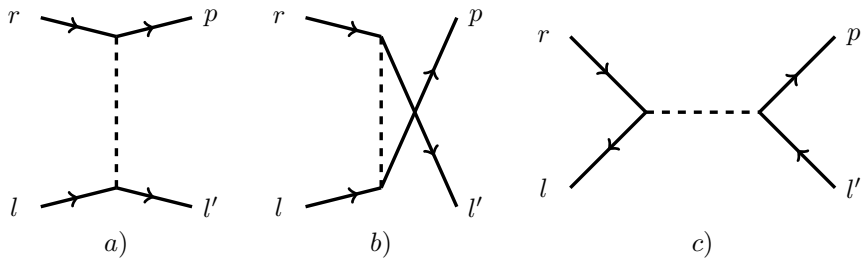

Figure 3.21: The contributions to the kernel of the kinetic equation of Λ_{++} in (3.227). The helicity indices are suppressed and are (r,d), (l,c), (l',d) and (p,a).

By using $\rho_D(b|\mathbf{r}|-a|\mathbf{p}|,\mathbf{r}-\mathbf{p}) = -2\,\mathrm{Im}\Pi_R(b|\mathbf{r}|-a|\mathbf{p}|,\mathbf{r}-\mathbf{p})\,|D_R(b|\mathbf{r}|-a|\mathbf{p}|,\mathbf{r}-\mathbf{p})|^2$ and (3.211),

$$\mathrm{Im}\Pi_R(b|\mathbf{r}|-a|\mathbf{p}|,\mathbf{r}-\mathbf{p}) = -\frac{1}{2}\sum_{c,d}\int_{\mathbf{L},\mathbf{L}'} K_{cd}(\mathbf{L},\mathbf{L}')\,(n_F(c|\mathbf{L}|)-n_F(d|\mathbf{L}'|))$$
$$(2\pi)\delta(b|\mathbf{r}|-a|\mathbf{p}|+c|\mathbf{L}|-d|\mathbf{L}'|)(2\pi)^2\delta^2(\mathbf{L}'+\mathbf{p}-\mathbf{r}-\mathbf{L}),$$

we get

$$\begin{aligned}
&\Gamma_{\mathbf{p},a} = \\
&= -\frac{1}{N}\sum_b\int_{\mathbf{r}}[n(b|\mathbf{r}|-a|\mathbf{p}|)+n_F(b|\mathbf{r}|)]K_{ab}(\mathbf{p},\mathbf{r})\mathrm{Im}\Pi_R(b|\mathbf{r}|-a|\mathbf{p}|,\mathbf{r}-\mathbf{p}) \\
&\qquad\qquad \times |D_R(b|\mathbf{r}|-a|\mathbf{p}|,\mathbf{r}-\mathbf{p})|^2 = \\
&= \frac{1}{2N}\sum_{bcd}\int_{\mathbf{rll}'}[n_B(b|\mathbf{r}|-a|\mathbf{p}|)+n_F(b|\mathbf{r}|)](n_F(c|\mathbf{L}|)-n_F(d|\mathbf{L}'|)) \\
&\qquad\qquad \times K_{ab}(\mathbf{p},\mathbf{r})K_{cd}(\mathbf{L},\mathbf{L}') \\
&\quad (2\pi)\delta(b|\mathbf{r}|-a|\mathbf{p}|+c|\mathbf{L}|-d|\mathbf{L}'|)(2\pi)^2\delta^2(\mathbf{L}'+\mathbf{p}-\mathbf{r}-\mathbf{L}) \\
&\qquad\qquad \times |D_R(b|\mathbf{r}|-a|\mathbf{p}|,\mathbf{r}-\mathbf{p})|^2.
\end{aligned}$$

By considering the only allowed kinematic contribution, the previous expression can be written as follows

$$2\Gamma_{\mathbf{p},a} = \frac{1/2}{1-n_F(aE_{\mathbf{p}})}\sum_{bcd}\int_{\mathbf{r},\mathbf{l},\mathbf{l}'}(2\pi)^3\delta(cE_{\mathbf{l}}+dE_{\mathbf{l}'}-E_{\mathbf{p}}-bE_{\mathbf{r}})\delta(\mathbf{l}+\mathbf{l}'-\mathbf{p}-\mathbf{r}) \\ \times n_F(bE_{\mathbf{r}})(1-n_F(cE_{\mathbf{l}}))(1-n_F(dE_{\mathbf{l}'}))\left|\mathcal{T}^{(P,R)\to(L,L')}_{abcd}\right|^2. \tag{3.231}$$

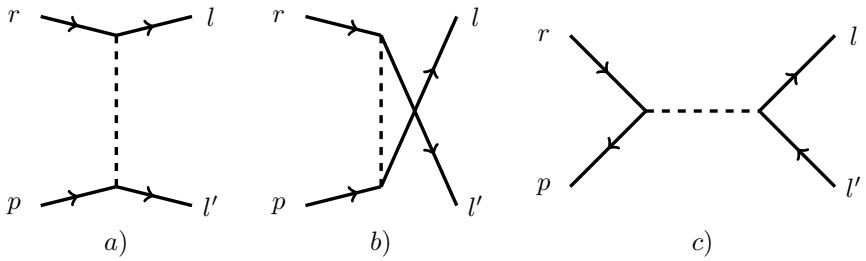

Figure 3.22: The contributions to the kernel of the kinetic equation of Λ_{+-} in (3.229). The helicity indices are suppressed and are (r,d), (l,b), (l',c) and (p,a).

This complete the proof of (3.226). Thus,

$$-iq^0\tilde{f}(q^0,\mathbf{p}) = \int_{\mathbf{r}}(R^{\wedge}(\mathbf{p},\mathbf{l})-R^{\vee}(\mathbf{p},\mathbf{l}))\tilde{f}(q^0,\mathbf{r}), \\ -iq^0 f(q^0,\mathbf{p}) = \int_{\mathbf{r}}(R^{\wedge}(\mathbf{p},\mathbf{l})+R^{\vee}(\mathbf{p},\mathbf{l}))-4(2\pi)^2\delta^2(\mathbf{p}-\mathbf{l})\Gamma_{\mathbf{l}})f(q^0,\mathbf{r}), \tag{3.232}$$

also for critical fermions. This is a highly non trivial result, that firmly establish the validity of our microscopic interpretation to scrambling in terms of a kinetic equation.

3.5.6 Towards the fermionic Quantum Critical Point

As for the bosonic $O(N)$ model, also for the GN model our results rely on the large N and hydrodynamic limit. The Gross-Neveu model,

$$\mathcal{L}_{GN} = \psi_i^{\dagger\,\alpha}(\partial_\tau - i\sigma\cdot\nabla)_\alpha^{\ \beta}\psi_{i,\beta} + \frac{1}{g}\phi^2 + \frac{1}{\sqrt{N}}\phi\,(\psi^\dagger\sigma^z\psi), \tag{3.233}$$

has a phase transition at

$$\frac{1}{g_c} = \frac{\Lambda}{4\pi}, \tag{3.234}$$

where Λ is the momentum cutoff. The analytical continuation of our results to the QCP is simply performed by substituting the value of g_c into the Hubbard-Stratonovich Green's function (3.186),

$$D(i\omega_n, \mathbf{k}) = \frac{1}{-2/g_c - \Pi(i\omega_n, \mathbf{k})}, \tag{3.235}$$

This completes our proof that the relation between chaos and scrambling. Such relation holds also for fermionic systems and it extends naturally to the (fermionic) quantum critical point. Furthermore, this strengthen the microscopic interpretation of chaos as a gross (energy) exchange.

3.6 Conclusion

We have shown the existence of an analytical relation between the *off-shell* BSE that defines the out-of-time order correlation function and the *off-shell* BSE that is used to described hydrodynamic transport In weakly coupled or large N QFTs. The remarkable askect of this relation is that it can be extended also beyond the regime of the quasiparticle framework and close to the quantum critical points, as we have proved for the bosonic $O(N)$ vector model and the Gross-Neveu model in $2+1$ dimensions. A straightforward consequence of this result is the microscopic understanding of scrambling, which is described by a Boltzmann-like equation that takes into account the gross energy exchange (compared to the standard BE that consider the net energy exchange). Moreover, since scrambling is related to the information spreading, we expect that an interpretation of our results in terms of more standard information theory quantities, as thermodynamic entropy of Kolmogorov-Sinai entropy, is viable. We refer these questions to future work.

3.A Notation for fermions

Given a fermion ψ_α with α labelling both spin and vector indices, the finite temperature correlation function in the Close Time Path (CTP) formalism are

$$S_{12|\alpha\beta}(x,y) = -\langle \bar{\psi}_\beta(y)\psi_\alpha(x)\rangle \tag{3.236}$$

$$S_{21|\alpha\beta}(x,y) = \langle \psi_\alpha(x)\bar{\psi}_\beta(y)\rangle \tag{3.237}$$

By writing the correlation function in terms of their Fourier transform in momentum space, and allowing a separation in the thermal circle of σ between the two operators, we get

$$S_{12}^{\sigma}(x) = S_{12}(\mathbf{x}, t + i\sigma) = \int d^4p\, e^{-ipx} e^{\sigma p^0} S_{12}^{\sigma=0}(p) \tag{3.238}$$

$$S_{21}^{\sigma}(x) = S_{21}(\mathbf{x}, t - i\sigma) = \int d^4p\, e^{-ipx} e^{-\sigma p^0} S_{21}^{\sigma=0}(p). \tag{3.239}$$

where the expression of the Green's function in momentum space are

$$S_{21}(p) = (1 - n_F(p^0))\rho_F(p) \tag{3.240}$$

$$S_{12}(p) = -n_F(p^0)\rho_F(p). \tag{3.241}$$

where $\rho_F(p)$ is the fermionic spectral function and it is related to the Green's function

$$\rho_{\alpha\beta}^{F}(p) = S_{21|\alpha\beta}(p) - S_{12|\alpha\beta}(p). \tag{3.242}$$

The system of equations (3.238) can be recast in momentum space as

$$S_{12}^{\sigma}(p) = e^{\sigma p^0} S_{12}^{\sigma=0}(p) \tag{3.243}$$

$$S_{21}^{\sigma}(p) = e^{-\sigma p^0} S_{21}^{\sigma=0}(p). \tag{3.244}$$

It is important to stress that the relation (3.242) holds only with the $\sigma = 0$ Wightman functions.

3.B Some identities

In this section we state some useful identities that we need to prove the relation among the kernel of the BSE for the OTOC and of the retarded Green's function of the bilocal density operator.

Bosonic O(N) vector model

We first focus on the kernel of the bosonic $O(N)$ vector model, which is

$$\Lambda^{NLO}(l,p) = \rho_D(l-p) + N \int_s (n(p_0 - s_0) - n(l_0 - s_0))\rho(p-s)\rho(l-s)D_R(s)D_A(s), \tag{3.245}$$

multiplied by the factor $(n(l_0 - p_0) - n(l_0))$. It is easy to see that the following identities hold:

$$n_B(l_0 - p_0) - n_B(l_0) = \frac{n_B(l_0)}{n_B(p_0)}(1 + n_B(l_0 - p_0)) \tag{3.246}$$

$$n_B(p^0 - s^0) - n_B(l^0 - s^0) = \frac{n_B(p^0 - s^0)}{1 + n_B(l_0 - p_0)}(1 + n_B(l^0 - s^0)). \tag{3.247}$$

Consequently the rung is equal to

$$(n(l_0 - p_0) - n(l_0))\Lambda^{NLO}(l,p) = \tag{3.248}$$
$$\frac{n_B(l_0)}{n_B(p_0)}\left[D_{21}^{\sigma=0}(l-p) + N\int_s G_{12}^{\sigma=0}(p-s)G_{21}^{\sigma=0}(l-s)D_R(s)D_A(s)\right].$$

rewriting in the Wightman functions in terms of the symmetric ones we get

$$(n(l_0 - p_0) - n(l_0))\Lambda^{NLO}(l,p) = \frac{\sinh(\beta \mathrm{p}_0/2)}{\sinh(\beta \mathrm{l}_0/2)}$$
$$\times\left[D_{21}^{\sigma=\beta/2}(l-p) + N\int_s G_{12}^{\sigma=\beta/2}(p-s)G_{21}^{\sigma=\beta/2}(l-s)D_R(s)D_A(s)\right].$$

Gross-Neveu model

Given the bosonic/fermionic equilibrium distribution function $n_{B/F}(p_0) = (e^{\beta p_0} \mp 1)^{-1}$, the following relations hold

$$n_B(r^0 - p^0) + n_F(r^0) = \frac{n_F(r^0)}{n_F(p^0)}(1 + n_B(r^0 - p^0)), \tag{3.249}$$

$$n_F(p^0 - l^0) - n_F(r^0 - l^0) = \frac{n_F(p^0 - l^0)}{1 + n_B(r^0 - p^0)}(1 - n_F(r^0 - l^0)). \tag{3.250}$$

The kernel of the BSE for the Gross-Neveu model is (3.201)

$$\tilde{\Lambda}(r,p)_{\gamma\delta'}^{\delta\gamma'} = (\sigma^z)_{\gamma}^{\gamma'}(\sigma^z)_{\delta'}^{\delta}\rho_D(r-p)$$
$$+\int_l (n_F(p^0 - l^0) - n_F(r^0 - l^0))(\sigma^z\,\rho_F(p-l)\sigma^z)_{\gamma}^{\delta}\,(\sigma^z\,\rho_F(r-l)\sigma^z)_{\delta'}^{\gamma'}$$

times $(n_B(r^0 - p^0) + n_F(r^0))$. By means of the (3.249), the first term is

$$(n_B(r^0 - p^0) + n_F(r^0))\rho_D(r^0 - p^0) = \frac{n_F(r^0)}{n_F(p^0)}e^{\beta(r^0 - p^0)/2}D_W^{\beta/2}(r-p) \tag{3.251}$$

where with the label $\beta/2$ we have indicated the correlation function with operator inserted at a distance $\beta/2$ over the thermal circle. They are defined as

$$G_W^{\beta/2}(r-p) = e^{-\beta(r^0-p^0)}(1+n_B(r^0-p^0))\rho_B(r-p), \tag{3.252}$$
$$S_W^{\beta/2}(r-p) = e^{-\beta(r^0-p^0)}(1-n_F(r^0-p^0))\rho_F(r-p), \tag{3.253}$$

and they can be rewritten in terms of the Wightman function with operator insertion almost coincident in the thermal circle

$$G_W^{\beta/2}(r-p) = e^{-\beta(r^0-p^0)}G_W(r-p), \tag{3.254}$$
$$S_W^{\beta/2}(r-p) = e^{-\beta(r^0-p^0)}S_W(r-p). \tag{3.255}$$

The second contribution to the kernel, corresponding to the second and third diagram in fig. 3.18, is

$$\begin{aligned}&(n_B(r^0-p^0)+n_F(r^0))(n_F(p^0-l^0)-n_F(r^0-l^0))\rho_F(r-l)\rho_F(p-l)\\ &=\frac{n_F(r^0)}{n_F(p^0)}S_{21}(r-l)S_{12}(l-p)=\frac{n_F(r^0)}{n_F(p^0)}e^{\beta(r^0-p^0)/2}S_W^{\beta/2}(r-l)S_W^{\beta/2}(l-p).\end{aligned} \tag{3.256}$$

Since the products of thermal factor simplifies as

$$\frac{n_F(r^0)}{n_F(p^0)}e^{\beta(r^0-p^0)/2}=\frac{\cosh(\beta p^0/2)}{\cosh(\beta r^0/2)}, \tag{3.257}$$

we can rewrite the kernel of the BSE of the bilocal density operator as

$$\begin{aligned}(n_B(r^0-p^0)+n_F(r^0))\tilde{\Lambda}(r,p)^{\delta\gamma'}_{\gamma\delta'} &= \frac{\cosh(\beta p^0/2)}{\cosh(\beta r^0/2)}\Bigg[(\sigma^z)^{\gamma'}_{\gamma}(\sigma^z)^{\delta}_{\delta'}G_W^{\beta/2}(r-p)\\ &+\int_l(\sigma^z\,S_W^{\beta/2}(l-p)\sigma^z)^{\delta}_{\gamma}\,(\sigma^z\,S_W^{\beta/2}(r-l)\sigma^z)^{\gamma'}_{\delta'}D^R(l+q)D^A(l)\Bigg].\end{aligned}$$

3.C Imaginary part of the self energy in the GN model

We start with the expression in imaginary time

$$\Pi(i\nu_n,\mathbf{p}) = -\sum_{\omega_m}\int_{\mathbf{k}}\mathrm{Tr}[G(i\omega_m-i\nu_n,\mathbf{k}-\mathbf{p})\sigma^z G(i\omega_m,\mathbf{k})\sigma^z] \tag{3.258}$$

now we insert the expression of the propagator in the helicity basis

$$\Pi(i\nu_n, \mathbf{p}) = -\sum_{\omega_m} \int_{\mathbf{k}} K_{ab}(\mathbf{k}-\mathbf{p}, \mathbf{k}) \frac{1}{i\omega_m - i\nu_n - a|\mathbf{k}-\mathbf{p}|} \frac{1}{i\omega_m - b|\mathbf{k}|} \tag{3.259}$$

and perform the Matsubara sum

$$\Pi(i\nu_n, \mathbf{p}) = -\int_{\mathbf{k}} K_{ab}(\mathbf{k}-\mathbf{p}, \mathbf{k}) \frac{n_F(a|\mathbf{k}-\mathbf{p}|) - n_F(b|\mathbf{k}|)}{i\nu_n + a|\mathbf{k}-\mathbf{p}| - b|\mathbf{k}|}. \tag{3.260}$$

To obtain the retarded, we perform the analytic continuation $i\nu_n \to \nu + i\epsilon$ and we can extract the imaginary part by simply use $\mathrm{Im}\,[1/(x \pm i\epsilon)] = \mp i\pi\delta(x)$ and shifting the integration variable $\mathbf{k} - \mathbf{p} \to \mathbf{k}$

$$\mathrm{Im}\,[\Pi_R(\nu, \mathbf{p})] = -\frac{1}{2} \int_{\mathbf{k}} K_{ab}(\mathbf{k}, \mathbf{k}+\mathbf{p}) (n_F(a|\mathbf{k}|) - n_F(b|\mathbf{k}+\mathbf{p}|)) \times (2\pi)\delta(\nu + a|\mathbf{k}| - b|\mathbf{k}+\mathbf{p}|)$$

3.D Pinching-poles approximation

Quantum field theories at finite temperature possess on-shell thermal excitations. The lifetime of such excitations is inversely proportional to the coupling constant and indeed, in a non-interacting theory, these excitations are stable and can live indefinitely long. This is the reason behind the appearance of the delta function in the spectral density. Besides this well-known effect, there is another consequence of the existence of those excitations and it is divergence of the product of two spectral functions with opposite-sign momentum, *i.e.* $\rho(k+p)\rho(-p)$, once the zero momentum ($\mathbf{k} = 0$) and vanishing frequency limit is taken ($k_0 \to 0$). The poles of the two spectral functions pinch the real axis in the complex energy plane both from below and above and cause a divergence. This is called pinching-pole divergence. Turning a coupling on, the lifetime becomes finite and regulates such divergence (which is commonly referred to as nearly-pinching pole divergence). Nevertheless it still provides the leading contributions in the weak coupling computations and allows to organize the diagrammatic expansion. In the latter case, the retarded and advanced Green's function take the form

$$G_{\mathrm{R}}(p) = \frac{1}{(p_0 + i\Gamma_{\mathbf{p}})^2 - E_{\mathbf{p}}^2}, \quad G_{\mathrm{A}}(p) = \frac{1}{(p_0 - i\Gamma_{\mathbf{p}})^2 - E_{\mathbf{p}}^2} \tag{3.261}$$

To understand the analytical structure of the terms $G_R(p+\omega)G_A(p)$, $G_R(p+\omega)G_R(p)$ and $G_A(p+\omega)G_A(p)^2$, we study the poles of the retarded

$(P_{1/2})$ and the advanced $(P_{3/4})$ Green's function. They are respectively located at

$$(P_1) : p_0 = -E_p - i\Gamma_p; \qquad (P_3) : p_0 = E_p + i\Gamma_p;$$
$$(P_2) : p_0 = E_p - i\Gamma_p; \qquad (P_4) : p_0 = -E_p + i\Gamma_p.$$

In the previous expressions, a non vanishing ω simply shifts the real part of $-\omega$. Since we will take the zero external momentum limit, we want to find the most divergent piece in ω.

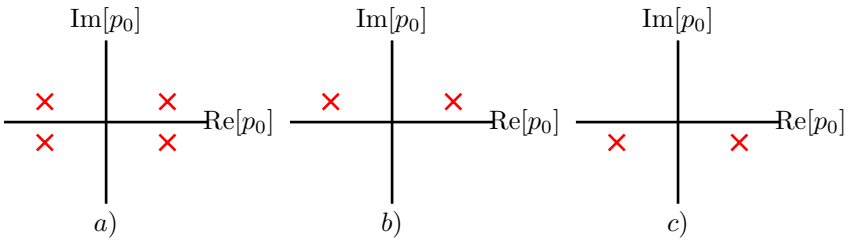

Figure 3.23: The pole structure of the product $G_R G_A$ (b), G_A^2 (c) and G_R^2 (a).

If we close the contour from below we get the following residues (times a $-2\pi i$ factor)

$$(P_1, P_3) : \frac{2\pi i}{4E_p^2}\frac{1}{\omega + 2E_p}; \;\; p_0 = -\omega - E_p;$$
$$(P_1, P_4) : \frac{2\pi i}{4E_p^2}\frac{1}{\omega + 2i\Gamma_p}; \;\; p_0 = -\omega - E_p;$$
$$(P_2, P_3) : \frac{2\pi i}{4E_p^2}\frac{1}{\omega + 2i\Gamma_p}; \;\; p_0 = -\omega + E_p;$$
$$(P_2, P_4) : \frac{2\pi i}{4E_p^2}\frac{1}{2E_p - \omega}; \;\; p_0 = -\omega + E_p;$$

If we close the contour above:

$$(P_1, P_3) : \frac{2\pi i}{4E_p^2}\frac{-1}{\omega + 2E_p}; \;\; p_0 = E_p; \qquad (P_1, P_4) : \frac{2\pi i}{4E_p^2}\frac{1}{\omega + 2i\Gamma_p}; \;\; p_0 = -E_p;$$
$$(P_2, P_3) : \frac{2\pi i}{4E_p^2}\frac{1}{\omega + 2i\Gamma_p}; \;\; p_0 = E_p; \qquad (P_2, P_4) : \frac{2\pi i}{4E_p^2}\frac{1}{2E_p - \omega}; \;\; p_0 = -E_p;$$

In the limit of vanishing ω, the most singular terms are (P_1, P_4) and (P_2, P_3), so that we can approximate

$$G_{ra}(p+k)G_{ra}(-p) \sim \frac{2\pi i}{4E_p^2}\frac{\delta(p_0 - E_p) + \delta(p_0 + E_p)}{\omega + 2i\Gamma_p} = \frac{\pi}{E_p}\frac{\delta(p_0^2 - E_p^2)}{-i\omega + 2\Gamma_p} \tag{3.262}$$

Now let's study

$$G_{ra}(p+\omega)G_{ra}(p) = \frac{1}{4E_p^2}\left(\frac{1}{p^0 + \omega + E_p + i\Gamma_p} - \frac{1}{p^0 + \omega - E_p + i\Gamma_p}\right) \times \left(\frac{1}{p^0 + E_p + i\Gamma_p} - \frac{1}{p^0 - E_p + i\Gamma_p}\right)$$

The previous expression has 4 poles, respectively at

$$\begin{aligned} &(P_1) : p_0 = -\omega - E_p - i\Gamma_p; \qquad (P_3) : p_0 = -E_p - i\Gamma_p; \\ &(P_2) : p_0 = -\omega + E_p - i\Gamma_p; \qquad (P_4) : p_0 = E_p - i\Gamma_p; \end{aligned}$$

If we close the contour above, the expression vanishes since there is no pole in the upper-half plane (this is equivalent to the statement that $G_R(t)^2 = 0$ for negative t). If we close the contour from below we get the following residues (times a $-2\pi i$ factor)

$$\begin{aligned} &(P_1, P_3) : 0; \;\; p_0 = -E_p; \\ &(P_1, P_4) : \frac{2\pi i}{4E_p^2}\frac{1}{-\omega + 2i\Gamma_p}; \;\; p_0 = -E_p; \\ &(P_2, P_3) : \frac{2\pi i}{4E_p^2}\frac{1}{-\omega + 2i\Gamma_p}; \;\; p_0 = E_p; \\ &(P_2, P_4) : \frac{2\pi i}{4E_p^2}\frac{1}{\omega - 2E_p}; \;\; p_0 = +E_p; \end{aligned}$$

By taking the complex conjugate of $G_{ra}(p+\omega)G_{ra}(p)$, we see that also the term $G_A(p+\omega)G_A(p)$ is subleading with respect to $G_R(p+\omega)G_A(p)$ in the limit of vanishing ω.

3.E Analytic continuation

Here we present the important steps to derive the analytical continuations to real time of the BSE. To do this, we closely follow the technique used

in [115, 183]. There, the authors make extensive use of the formula, valid for a generic function $\tilde{G}(i\omega_n + i\nu_m, i\omega_n)$,

$$T\sum_n \tilde{G}(i\omega_n + i\nu_m, i\omega_n) = \sum_{\text{cuts}} \int_{-\infty}^{\infty} \frac{d\xi}{2\pi i} n(\xi) \text{Disc}\, \tilde{G}(\xi + i\nu_m, \xi) - \sum_{\text{poles}} n(\xi_i) \text{Res}[\tilde{G}(\xi + i\nu_m, \xi), \xi_i]. \quad (3.263)$$

Because of the recursive BSE (3.128), the analytical structures of $\tilde{G}(i\omega_n + i\nu_m, i\omega_n)$ is represented by two branch cuts at $\text{Im}[\xi + i\nu_n] = 0$ and $\text{Im}[\xi] = 0$. The BSE resums the full series of correlation function with n rungs, relating the $n+1$ to the n, and taking the $n \to \infty$ limit. The $n = 0$ correlation function is simply $G(P+Q)G(P)$, so it has two branch cuts at $\text{Im}[\xi + i\nu_n] = 0$ and $\text{Im}[\xi] = 0$. By induction, it is easy to see that any n has the same analytical structure, and so for a general BSE of the form (3.128), the singularities correspond to the singularities of the product $G(P+Q)G(P)$ [115]. This means that the expression for the Matsubara sum is

$$\begin{aligned} T\sum_m \tilde{G}(i\omega_m + i\nu_n, i\omega_n) &= \sum_{\text{cuts}} \int_{-\infty}^{\infty} \frac{d\xi}{2\pi i} n(\xi)\, \text{Disc}\, \tilde{G}(\xi + i\nu_m, \xi) \quad (3.264) \\ &= -\int_{-\infty}^{\infty} \frac{d\xi}{2\pi i} n(\xi) \left[\tilde{G}(\xi + i\nu_n, \omega + i0^+) - \tilde{G}(\xi + i\nu_n, \xi + i0^-)\right] \\ &\quad - \int_{-\infty}^{\infty} \frac{d\xi}{2\pi i} n(\xi) \left[\tilde{G}(\xi + i0^+, \xi - i\nu_n) - \tilde{G}(\xi + i0^-, \xi - i\nu_n)\right] \end{aligned}$$

Plugging (3.127) in the previous equation and using $G(\omega + i0^+) = G_R(\omega)$ and $G(\omega + i0^-) = G_A(\omega)$, we get

$$\begin{aligned} &T\sum_m \tilde{G}(i\omega_m + i\nu_n, i\omega_m) = \\ &-\int_{-\infty}^{\infty} \frac{d\xi}{2\pi i}\, n(\xi)[G(\xi+i\nu_m)\Gamma(\xi+i\nu_m, \xi+i0^+)+G(\xi-i\nu_n)\Gamma(\xi+i0^+, \xi-i\nu_n)]G_R(\xi) \\ &+\int_{-\infty}^{\infty} \frac{d\xi}{2\pi i} n(\xi)[G(\xi+i\nu_n)\Gamma(\xi+i\nu_n, \xi+i0^-)+G(\xi-i\nu_n)\Gamma(\xi+i0^-, \xi-i\nu_n)]G_A(\xi) \end{aligned}$$

We now use the fact that we are interested in the following analytical continuation in the external frequency: $i\nu_n \to \nu + i0^+$. Thus

$$
\begin{aligned}
&T\sum_m \tilde{G}(i\omega_m + \nu + i0^+, i\omega_m) = \\
&\quad - \int_{-\infty}^{\infty} \frac{d\xi}{2\pi i}\, n(\xi) \left[G(\xi + \nu + i0^+)\Gamma(\xi + \nu + i0^+, \xi + i0^+) \right. \\
&\qquad\qquad \left. + G(\xi - \nu + i0^-)\Gamma(\xi + i0^+, \xi - \nu + i0^-) \right] G_R(\xi) \\
&\quad + \int_{-\infty}^{\infty} \frac{d\xi}{2\pi i} n(\xi) \left[G(\xi + \nu + i0^+)\Gamma(\xi + \nu + i0^+, \xi + i0^-) \right. \\
&\qquad\qquad \left. + G(\xi - \nu + i0^-)\Gamma(\xi + i0^-, \xi - \nu + i0^-) \right] G_A(\xi) = \\
&\quad - \int_{-\infty}^{\infty} \frac{d\xi}{2\pi i}\, n(\xi) \left[G_R(\xi + \nu)\Gamma(\xi + \nu + i0^+, \xi + i0^+) \right. \\
&\qquad\qquad \left. + G_A(\xi - \nu)\Gamma(\xi + i0^+, \xi - \nu + i0^-) \right] G_R(\xi) \\
&\quad + \int_{-\infty}^{\infty} \frac{d\xi}{2\pi i} n(\xi) \left[G_R(\xi + \nu)\Gamma(\xi + \nu + i0^+, \xi + i0^-) \right. \\
&\qquad\qquad \left. + G_A(\xi - \nu)\Gamma(\xi + i0^-, \xi - \nu + i0^-) \right] G_A(\xi).
\end{aligned}
$$

In the previous expression, we can shift the integration variable in the second and last term and we get

$$
\begin{aligned}
&T\sum_m \tilde{G}(i\omega_m + \nu + i0^+, i\omega_m) = \\
&\quad - \int_{-\infty}^{\infty} \frac{d\xi}{2\pi i} \left[n(\xi) G_R(\xi + \nu)\Gamma(\xi + \nu + i0^+, \xi + i0^+) G_R(\xi) \right. \\
&\qquad\qquad \left. - n(\xi + \nu) G_A(\xi)\Gamma(\xi + \nu + i0^-, \xi + i0^-) G_A(\xi + \nu) \right] \\
&\quad - \int_{-\infty}^{\infty} \frac{d\xi}{2\pi i} \left(n(\xi + \nu) - n(\xi) \right) \left[G_A(\xi) G_R(\xi + \nu)\Gamma(\xi + \nu + i0^+, \xi + i0^-) \right].
\end{aligned}
$$

As we are interested in the $\nu \to 0$ limit, we know that the product $G_A(\xi)G_R(\xi + \nu)$ dominates the sum. This allows us to write

$$
\begin{aligned}
T\sum_m \tilde{G}(i\omega_m + \nu + i0^+, i\omega_m) = &\int_{-\infty}^{\infty} \frac{d\xi}{2\pi i} \left(n(\xi + \nu) - n(\xi) \right) \\
&\times G_A(\xi) G_R(\xi + \nu)\Gamma(\xi + \nu + i0^+, \xi + i0^-).
\end{aligned}
$$

The previous analysis has to be carried out with all the Matsubara frequency terms in the RHS of the BSE. The full correlation function will

involve the Matsubara sum over the frequencies p_n, which satisfies the BSE

$$\sum_{p_n} \int_{\mathbf{p}} \tilde{G}(ip_n + i\nu_{n'}, ip_n) = \sum_{p_n} \int_{\mathbf{p}} G(ip_n + i\nu_{n'}) G(ip_n) \times \left[1 + \frac{1}{N} \sum_m \int_{\mathbf{l}} \tilde{G}(il_m + i\nu_{n'}, il_m) \left[\Lambda^{LO} + \Lambda^{NLO}(il_m, ip_n; i\nu_{n'}) \right] \right]. \tag{3.265}$$

A similar treatment was done in [135], where the authors considered a strict zero external frequency limit. We performed a similar analysis by retaining the small but still non zero external frequency. In both cases, the crucial consequences of the Matsubara sum are the following: since the leading order kernel Λ^{LO} does not present any singularity, it vanishes in the Matsubara sum. So we are left with only the Λ^{NLO} kernel in the BSE. Moreover, together with the pinching-pole approximation, the matsubara sum pick only a particular analytic continuation which can be shown reproduces the result obtained in real time formalism [115].

3.F Consistency of the result for the $N \times N$ matrix model

As we anticipated earlier, we can verify our result by means of the identity (3.32). We study the BSE for $G^{AaRr}(p, q|k)$ and then send $k \to -k$:

$$\begin{aligned} G^{AaRr}(p, q|k) &= iG^{AR}(p+k)G^{ar}(-p)(2\pi)^4\delta^4(p-q) + \\ -G^{A\alpha_1}(p+k)G^{a\beta_1}(-p) &\int_l K_{\alpha_1\beta_1\alpha_4\beta_4}(p+k, -p, -l-k, l) G^{\alpha_4\beta_4 Rr}(p, q|k). \end{aligned} \tag{3.266}$$

By expanding the sum over the extended SK indices, we observe that since $G^{AA} = G^{aa} = 0$, only one combination has a non vanishing contribution

$$\begin{aligned} G^{AaRr}(p, q|k) =& iG^{AR}(p+k)G^{ar}(-p)(2\pi)^4\delta^4(p-q) \\ &- G^{AR}(p+k)G^{ar}(-p) \int_l K_{Rr\alpha_4\beta_4}(p, l|k) G^{\alpha_4\beta_4 Rr}(l, q|k) \\ =& iG^{AR}(p+k)G^{ar}(-p)(2\pi)^4\delta^4(p-q) \\ &- G^{AR}(p+k)G^{ar}(-p) \int_l K_{RrAa}(p, l|k) G^{AaRr}(l, q|k). \end{aligned}$$

By writing the kernel K_{RrAa},

$$K_{RrAa}(p,l|k) = \frac{1}{4}\frac{N^2+5}{6}\int_s G_{Rr}(s)G_{Rr}(s-l+p) = K_{AaRr}(p,l|k), \tag{3.267}$$

we arrive to the BSE for the $G^{AaRr}(p,q|k)$ Green's function

$$G^{AaRr}(p,q|k) = G^{AR}(p+k)G^{ar}(-p)\Bigg(i(2\pi)^4\delta^4(p-q) - \frac{1}{2}\int_l K_{AaRr}(p,l|k)G^{AaRr}(l,q|k)\Bigg). \tag{3.268}$$

By sending $k \to -k$ and using the pinching-pole approximation, we obtain the identity (3.32).

3.G From the BSE to the kinetic equation in the ϕ^4 matrix model

In this appendix we explicitly show how the kernel of the BSE for transport (3.41), once on-shell, reproduces the kinetic equation for transport (3.62). In the case of the bosonic matrix model, the scattering amplitude is independent of the momenta and equals, for any N,

$$|\mathcal{T}|^2 = g^4\frac{N^2+5}{6}. \tag{3.269}$$

In the following we will need some identity for the Bose-Einstein distribution function

$$n(p_1)n(p_2)(1+n(p_3))(1+n(p_4))\delta(p_1^0+p_2^0-p_3^0-p_4^0) = (1+n(p_1))(1+n(p_2))n(p_3)n(p_4)\delta(p_1^0+p_2^0-p_3^0-p_4^0), \tag{3.270}$$

together with the symmetry property of the Bose-Einstein distribution function and the spectral density with respect to the $s \to -s$ transformation

$$(1+n(-s)) = -n(s) \quad \Leftrightarrow \quad n(-s) = -(1+n(s)), \tag{3.271}$$

$$\rho^{free}(s) = \frac{2\pi}{2E_{\mathbf{s}}}\left(\delta(s^0-E_{\mathbf{s}}) - \delta(s^0+E_{\mathbf{s}})\right) = -\rho^{free}(-s). \tag{3.272}$$

Now, the kernel of the BSE equals (3.41)

$$R^{\text{transp}}(p,l) = -\frac{|\mathcal{T}|^2}{2}\frac{1+n(l_0)}{1+n(p_0)}\int\limits_{s_1,s_2}\rho(s_1)\rho(s_2)(1+n(s_1))n(s_2) \times (2\pi)^4\delta^4(s_1-s_2+l-p). \quad (3.273)$$

In the BSE, the structure of the expansion is such that the propagator occurring in the rungs are taken as free propagators. So we can insert the free spectral density in the previous equation and we get

$$R^{\text{transp}}(p,l) = -\frac{1}{2}|\mathcal{T}|^2(2\pi)^2\frac{1+n(l_0)}{1+n(p_0)}\int\limits_{s_1,s_2}\frac{(1+n(s_1))n(s_2)}{4E_{\mathbf{s_1}}E_{\mathbf{s_2}}}(2\pi)^4\delta^4(s_1-s_2+l-p) \times (\delta(s_1^0-E_{\mathbf{s_1}})-\delta(s_1^0+E_{\mathbf{s_1}}))(\delta(s_2^0-E_{\mathbf{s_2}})-\delta(s_2^0+E_{\mathbf{s_2}})).$$

We now have to evaluate the delta function, which constraints the dynamics

$$\int\limits_{s_1,s_2}\rho^{free}(s_1)\rho^{free}(s_2)(1+n(s_1))n(s_2)(2\pi)^4\delta^4(s_1-s_2+l-p) =$$

$$= \int\limits_{\mathbf{s}_1,\mathbf{s}_2}(2\pi)^4\delta^3(s_1-s_2+l-p)\Big[(1+n(E_{\mathbf{s_1}}))n(E_{\mathbf{s_2}})\delta(E_{\mathbf{s_1}}-E_{\mathbf{s_2}}+l-p)+$$

$$(1+n(E_{\mathbf{s_2}}))n(E_{\mathbf{s_1}})\delta(-E_{\mathbf{s_1}}+E_{\mathbf{s_2}}+l-p)+n(E_{\mathbf{s_1}})n(E_{\mathbf{s_2}})\delta(-E_{\mathbf{s_1}}-E_{\mathbf{s_2}}+l-p)$$

$$+(1+n(E_{\mathbf{s_1}}))(1+n(E_{\mathbf{s_2}}))\delta(E_{\mathbf{s_1}}+E_{\mathbf{s_2}}+l-p)\Big]$$

$$= \int\limits_{\mathbf{s}_1,\mathbf{s}_2}(2\pi)^4\delta^3(s_1-s_2+l-p)\Big[2(1+n(E_{\mathbf{s_1}}))n(E_{\mathbf{s_2}})\delta(E_{\mathbf{s_1}}-E_{\mathbf{s_2}}+l-p)+$$

$$+n(E_{\mathbf{s_1}})n(E_{\mathbf{s_2}})\delta(-E_{\mathbf{s_1}}-E_{\mathbf{s_2}}+l-p)+(1+n(E_{\mathbf{s_1}}))(1+n(E_{\mathbf{s_2}}))\delta(E_{\mathbf{s_1}}+E_{\mathbf{s_2}}+l-p)\Big].$$

Thus

$$R^{\text{transp}}(p,l) = -\frac{1}{2}|\mathcal{T}|^2\frac{2\pi}{1+n(p_0)}\int\limits_{\substack{\mathbf{s}_1,\mathbf{s}_2\\ \mathbf{l}=\mathbf{p}+\mathbf{s}_2-\mathbf{s}_1}} \quad (3.274)$$

$$[\delta(E_{\mathbf{s_1}}-E_{\mathbf{s_2}}+l-p)2(1+n(l_0))(1+n(E_{\mathbf{s_1}}))n(E_{\mathbf{s_2}}) + \delta(-E_{\mathbf{s_1}}-E_{\mathbf{s_2}}+l-p)(1+n(l_0))n(E_{\mathbf{s_1}})n(E_{\mathbf{s_2}}) + \delta(E_{\mathbf{s_1}}+E_{\mathbf{s_2}}+l-p)(1+n(l_0))(1+n(E_{\mathbf{s_1}}))(1+n(E_{\mathbf{s_2}}))].$$

In the pinching pole approximation, the product of retarded and advanced Green's function gives a delta function which puts the momentum p *on-shell*. This in turn places *on-shell* also the momentum l, since the only non trivial solution is supported on physical states. Consequently

$$R^{\text{transp}}(\mathbf{p}, E_{\mathbf{p}}; \mathbf{l}, E_{\mathbf{l}}) = -\frac{1}{2}|\mathcal{T}|^2 \frac{2\pi}{1+n(p_0)} \int\limits_{\substack{\mathbf{s_1},\mathbf{s_2} \\ \mathbf{l}=\mathbf{p}+\mathbf{s_2}-\mathbf{s_1}}} [\delta(E_{\mathbf{s_1}} - E_{\mathbf{s_2}} + E_{\mathbf{l}} - p)2(1+n(E_{\mathbf{l}}))(1+n(E_{\mathbf{s_1}}))n(E_{\mathbf{s_2}}) + \delta(-E_{\mathbf{s_1}} - E_{\mathbf{s_2}} + E_{\mathbf{l}} - p)(1+n(E_{\mathbf{l}}))n(E_{\mathbf{s_1}})n(E_{\mathbf{s_2}}) + \delta(E_{\mathbf{s_1}} + E_{\mathbf{s_2}} + E_{\mathbf{l}} - p)(1+n(E_{\mathbf{l}}))(1+n(E_{\mathbf{s_1}}))(1+n(E_{\mathbf{s_2}}))] .$$

We recognize the processes $ps_2 \to ls_1$ (with a factor 2 for $s_2 \leftrightarrow s_1$; $ps_2s_1 \to 1$ and $p \to s_1s_2l$). These are all "loss-"rates. The last two terms cancel, however, as it is kinematically forbidden for a *on-shell* particle of mass m to decay to three *on-shell* particles of the same mass m and vice versa. The previous term notably simplifies into

$$R^{\text{transp}}(\mathbf{p}, E_{\mathbf{p}}; \mathbf{l}, E_{\mathbf{l}}) = -\frac{1}{2}|\mathcal{T}|^2 \frac{2\pi}{1+n(E_{\mathbf{p}})} \int\limits_{\substack{\mathbf{s_1},\mathbf{s_2} \\ \mathbf{l}=\mathbf{p}+\mathbf{s_2}-\mathbf{s_1}}} [\delta(E_{\mathbf{s_1}} - E_{\mathbf{s_2}} + E_{\mathbf{l}} - E_{\mathbf{p}})2(1+n(E_{\mathbf{l}}))(1+n(E_{\mathbf{s_1}}))n(E_{\mathbf{s_2}})] . \tag{3.275}$$

The other "negative"-energy kernel gives – using $(1+n(-s)) = -n(s)$

$$R^{\text{transp}}(\mathbf{p}, E_{\mathbf{p}}|\mathbf{l}, -E_{\mathbf{l}}) = \frac{1}{2}|\mathcal{T}|^2 \frac{2\pi}{1+n(E_{\mathbf{p}})} \int\limits_{\substack{\mathbf{s_1},\mathbf{s_2} \\ \mathbf{l}=\mathbf{p}+\mathbf{s_2}-\mathbf{s_1}}} \tag{3.276}$$

$$[\delta(E_{\mathbf{s_1}} - E_{\mathbf{s_2}} - E_{\mathbf{l}} - E_{\mathbf{p}})2n(E_{\mathbf{l}})(1+n(E_{\mathbf{s_1}}))n(E_{\mathbf{s_2}}) + \delta(-E_{\mathbf{s_1}} - E_{\mathbf{s_2}} - E_{\mathbf{l}} - E_{\mathbf{p}})n(E_{\mathbf{l}})n(E_{\mathbf{s_1}})n(E_{\mathbf{s_2}}) + \delta(E_{\mathbf{s_1}} + E_{\mathbf{s_2}} - E_{\mathbf{l}} - E_{\mathbf{p}})n(E_{\mathbf{l}})(1+n(E_{\mathbf{s_1}}))(1+n(E_{\mathbf{s_2}}))] . \tag{3.277}$$

We recognize the processes $pls_2 \to s_1$, $pls_1s_2 \to 0$, $pl \to s_1s_2$. Using total energy conservation, these should be interpreted as "gains" $pls_2 \leftarrow s_1$, $pls_1s_2 \leftarrow 0$, $pl \leftarrow s_1s_2$. Again, the first two processes are kinematically not allowed. Thus

$$R^{\text{transp}}(\mathbf{p}, E_{\mathbf{p}}|\mathbf{l}, -E_{\mathbf{l}}) = \frac{1}{2}|\mathcal{T}|^2 \frac{2\pi}{1+n(E_{\mathbf{p}})} \int\limits_{\substack{\mathbf{s_1},\mathbf{s_2} \\ \mathbf{l}=\mathbf{p}+\mathbf{s_2}-\mathbf{s_1}}} \tag{3.278}$$

$$[\delta(E_{\mathbf{s_1}} + E_{\mathbf{s_2}} - E_{\mathbf{l}} - E_{\mathbf{p}})n(E_{\mathbf{l}})(1+n(E_{\mathbf{s_1}}))(1+n(E_{\mathbf{s_2}}))] .$$

The object to prove is that the collision kernel equals

$$\hat{C}(\mathbf{p},\mathbf{l}) = -\left[\int_{\mathbf{l}} 2\Gamma_{\mathbf{p}}\delta(\mathbf{p}-\mathbf{l}) + \frac{1}{2E_{\mathbf{p}}}\left(R^{\text{transp}}(\mathbf{p},E_{\mathbf{p}}|\mathbf{l},E_{\mathbf{l}}) + R^{\text{transp}}(\mathbf{p},E_{\mathbf{p}}|\mathbf{l},-E_{\mathbf{l}})\right)\right]. \tag{3.279}$$

Comparing (3.275) and (3.278) to the Boltzmann equation (3.62) which, in a more compact form, reads

$$\begin{aligned}\partial_t f(\mathbf{p},t) =& \frac{1}{(1+n(\mathbf{p}))}\int\limits_{\substack{\mathbf{l},\mathbf{s_1},\mathbf{s_2}\\ \mathbf{l}=\mathbf{p}+\mathbf{s_2}-\mathbf{s_1}}} \frac{|\mathcal{T}|^2/2}{2E_{\mathbf{p}}} \\ &\times[(2\pi)\delta(E_{\mathbf{s_1}}-E_{\mathbf{s_2}}+E_{\mathbf{l}}-p)2(1+n(E_{\mathbf{l}}))(1+n(E_{\mathbf{s_1}}))n(E_{\mathbf{s_2}}) \\ &-(2\pi)\delta(E_{\mathbf{s_1}}+E_{\mathbf{s_2}}-E_{\mathbf{l}}-p)n(E_{\mathbf{l}})(1+n(E_{\mathbf{s_1}}))(1+n(E_{\mathbf{s_2}})) \\ &-\int\limits_{\mathbf{l}'}(2\pi)\delta(E_{\mathbf{s_1}}+E_{\mathbf{s_2}}-E_{\mathbf{l}}-p)n(E_{\mathbf{l}})(1+n(E_{\mathbf{s_1}}))(1+n(E_{\mathbf{s_2}}))\delta(\mathbf{p}-\mathbf{l}')f(\mathbf{l}',t)\Bigg],\end{aligned} \tag{3.280}$$

we realize that we are missing the last term. As we are going to show, this is represented by imaginary part of the self-energy $2\Gamma_{\mathbf{p}}$. We thus wish to check that

$$-2\Gamma_{\mathbf{p}} = -\frac{2}{1+n(\mathbf{p})}f(\mathbf{p},t)\int_{\mathbf{l},\mathbf{p_2},\mathbf{p}_4}\frac{(2\pi)^4\delta^4(\mathbf{p}^{\text{os}}+\mathbf{l}^{\text{os}}-\mathbf{p_2}^{\text{os}}-\mathbf{p_4}^{\text{os}})|\mathcal{T}|^2}{2E_{\mathbf{p}}} n(E_{\mathbf{l}})(1+n(E_{\mathbf{p_2}}))(1+n(E_{\mathbf{4}})). \tag{3.281}$$

The imaginary part of the self-energy can be easily expressed in terms of the kernel as

$$\Gamma_{\mathbf{p}} = -\frac{1}{6}\int\frac{d^3l}{(2\pi)^3}\frac{1}{4E_{\mathbf{p}}E_{\mathbf{l}}}(R^{\text{transp}}(\mathbf{p},E_{\mathbf{p}}|\mathbf{l},E_{\mathbf{l}}) - R^{\text{transp}}(\mathbf{p},E_{\mathbf{p}}|\mathbf{l},-E_{\mathbf{l}})). \tag{3.282}$$

Now expanding the kernel, we obtain

$$
\begin{aligned}
-2\Gamma_{\mathbf{p}} &= \frac{1}{3}\int \frac{d^3l}{(2\pi)^3}\frac{1}{4E_{\mathbf{p}}E_{\mathbf{l}}}(\mathcal{K}(\mathbf{p},E_{\mathbf{p}}|\mathbf{l},E_{\mathbf{l}})-\mathcal{K}(\mathbf{p},E_{\mathbf{p}}|\mathbf{l},-E_{\mathbf{l}}))= \\
&= -\frac{1}{3}\frac{|\mathcal{T}|^2}{2}\frac{1}{1+n(E_{\mathbf{p}})}\int_{\mathbf{l},\mathbf{s_1},\mathbf{s_2}}\frac{(2\pi)^4\delta^4({\mathbf{s_1}}^{\mathrm{os}}-{\mathbf{s_2}}^{\mathrm{os}}+\mathbf{l}^{\mathrm{os}}-\mathbf{p}^{\mathrm{os}})}{2E_{\mathbf{p}}} \\
&\qquad 2(1+n(E_{\mathbf{l}}))(1+n(E_{\mathbf{s_1}}))n(E_{\mathbf{s_2}})+ \\
&\quad -\frac{1}{3}\frac{|\mathcal{T}|^2}{2}\frac{1}{1+n(E_{\mathbf{p}})}\int_{\mathbf{l},\mathbf{s_1},\mathbf{s_2}}\frac{(2\pi)^4\delta^4({\mathbf{s_1}}^{\mathrm{os}}-{\mathbf{s_2}}^{\mathrm{os}}+\mathbf{l}^{\mathrm{os}}-\mathbf{p}^{\mathrm{os}})}{2E_{\mathbf{p}}} \\
&\qquad\qquad n(E_{\mathbf{l}})(1+n(E_{\mathbf{s_1}}))(1+n(E_{\mathbf{s_2}})). \quad (3.283)
\end{aligned}
$$

By relabeling $s_2 \leftrightarrow \ell$ in the first line (and switching $\mathbf{p} \to -\mathbf{p}$ and $\mathbf{s_1} \to -\mathbf{s_1}$), we note that the two lines add into

$$
\begin{aligned}
-2\Gamma_{\mathbf{p}} &= -\frac{|\mathcal{T}|^2}{2}\frac{1}{1+n(E_{\mathbf{p}})}\int_{\mathbf{l},\mathbf{s_1},\mathbf{s_2}}\frac{(2\pi)^4\delta^4({\mathbf{s_1}}^{\mathrm{os}}-{\mathbf{s_2}}^{\mathrm{os}}+\mathbf{l}^{\mathrm{os}}-\mathbf{p}^{\mathrm{os}})}{2E_{\mathbf{p}}} \\
&\qquad n(E_{\mathbf{l}})(1+n(E_{\mathbf{s_1}}))(1+n(E_{\mathbf{s_2}}))= \\
&= -\frac{1/2}{1+n(\mathbf{p})}\int_{\mathbf{l},\mathbf{s_1},\mathbf{s_2}}\frac{(2\pi)^4\delta^4(\mathbf{p}^{\mathrm{os}}+\mathbf{l}^{\mathrm{os}}-{\mathbf{s_1}}^{\mathrm{os}}-{\mathbf{s_2}}^{\mathrm{os}})|\mathcal{T}|^2}{2E_{\mathbf{p}}} \\
&\qquad\qquad n(E_{\mathbf{l}})(1+n(E_{\mathbf{s_1}}))(1+n(E_{\mathbf{s_2}})). \quad (3.284)
\end{aligned}
$$

The last equation completes the proof that in the late time limit, the BSE for the retarded Green's function of the bilocal density operator precisely reproduces the Boltzmann equation. Thus we conclude that, in terms of our earlier notation, (3.74) and (3.75) are satisfied.

4 Black Hole scrambling from hydrodynamics

We argue that the gravitational shock wave computation used to extract the scrambling rate in strongly coupled quantum theories with a holographic dual is directly related to probing the system's hydrodynamic sound modes. The information recovered from the shock wave can be reconstructed in terms of purely diffusion-like, linearized gravitational waves at the horizon of a single-sided black hole with specific regularity-enforced imaginary values of frequency and momentum. In two-derivative bulk theories, this horizon "diffusion" can be related to late-time momentum diffusion via a simple relation, which ceases to hold in higher-derivative theories. We then show that the same values of imaginary frequency and momentum follow from a dispersion relation of a hydrodynamic sound mode. The frequency, momentum and group velocity give the holographic Lyapunov exponent and the butterfly velocity. Moreover, at this special point along the sound dispersion relation curve, the residue of the retarded longitudinal stress-energy tensor two-point function vanishes. This establishes a direct link between a hydrodynamic sound mode at an analytically continued, imaginary momentum and the holographic butterfly effect. Furthermore, our results imply that infinitely strongly coupled, large-N_c holographic theories exhibit properties similar to classical dilute gasses; there, late-time equilibration and early-time scrambling are also controlled by the same dynamics.[1]

4.1 Introduction

The notion that dynamics at widely separated timescales is governed by independent processes lies at the heart of modern physics. The emergence of collective phenomena is a clear example. At very short timescales, the physics is described by microscopic "far-from-equilibrium" dynamics; at long timescales, it is the universal statistics-dominated processes that

[1] The contents of this chapter have been published in S. Grozdanov, K. E. Schalm and V. Scopelliti, Phys. Rev. Lett. **120** (2018) no.23, 231601.

control the onset of equilibrium. Ironically, the most prevalent textbook example of collective emergence, the computation by Maxwell of the shear viscosity of a classical ideal gas, fails this guideline. As is well known, in dilute gases the shear viscosity and some other transport coefficients are directly related to the 2-to-2 scattering rates of the microscopic constituents. In dilute gases, the early-time physics thus also controls the late-time approach to equilibrium. Our full understanding of kinetic theory explains why dilute gases violate the canonical notion of separation of scales. The dilute gas is a special case for which the BBGKY hierarchy that builds up the long-time behavior from microscopic processes truncates [127, 139–146].

On the other hand, in generic (e.g. dense) many-body systems, the early-time physics is distinct from late-time evolution. Of course, this does not imply that the early-time physics is irrelevant to collective behavior, as indeed, it crucially ensures ergodicity or mixing (scrambling). Nevertheless, one generically distinguishes (at least) two timescales: an early-time ergodic and a late-time collective scale. In classical systems, ergodicity is driven by chaotic non-linear dynamics, whereas statistics and universality drive collective behavior. These two different scales have a direct manifestation in classical dynamical systems analysis. Chaotic dynamics is characterized by Lyapunov exponents encoding the exponential divergence of trajectories with infinitesimally different initial conditions—the butterfly effect. A Gibbs ensemble of such initial conditions, however, equilibrates with a generically distinct characteristic timescale set by Pollicott-Ruelle resonances [151, 205, 206], again exemplifying the notion that widely separated timescales are driven by different physics.

Perturbative quantum field theories are usually studied in the dilute regime and as in the classical gas, both timescales are driven by the same physics [44, 69, 136, 152–154]. Strongly coupled, dense, quantum theories on the other hand are expected to have distinct scales. Triggered by studies [12, 16, 151, 207, 208] on collective dynamics in strongly coupled large-N_c quantum systems holographically dual to black holes, Blake observed that in the simplest such systems, late-time diffusion and early-time ergodic dynamics do appear to be governed by the same physics [64], similar to the dilute gas rather than the generic expectation. Follow-up studies extended the range of systems [33, 65, 67, 209, 210], found counterexamples [211] and observed that it only applied to thermal diffusivity [66, 212].

In this work, we will show how the holographic computations of quantum ergodic dynamics—the holographic butterfly effect—and hydrodynamics are related. In particular, we will show that the characteristic exponential growth exists on the level of (retarded) two-point functions when the

hydrodynamic sound mode is driven to instability by a choice of a specific value of momentum. This result indicates an intriguing similarity between the behavior of infinitely strongly coupled large-N_c theories holographically dual to two-derivative gravity and classical dilute gases in the sense that chaotic dynamics is entirely describable by the same physics of hydrodynamic modes, albeit excited outside of the hydrodynamic regime of small frequency ω and momentum k compared to the temperature scale T of the CFT. In this Letter, we will only focus on charge-neutral systems, although we expect our findings to be valid also for charged states and for systems with momentum relaxation in which long-lived longitudinal modes are controlled by diffusion.

4.2 Scrambling and hydrodynamical transport

By convention, the early-time onset of ergodicity is characterized by the scrambling rate λ and the butterfly velocity v_B, which are defined from the early-time rate of exponential growth of out-of-time-ordered correlation function (OTOC) of local (unbounded) operators,

$$C(t,x) = -\frac{\langle [\hat{W}(t,x),\hat{V}(0)]^\dagger [\hat{W}(t,x),\hat{V}(0)]\rangle_\beta}{2\langle \hat{W}(t,x)\hat{W}(t,x)\rangle_\beta \langle \hat{V}(0)\hat{V}(0)\rangle_\beta} \simeq e^{2\lambda(t-x/v_B)}\,. \tag{4.1}$$

Here, $\hat{V}(t,x)$ and $\hat{W}(t,x)$ are generic operators, and expectation values are taken in the thermal ensemble with temperature $T = 1/\beta$. In systems with a classical analogue for which such growth persists as $t \to \infty$ and for special (unbounded) operators, this indeed computes the Lyapunov exponent $\lambda_L = \lambda$ associated with chaotic behavior underpinning classical ergodicity [148–150].

Not all systems exhibit late-time regime of exponential growth of this correlator—in fact, most quantum systems do not [155, 156], illustrating the tension between classical chaos and quantum dynamics. Large-N_c systems with a holographic dual do exhibit such growth. Extrapolating from the insight that any perturbation carries energy, it has been argued that this exponential rate can be read off from a gravitational shock wave propagating along the double-sided (maximally extended) black hole horizon [12].

The non-linear shock wave calculation implicitly focusses on energy-momentum dynamics in the dual theory, rather than generic dynamics, as

this is what purely gravitational spacetime dynamics and waves encode. On the other hand, the collective late-time dynamics of energy-momentum is also well-understood with its IR dynamics governed by hydrodynamics. Its behavior can be computed from linearized gravitational perturbations (see e.g. [100, 120, 213]). The mere fact that the gravitational shock wave encoding early-time ergodicity describes the dynamics of energy-momentum, as do hydrodynamic excitations, is far from sufficient for establishing any relation between them. A more telling fact is that the exact non-linear shock wave solution is actually also a solution to linearized gravitational equations. This is what we show now. This results then leads to our discovery that when perturbed with a special imaginary momentum, the late-time hydrodynamic sound mode reflects the leading-order early-time instability of the system with the exponential growth set by λ_L and the butterfly velocity v_B.

4.3 Shock waves from linearized gravitational perturbations

Chaotic properties normally extracted from shock waves can be inferred directly from a single-sided, linearized analysis of the bulk gravitational equations. We study five-dimensional, two-derivative, classical gravity with the action

$$S = \frac{1}{2\kappa_5^2}\int d^5x\sqrt{-g}\left[R + \frac{12}{L^2} + \mathcal{L}_{matter}\right], \tag{4.2}$$

which gives rise to the following Einstein's equations (in units where $L = 1$):

$$\mathbf{G}_{\mu\nu} \equiv R_{\mu\nu} - \frac{1}{2}g_{\mu\nu}R - 6g_{\mu\nu} = \kappa_5^2\, T_{\mu\nu}^{matter}\,. \tag{4.3}$$

In the longitudinal sound channel, in the $h_{\mu z} = 0$ gauge with momentum in the z-direction, we write a first-order perturbed metric as

$$\begin{aligned} ds^2 = &-f(r)dt^2 + \frac{dr^2}{f(r)} + b(r)\left(dx^2 + dy^2 + dz^2\right) \\ &- \left[f(r)H_1 dt^2 - 2H_2 dtdr + \frac{H_3 dr^2}{f(r)} + H_4\left(dx^2 + dy^2\right)\right], \end{aligned} \tag{4.4}$$

where H_i are functions of t, z and r, and $f(r_h) = 0$. We demand that the perturbation is null in the radial direction at the horizon, set $H_4(r_h) = 0$

and write

$$H_1 = H_3 = (C_+ W_+(t,z,r) + C_- W_-(t,z,r))\,, \tag{4.5}$$
$$H_2 = (C_+ W_+(t,z,r) - C_- W_-(t,z,r))\,. \tag{4.6}$$

First, consider $T^{matter}_{\mu\nu} = 0$ to focus on the AdS-Schwarzschild black brane background with $b(r) = r^2$ dual to thermal $\mathcal{N} = 4$ supersymmetric Yang-Mills (SYM) theory. We can write $W_\pm$ as

$$W_\pm(t,z,r) = e^{-i\omega\left[t \pm \int^r \frac{dr'}{f(r')}\right] + ikz}\, h_\pm(r)\,, \tag{4.7}$$

where $h_\pm(r)$ are regular at $r = r_h$. Using $\mathbf{G}_{rr} = 0$, then

$$h_\pm(r) = e^{\int^r \frac{k^2 \pm 9i\omega r' - 12 r'^2}{3 r' f(r')} dr'}\,. \tag{4.8}$$

Imposing regularity [214, 215] on (4.8) fixes a single relation between ω, k^2 and r_h. Ensuring the remaining equations of motion (4.3) are solved at $r = r_h$, gives a second, (advanced and retarded) *diffusive* condition,

$$\omega_\pm \equiv \pm i\mathfrak{D}k^2 = \pm\, i\frac{1}{3\pi T}k^2\,. \tag{4.9}$$

Combined with the horizon-regularity, this fixes the solution in terms of a specific imaginary momentum mode

$$k^2 \equiv -\mu^2 = -6\pi^2 T^2\,, \tag{4.10}$$

which gives the Lyapunov exponent and the butterfly velocity, i.e. for modes with $e^{-i\omega t + ikz}$,

$$\omega_\pm \equiv \mp i\lambda_L\,, \quad \lambda_L = 2\pi T\,, \tag{4.11}$$
$$v_B \equiv \left|\frac{\omega_\pm}{k}\right| = \sqrt{\lambda_L \mathfrak{D}}\,. \tag{4.12}$$

Away from the horizon, the corrections to the present solution can be consistently constructed in a small $\sqrt{r - r_h}$ expansion, requiring $H_4 \neq 0$.

For a regular $T^{matter}_{\mu\nu} \neq 0$, one can see the horizon diffusion arise more generally. For a background metric (4.4), the regularity of $\mathbf{G}_{rr}$ implies

$$b(r_h) = b'(r_h) f'(r_h)/8\,. \tag{4.13}$$

Assuming that $T_{tr}(r_h) = 0$, it follows immediately from $\mathbf{G}_{tr}(r_h) = 0$ that at $r = r_h$,

$$\partial_t W_\pm = \mp\, \mathfrak{D}\, \partial_z^2 W_\pm\,, \tag{4.14}$$

with the horizon diffusion coefficient, as in [64]:

$$\mathfrak{D} = \frac{v_B^2}{\lambda_L} = \frac{2}{3}\frac{1}{b'(r_h)} = \frac{1}{12}\frac{f'(r_h)}{b(r_h)}\,. \tag{4.15}$$

Assuming that the solution is not supported by $T_{\mu\nu}^{matter}$ and requiring regularity in $\mathbf{G}_{rr}$, we again obtain the Lyapunov exponent from Eq. (4.11) and imaginary momentum

$$k^2 = -\frac{3}{4}b'(r_h)f'(r_h) = -3\pi T\, b'(r_h)\,. \tag{4.16}$$

Therefore, we have recovered all known shock wave results from a linear gravitational perturbation of a single-sided black brane. The validity of this solution requires sufficient decoupling of $\mathcal{L}_{matter}$ at the horizon, which is implicitly assumed in the shock wave computation. Generically, this will not be the case. The sound channel couples all scalar excitations, and one needs to demand that all their equations of motion are satisfied as well.

Higher-derivative gravity corrections encode (inverse) coupling constant corrections in the dual field theory [165, 216–223]. An analogous calculation as in two-derivative theories can now be done e.g. in Gauss-Bonnet theory (for details regarding the theory see e.g. [223]), where we also recover the known results of Ref. [15], [2]

$$\omega_\pm = \mp 2i\pi T\,, \qquad k^2 = -\frac{6\pi^2 T^2}{N_{GB}^2}\,, \qquad v_B^2 = \frac{2}{3}N_{GB}^2\,. \tag{4.17}$$

Focusing again on the two-derivative action (5.7) dual to $\mathcal{N}=4$ SYM at large N_c and infinite coupling, and transforming the metric (4.4) to Kruskal-Szekeres coordinates, one finds

$$\begin{aligned} ds^2 = {} & A(UV)\,dUdV + B(UV)d\mathbf{x}^2 \\ & - A(UV)\,e^{ikz}\left(C_+\frac{dU^2}{U} - C_-\frac{dV^2}{V}\right). \end{aligned} \tag{4.18}$$

Our solution thus takes the form of the exact shock wave solution $ds^2 = A(UV)dUdV + B(UV)d\mathbf{x}^2 - A(UV)\delta(U)h(x)dU^2$, but travelling along both null $U=0$ and $V=0$. The only difference is that the shock solution has a Dirac delta function support $h_{UU} \propto \delta(U)$, whereas the solution presented here has support given by a (smeared) $h_{UU} \propto \Delta(U) \equiv 1/U$. At the level

[2] N_{GB} is conventionally set to $N_{GB}^2 = \left(1+\sqrt{1-4\lambda_{GB}}\right)/2$, which ensures that the boundary speed of light is one.

of the linearized Einstein's equations, the function $\Delta(U) \equiv 1/U$ satisfies the distributional identities used to construct the shock wave solution: $U\partial_U\Delta(U) = -\Delta(U)$ and $U^2\partial_U^2\Delta(U) = 2\Delta(U)$. Distributional identities of the type $F(U)\Delta^2(U) \approx 0$, when integrated over U for sufficiently smooth $F(U)$, are satisfied approximately but not exactly as with $\delta^2(U)$ (see e.g. [224]). A distinct difference is that the $\delta(U)$-shock is supported by energy-momentum at the horizon. The linearized solution (4.18) with a less singular support is a leading-order in $1/U$ approximation of an exact smooth solution to Einstein's equation with no source of energy-momentum. It is a longitudinal (sound) mode, which encodes the correct Lyapunov exponent and the butterfly velocity.

4.4 Hydrodynamics and the sound mode

Sound is well understood as a hydrodynamical phenomenon. In holography, it is encoded by the low-energy limit of the sound channel spectrum [120, 225] and is described by a pair of longest-lived modes $\omega_\pm^*(k)$. Within the hydrodynamic approximation (expansion of $\omega_\pm^*$ for $|k|/T \ll 1$),

$$\omega_\pm^*(k) \approx \pm \sum_{n=0}^{\infty} \mathcal{V}_{2n+1} k^{2n+1} - i \sum_{n=0}^{\infty} \Gamma_{2n+2} k^{2n+2}, \tag{4.19}$$

which is analytically known for $\mathcal{N} = 4$ SYM to $\mathcal{O}(k^4)$ at infinite coupling, i.e. to third order in the hydrodynamic expansion [226]. All $\mathcal{V}_n$ and Γ_n are real and for $\mathcal{N} = 4$ SYM at infinite coupling, $\mathcal{V}_1 = 1/\sqrt{3}$, $\Gamma_2 = 1/(6\pi T)$, $\mathcal{V}_3 = (3 - 2\ln 2)/(24\sqrt{3}\pi^2 T^2)$ and $\Gamma_4 = (\pi^2 - 24 + 24\ln 2 - 12\ln^2 2)/(864\pi^3 T^3)$. For real k, Eq. (4.19) describes attenuated propagating modes. However, for imaginary k, which is required to construct the above gravitational solution, both $\omega_\pm^*$ and k are purely imaginary. To find $\omega_\pm^*(k)$ for imaginary k, we compute the quasinormal mode spectrum (poles of the retarded sound channel stress-energy tensor two-point function, e.g. the energy-energy $G^R_{T^{00}T^{00}}(\omega, k)$) [120], which can be done analytically in the hydrodynamic expansion (small $|\omega|/T \ll 1$, $|k|/T \ll 1$) or numerically in the holographic model for any ω and k. Our first observation is that for imaginary k, the system is driven to instability, which results in at least one of the two sound modes in (4.19) having $\mathrm{Im}[\omega] > 0$. Our main result, however, is that the fully numerically computed frequency (dispersion relation) of the most unstable sound mode ω_+^* asymptotically approaches the Lyapunov exponent growth rate $k = i\mu = \sqrt{6}i\pi T$:

$$\omega_+^*(i\mu) = i\lambda_L\,. \tag{4.20}$$

Precisely at $k = i\mu$, the quasinormal mode solution does not exist, even though it exists infinitesimally close to this point when approached from either side along the imaginary k dispersion curve. This allows us to deduce that at the special point $\omega_+^*(i\mu)$, cf. Eqs. (4.10) and (4.11), the retarded longitudinal two-point function of the stress-energy tensor has a hydrodynamic pole which contains all information about many-body chaos, λ_L and v_B. Furthermore, at the point of chaos, its residue vanishes:

$$\operatorname{Res} G^R_{T^{00}T^{00}}(\omega = \omega_+^*(i\mu) = i\lambda_L, k = i\mu) = 0\,. \tag{4.21}$$

The two-point correlator identity (4.21) is sufficient for uniquely specifying the point of chaos in the CFT, eliminating the need for the OTOC considerations to find μ.

We note that, intriguingly, the dispersion relation around this point can be reasonably well approximated by $\omega = v_B k$. This is evident from the numerical computations and from the third-order hydrodynamic approximation to $\omega_+(k)$, which reproduces the full dispersion relation of the dominant mode rather well, giving $\omega_+^*(i\mu) \approx 0.990 \times i\lambda_L$. Our results are presented in Fig. 4.1.

4.5 Discussion

These results show that the holographic butterfly effect and black hole scrambling can be understood in terms of a hydrodynamic sound mode at a specific imaginary momentum (exponentially spatially growing fluid profile), which is fixed by dual Einstein's equations governing a radially null sound mode and the condition of regularity (without additional energy-momentum) at the horizon. At $\omega_+^*(i\mu)$, the sound mode dispersion relation gives the Lyapunov exponent associated with holographic many-body chaos. Furthermore, even though $|k|/T$ lies at the edge or outside of the hydrodynamic regime [165, 227], the full dispersion relation is well described by the hydrodynamic approximation.

What are the physical implications of our observations? Several recent papers have speculated on relations between late-time diffusion and the butterfly effect [64–67, 136, 154, 211, 228, 229]. The late-time behavior of hydrodynamic excitations in a translationally invariant, uncharged CFTs is controlled by momentum diffusion. In theories holographically dual to two-derivative gravity, momentum diffusion D is completely determined by horizon data [119] while charge diffusion is not. Given a (background)

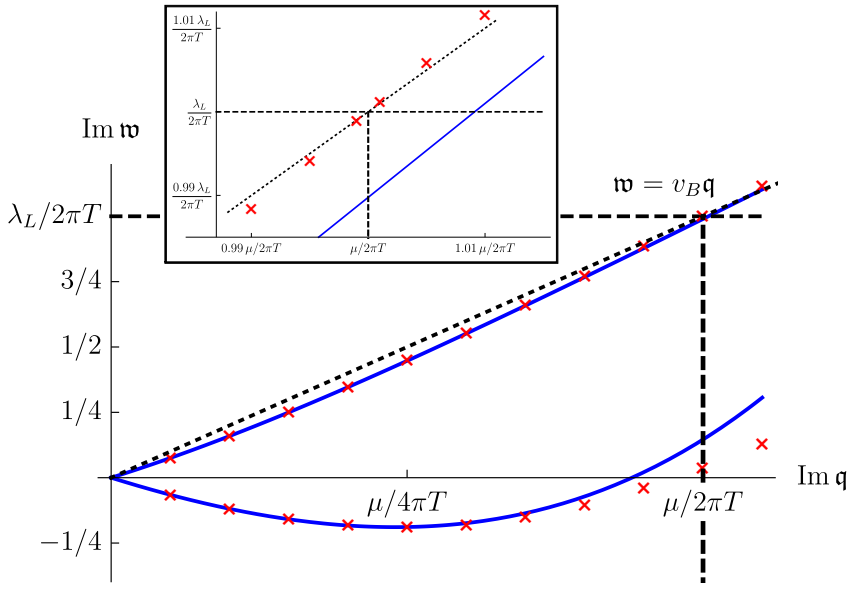

Figure 4.1: Dispersion relations of the hydrodynamic sound modes, plotted for imaginary dimensionless $\mathfrak{w} \equiv \omega/2\pi T$ and $\mathfrak{q} \equiv k/2\pi T$. The blue lines depict the third-order hydrodynamic result [226] and the red crosses the numerically computed $\mathfrak{w}^*_\pm(\mathfrak{q})$. Dashed lines indicate the values of $\omega = i\lambda_L$ and $k = i\mu$. The dotted line is the linear dispersion relation $\mathfrak{w} = v_B\mathfrak{q}$. The inlay depicts a zoomed-in plot around $k = i\mu$.

metric (4.4) and the shock wave diffusivity $\mathfrak{D}$ (cf. Eq. (4.15)):

$$\frac{D}{\mathfrak{D}} = \frac{3\,b'(r_h)}{8\pi T}\,. \tag{4.22}$$

In large-N_c $\mathcal{N} = 4$ SYM theory at infinite coupling, this reduces to $D/\mathfrak{D} = 3/4$. However, as we move away from infinite coupling and consider higher-derivative bulk theories, D is no longer computable in terms of simple horizon data, which results in deviations of η/s from $1/4\pi$. Since the butterfly velocity and the Lyapunov exponent are by construction computed only at the horizon, we have a-priori no reason to expect that there continues to exist a simple relation between D and $\mathfrak{D}$ in holographic duals with more then two derivatives. Indeed, the ratio of $D/\mathfrak{D}$ in Gauss-Bonnet has non-trivial coupling dependence [15, 223], and is thus not universal [3].

[3] For a discussion regarding the validity of hydrodynamics in the presence of coupling constant corrections, see [121, 165, 222, 223, 230, 231].

As we emphasized in the Introduction, a relation, such as (4.22), which depends only on $r_h \sim T$, between late-time and early-time physics is rather unexpected. The exception is the classical dilute gas. Its early-time chaos and late-time diffusion are controlled by the same process (2-to-2 scattering). Our findings show that the situation is similar in an infinitely strongly coupled, large-N_c CFT. As a result, early-time scrambling and late-time hydrodynamics are qualitatively related and appear to be driven by the same physics—hydrodynamics.

The reason that an obtuse relation between microscopic ergodicity from shock waves and late-time diffusion is sought after is that black holes are special in that their ergodicity rate λ_L saturates a conjectured bound $\lambda_L \leq 2\pi T$ [16]. If early-time ergodicity indeed controlled late-time diffusion, this bound could imply a long-sought fundamental diffusion bound [229, 232] [4]. Such a fundamental bound was re-postulated several years ago based on early results on collective dynamics in holography by noting that the shear viscosity in these systems only depends on horizon data [118, 236]. Expressions such as Eq. (4.22) make it clear, however, that the Lyapunov exponent bound does not yield a diffusion bound. The dependence on the temperature through r_h or the presence of additional scales allows this ratio to take any value. We note that such temperature dependence is also present in the classical dilute gas of particles with mass m and density ρ through the average velocity v. Its shear viscosity η and the Lyapunov exponent [161] behave as

$$\eta \sim m\frac{\sqrt{\langle v^2(T)\rangle}}{\sigma_{2-2}}\,, \qquad \lambda_L \sim \rho(T)\sqrt{\langle v^2(T)\rangle}\sigma_{2-2}\,, \tag{4.23}$$

with σ_{2-2} the 2-to-2 scattering rate. As a final comment, we note that the evolution of the unstable hydrodynamic mode, albeit driven to instability with a choice of an imaginary momentum, may not only grow with exponential growth faster than $\mathrm{Im}[\omega] > \lambda_L = 2\pi T$ but can also have a local group velocity larger than v_B at various values of imaginary k (cf. Fig. 4.1). As also found in [160, 229], this indicates that the butterfly velocity may not in all generality be a bounding velocity. Understanding the relation between these observations and bounds on λ_L and the speed of propagation of quantum correlations remains an important open problem, as does a better understanding of the relation between many-body microscopic chaos and instability-induced collective hydrodynamic turbulence.

[4] For two examples of rigorous diffusion bounds in one-dimensional systems, see [233]. In holography, one can derive bounds on conductivities in disordered systems [234, 235] but as of yet, not on diffusion.

5 Regulator dependence of the OTOC and kinetic theory at rescue

We study the contour dependence of the out-of-time-ordered correlation function (OTOC) both in weakly coupled field theory and in the Sachdev-Ye-Kitaev (SYK) model. We show that its value, including its Lyapunov spectrum, depends sensitively on the shape of the complex time contour in generic weakly coupled field theories. For gapless theories with no thermal mass, such as SYK, the Lyapunov spectrum turns out to be an exception; their Lyapunov spectra do not exhibit contour dependence, though the full OTOCs do. Our result puts into question which of the Lyapunov exponents computed from the exponential growth of the OTOC reflects the actual physical dynamics of the system. We argue that, in a weakly coupled Φ^4 theory, a kinetic theory argument indicates that the symmetric configuration of the time contour, namely the one for which the bound on chaos has been proven, has a proper interpretation in terms of dynamical chaos. Finally, we point out that a relation between these OTOCs and a quantity which may be measured experimentally — the Loschmidt echo — also suggests a symmetric contour configuration, with the subtlety that the inverse periodicity in Euclidean time is half the physical temperature. In this interpretation the chaos bound reads $\lambda \leq \frac{2\pi}{\beta} = \pi T_{\text{physical}}$.[1]

5.1 Introduction

It has long been known that chaos, understood as the exponential sensitivity of the dynamics to initial conditions, does not have an immediate equivalent in the quantum dynamics governed by the Schrödinger equation. In quantum systems one needs to define quantum chaos in a more indirect way. One way to do so, is to measure the correlation between an operator $W(t)$ and some earlier perturbation $V(0)$ and compare this with the

[1] The contents of this chapter have been published in A. Romero-Bermúdez, K. E. Schalm and V. Scopelliti, J. High Energ. Phys. **2019**, 107 (2019).

correlation where the perturbation $V(0)$ is performed after operator $W(t)$ is inserted:

$$\langle\psi_{\text{final}}|W(t)V(0)|\psi_{\text{initial}}\rangle - \langle\psi_{\text{final}}|V(0)W(t)|\psi_{\text{initial}}\rangle \tag{5.1}$$
$$= \langle\psi_{\text{final}}|[W(t),V(0)]|\psi_{\text{initial}}\rangle\,. \tag{5.2}$$

Choosing $W(t) = q(t)$ and $V(0) = p(0)$ this commutator formally equals $[W(t),V(0)] = i\hbar\frac{\partial q(t)}{\partial q(0)}$ and in that sense the above measures the sensitivity to initial conditions. The commutator is evaluated between two wave-functions, however. For a generic $|\psi_{\text{initial}}\rangle$ and $|\psi_{\text{final}}\rangle$, this is a complex amplitude that also depends on the details of both. An obvious step is to sum over final states, which converts this to an expectation value

$$C(t;\psi_{\text{initial}}) = \sum_{\text{final}}\langle\psi_{\text{initial}}|[W(t),V(0)]^\dagger|\psi_{\text{final}}\rangle\langle\psi_{\text{final}}|[W(t),V(0)]|\psi_{\text{initial}}\rangle$$
$$= \langle\psi_{\text{initial}}|[W(t),V(0)]^\dagger[W(t),V(0)]|\psi_{\text{initial}}\rangle\,. \tag{5.3}$$

To also isolate the dynamics driven by $V(0)$ and $W(t)$ as much from the details of the initial state, one can average over a suitable ensemble. A physically natural choice is the thermal one

$$C(t;\beta) = \sum_{\text{initial}} e^{-\beta E[\psi_{\text{initial}}]}\langle\psi_{\text{initial}}|[W(t),V(0)]^\dagger[W(t),V(0)]|\psi_{\text{initial}}\rangle$$
$$= \text{Tr}\rho_\beta[W(t),V(0)]^\dagger[W(t),V(0)]\,. \tag{5.4}$$

This commutator-squared $C(t;\beta)$ or, equivalently, this out-of-time ordered correlation function (OTOC) has been of much interest as a diagnostic of chaotic behaviour in many-body systems [16, 237, 238]. Specifically, if this OTOC has a regime where it exhibits an exponential time dependence, $C(t) \sim e^{\lambda t}$, this behaviour has been proposed to be a signature of chaos, with λ being the *quantum* Lyapunov exponent.[2] Moreover, this quantum Lyapunov exponent has been conjectured to be bounded from above $\lambda \leq 2\pi k_B T/\hbar$ [16].

In practice most computations do not compute $C(t)$ as defined above. Rather one "smears" the thermal distribution between the two commutators [16, 239]

$$C(t;\beta)_{\text{regulated}} \equiv \text{Tr}\left(\rho^{\frac{1}{2}}[W(t),V]^\dagger\rho^{\frac{1}{2}}[W(t),V]\right)\,. \tag{5.5}$$

[2] Note that the Lyupanov exponent defined this way is in fact twice the chaos exponent one would surmise from the choice $W(t) = q(t)$, $V(0) = p(0)$ with $q(t) \sim e^{\lambda_{\text{chaos}}t}q(0)$, i.e. $\lambda = 2\lambda_{\text{chaos}}$.

Mathematically, this has the advantage of being manifestly Hermitian (see e.g. [239]). The physical intuition is that in a QFT this correlation function naively suffers from a short-distance divergences caused by the insertion of two operators at the same time. As chaos is in principle a long-time characteristic, the claim is that the information about chaos, and in particular the Lyapunov exponents λ, do not depend on this regularization [16, 239].

We will show that this intuition is incorrect, as was also pointed out earlier in [240] for the specific case of 2D fermions with quenched disorder. By explicit computation we will show that in the two-parameter family of "regularized" OTOCs

$$C(t;\beta)_{(\alpha,\sigma)} \equiv \tag{5.6}$$
$$-\operatorname{Tr}\left[\rho^{1-\alpha-\sigma}\Big(W^\dagger(t)\rho^\sigma V^\dagger - V^\dagger\rho^\sigma W^\dagger(t)\Big)\rho^{\alpha-\sigma}\Big(W(t)\rho^\sigma V - V\rho^\sigma W(t)\Big)\right],$$

the Lyapunov exponents are independent of σ but do depend on α. Our computation shows that this regularization dependence is an IR-effect and has nothing to do with short-distance singularities. The more appropriate comparison for the regularization dependence of the OTOC is the proof in Schwinger-Keldysh theory that physical correlation functions are independent on the choice of contour. In Schwinger-Keldysh theory, there is a diagrammatic proof that *physical* Green's functions involving operator insertions either on only forward or only backward branches are independent of the contour due to energy conservation; this can be found in e.g. [241, 242]. The OTOC, however, is a correlation on a doubled Schwinger-Keldysh contour [243] and the two-body Green's functions involved in the commutator-squared involve operators inserted on both forward and backward branches. The arguments of [241, 242] do not generalize to prove that the correlation functions that appear in $C(t;\beta)_{(\alpha,\sigma)}$ must be independent on the contour. Our explicit computation in Section 5.3 shows that they indeed are not.

Gapless theories are notoriously more IR sensitive than gapped theories. Perhaps somewhat counterintuitively, our results show that weakly coupled gapless theories are in fact less contour-dependent than explicitly gapped theories, although the thermally generated mass does imbue a suppressed dependence. The SYK model on the other hand, which has been at the forefront of many OTOC studies, has no thermally induced mass. In this model specifically the contour dependence is extremely weak. In fact its Lyapunov spectrum turns out to be always contour-independent, as we show in Section 5.4.

Let us stress that the found contour dependence in generic models is not a pedantic point. As also pointed out by [240], OTOCs are now being measured either in numerical or actual physical experiments. Often one massages the regulator to be the most convenient for the set-up. For instance, Das et. al. [244] use the canonical thermal OTOC $C(t;\beta)_{(0,0)}$ in a numerical study, whereas a cold atom experiment measures a Loschmidt echo [245], which can be related to $C(t;\beta)_{(\frac{1}{2},0)}$. As the theoretical prediction for these two correlation functions is different due to the regulator dependence, these two experimental results cannot be compared to each other.

Given the regularization dependence that we and [240] observe, the immediate question arises: which is the proper regularization that measures quantum chaos. As the previous paragraph shows, to some extent this is in the eye of the beholder. One can devise experimental set-ups that measure either. Nevertheless, we will argue that the OTOC that most closely reflects physical microscopic chaos is the symmetrized one $C(t;\beta)_{(\frac{1}{2},0)}$ used originally for hermiticity reasons. Our argument rests on the following fact: in weakly coupled field theories the computation of any of the OTOCs $C(t;\beta)_{(\alpha,\sigma)}$ can be cast in the form of a kinetic equation [44]. This kinetic equation reveals most closely the physical process one is actually computing. In terms of the kinetic equation, only the symmetrized OTOC with $\alpha = 1/2$ can be understood as a microscopic unbiased "collision"-counter. Such unbiased collision counters have long been successfully proposed as tracking microscopic classical chaos [161, 246]. This is explained in Section 5.3.2.

We conclude by showing the symmetric OTOC $C(t;\beta)_{(\frac{1}{2},0)}$ regulated this way has a natural interpretation as a Loschmidt echo, rather than an expectation value in a thermal ensemble as in the introductory thought experiment. This has as subtle physical consequence that the physical temperature is set by twice the inverse periodicity in Euclidean time. In this interpretation the MSS bound reads

$$\lambda \leq \frac{k_B}{\hbar}\frac{2\pi}{\beta} = \frac{\pi k_B T_{\text{physical}}}{\hbar} \ . \tag{5.7}$$

5.2 A two-parameter family of extended Schwinger-Keldysh contours

We will assume that $W(t)$ and $V(0)$ are hermitian from here on.
We formally consider the following regularization of the commutator-

squared of Eq. (5.4):

$$C(t;\beta)_{(\alpha,\sigma)} = \mathrm{Tr}\left[\mathcal{A}^\dagger \mathcal{A}\right] \geq 0\,, \tag{5.8}$$

$$\mathcal{A} \equiv \rho^{\frac{\alpha-\sigma}{2}}\ [W(t), V(0)]_\sigma\ \rho^{\frac{1-\alpha-\sigma}{2}}\,, \quad [A,B]_\sigma \equiv A\rho^\sigma B - B\rho^\sigma A\,, \tag{5.9}$$

with $\sigma \in [0, 1/4]$. First, we note that for $0 \leq \alpha \leq 1$, $C(t;\beta)_{(\alpha,0)}$ is positive definite and for $\alpha = \{0,1\}$, $\sigma = 0$ we recover the unregulated thermal commutator-squaredd in the thermal state.

Expanding the terms in $C(t;\beta)_{(\alpha,\sigma)}$ gives Eq. (5.6)

$$\begin{aligned} C(t;\beta)_{(\alpha,\sigma)} = &-\mathrm{Tr}\left[\rho^{1-\alpha-\sigma}W(t)\rho^\sigma V\rho^{\alpha-\sigma}W(t)\rho^\sigma V + \rho^{1-\alpha-\sigma}V\rho^\sigma W(t)\rho^{\alpha-\sigma}V\rho^\sigma W(t)\right] \\ &+ \mathrm{Tr}\left[\rho^{1-\alpha-\sigma}W(t)\rho^\sigma V\rho^{\alpha-\sigma}V\rho^\sigma W(t) + \rho^{1-\alpha-\sigma}V\rho^\sigma W(t)\rho^{\alpha-\sigma}W(t)\rho^\sigma V\right]\,, \end{aligned}$$

The last two are conventional Schwinger-Keldysh time-ordered correlation functions (TOCs), whereas the first two are true out-of-time-ordered correlators of the type

$$F(t_1,t_2)_{(\alpha,\sigma)} \equiv \mathrm{Tr}[\rho^{1-\alpha-\sigma}W(t_1)\rho^\sigma V\rho^{\alpha-\sigma}W(t_2)\rho^\sigma V] \tag{5.10}$$

$$= \mathrm{Tr}[\rho^{1-\alpha}\ W(t_1 - i\sigma\beta)V\ \rho^\alpha\ W(t_2 - i\sigma\beta)V] \tag{5.11}$$

$$= F(t_1 - i\sigma\beta, t_2 - i\sigma\beta)_{(\alpha,0)}\,. \tag{5.12}$$

Schematically $C(t;\beta)_{(\alpha,\sigma)}$ equals

$$C(t;\beta)_{(\alpha,\sigma)} = \mathrm{TOCs} - F\Big(t - i\sigma\beta, t - i\sigma\beta\Big)_{(\alpha,0)} - F\Big(t - i(1-\alpha-\sigma)\beta, t - i(\alpha-\sigma)\beta\Big)_{(\alpha,0)}\,. \tag{5.13}$$

Each out-of-time ordered correlator $F(t_1,t_2)_{(\alpha,\sigma)}$ may be seen as a correlation function in the extended Schwinger-Keldysh contour. The usual choice with $\alpha = 1/2$, $\sigma = 1/4$ is shown in Fig. 5.1-(a); the more general $F(t_1,t_2)_{(\alpha,\sigma)}$ corresponds to a more complicated contour like the one shown in Fig. 5.1-(b) with different separations in imaginary time between each of the branches.

It is this OTOC $F(t_1,t_2)_{(\alpha,\sigma)}$ that controls the regime of exponential growth and the Lyapunov spectrum $F(t_1,t_2)_{(\alpha,\sigma)} \sim 1 - \mathsf{A}(t_1-t_2)e^{\lambda_{(\alpha,\sigma)}\frac{(t_1+t_2)}{2}}$, with $\mathsf{A}(0)$ a finite positive number. We will now show that the same exponential time dependence and thus the same Lyapunov exponent is obtained independent of the value of σ if $\alpha = 1/2$. This follows directly from the

analyticity property of the function highlighted above: $F(t_1,t_2)_{(\alpha,\sigma)} = F(t_1 - i\sigma\beta, t_2 - i\sigma\beta)_{(\alpha,0)}$ for $0 \leq \sigma \leq \min\{\alpha, 1-\alpha\}$ [16]. Suppose for the particular value $\sigma = 0$ the function $F(t_1,t_2)_{(\alpha,0)}$ has the exponential behavior $F(t_1,t_2)_{(\alpha,0)} \simeq \mathsf{A}(t_1 - t_2)e^{\lambda_\alpha \frac{t_1+t_2}{2}}$ with $\lambda_\alpha = \lambda_{(\alpha,0)}$. Analyticity implies that $F(t_1+i\xi\beta, t_2+i\gamma\beta)_{(\alpha,0)} \simeq \mathsf{A}(t_1 - t_2 + i\beta(\gamma - \xi \bmod 1))e^{i\frac{\xi+\gamma}{2}\beta\lambda_\alpha} e^{\lambda_\alpha \frac{t_1+t_2}{2}}$. Substituting this into Eq. (5.13), we get

$$C(t;\beta)_{(\alpha,\sigma)} \simeq \text{TOCs} + \Big[\mathsf{A}(0)e^{-i\sigma\beta\lambda_\alpha} + \mathsf{A}\big(i\beta(1-2\alpha \bmod 1)\big)e^{-i\frac{\beta\lambda_\alpha}{2}(1-\alpha-\sigma+\alpha-\sigma)}\Big]e^{\lambda_\alpha t} \,. \tag{5.14}$$

For the specific choice $\alpha = 1/2$ — the one that is made in almost all previous studies — the prefactor $\mathsf{A}(i\beta(1-2\alpha \bmod 1))|_{\alpha=1/2} = \mathsf{A}(0)$ is the same in both cases and equal to the one computed for the $\alpha = 1/2$. Thus

$$C(t;\beta)_{(\frac{1}{2},\sigma)} = \text{TOCs} + 2\mathsf{A}(0)e^{-i\beta\frac{\lambda_{1/2}}{4}} \cos\left[\left(\sigma - \frac{1}{4}\right)\beta\lambda_{1/2}\right] e^{\lambda_{1/2}t}\,, \tag{5.15}$$

with $\lambda_{1/2} = \lambda_{(\frac{1}{2},\sigma)}$, $\forall\sigma$. Although the Lyapunov exponent is not affected by the deformation parametrized by σ away from $(\alpha,\sigma) = (\frac{1}{2},0)$, we do see that the prefactor of the exponential depends on the σ-deformation of the contour. Therefore, similarly to a Wightman function in Schwinger-Keldysh theory, the full commutator-squared $C(t;\beta)_{(\frac{1}{2},\sigma)}$ cannot be an observable measurable in an experiment, even though it may contain physical information.

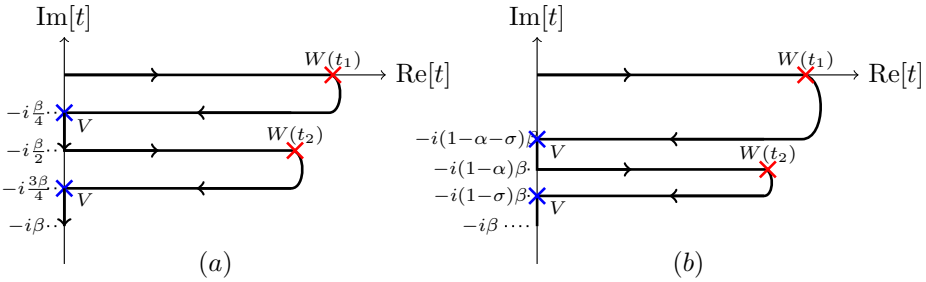

Figure 5.1: (a) Extended Schwinger-Keldysh contour corresponding to $\mathrm{Tr}[\rho^{\frac{1}{4}} V \rho^{\frac{1}{4}} W(t_2) \rho^{\frac{1}{4}} V \rho^{\frac{1}{4}} W(t_1)]$. (b) Contour corresponding to a general regularization of the OTOC $\mathrm{Tr}[\rho^{\sigma} V \rho^{\alpha-\sigma} W(t_2) \rho^{\sigma} V \rho^{1-\alpha-\sigma} W(t_1)]$, which contributes to $C_{(\alpha,\sigma)}(t_1,t_2)$.

We also point out that the dependence of the prefactor on the contour seems to be in tension with the recent attempts to associate *maximal chaos*, defined as maximal Lyapunov exponent $\lambda = 2\pi/\beta$, to *destructive interference* of the commutator-squared [247, 248]. The destructive interference refers to the fact that, if the decoherence factor equals $\cos(\lambda\beta/4)$, it vanishes for maximal chaos $\lambda = 2\pi/\beta$. This implies that for maximal chaos the exponential time-dependence should be absent in the symmetric commutator-squared. Our derivation shows, however, that this is an artefact of the analytical continuation. In our case, the decoherence factor of commutator-squared of Eq. (5.15) is $\cos((1/4-\sigma)\lambda\beta)$, which does not vanish for maximal chaos $\lambda = 2\pi/\beta$, provided $0 < \sigma \leq 1/4$. This casts doubts on how universal the relation between maximal chaos destructive interference may be.

Moreover, it has also been suggested that in SYK the prefactor of the OTOCs $A\cos(\lambda\beta/4)$, where $A = \beta J/N$, is an observable which is finite at zero temperature [249]. However, as we have shown above this quantity is contour-dependent and therefore, it is not manifestly a physical observable.

To summarize, since the commutator-squared depends on the contour it is not clear whether the regularised commutator-squared is actually an observable. Another possibility may be that not all regularizations of the commutator-squared are physically allowed and one value of σ is preferred. For the specific deformation parametrized by σ, we could not find an argument for such case.

5.2.1 The α-contour

Starting from $\alpha = 1/2$, the parameter σ affects only the decoherence factor of the commutator-squared but leaves the Lyapunov spectrum invariant. There is therefore a possibility that the Lyapunov spectrum as defined through the OTOC does measure a physical quantity. We set $\sigma = 0$ from here on and now explore its dependence on the other contour parameter α which fixes the distance between the forwards branches, as shown in Fig 5.2:

$$C(t;\beta)_{(\alpha,0)} = \mathrm{Tr}\left[\mathcal{A}^\dagger\mathcal{A}\right] \geq 0\,, \quad \mathcal{A} \equiv \rho^{\frac{1-\alpha}{2}}\,[W(t),V(0)]\,\rho^{\frac{\alpha}{2}}\,. \tag{5.16}$$

We have already seen that, for $\alpha \neq \frac{1}{2}$, different choices of σ cannot be related by analytic continuation. Neither can $C(t;\beta)_{(\alpha,0)}$ and $C(t;\beta)_{(\alpha',0)}$ be related to each other by analytic continuation. In other words, the distance in imaginary time between the forwards branches cannot be

compensated by analytic continuation of time. This may be seen explicitly by rewriting the OTOCs in $C(t;\beta)_{(\alpha,0)}$ as follows

$$\mathcal{H}_\alpha(t_1,t_2;t_3,t_4) \equiv \mathrm{Tr}\left[\rho^\alpha V(t_3)W(t_1)\rho^{1-\alpha}V(t_4)W(t_2)\right]$$
$$= \mathrm{Tr}\left[V\left(t_3+i\beta\Big(\alpha-\frac{1}{4}\Big)\right)\rho^{\frac{1}{4}}W\left(t_1+i\beta\Big(\alpha-\frac{1}{2}\Big)\right)\rho^{\frac{1}{4}}V\left(t_4+i\frac{\beta}{4}\right)\rho^{\frac{1}{4}}W(t_2)\rho^{\frac{1}{4}}\right], \tag{5.17}$$

$$\mathcal{G}_\alpha(t_1,t_2) \equiv \mathrm{Tr}\left[\rho^\alpha W(t_1)V(t_3)\rho^{1-\alpha}W(t_2)V(t_4)\right]$$
$$= \mathrm{Tr}\left[W\left(t_1+i\beta\Big(\alpha-\frac{1}{4}\Big)\right)\rho^{\frac{1}{4}}V\left(t_3+i\beta\Big(\alpha-\frac{1}{2}\Big)\right)\rho^{\frac{1}{4}}W\left(t_2+i\frac{\beta}{4}\right)\rho^{\frac{1}{4}}V(t_4)\rho^{\frac{1}{4}}\right], \tag{5.18}$$

where we have chosen to compare to the standard contour with $\rho^{1/4}$ separation. The differences between the complexified times, $t_1+i\beta(\alpha-\frac{1}{2}), t_2, t_3+i\beta(\alpha-\frac{1}{4})$ and $t_4+i\beta/4$ in Eq. (5.18), no longer vanish in the analytically continued OTOCs and this prevents relating one Lyapunov exponent to another. In particular, the imaginary-time separation between the two operators $V(0)$ in both $\mathcal{G}_\alpha$ and $\mathcal{H}_\alpha$ depends on α. The standard choice, $F(t)_{\left(\frac{1}{2},\frac{1}{4}\right)}$, which is the building block used to derive the bound on the Lyapunov exponent [16], is computed on a contour where the separation is $\beta/2$ and $\alpha = 1/2$. Therefore, $\mathcal{G}_\alpha$ and $\mathcal{H}_\alpha$ cannot be related to $F(t)_{\left(\frac{1}{2},\frac{1}{4}\right)}$ by a simple analytic continuation whenever $\alpha \neq 1/2$ and we have to study the behavior of these OTOCs separately.

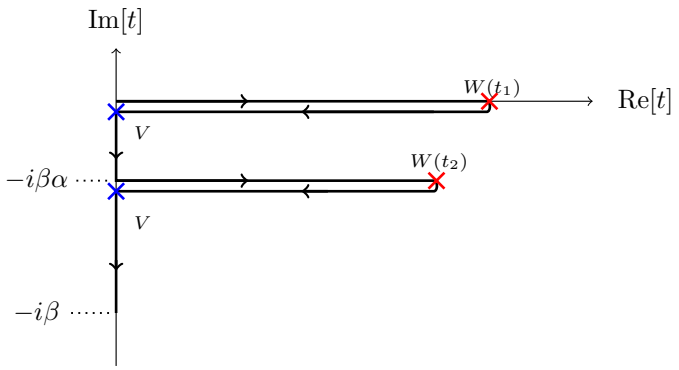

Figure 5.2: Extended Schwinger-Keldysh contour corresponding to $tr[\rho^\alpha W(t_1)V\rho^{1-\alpha}W(t_2)V]$ which enters in $C(t;\beta)_{(\alpha,0)}$ defined in Eq. (5.16).

5.2.2 OTOCS and physical observables in SK formalism

As one may extrapolate from the previous section, the OTOC and its Lyapunov spectrum will in general depend on the Schwinger-Keldysh contour on which it is computed. At first, this result may be surprising because, in standard Schwinger-Keldysh, it is known that *physical* Green's functions are independent of the contour due to energy conservation [241, 242]. Indeed, since the doubling of the contour is an artificial mathematical convenience, a priori only correlation functions with external insertions on a single branch should considered physical, e.g.,

$$\langle \mathcal{O}^{(1)}(x_1)\mathcal{O}^{(1)}(x_2)\mathcal{O}^{(1)}(x_3)\rangle, \quad \langle \mathcal{O}^{(2)}(x_1)\mathcal{O}^{(2)}(x_2)\mathcal{O}^{(2)}(x_3)\mathcal{O}^{(2)}(x_4)\rangle\,, \tag{5.19}$$

where we indicated with (i) the branch where each operator is inserted. With this definition, the fact that the correlation functions do not depend on the contour is a simple diagrammatic proof. We restate it here for the sake of clarity; it can be found in [241, 242].

By inspecting the SK effective action, we know that the interaction vertices are of the form

$$\mathcal{L}_{int} = \mathcal{L}^{(1)}_{int} - \mathcal{L}^{(2)}_{int}. \tag{5.20}$$

Consequently, in the diagrammatic expansion each vertex is either of type 1 or of type 2. The external legs of the vertices are connected to each other or to external operator insertions with the propagators

$$\langle \phi^{(i)}(-k)\phi^{(j)}(k)\rangle = \begin{pmatrix} G_{\text{Feynman}}(k) & G^{<}_{\text{Wightman}}(k) \\ G^{>}_{\text{Wightman}}(k) & G_{\text{anti-Feyman}}(k) \end{pmatrix}_{ij} \tag{5.21}$$

Without loss of generality, we focus on the simple lowest order 1PI diagram with n operators inserted the branch 1 and only one n-point vertex: $\langle \mathcal{O}^{(1)}_1(k_1)....\mathcal{O}^{(1)}_n(k_n)\rangle_\alpha$. Clearly if the vertex is of type 1, there is no contour dependence in the diagram. When the vertex is of type 2, as in Fig. 5.3, we need to use a Wightman function. For a general contour where the forward and backward branches are separated by ρ^α this is one of the Wightman functions[3]

$$\begin{aligned} G^{\beta\alpha}_{12}(k) &= \mathrm{Tr}\rho^{1-\alpha}\phi^{(1)}(-k)\rho^\alpha\phi^{(2)}(k) \\ G^{\beta\alpha}_{21}(k) &= \mathrm{Tr}\rho^{1-\alpha}\phi^{(2)}(-k)\rho^\alpha\phi^{(1)}(k) = e^{\beta(1-2\alpha)k^0}G^{\beta\alpha}_{12}(k) \end{aligned} \tag{5.22}$$

[3] In the literature the following notation is sometimes used: $G_{12}(k) = G^{<}(k)$ and $G_{21}(k) = G^{>}(k)$.

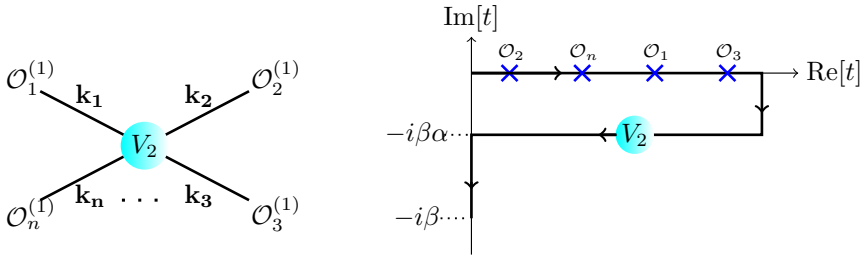

Figure 5.3: A diagrammatic expansion of the correlator with the external legs on the same branch of the SK contour. The result does not depend on the width $\beta\alpha$.

By Fourier transforming the time direction, using $\rho^{\alpha}\hat{O}(t)\rho^{-\alpha} = \hat{O}(t+i\alpha)$ and Fourier transforming back, one readily derives that

$$G_{12}^{\beta\alpha}(k) = e^{\beta\alpha k^0} G_{12}^{\alpha=0}(k),$$
$$G_{21}^{\beta\alpha}(k) = e^{-\beta\alpha k^0} G_{21}^{\alpha=0}(k). \tag{5.23}$$

At lowest order, there is a single n-point vertex on branch 2. Contracting each of the legs of the vertex with the external operators on branch 1, and by using (5.23), this means that the relation between correlation function on different contours is

$$\langle \mathcal{O}_1^{(1)}(k_1)....\mathcal{O}_n^{(1)}(k_n)\rangle_{\alpha} \sim e^{\beta\alpha \sum_{i=1,..,n} k_i^0} \langle \mathcal{O}_1^{(1)}(k_1)....\mathcal{O}_n^{(1)}(k_n)\rangle_{\alpha=0} \tag{5.24}$$
$$= \langle \mathcal{O}_1^{(1)}(k_1)....\mathcal{O}_n^{(1)}(k_n)\rangle_{\alpha=0}.$$

Because of energy conservation at the vertex, $\sum_{i=1,..,n} k_i = 0$, the overall factor vanishes and this proves the contour independence of these types of diagrams.

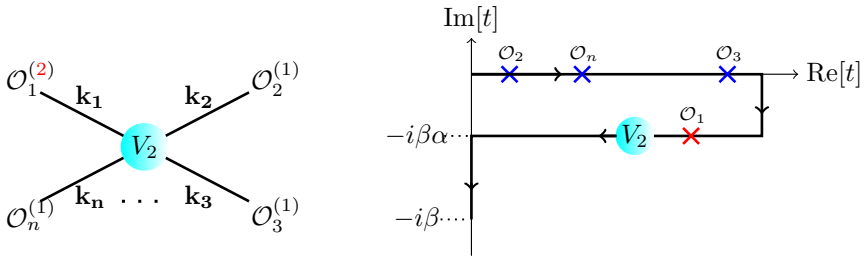

Figure 5.4: A diagrammatic expansion of the correlator with all but one external legs on the same branch of the SK contour. The result does depend on the width $\beta\alpha$

However, if one of the external legs is in the branch 2, see Fig. 5.4, it is easy to see that now one of the Green's function no longer depends on the separation α at all, so the global factor in the n point function does not simplify anymore. The simplest example of this is the Wightman function itself. There is no vertex, but we have already shown that $G^{\alpha}_{12} \neq G^{0}_{12}$ above in Eq. (5.22). Extending to an n-point correlation functions with a single n-point vertex, one has

$$\begin{aligned}\langle \mathcal{O}_1^{(2)}(k_1)....\mathcal{O}_n^{(1)}(k_n)\rangle_\alpha &\sim e^{\beta\alpha\sum_{i=2,..,n}k_i^0}\langle \mathcal{O}_1^{(2)}(k_1)....\mathcal{O}_n^{(1)}(k_n)\rangle_{\alpha=0} \\ &\neq \langle \mathcal{O}_1^{(2)}(k_1)....\mathcal{O}^{(1)}n(k_n)\rangle_{\alpha=0}\ , \end{aligned} \tag{5.25}$$

but now the exponent in the prefactor $\sum_{i=2,..,n} k_i^0 = -k_1^0 \neq 0$.

It is not difficult to see that the simple proof shown above extends to any diagrams. Indeed, given any diagram of the expansion, it is sufficient to divide it in subdiagrams and to use the momentum conservation in each vertex.

Turning our attention back to the OTOC, by construction each insertion occurs on one of four different branches. This indicates that the OTOC will be contour dependent, similar to two-branch correlation function in Schwinger-Keldysh theory as depicted in Fig. 5.4. If so, this does not immediately mean that the OTOC does not measure a physical quantity (in part). For example, the (bosonic) Wightman function $G_{12}^{\beta\alpha}(k) = e^{\beta k^0}(1+n(k^0))\rho(k)$ depends on the contour, but still encodes a physical quantity, namely the spectral density $\rho(k)$. Therefore, more care is needed to understand the relation between the contour-dependent OTOC and physical properties of the system.

5.3 Contour dependence of the Lyapunov spectrum in a weakly coupled Φ^4 theory

We now prove by direct computation that the OTOC indeed depends in detail on the contour chosed. In this section, we compute Lyapunov spectrum obtained from the commutator-squared $C(t;\beta)_{(\alpha,0)}$ in a perturbative matrix field theory, which has been studied in detail for $\alpha = 1/2$ in [243]. The advantage of the perturbative field theory calculation is that the commutator-squared can be related to a kinetic equation encoding the microscopic dynamics [44]. From this, we will suggests that this microscopic insight argues that one specific contour, the one with $\alpha = 1/2$ is the one that computes microscopic chaos.

We consider a 3+1 dimensional QFT with a Hermitian matrix field Φ_{ab} whose Lagrangian is given by

$$\mathcal{L} = \mathrm{Tr}\left(\frac{1}{2}\dot{\Phi}^2 - \frac{1}{2}(\nabla\Phi)^2 - \frac{1}{2}m^2\Phi^2 - \frac{g^2}{4!}\Phi^4\right), \tag{5.26}$$

with $g^2 = \lambda N$.
The commutator-squared of Eq. (5.16) in this matrix model is

$$C(t;\beta)_{(\alpha,0)} = \frac{1}{N^4}\sum_{aba'b'}\int d^3\mathbf{x}\,\mathrm{Tr}\Big(\rho^{1-\alpha}\,[\Phi_{ab}(t,\mathbf{x}),\Phi_{a'b'}]\rho^{\alpha}\,[\Phi_{ab}(t,\mathbf{x}),\Phi_{a'b'}]^{\dagger}\Big). \tag{5.27}$$

For $t > 0$, which we shall assume, the lowest order (disconnected) contribution is the product of two retarded Green's function arising from a contraction on the top two folds and the bottom folds separately; there is therefore no contour dependence. The non-trivial contribution at the next order, that can seed exponential growth, is the contribution with two Wightman functions connecting the two retarded Green's functions. For $\alpha = 1/2$, this equals [243]:

$$C(\omega)^{(1)}_{(\frac{1}{2},0)} = \frac{1}{N^2}\int\frac{d^4p}{(2\pi)^4}\frac{d^4p'}{(2\pi)^4}G_R(\omega-p)G_R(p)R(p-p')G_R(\omega-p')G_R(p') \tag{5.28}$$

where the kernel $R(p)$ is determined in terms of Wightman functions with operators separated by $i\beta/2$:

$$R(p) = \frac{g^4(N^2+5)}{12}\int\frac{d^4\ell}{(2\pi)^4}G_{12}^{\beta/2}(p/2+\ell)G_{12}^{\beta/2}(p/2-\ell)\,, \tag{5.29}$$

Note that it is only $G_{12}(k)$ and not $G_{21}(k)$, independent of the deformation $\alpha = 1/2$, which appears inside the kernel. This choice is due to the identity $G_{12}(k) = G_{21}(-k)$. We will consistently use G_{12} only; this will not affect the final result. Defining a function $f(\omega,p)$,

$$C(\omega)_{(\frac{1}{2},0)} = \frac{1}{N^2}\int\frac{d^4p}{(2\pi)^4}f(\omega,p)\,, \tag{5.30}$$

at the next order one of the contributions is

$$C(\omega)^{(2)}_{(\frac{1}{2},0)} = \frac{1}{N^2}\int\frac{d^4p}{(2\pi)^4}\frac{d^4p'}{(2\pi)^4}G_R(\omega-p)G_R(p)R(p-p')f^{(1)}(\omega,p') \tag{5.31}$$

and by rewriting $C(\omega)^{(2)}_{(\frac{1}{2},0)} = \frac{1}{N^2}\int\frac{d^4p}{(2\pi)^4}f^{(2)}(\omega,p)$, one can set up a recursive Bethe-Salpeter equation to determine $f(\omega,p)$ and hence $C(\omega)_{(\frac{1}{2},0)}$ to

all orders. Since we are interested in the late-time exponential growth, we focus on the homogeneous part of the Bethe-Salpeter equation, which in the low-frequency, late time limit equals

$$f(\omega,p) \simeq -G^R(p)G^R(\omega-p)\int \frac{d^4k}{(2\pi)^4} R(k-p) f(\omega,k)\,, \tag{5.32}$$

Equation (5.32) is only appropriate in the low ω limit. In this limit the product of retarded Green's functions is dominated by a *pinching pole singularity*, which amounts to the following approximation [243]

$$G^R(p)G^R(\omega-p) = \frac{\pi}{E_{\mathbf{p}}}\frac{\delta({p_0}^2-E_{\mathbf{p}}^2)}{i\omega-2\Gamma_p}+\dots\quad. \tag{5.33}$$

As this concentrates the support of the right hand side of the BSE on the on-shell delta-function, there is natural ansatz for the solution of $f(\omega,p)$ to be proportional to the same delta-function

$$f(\omega,p)_{\rm ansatz} = f(\omega,\mathbf{p})\delta(p_0^2-E_{\mathbf{p}}^2). \tag{5.34}$$

The imaginary part of the two-loop (α-independent) self energy Γ_p also happens to be determined in terms of (the $\alpha=1/2$) $R(k)$ defined in Eq. (5.29):

$$\Gamma_{\mathbf{p}} = \frac{\sinh\left(\frac{\beta E_{\mathbf{p}}}{2}\right)}{24E_{\mathbf{p}}}\int\frac{d^3k}{(2\pi)^3}\frac{R(E_{\mathbf{p}}-E_{\boldsymbol{k}},\mathbf{p}-\boldsymbol{k})+R(E_{\mathbf{p}}+E_{\boldsymbol{k}},\mathbf{p}-\boldsymbol{k})}{E_{\boldsymbol{k}}\sinh\left(\frac{\beta E_{\boldsymbol{k}}}{2}\right)}\,. \tag{5.35}$$

Including both the pinching pole approximation and the self-energy rewriting in terms of the rung function $R(k-p)$, the low-energy approximation of the BSE reads

$$-i\omega f(\omega,\mathbf{p}) = \int\frac{d^3k}{(2\pi)^3}\left(\mathcal{K}(\mathbf{p},\boldsymbol{k})-2\Gamma_{\boldsymbol{k}}(2\pi)^3\delta^3(\mathbf{p}-\boldsymbol{k})\right)f(\omega,\boldsymbol{k}), \tag{5.36}$$

where $\mathcal{K}(\mathbf{p},\boldsymbol{k}) = \frac{R(E_{\mathbf{p}}-E_{\boldsymbol{k}},\mathbf{p}-\boldsymbol{k})+R(E_{\mathbf{p}}+E_{\boldsymbol{k}},\mathbf{p}-\boldsymbol{k})}{4E_{\boldsymbol{k}}E_{\mathbf{p}}}$. The positive eigenvalues of the kernel $\mathcal{K}(\mathbf{p},\boldsymbol{k})-2\Gamma_{\mathbf{p}}\delta^3(\mathbf{p}-\boldsymbol{k})$, considered as a matrix in k and p, form the Lyapunov spectrum characterizing the exponential growth at late times, as we will review below.

Importantly, the Lyapunov spectrum is *not* set by the off-shell rung function $R(p-k)$ or the off-shell BSE Eq. (5.39) [44]. Specifically, the "on-shell" delta-function ansatz for $f(\omega,p)=f(\omega,\mathbf{p})\delta(p_0^2-E_p)$, that naturally

follows the pinching pole approximation, acts as a projector on the set of functions $f(\omega, p)$. Therefore the set of eigenvalues and eigenvectors of $R(k-p)$ are not the same as those of the kernel in Eq.(5.36) which sets the Lyapunov spectrum.

This derivation makes clear that the only α-contour-deformation dependence arises from the Wightman functions in the rung function. It is then straightforward to derive the contour-dependence of the OTOC. For $\alpha \neq 1/2$, the rung function should be modified as sketched in Fig. 5.5. Mathematically

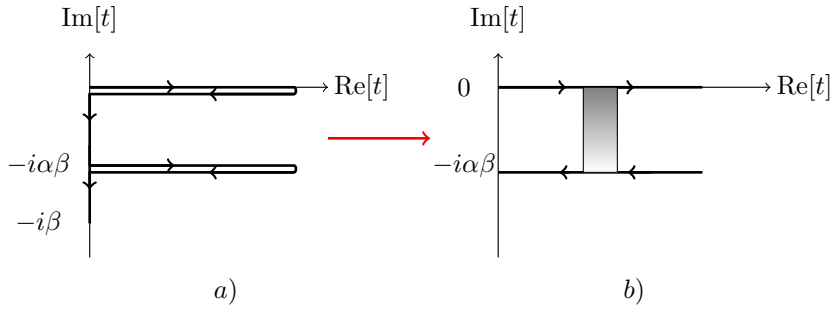

Figure 5.5: A pictorial representation of a general time contour (a) and of the 4-points function in the ladder approximation (b) . The external legs lay on the first time fold and the second time fold. On the contrary, the rung joins the two time folds and include Wightman functions which by definition are contour dependent.

$$R(p) \to e^{\beta p^0(\alpha-1/2)} R(p)\,. \tag{5.37}$$

Again, defining

$$C(\omega;\beta)_{(\alpha,0)} = \frac{1}{N^2}\int \frac{d^4p}{(2\pi)^4} f(\omega,p), \tag{5.38}$$

this will now obey the equation:

$$f(\omega,p) \simeq -G^R(p)G^R(\omega-p)\int \frac{d^4k}{(2\pi)^4} e^{\eta(k^0-p^0)} R(k-p) f(\omega,k)\,, \tag{5.39}$$

with $\eta \equiv \beta(\alpha-1/2)$. Note that the change in the rung function does not depend on whether it is constructed from $G_{12}(k)$ or $G_{21}(-k)$. This can be confirmed by the fact that the commutator-squared should obey

a KMS type symmetry $\alpha \to 1-\alpha$ on the doubled time contour. This follows by redefining $k \to \omega - k$ and $p \to \omega - p$. The kernel $R(k-p)$ is even in $k-p$ as can be readily seen from its definition Eq. (5.29). The product $G^R(p)G^R(\omega-p)$ changes into itself, and one obtains an equation for $f(\omega;\omega-p^0,-\mathbf{p})$ which identical to the original equation.

To solve the Bethe-Salpeter equation (5.39) after the pinching pole approximation in the late time limit,

$$f(\omega,p) \simeq \frac{\pi}{E_{\mathbf{p}}}\frac{\delta({p_0}^2-E_{\mathbf{p}}^2)}{-i\omega+2\Gamma_p}\int\frac{d^4k}{(2\pi)^4}e^{\eta(k^0-p^0)}R(k-p)f(\omega,k)\,, \tag{5.40}$$

one then makes the natural ansatz

$$f(\omega,p) = f(\omega,\mathbf{p})\delta(p_0^2-E_{\mathbf{p}}^2)\,. \tag{5.41}$$

However, note that the choice of the ansatz is very subtle and might lead to a different physical solution. By inspecting eq. (5.39), one might be tempted to argue that, since the η dependent term resembles a similarity transformation, the eigenvalues are unchanged. This conclusion is not correct. Indeed, as briefly recalled above, we showed in [44] that there are physical implications in this choice. Most notably, the $\eta=0$ BSE with the kernel replacement $R(k-p)\to\frac{\sinh(\beta p_0/2))}{\sinh(\beta k_0/2)}R(k-p)$ corresponds to the evaluation of a *different* analytic continuation of the commutator-squared. This analytic continuation is the retarded correlation function of the Wigner transform of the bilocal density operator, namely the correlation function that appears in the Kubo formula of the shear viscosity. From Boltzmann's kinetic theory, the spectrum with this ansatz is manifestly negative definite (*i.e.* there are only decaying modes). In other words, the choice of contour dictates the ansatz to solve the BSE. At the same time, all the contours that are related through analytic continuation arise from the same contour-independent off shell BSE Eq. (5.40).

Substituting this *appropriate* ansatz (5.41) into eq. (5.39), we then perform the integral over p_0. This yields

$$(-i\omega+2\Gamma_p)f(\omega,\mathbf{p}) = \int\frac{d^3k}{(2\pi)^3}f(\omega,\boldsymbol{k})\mathcal{K}(\boldsymbol{k},\mathbf{p},\eta), \tag{5.42}$$

with

$$\mathcal{K}(\boldsymbol{k},\mathbf{p},\eta)\equiv \frac{\cosh\left[\eta(E_{\mathbf{p}}-E_{\boldsymbol{k}})\right]R\big(E_{\mathbf{p}}-E_{\boldsymbol{k}},\mathbf{p}-\boldsymbol{k}\big)+\cosh\left[\eta(E_{\mathbf{p}}+E_{\boldsymbol{k}})\right]R\big(E_{\mathbf{p}}+E_{\boldsymbol{k}},\mathbf{p}-\boldsymbol{k}\big)}{4E_{\boldsymbol{k}}E_{\mathbf{p}}}\,,$$

where we have explicitly used that the rung kernel is even in the energy argument: $R(k_0, \boldsymbol{k}) = R(-k_0, \boldsymbol{k})$. Substituting Eq. (5.35) into Eq. (5.42), we arrive at the final Bethe-Salpeter equation for $C(\omega)_{(\alpha,0)} = \frac{1}{N^2}\int \frac{d^4p}{(2\pi)^4} f(\omega, p)$ in the frequency domain:

$$-i\omega f(\omega, \mathbf{p}) = \int \frac{d^3k}{(2\pi)^3} \Big[f(\omega, \boldsymbol{k}) \mathcal{K}(\boldsymbol{k}, \mathbf{p}, \eta) - f(\omega, \mathbf{p}) \frac{\sinh\left(\frac{\beta E_{\mathbf{p}}}{2}\right)}{\sinh\left(\frac{\beta E_{\boldsymbol{k}}}{2}\right)} \frac{R\big(E_-, \mathbf{p}-\boldsymbol{k}\big) + R\big(E_+, \mathbf{p}-\boldsymbol{k}\big)}{12 E_{\mathbf{p}} E_{\boldsymbol{k}}} \Big], \tag{5.43}$$

where $E_\pm \equiv E_{\mathbf{p}} \pm E_{\boldsymbol{k}}$. In the time domain this is an equation of the type

$$\frac{\partial}{\partial t} f(t)_{\mathbf{p}} = \mathcal{M}_{\mathbf{p}\boldsymbol{k}} f_{\boldsymbol{k}}(t). \tag{5.44}$$

The solutions are the eigenvectors of $\mathcal{M}_{\mathbf{p}\boldsymbol{k}}$ with an exponential growth/decay in time proportional to the eigenvalue. The positive eigenvalues of $\mathcal{M}_{\mathbf{p}\boldsymbol{k}}$ are the Lyapunov spectrum. This can be found numerically; the precise method used to solve this equation may be found in Appendix 5.A. Without computation it is already clear, however, that the result will depend on the α-deformed contour, as the defining Bethe-Salpeter equation does so.

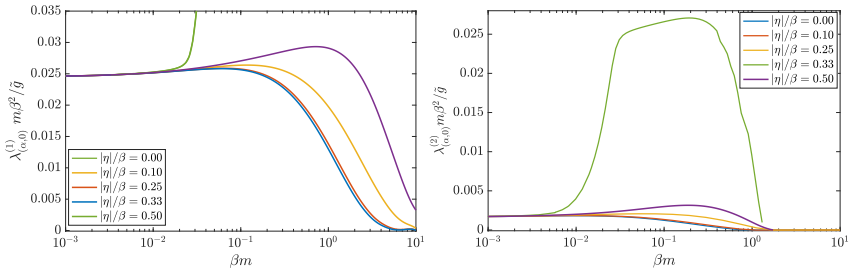

Figure 5.6: Contour dependence of the Lyapunov spectrum in the weakly coupled Φ^4-matrix model. Two largest Lyapunov exponents of Lyapunov spectrum of the matrix Φ^4 theory as a function of the coupling. Each value of η, defined in Eq. (5.39), corresponds to a different contour choice: $\eta = 0$ corresponds to the common symmetric regularization. For brevity, we defined $\tilde{g} = \frac{g^4(N^2+5)}{4\cdot 144}$.

The result is presented in Fig. 5.6. We clearly see the dependence of the two positive Lyapunov exponents on the contour. The spectrum does

become contour-independent in the high-temperature limit. This follows directly from the fact that the deformation parametrized by $\eta = \beta(\alpha - 1/2)$ becomes negligible for small β (compared to the mass).

That in these models the Lyapunov spectrum is contour independent for zero mass, will be crucial to understand the SYK model, which we study in the next section. There, there are only gapless excitations and not even a thermal mass, and we can therefore expect the same contour independence of the Lyapunov spectrum as the $\beta m \to 0$ limit of weakly coupled field theories as exhibited in Fig.5.6. Do recall that the full OTOC always depends on the contour.

For intermediate and small β, the Lyapunov spectrum sensitively depends on the choice of contour. As also noted already in [243], in the extreme low temperature limit $\beta m \to \infty$, the Lyapunov spectrum vanishes exponentially in βm. Even though this decreases the relative dependence on the contour, the contour dependence still persists and is given by $e^{-(\beta+2|\eta|)m}$, as shown in Fig. 5.7.

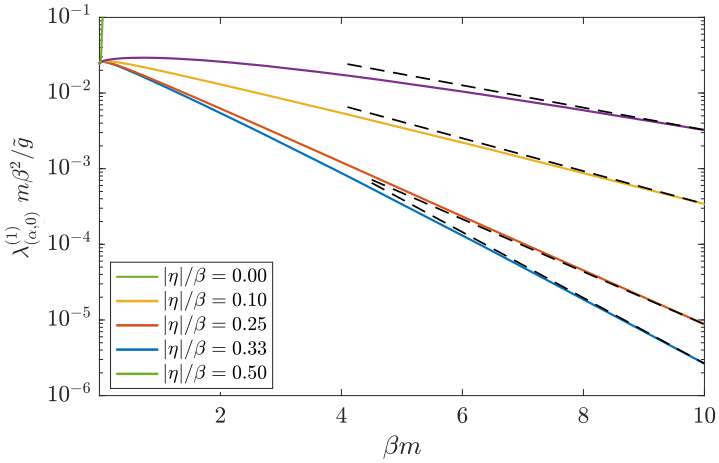

Figure 5.7: Exponential decay of the first Lyapunov exponent for various contours. Dashed lines correspond to the analytical expression $Ce^{-(\beta+2|\eta|)m}$, where C is fixed so that the dashed line passes through the last point available $\beta m = 10$. For brevity, we defined $\tilde{g} = \frac{g^4(N^2+5)}{4\cdot 144}$.

Let us make one final comment on the connection between the choice of ansatz and the contour dependence of the Lyapunov spectrum. One

readily observes that another possible ansatz to the BSE is

$$\begin{aligned} f(\omega,p) &= f(\omega,\mathbf{p})e^{\eta p^0}\delta(p_0^2-E_{\mathbf{p}}^2) \\ &= f(\omega,\mathbf{p})\left(e^{\eta E_{\mathbf{p}}}\frac{\delta(p^0-E_{\mathbf{p}})}{2E_{\mathbf{p}}}+e^{-\eta E_{\mathbf{p}}}\frac{\delta(p^0+E_{\mathbf{p}})}{2E_{\mathbf{p}}}\right). \end{aligned} \tag{5.45}$$

This η-contour skewed ansatz gives a contour independent Lyapunov exponent as solution for Eq. (5.40) and coincides with the solution for $\eta = 0$. One may ask why one ansatz is preferred over the other. As is clear from fig. 5.6, the natural ansatz (5.41) represents a solution with a larger eigenvalue of the Lyapunov exponent. We therefore argue that this solution is what a general computation, *i.e.* using different techniques than the BSE, of the leading exponential rate of growth in the OTOC would capture. In support of this, we also refer to the results of [240]. There, the authors computed the OTOC for a $2+1$ disordered systems by means of a Keldysh nonlinear sigma model technique that they developed. Within this framework, the computation of the largest exponent for the unregularised $\eta = 1/2$ case and the regularised $\eta = 0$ case gives a different result. Moreover, the unregularised case has a larger exponetial growth rate. The explanation is the one we give above.

This is the message to take from these results. When one computes the OTOC, one is inherently concerned with the late time regime of the correlator and with the largest term in the exponential growth. Mathematically the Lyapunov exponent of the fastest growing mode is contour dependent. This gives rise to the physics question of how we can understand the different contour dependent growing rates. We will answer this question in sec. 5.3.2.

5.3.1 The contour dependence regulates the IR

The contour dependence of the Lyapunov spectrum explicitly exhibited above emphasizes an important point regarding the physics behind the contour deformation. One of the arguments made for deforming contour symmetrically

$$C(t;\beta)_{\text{regulated}} = \text{Tr}\left(\rho^{\frac{1}{2}}[W(t),V]^\dagger\rho^{\frac{1}{2}}[W(t),V]\right), \tag{5.46}$$

or

$$F(t,t)_{(\frac{1}{2},\frac{1}{4})} = \text{Tr}\left(\rho^{\frac{1}{4}}W(t)\rho^{\frac{1}{4}}V\rho^{\frac{1}{4}}W(t)\rho^{\frac{1}{4}}V\right), \tag{5.47}$$

is that the smearing of the density matrix regulates a short distance singularity by separating the local operators in imaginary time. If this were indeed what the smearing should accomplish, then (1) at any finite value of regulator η we should expect the *low*-temperature limit to be universal, and (2) at any finite temperature β in units of the mass m the answer for the OTOC should diverge as one removes the regulator $|\eta| \to \frac{\beta}{2}$. The result, however, shows the opposite. The high-temperature limit is universal, indicating that this is the regime that is insensitive to the regulator, and, though we do not compute the full OTOC, the Lyapunov spectrum at fixed βm stays finite for any value of regulator. This argues strongly that the contour-deformation regulates the IR rather than the UV. This in fact agrees with Schwinger-Keldysh theory. There, the "contour-deformation" is the introduction of temperature itself, and this is a well-known IR regulator.

For results in the literature in perturbative QFTs, this diametrically opposite interpretation of the contour deformation has little effect. As in e.g [44, 243, 250, 251] usually the focus is on the universal high temperature regime. However, for the SYK model, the focus has often been on the emergent regime at low temperatures. There, this realization that the contour deformation regulates the IR may imply that the results are in fact regulator dependent and do not reflect physical information about the true dynamics. As we will show in Section 5.4, SYK is special in that its gapless nature and the absence of a thermal mass imply contour independence of the Lyapunov spectrum even at low temperature, extending from the $\beta m \to 0$ regime of weakly coupled field theories. Before we turn to this, we first address how to obtain the physical information about the true chaos/scrambling dynamics at low temperatures.

5.3.2 Kinetic theory interpretation of the α-deformed OTOC

IR regulators often encode real physical circumstances. The correct question to ask therefore is which contour properly reflects physical information of microscopic chaos. In this section we will argue that this can be decided by interpreting the result of the previous section in terms of the kinetic theory for many body chaos derived in [44]. There, the authors showed that the computation of the $\alpha = 1/2, \sigma = 1/4$ OTOC is equivalent to a Boltzmann-like equation that tracks the time evolution of the gross energy exchange.

We briefly review this result. The standard Boltzmann equation describes the time evolution of the single-particle distribution function

$f(t, \mathbf{r}, \mathbf{p})$,[4] parametrizing the deviation of the single-particle distribution function from its equilibrium value:

$$f(t, \mathbf{p}) = \frac{\delta n(t, \mathbf{p})}{(1 + n(\mathbf{p}))n(\mathbf{p})}\,, \tag{5.48}$$

and $n(\mathbf{p})$ is the Bose-Einstein distribution. For small deviations from the equilibrium value, the Boltzmann equation can be linearized and, focusing on the homogeneous case, it reads

$$\partial_t f(t, \mathbf{p}) = -\int_{\mathbf{l}} \mathcal{L}(\mathbf{p}, \mathbf{l}) f(t, \mathbf{l})\,, \tag{5.49}$$

where $\mathcal{L}(\mathbf{p}, \mathbf{l})$ represents the collision integral. $\mathcal{L}(\mathbf{p}, \mathbf{l})$ contains two contributions, namely the *gain* term $R^{\wedge}(\mathbf{p}, \mathbf{l})$, counting increase of the density of the phase-space cell, and the *loss* term $R^{\vee}(\mathbf{p}, \mathbf{l})$, which accounts for scattering out of the phase-space cell. In terms of these two contribution, the Boltzmann equation is

$$\partial_t f(t, \mathbf{p}) = \int_{\mathbf{l}} \left[R^{\wedge}(\mathbf{p}, \mathbf{l}) - R^{\vee}(\mathbf{p}, \mathbf{l})\right] f(t, \mathbf{l}). \tag{5.50}$$

As shown in [44], the Bethe-Salpeter equation of the symmetrised commutator-squared $C(t; \beta)_{(\frac{1}{2},0)}$ is equivalent to considering a Boltzman-like equation where the sign of the contribution of the true loss term is changed, so that we account for a gross exchange rather than a net exchange. More precisely, the gross exchange is given by

$$\partial_t f^{\mathrm{EX}}(t, \mathbf{p}) = \int_{\mathbf{l}} \frac{\mathcal{E}[E_{\mathbf{p}}]}{\mathcal{E}[E_{\mathbf{l}}]} \left[R^{\wedge}(\mathbf{p}, \mathbf{l}) + R^{\vee}(\mathbf{p}, \mathbf{l}) - 4\Gamma_{\mathbf{l}}\delta(\mathbf{p} - \mathbf{l})\right] f^{\mathrm{EX}}(t, \mathbf{l})\,, \tag{5.51}$$

where $\mathcal{E}[E_{\mathbf{p}}] = 1/\sinh(E_{\mathbf{p}}\beta/2)$ is an energy-related observable which does not alter the spectrum of the collision integral, as it enters in the form of a similarity transformation. The extra factor $\Gamma_{\mathbf{l}}$, the self-energy due to the thermal environment, is present to avoid over-counting. It can be understood as follows: $R^{\vee_T}(\mathbf{p}, \mathbf{l}) \equiv R^{\vee}(\mathbf{p}, \mathbf{l}) - 2\Gamma_{\mathbf{l}}\delta(\mathbf{p} - \mathbf{l})$ counts the changes in the particle number $f(t, \mathbf{p})$ due only to processes with $\mathbf{p} \neq \mathbf{l}$. Therefore, changing the sign of $R^{\vee}$ in Eq. (5.50) would over-count the contribution from the bath. If one changes only the sign of the true loss term $R^{\vee_T}(\mathbf{p}, \mathbf{l})$, the gross exchange is exactly given by $R^{\wedge}(\mathbf{p}, \mathbf{l}) + R^{\vee}(\mathbf{p}, \mathbf{l}) - 4\Gamma_{\mathbf{l}}\delta(\mathbf{p} - \mathbf{l})$

[4] Not to be confused with the commutator-squared function defined in Eq. (5.38).

[44]. The eigenvalues of the integral operator (5.51) are equivalent to those measuring the exponential growth rate of the OTOC, and thus give the Lyapunov spectrum of the theory.

As the α-deformation only changes the rung function in the Bethe-Salpeter equation, resulting in result (5.43), it is immediately recognized that the kinetic equation encoding the late time behavior of these families of OTOC is modified as follows

$$\begin{aligned}\partial_t f^{\rm EX}(t,\mathbf{p}) = \int_{\mathbf{l}} \frac{\mathcal{E}[E_{\mathbf{p}}]}{\mathcal{E}[E_{\mathbf{l}}]} \Big\{ & \cosh\left[\eta(E_{\mathbf{p}} - E_{\mathbf{l}})\right] R^{\wedge}(\mathbf{p},\mathbf{l}) \\ & + \cosh\left[\eta(E_{\mathbf{p}} + E_{\mathbf{l}})\right] R^{\vee}(\mathbf{p},\mathbf{l}) \\ & - 2\big[\cosh\left[2\eta(E_{\mathbf{p}})\right] + 1\big]\Gamma_{\mathbf{l}}\delta(\mathbf{p}-\mathbf{l})\Big\} f^{\rm EX}(t,\mathbf{l})\,. \end{aligned} \tag{5.52}$$

The kinetic equation equivalent of the contour-dependent commutator square gives us a direct physical interpretation of what is computed, as we understand each term as loss, gain and self-energy terms in the microscopic dynamics. The explicit $\eta = \beta(\alpha - 1/2)$ dependence in Eq. (5.52) shows that the different contours in the α-family have a different physical origin. While for $\eta = 0$ (symmetric regularization) both the gain and loss processes are weighted equally, for other contours $\eta \neq 0$, their relative weight is different. For none of these values does the kinetic equation have an obvious natural physical interpretation in terms of gross, net or otherwise simple exchange dynamics.

On the other hand, the gross exchange equation has been put forward independently already a long time ago as a measure of microscopic classical chaos [246]. This conclusion from the weakly coupled field theory computation above therefore strongly suggests that, in order to probe dynamical many-body chaos in QFT, the correct choice for the out-of-time correlation function is the symmetrically regularized choice with $\eta = 0$. Fortuitously, this is the one that has predominated all the calculations in the literature, including the derivation of the MSS bound on chaos [16]. It also means that the naive *thermal* expectation value of the commutator-squared $\mathrm{Tr}[\rho[W(t),V]^2]$ does *not* measure microscopic quantum chaos. One is therefore left with the reversed question: how does one justify from first principles the symmetrically regularized commutator-squared as a measure of quantum chaos. We will return to this question in the last section. First, we will consider the same question of contour-dependence of the commutator-squared and its Lyapunov spectrum for the case of the SYK model.

5.4 Contour dependence of the Lyapunov exponent in the SYK model

One of the research directions where the commutator-squared has had important impact is in the emergent strongly coupled low energy regime of the Sachdev-Ye-Kitaev model. The exponential growth of the symmetrically regularized commutator-squared saturates the MSS bound on chaos $\lambda_L \leq 2\pi T$; this has given great impetus to the notion that the SYK model provides a microscopic theory for AdS black holes.

Now that we know that the commutator-squared and its Lyapunov spectrum depend on the way the contour is regulated, the natural question on how this affects the insights in the SYK model arises. We shall first show that, in contrast to the previous weakly coupled massive QFT results, in the SYK model the Lyapunov spectrum is contour regularization independent.

The SYK Hamiltonian with $q/2$-body interactions is

$$H = i^{\frac{q}{2}} \sum_{1\leq i_1<i_2<\cdots<i_q\leq N} J_{i_1,i_2,\ldots,i_q}\ \chi_{i_1}\chi_{i_2}\cdots\chi_{i_q}\,, \tag{5.53}$$

where χ_i are Majorana fermions so $\{\chi_i,\chi_j\} = \delta_{ij}$ and the coupling $J_{i_1,i_2,\ldots,i_q}$ is a Gaussian-distributed random variable with zero average and diagonal (i.e. for each $J_{i_1,i_2,\ldots,i_q}$ independently) variance $\frac{2^{q-1}}{q}\frac{J^2(q-1)!}{N^{q-1}}$ [18]. The fermionic two-point function $G(\tau) = -\langle \mathcal{T}\chi(\tau)\chi(0)\rangle$ satisfies the following averaged Dyson equation in the large-N limit [18]:

$$G_n^{-1} = -i\omega_n - \Sigma_n\,,\ \Sigma(\tau) = -J^2 G(\tau)^{q-2}G(-\tau)\,, \tag{5.54}$$

with $\omega_n = (2\pi/\beta)(n+1/2)$, $G_n \equiv G(i\omega_n)$ and $\Sigma_n \equiv \Sigma(i\omega_n)$. In the same way as for weakly coupled QFT, the symmetrical contour regularized commutator-squared $C(t;\beta)_{(\frac{1}{2},0)}$ satisfies a Bethe-Salpeter equation. In the large-N limit, for arbitrary coupling, the homogeneous part of the BS-equation governs the large time limit and is [18]:

$$F(t_1,t_2) = J^2(q-1)\int dt_3 dt_4 G^R(t_{13})G^R(t_{24})\left[G^W(t_{34})\right]^{q-2}F(t_3,t_4)\,, \tag{5.55}$$

where G^R and G^W are the retarded and Wightman two-point functions.

There is now a difference with the the perturbative QFT approach. As recalled in the previous section, there the late time approximation also involves a pinching pole "on-shell" reduction of the retarded Green's

functions. The large N late time limit in SYK, on the other hand, is a conformal field theory with no on-shell particle-like excitations. There is no natural simplification of the retarded SYK Green's functions in this limit. In contrast to the perturbative QFT solution, the full large N Green's functions are obtained by analytically continuing the Dyson equation Eq. (5.54) to real time and solving these equations numerically with an iterative procedure [252].[5] Then one solves the SYK BSE Eq.(5.55) by making the explicit ansatz $F(t_1,t_2)=e^{\lambda_L(t_1+t_2)/2}f(t_{12})$ and rewriting it as an integral eigenvalue equation in frequency space:

$$f(\omega')=(q-1)J^2\left|G^R\left(\omega'+i\frac{\lambda_L}{2}\right)\right|^2\int\frac{d\omega}{2\pi}g_{lr}(\omega'-\omega)f(\omega)\,, \tag{5.56}$$

$$g_{lr}(\omega)\equiv\int dte^{i\omega t}G^W(t)^{q-2}\,. \tag{5.57}$$

One finally (numerically or analytically) searches for which value of λ_L the kernel has an eigenvector with eigenvalue 1 [18].

We can now ask how the subtly different SYK computation of its Lyapunov spectrum depends on the contour. As in the perturbative QFT of the Sec. 5.3, the only place the contour regularization shows up is in the Wightman functions.[6] Instead of parametrizing with respect to the $\alpha=0$ Wightman function, let us parametrize with respect to the $\alpha=1/2$ Wightman function:

$$G^\eta(\omega)=e^{\eta\omega}G^{\eta=0}(\omega)\,. \tag{5.58}$$

The Bethe-Salpeter equation (5.55) for the commutator square in frequency space for arbitrary α-deformed contour is then the same as before, but with a modified kernel $\tilde{g}_{lr}(\omega)$:

$$\tilde{f}(\omega')=(q-1)J^2\left|G^R\left(\omega'+i\frac{\lambda_\alpha}{2}\right)\right|^2\int\frac{d\omega}{2\pi}\tilde{g}_{lr}(\omega'-\omega)\tilde{f}(\omega)\,, \tag{5.59}$$

$$\tilde{g}_{lr}(\omega)\equiv\int dte^{i\omega t}G^\eta(t)^{q-2}\,,\quad G^\eta(t)=\int d\omega e^{-i\omega t}G^\eta(\omega)\,. \tag{5.60}$$

[5] As we are using the symmetric regularization, $G^W(\omega)=\rho(\omega)\frac{e^{-\omega\frac{\beta}{2}}}{1+e^{-\beta\omega}}$ is the Wightman function with operators separated by $i\beta/2$.

[6] This can also be seen explicitly by analytically continuing Eq. (5.55) $t_1\to t_1+i\beta\left(\alpha-\frac{1}{4}\right)$, $t_2\to t_2+i\frac{\beta}{4}$, $t_3\to t_3+i\beta\left(\alpha-\frac{1}{2}\right)$, $t_4\to t_4$.

We evaluate the modification in the kernel $\tilde{g}_{lr}(\omega)$, compared to the original kernel $g_{lr}(\omega)$, by using the convolution of the Wightman functions:

$$\tilde{g}_{lr}(\omega) = \int dt e^{i\omega t} G^{\eta}(t)^{q-2} = \int d\omega_1 \dots d\omega_{q-3} G^{\eta}\big(\omega_1\big) G^{\eta}\big(\omega_2\big) \dots \times G^{\eta}\big(\omega - \omega_1 - \dots - \omega_{q-3}\big)\,,$$

and substituting $G^{\eta}(\omega) = e^{\omega\eta} G^{W}(\omega)$ in each term inside the integral:

$$\begin{aligned}\tilde{g}_{lr}(\omega) &= \int\limits_{\omega_1,\dots,\omega_{q-3}} e^{\eta\omega_1} G^{\eta}\big(\omega_1\big)\; e^{\eta\omega_2} G^{\eta}\big(\omega_2\big) \dots e^{\eta(\omega-\omega_1-\dots-\omega_{q-3})} \\ &\qquad \times G^{\eta}\big(\omega - \omega_1 - \dots - \omega_{q-3}\big) \\ &= e^{\eta\omega} \int dt e^{i\omega t} G^{W}(t)^{q-2} = e^{\eta\omega} g_{lr}(\omega)\,.\end{aligned}$$

Therefore, Eq. (5.59) reduces to

$$\tilde{f}(\omega') = (q-1) J^2 \left| G^R\left(\omega' + i\frac{\lambda_\alpha}{2}\right)\right|^2 \int \frac{d\omega}{2\pi} e^{\eta(\omega'-\omega)} g_{lr}(\omega'-\omega) \tilde{f}(\omega)\,, \quad (5.61)$$

The crucial difference with weakly coupled QFT is that, because of the gapless nature of SYK even at finite temperature and the absence of a pinched pole on-shell condition, the product of retarded Green's functions remains a smooth function and not a distribution. This allows one to re-absorb the contour dependence with the redefinition $\tilde{f}(\omega') \to \tilde{e}^{-\eta\omega'} f(\omega')$.[7] In the late time SYK-BSE, this acts as a similarity transformation on the kernel, and its eigenvalues equal to its Lyapunov spectrum is therefore contour independent. Note again that the OTOC is still contour dependent, yet the Lyapunov exponent is independent of the regularization. As mentioned before, this can be qualitatively understood from the weakly coupled case, where in the massless case the dependence of the contour on the Lyapunov exponent vanishes.

To check the solution obtained with the BSE, we now consider the two regimes of the SYK model where some analytical control is possible: the strong coupling limit $\beta J \gg 1$ and the large-q limit.

[7] We thank Subir Sachdev and Yingfei Gu for emphasizing that this should be the case.

5.4.1 Study of the OTOC in SYK in the strongly coupled limit: conformal limit analysis

In the strongly-coupled regime $\beta J \gg 1$ of the SYK model, where conformal symmetry emerges asymptotically, the OTOC may also be computed analytically by studying the spectrum of the Casimir operator. More specifcally, for $\beta J \gg 1$ the eigenvectors of the Casimir operator, with eigenvalue $h(h-1)$, are also eigenvectors of the Euclidean kernel of the Bethe-Salpeter equation [18]. In this regime, the kernel of the Bethe-Salpeter equation is:

$$K_c(\tau_1,\tau_2;\tau_3,\tau_4) \propto \frac{\mathrm{sgn}(\tau_{13})\mathrm{sgn}(\tau_{24})}{|\tau_{13}|^{2\Delta}|\tau_{24}|^{2\Delta}|\tau_{34}|^{2-4\Delta}}\,, \quad \Delta = 1/q\,, \tag{5.62}$$

where the eigenvalues of K_c depend on q and h. Moreover, the allowed values of h are constrained, because the Bethe-Salpeter equation for the OTOC selects the eigenvalue unity of K_c. For $q=4$, the leading contribution to the OTOC turns out to be $h=2$ and is given by [18]:

$$\frac{\mathcal{F}(\theta_1...\theta_4)}{G(\theta_{12})G(\theta_{34})} = \frac{6\alpha_0}{\pi^2\alpha_K}\beta\mathcal{J}\sum_{|n|\geq 2}\frac{e^{in(y'-y)}}{n^2(n^2-1)}\left[\frac{\sin\frac{nx}{2}}{\tan\frac{x}{2}} - n\cos\frac{nx}{2}\right]\left[\frac{\sin\frac{nx'}{2}}{\tan\frac{x'}{2}} - n\cos\frac{nx'}{2}\right] \tag{5.63}$$

$$x = \theta_{12} \qquad x' = \theta_{34} \qquad y = \frac{\theta_1+\theta_2}{2} \qquad y' = \frac{\theta_3+\theta_4}{2}\,, \tag{5.64}$$

where θ is the rescaled Euclidean time $\theta = \tau/\beta$. This equation must now be analytically continued to real time by choosing the operator insertions. We consider the contour shown in Fig. 5.8, which allows us to consider both the σ- and α-families simultaneously.

More specifically, we choose

$$\theta_1 = i\frac{2\pi t}{\beta} + 2\pi(\sigma+\alpha)\,, \qquad \theta_2 = i\frac{2\pi t}{\beta} + 2\pi\sigma\,, \qquad \theta_3 = 2\pi\alpha\,, \qquad \theta_4 = 0\,. \tag{5.65}$$

In terms of x, x', y, y', we have:

$$x = x' = 2\pi\alpha\,, \qquad y = i\frac{2\pi t}{\beta} + 2\pi\sigma + \pi\alpha\,, \qquad y' = \pi\alpha. \tag{5.66}$$

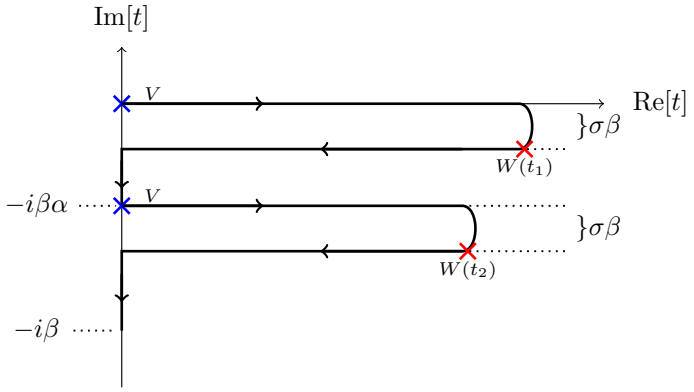

Figure 5.8: Extended Schwinger-Keldysh contour corresponding to the two-parameter OTOC $\mathrm{Tr}[\rho^{\alpha} W(t_1 + i\sigma\beta) V \rho^{1-\alpha} W(t_2 + i\sigma\beta) V]$.

In order compute Eq. (5.63) explicitly, we set $x = x'$, sum over n and then substitute Eq. (5.66) to get:

$$\frac{\mathcal{F}(t)}{G(2\pi\alpha)G(2\pi\alpha)} \propto \frac{1}{2} - \frac{\pi}{4}\left\{2\pi\cot^2(\pi\alpha)\left[(\alpha-1)\alpha + \sigma + i\frac{t}{\beta}\right] + (4\alpha - 2)\cot(\pi\alpha)\right. \tag{5.67}$$

$$\left. + i\csc^2(\pi\alpha)\sinh\left(\frac{2\pi t}{\beta} - 2i\pi\sigma\right)\right\}, \tag{5.68}$$

which for large t behaves as:

$$\frac{\mathcal{F}(t)}{G(2\pi\alpha)G(2\pi\alpha)} \propto -i\frac{\pi^2}{4}\csc^2(\pi\alpha)e^{-2i\pi\sigma}e^{\frac{2\pi t}{\beta}}. \tag{5.69}$$

We first note that $\mathcal{F}(t)$ is symmetric over $\alpha \to 1 - \alpha$, as expected. Second, the long-time regime is controlled by a growth rate given by $2\pi/\beta$, independent of the distance between the forward branches α. This confirms the contour dependence of the OTOC while the Lyapunov spectrum is nevertheless independent.

5.4.2 Study of the OTOC in SYK in the limit of large interaction order

In the SYK model, analytical control is also possible when one increases the order of the interaction in the Hamiltonian (5.53), which is set by q

[18]. Here we consider the calculation of the Lyapunov exponent in SYK in the large-q limit, and show that it is also contour independent.

We start with the two-point function in Euclidean signature in the large-q expansion [18]:

$$G(\tau) \underset{q\gg 1}{=} \frac{1}{2}\mathrm{sgn}(\tau)\left(1+\frac{1}{q}g(\tau)+O(q^{-2})\right), \tag{5.70}$$

where $g(\tau)$ is obtained by inserting the above ansatz in the saddle point equation for the two-point function. This gives the equation

$$\partial_\theta^2 g = 2(\beta\mathcal{J})^2 e^{g(\theta)}, \tag{5.71}$$

where $\theta=\tau/\beta\in[0,1)$ and $\mathcal{J}^2=q2^{1-q}J^2$, and with boundary conditions $g(0)=g(1)=0$. The solution of Eq. (5.71) is

$$e^{g_{(0)}(\theta)} = \left[\frac{\cos\frac{\pi\nu}{2}}{\cos\left[\pi\nu\left(\frac{1}{2}-\theta\right)\right]}\right]^2, \qquad \beta\mathcal{J}=\frac{\pi\nu}{\cos\frac{\pi\nu}{2}}, \tag{5.72}$$

with $\nu\in[0,1]$ parametrising the flow from weak $\beta J\sim 0$ coupling ($\nu\sim 0$), to strong coupling $\beta J\gg 1$ ($\nu\sim 1$). The analytic continuation to real time reads

$$G^R(t)=\theta(t)\left[G(\tau\to it+\epsilon)-G(\tau\to it-\epsilon)\right]=\theta(t)+\mathcal{O}(1/q), \tag{5.73}$$

$$G^{(\alpha)}(t)=G(\tau\to it+\alpha\beta), \tag{5.74}$$

for $\alpha=1/2$, and $G^{(\alpha)}(t)$ gives the Wightman function with operators separated by $i\beta/2$. Instead of working in frequency space with Eq. (5.61), we work in the time domain and use the following simplification for large q:

$$J^2(q-1)G(\tau)^{q-2} \underset{q\gg 1}{\simeq} J^2q2^{2-q}\mathrm{sgn}(\tau)^{q-2}e^{g(\tau)} = 2\mathcal{J}^2e^{g(\tau)}. \tag{5.75}$$

Therefore, using Eqs. (5.74) and (5.75), the kernel of the Bethe-Salpeter equation, Eq. (5.55), for large-q is

$$\begin{aligned} K^{(\alpha)}(t_1,\ldots,t_4) &= J^2(q-1)G^R(t_{13})G^R(t_{24})G^\alpha(t_{34})^{q-2} \\ &\underset{q\gg 1}{\simeq} \theta(t_{13})\theta(t_{24})2\mathcal{J}^2e^{g(\tau\to it_{34}+\beta\alpha)} \\ &= \theta(t_{13})\theta(t_{24})\frac{2\pi^2\nu^2}{\beta^2\cosh^2\left(\frac{\pi\nu}{\beta}(t_{34}+i\eta)\right)}, \qquad \eta=\beta(\alpha-1/2), \end{aligned} \tag{5.76}$$

where $0 < \nu < 1$ and we take $0 < \alpha < 1/2$. Finally, we use $\partial_t \theta(t) = \delta(t)$ to simplify the Bethe-Salpeter equation

$$\begin{aligned}\partial_{t_1}\partial_{t_2}\left[F(t_1,t_2) = \int dt_3 dt_4 K^{(\alpha)}(t_1,\ldots,t_4)F(t_3,t_4)\right],\\ \partial_{t_1}\partial_{t_2}F(t_1,t_2) = 2\mathcal{J}^2 e^{g(\tau\to it_{12}+\beta\alpha)}F(t_1,t_2)\,.\end{aligned} \tag{5.77}$$

Making the ansatz $F(t,t') = e^{\lambda_L \frac{t+t'}{2}} f(t-t')$:

$$\begin{aligned}\left[\partial_{t_{12}}^2 + 2\mathcal{J}^2 e^{g(\tau\to it_{12}+\beta\alpha)}\right] f(t_{12}) =& \frac{\lambda_L^2}{4} f(t_{12}),\\ \left[\partial_{t_{12}}^2 + \frac{\pi^2\nu^2}{\beta^2}\frac{2}{\cosh^2\left(\frac{\pi\nu}{\beta}(t_{12}+i\eta)\right)}\right] f(t_{12}) =& \frac{\lambda_L^2}{4} f(t_{12}),\\ \left[-\partial_y^2 - \frac{2}{\cosh^2\left(y + i\frac{\pi\nu}{\beta}\eta\right)}\right] f(y) =& -\left(\frac{\lambda_L\beta}{2\pi\nu}\right)^2 f(y)\,.\end{aligned}$$

This is the Schrödinger equation with a *complex* Pöschl-Teller potential, which has a boundstate, $f(y) = \sqrt{\frac{\tan(\pi\nu\eta/\beta)}{4\eta\cos(\pi\nu\eta/\beta)}}\mathrm{sech}(y + i\frac{\pi\nu}{\beta}\eta)$, with real eigenvalue $E = -1$. The value of the eigenenergy gives the value of the Lyapunov exponent $\lambda_L = 2\pi\nu/\beta$, which is independent on the contour parameter α.

The large q analysis allows us a qualitative insight into the role of the gapless nature of SYK by taking a closer look to the SYK-BSE Eq. (5.61). Take the kernel of the Bethe-Salpeter equation in the regime where conformal symmetry is only weakly broken $\beta J \gg 1$. In this regime, the symmetric $\eta = 0$ Wightman function is $G^W(t) = b\left[\frac{\pi}{\beta\cosh\frac{\pi t}{\beta}}\right]^{2/q}$, $b^q = \left(\frac{1}{2} - \frac{1}{q}\right)\tan(\pi/q)/(J^2\pi)$ [18]. Consequently, the $\eta = 0$ kernel $g_{lr}(\omega)$ is

$$g_{lr}(\omega'-\omega) = \int dt e^{i\omega t} G^W(t)^{q-2} = b^{q-2}\left(\frac{\pi}{\beta}\right)^{2-4/q}\frac{2^{1-4/q}}{\Gamma\left(2-\frac{4}{q}\right)}\left|\Gamma\left(1-\frac{2}{q}-i\frac{\beta(\omega'-\omega)}{2\pi}\right)\right|^2.$$

Using the identity $|\Gamma(a+ib)|^2 = \Gamma(a)^2\prod_{k=0}^{\infty}\frac{1}{1+b^2/(a+k)^2}$, one immediately sees that this kernel is strongly peaked around the origin $\beta(\omega'-\omega)\to 0$.

On the other hand, changing the regularization changes the kernel by an overall factor $e^{(\alpha-1/2)\beta(\omega'-\omega)}$. Thus, as the integral in Eq. (5.61) is dominated by $\omega' \sim \omega$, the dependence on the contour proportional to $e^{\eta(\omega'-\omega)} \sim 1$ essentially drops out.

In a theory with gapped excitation, on the other hand, one can see for the case of the matrix model by numerically inspecting the expression of the on-shell kernel (5.93) and (5.94), that the kernels are peaked around the value of the gap. This gives a contribution of the order $e^{\eta\Delta_{gap}}$. Physically it may be seen as a consequence of a combination of an on-shell particle and anti-particle process that dominates the kernel.

5.5 The Lyapunov spectrum and the Loschmidt echo

In previous sections we have seen how the regularization dependence can afflict the commutator-squared. This shows that without more detailed specification one cannot directly relate this quantity to an observable that can be measured in experiments. We have also shown that the regularization dependence is dominant in the IR rather than the UV. This is analogous to Schwinger-Keldysh theory where contour dependence is related to the temperature, and the latter is a well known IR regulator. IR regularization issues are usually not solved by counterterms and renormalization. Instead they often encode physics on their own. This suggests that a way to resolve the regulator dependence is to *define* which member of family of "regularized" correlation functions computes a proper physical observable. The weakly coupled QFT result, through the mapping of the commutator-squared to a kinetic equation, indicates that the symmetrically regularized commutator-squared is the correct one.

Fortuitously this is the one almost exclusively studied in the literature and the one for which the MSS bound on chaos is derived. Nevertheless, one would like to understand from first principles why the symmetrized contour is an appropriate physical observable. The first attempt construction in the introduction points to the thermally averaged commutator-squared instead. In this section we show that the symmetrized commutator-squared follows directly from an alternative measure of chaos, which is related to standard measurements of information spreading: the Loschmidt echo. This quantity contains not only the commutator-squared but also higher-order out-of time correlation functions. The Loschmidt echo and related quantities have been used in the context of quantum chaos for a long

time [253–257]. Therefore, it is not surprising that the OTOCs may be extracted from echo spectroscopy as proposed in [258–261] and measured experimentally in [245].

5.5.1 Loschmidt echo

The Loschmidt echo is based on a old thought experiment trying to disprove the irreversibility inherent in Boltzmann's equations by imaging a dynamical system where at time t after $t_0 = 0$ one reverses all velocities and compare the resulting state at time $2t$ with the original state. Microscopically the answer is of course identical, but supposing one makes a tiny "erroneous" perturbation at the time when one reverses all velocities, one immediately sees that in a chaotic non-integrable system the resulting state will be exponentially different from the original state.

This thought experiment can be directly mapped to a quantum quench experiment. One evolves a quantum state forward in time for a time t, perturbs it with an instantaneous quench $e^{i\delta W}$, evolves backward for the same time t and projects onto the original state,

$$M(t) \equiv \langle\psi|e^{iHt}e^{i\delta W}e^{-iHt}|\psi\rangle\,. \tag{5.78}$$

For a generic initial state, the echo will have a universal late time exponential fall off independent of the type of quench W that encodes the lack of overlap between the initial and final state,

$$M(t) = \langle\psi_{\text{initial}}|\psi_{\text{Loschmidt}}(2t)\rangle \sim e^{-\lambda t}. \tag{5.79}$$

The Lyapunov exponent λ is then a property of the system characterized by its Hamiltonian H alone.

The Loschmidt echo is the expectation value of a complex operator. To avoid phases one often takes the absolute value squared, which is known as the fidelity [262]

$$F(t) \equiv \left|\langle\psi|e^{iHt}e^{i\delta W}e^{-iHt}|\psi\rangle\right|^2 \sim \left|\frac{1}{1+\delta e^{\lambda t}}\right|^2 \overset{t\to\infty}{\sim} e^{-2\lambda t}\,. \tag{5.80}$$

The intermediate step is a well-known result from Jalabert and Pastawski [254]. A second practical step with an eye on experiment is to consider the fidelity for an ensemble of states, rather than a single state. Choosing

the thermal ensemble one has

$$\begin{aligned} F(t) &\equiv \left| \frac{1}{Z_\beta} \sum_\psi e^{-\beta E[\psi]} \langle \psi | e^{iHt} e^{-i\delta W} e^{-iHt} | \psi \rangle \right|^2 \\ &= \left| \mathrm{Tr}\, \rho e^{iHt} e^{-i\delta W} e^{-iHt} \right|^2 \\ &= \mathrm{Tr}\, \rho e^{iHt} e^{-i\delta W} e^{-iHt} \rho e^{iHt} e^{i\delta W} e^{-iHt} + \mathcal{O}\left(1/t\right) \\ &= \mathrm{Tr}\, \rho e^{-i\delta W(t)} \rho e^{i\delta W(t)}. \end{aligned} \tag{5.81}$$

Defining $e^{-iHt}\rho e^{iHt} \equiv X$ and $e^{-i\delta W} e^{-iHt} \rho e^{iHt} e^{i\delta W} = Y$, the fidelity $F(t)$ above is a specific case of the more general operator fidelity $\mathcal{F} = \mathrm{Tr} X^\dagger Y$ applied to density matrices as operators.[8] Three remarks are in order. (1) In the intermediate step we used that the *leading* Lyapunov decay rate in t is the same when computed via $\left|\mathrm{Tr}\rho e^{-i\delta W(t)}\right|^2$ or $\mathrm{Tr}\rho e^{-i\delta W(t)} \rho e^{i\delta W(t)}$. (2) Naively, as the late time Lyapunov exponent of interest is a property of the system and not of the initial state, the averaging should not matter. However, it is well known from classical dynamical systems that the late time behavior of an ensemble of classical trajectories is governed by Policott-Ruelle decay, rather than the microscopic exponential growth. Even though these are qualitatively related in weakly coupled theories, they are not quantitatively the same [44]. (3) Note both the symmetrized appearance of the density matrix, and the fact that the cumulative power of the density matrix is 2. Computed through a path-integral this implies that the periodicity in Euclidean time is twice the inverse temperature $\beta = 2/T_{\mathrm{phys}}$.

To connect with the commutator-squared, we expand to second order in δ

$$\begin{aligned} F(t) &= \mathrm{Tr}\rho^2 + \mathrm{Tr}\, \rho(-\delta^2 W(t)^2)\rho + \mathrm{Tr}\, \rho(\delta W(t))\rho \delta W(t) \\ &= \mathrm{Tr}\rho^2 + \frac{\delta^2}{2} \mathrm{Tr}\, [\rho, W(t)][\rho, W(t)] + \dots \end{aligned} \tag{5.83}$$

[8] The operator fidelity is a weaker version of state fidelity encoding the notion of how close a state is to a maximally entangled one [263] or, if referring to teleportation, it quantifies the quality of the teleportation that can be achieved with the given state [264]. The state fidelity between two quantum states given by the density matrices ρ_0 and ρ_1 equals [265, 266]:

$$F(\rho_0, \rho_1) \equiv \mathrm{Tr} \sqrt{\rho_1^{1/2} \rho_0 \rho_1^{1/2}}\,. \tag{5.82}$$

with the difference that the density matrix itself takes the role of the operator $V(0)$. The second time dependent term, the density-matrix commutator-squared, is a variant of the Wigner-Yanase-Dyson skew information.

$$I_\alpha(\rho, A) \equiv \frac{1}{2}\mathrm{Tr}[i[\rho^{2\alpha}, A^\dagger](i[\rho^{2-2\alpha}, A])]\,, 0 \leq \alpha \leq 1\,, \tag{5.84}$$

for the symmetric value $\alpha = 1/2$ [267]. Writing out the symmetric case for hermitian A,

$$I_{\frac{1}{2}}(\rho, A) = (\mathrm{Tr}\rho A\rho A - \mathrm{Tr}\rho AA\rho) \tag{5.85}$$

and replacing the thermal density matrix ρ with a pure state density matrix,

$$I_{\frac{1}{2}}(|\psi\rangle\langle\psi|, A) = -(\langle A^2\rangle - \langle A\rangle^2), \tag{5.86}$$

one can recognize that the WYD skew information is an extension of the variance for pure states to mixed states. If, by the same argument as above, one may assume that it is dominated by some largest eigenvalue $\mathrm{Tr}\rho A\rho A \sim (\mathrm{Tr}\rho A)^2$, it computes something akin to the (largest eigenvalue) variance for the operator $\mathcal{O} = \rho A$. In that sense it is again natural that the density matrix appears with cumulative power 2. Put differently, in computing the WYD skew information the periodicity in Euclidean time is twice the inverse temperature $\beta = 2/T_{\mathrm{phys}}$.

However, this is not yet the commutator-squared we are interested in. A guess might be the case where the thermal density matrix is rotated by a small similarity transformation $\rho = e^{iV}\rho_0 e^{-iV}$. This is equivalent to an instantaneous quench by V at time $t = 1$. Then in the limit of small δ the late time fidelity equals

$$\begin{aligned} F(t) &= \mathrm{Tr}\,\rho e^{iHt}e^{-i\delta W}e^{-iHt}\rho e^{iHt}e^{i\delta W}e^{-iHt} \\ &= \mathrm{Tr}\,\rho_0 e^{iV(0)}e^{-i\delta W(t)}e^{-iV(0)}\rho_0 e^{iV(0)}e^{i\delta W(t)}e^{-iV(0)} \\ &= \mathrm{Tr}\rho_0^2 + \frac{\delta^2}{2}\mathrm{Tr}[\rho_0, e^{iV(0)}W(t)e^{-iV(0)}][\rho_0, e^{iV(0)}W(t)e^{-iV(0)}] + \dots \\ &= \mathrm{Tr}\rho_0^2 + \delta^2\Big(\mathrm{Tr}\rho_0 e^{iV(0)}W(t)e^{-iV(0)}\rho_0 e^{iV(0)}W(t)e^{-iV(0)} \\ &\qquad\qquad -\mathrm{Tr}\rho_0 e^{iV(0)}W(t)^2 e^{-iV(0)}\rho_0\Big)\,. \end{aligned} \tag{5.87}$$

The first and the last term can never give an OTOC; ignoring those, one

has in the limit of small V

$$F(t) = \text{TOC} + \delta^2 \left(\text{Tr}\rho_0 W(t)\rho_0 W(t) + 2\text{Tr}\rho_0 W(t)\rho_0[V, W(t)] + \right. \\ \left. + \text{Tr}\rho_0 W(t)\rho_0[V,[V,W(t)]] + \text{Tr}\rho_0[V,W(t)]\rho_0[V,W(t)] + \ldots\right). \tag{5.88}$$

The two terms of order δ^2 in the first line are also TOC. The terms on the second line contain the symmetric commutator-squared and a second term which is also an OTOC but on a different contour.[9] As we know by now, generically the Lyapunov behavior of this other OTOC will be different. This is not yet the answer.

Tracing the origin of Eq. (5.88), it is easy to see how the fidelity and the symmetrized commutator-squared are related. Eq. (5.88) follows from taking the long time limit and then taking V and δW small in the fundamental definition of the ensemble averaged fidelity — the first line of Eq. (5.81). If, however, we take the limit of V and δW small, with $\rho = e^{iV}\rho_0 e^{-iV}$, the ensemble averaged fidelity equals

$$\begin{aligned} F(t) &= \left|\text{Tr}e^{iV(0)}\rho_0 e^{-iV(0)}e^{-i\delta W(t)}\right|^2 \\ &= \left|\text{Tr}\rho_0\left(1 - i\delta W(t) - \frac{\delta^2}{2}W(t)^2 - \delta[V,W(t)] + \ldots\right)\right|^2 \\ &= |\text{Tr}\rho_0|^2 - \delta\text{Tr}\rho_0\text{Tr}\rho_0[V,W(t)] - \delta\text{Tr}\overline{\rho_0[V,W(t)]}\text{Tr}\rho_0 \\ &\quad + \delta^2\text{Tr}\overline{\rho_0[V,W(t)]}\text{Tr}\rho_0[V,W(t)]. \end{aligned} \tag{5.89}$$

We now use the late time approximation, where we assume that $\rho_0[V, W(t)]$ is dominated by an eigenvalue $\text{Eig}(\rho_0[V, W(t)]) \sim e^{\frac{1}{2}(\lambda+i\phi)t}$. In that limit, the middle two terms give a strongly oscillatory contribution, which is hard to measure. We therefore ignore it. As to the last term in Eq.(5.89), there the late time limit allows us to make again the approximation

$$\begin{aligned} F(t) &= \ldots + \text{Tr}\overline{\rho_0[V,W(t)]}\text{Tr}\rho_0[V,W(t)] \\ &= \ldots + \text{Tr}\overline{\rho_0[V,W(t)]}\rho_0[V,W(t)] + \mathcal{O}(1/t). \end{aligned} \tag{5.90}$$

[9] Note that, at higher orders in δ, the fidelity contains higher-order correlation functions, which are still represented by a Schwinger-Keldysh contour with only two folds but with multiple insertions of operators. These correlation functions differ from higher-point OTOCs in Schwinger-Keldysh contours with more than two folds [268]. The latter correspond to multiple repetitions of the Loschmidt experiment and, consequently, the largest growth rate is simply a multiple of the Lyapunov exponent of the 4-point function OTOC corresponding to a single repetition of the Loschmidt experiment.

We recognize precisely the symmetrized commutator-squared with one already noted difference. The cumulative power of the density matrix is 2. This implies that the connection between the periodicity in Euclidean time and the physical temperature differs with a factor two compared to what the naive smearing procedured assumes: $\beta = 2/T_{\text{phys}}$. In particular this means the proper MSS bound on chaos should read $\lambda \leq \pi T_{\text{phys}}$.

The above is a strong argument that the natural observable which measures the symmetrized commutator-squared is the Loschmidt echo in the limit of small quenches first and late time subsequent with the sublety that $\beta = 2/T_{\text{phys}}$.

5.6 Conclusion

In this article we have explored the role of the regularization scheme of the commutator-squared and of the OTOC. Quantum chaotic systems may display an exponential growth parametrized by a quantum Lyapunov exponent which is bounded by above $\lambda \leq 2\pi k_B T/\hbar$ [16]. The proof of this bound involves regularising the OTOC by thermally spreading the operators. Purportedly, this is done to regulate short distance singularities and any physical property of a system should be independent of the short distance regularization scheme.

Here, we have shown that for those regularizations consisting on a contour with a $i\beta/2$ separation between the forward branches, shifting the backwards branches induces a change in the decoherence factor, defined as the prefactor of the sum of the OTOCs [247]. Therefore, the decoherence factor cannot be a physical quantity as previously suggested. On the other hand, the Lyapunov exponent is the same for all of these contours, suggesting that indeed it may be measurable.

However, we have then shown that for a different choice of contours, where the separation between the forward branches is changed, the Lyapunov spectrum also depends on the contour chosen. While the contour dependence of the commutator-squared has been mostly overlooked in the literature, it is not surprising that this is the case. Similarly to the Wightman function, the commutator-squared involves operators inserted on forward and backward branches of the Schwinger-Keldysh contour, and so there is no reason to expect that it should be a physical quantity. Therefore, it is important to know how to extract physical information from it, in the same way that the spectral density, a physical quantity, may be obtained from the Wightman function, even though the Wightman function itself is not physical. The one notable exception in the literature is

[240]. There, the authors studied many body chaos in a weakly interacting 2D system of fermions with quenched disorder and computed the Lyapunov exponent both for the unregularized $\eta = 1/2$ case and the symmetrically regularized one, $\eta = 0$ (in our notation). They indeed found that the two results disagree, and pointed out the regulator dependence of the OTOC. The conclusion that they drew is that, in the model considered, the only special feature of the symmetrically regularized OTOC is a particular cancellations of divergencies in the computation, but the physical meaning behind this correlator remained obscure.

Here we have performed a more thorough analysis showing the regulator dependence of the OTOC for two paradigmatic models, a weakly coupled ϕ^4 matrix boson (at any N) and the SYK model. By comparing to ordinary Schwinger-Keldysh theory, we provide a simple diagrammatic proof regarding the reason why the choice of the contour affects the OTOC, although the Lyapunov spectrum becomes contour independent for theories that stay massless/gapless even at finite temperature. This is particularly relevant for the SYK model, which has been extensively studied over the last years. Its largest Lyaponuv exponent, which saturates the MSS bound, is indeed contour independent.

These detailed studies allow us to recognize that the regulator dependence is an IR issue, and not an alleviation of purported UV singularities. This means one has to take more care in understanding the role of the regulator as it may contain physical information. One crucial insight of this chapter is to recognise the special physical meaning of the symmetrically regularised OTOC, by means of kinetic theory [44]. The OTOC computed on this contour is the one which one can properly claim to compute chaos or scrambling. That the fact that the bound on chaos holds for this physically meaningful definition of OTOC is remarkable and open new directions on possible still unknown dynamical constraints that the bound can impose.

This does then raise the question which simple observable naturally gives rise to such a symmetric insertion of a thermal density matrix. We proposed a simple observable, related to the operator fidelity, which contains information beyond the commutator-squared and can be measured experimentally using echo spectroscopy. The corollary of using this observable to define the OTOC is that is based on a double insertion of density matrices, i.e. the periodicity in Euclidean time is twice the inverse temperature. From this point of view the bound on chaos should read $\lambda \leq \pi k_B T_{\text{phys}}/\hbar$.

Overall, our results pose the question on the usefulness of the commutator-squared to probe quantum chaos. The contour dependence of the commutator-

squared and of the Lyapunov spectrum extracted from it casts doubts on whether the commutator square is physical and how physical information should be extracted from it. However, even though a natural way to define chaotic quantum system is that in which the OTOC displays an exponential growth, this growth regime actually clashes with the other notion of a quantum chaotic theory that it should display random matrix behaviour. In the SYK model, even though one has exponential growth at shorter times similar to *classical* weakly interacting chaos, spectral properties, such as the spectral form factor, are similar to that of random matrix theory for times of order of $N\log(N)$ and larger [269–271]. This suggests that the model becomes truly *quantum* chaotic after this time-scale. A gorgeous example of true *quantum* chaos embodied by random matrix behaviour has been observed on the kicked Ising spin-1/2 chain for much shorter timescales [272]. There is no exponential growth in the OTOC in this model, which challenges the notion of how quantum chaos and especially maximal chaos should be defined.

5.A Numerical calculation in matrix model

In this appendix we outline the simplifications used to solve numerically the Bethe-Salpeter equation Eq. (5.43). Following [243], we define

$$P = |\mathbf{p}|, \quad K = |\boldsymbol{k}|, \quad y = |\boldsymbol{k} - \mathbf{p}| \tag{5.91}$$

and express the momentum integral as follows

$$\int d^3k = 2\pi \int_0^\infty K^2 dK \int_{|K-P|}^{K+P} \frac{y dy}{KP}. \tag{5.92}$$

Rewriting Eq. (5.43) in the time domain and replacing the momentum integral, we arrive at the simplified version of the Bethe-Salpeter equation, which we solve numerically following the strategy described in [243]:

$$\begin{aligned}\lambda_L f(P) = \int_0^\infty dK \Bigg[&\left(\cosh(\eta E_+) f(K) - \frac{f(P)}{3} \frac{\sinh\left(\frac{\beta E_P}{2}\right)}{\sinh\left(\frac{\beta E_K}{2}\right)} \right) I_+(P,K) \\ &+ \left(\cosh(\eta E_-) f(K) - \frac{f(P)}{3} \frac{\sinh\left(\frac{\beta E_P}{2}\right)}{\sinh\left(\frac{\beta E_K}{2}\right)} \right) I_-(P,K) \Bigg],\end{aligned} \tag{5.93}$$

where

$$I_+(P,K) \equiv \frac{K}{(2\pi)^2 P 4 E_P E_K} \int_{|K-P|}^{K+P} dy y R(E_+, y) = \frac{\frac{3\tilde{g}K}{(2\pi)^3 \beta P E_P E_K}}{\sinh(\beta E_+/2)} \int_{|K-P|}^{K+P} dy \log \frac{\sinh x_+^+}{\sinh x_-^+}$$

$$I_-(P,K) \equiv \frac{K}{(2\pi)^2 P 4 E_P E_K} \int_{|K-P|}^{K+P} dy y R(E_-, y) = \frac{\frac{3\tilde{g}K}{(2\pi)^3 \beta P E_P E_K}}{\sinh(\beta E_-/2)} \int_{|K-P|}^{K+P} dy \log \frac{1 - e^{-2x_+^-}}{1 - e^{2x_-^-}}$$

$$x_\pm^+ = \frac{\beta}{4}\left(E_+ \pm y\sqrt{1 + \frac{4m^2}{y^2 - E_+^2}}\right) \qquad x_\pm^- = \frac{\beta}{4}\left(E_- \pm y\sqrt{1 + \frac{4m^2}{y^2 - E_-^2}}\right), \tag{5.94}$$

and we defined $\tilde{g} = g^4(N^2+5)/(4 \cdot 144)$.

Bibliography

[1] H. Poincaré. "Sur le problème des trois corps et les équations de la dynamique". In: *Acta Math.* 13 (1980), pp. 1–270.

[2] Marcos Rigol, Vanja Dunjko, and Maxim Olshanii. "Thermalization and its mechanism for generic isolated quantum systems". In: *Nature* 452.7189 (2008), pp. 854–858. DOI: 10.1038/nature06838. arXiv: 0708.1324 [cond-mat.stat-mech].

[3] Luca D'Alessio et al. "From quantum chaos and eigenstate thermalization to statistical mechanics and thermodynamics". In: *Advances in Physics* 65.3 (2016), pp. 239–362. DOI: 10.1080/00018732.2016.1198134. eprint: https://doi.org/10.1080/00018732.2016.1198134. URL: https://doi.org/10.1080/00018732.2016.1198134.

[4] S. Sachdev. "Strange metals and black holes". In: *talk at Dirac medal award cerimony, Trieste* (2019). URL: http://qpt.physics.harvard.edu/talks/trieste19.pdf.

[5] J. M. Deutsch. "Quantum statistical mechanics in a closed system". In: *Phys. Rev. A* 43 (4 1991), pp. 2046–2049. DOI: 10.1103/PhysRevA.43.2046. URL: https://link.aps.org/doi/10.1103/PhysRevA.43.2046.

[6] Mark Srednicki. "Chaos and quantum thermalization". In: *Phys. Rev. E* 50 (2 1994), pp. 888–901. DOI: 10.1103/PhysRevE.50.888. URL: https://link.aps.org/doi/10.1103/PhysRevE.50.888.

[7] Mark Srednicki. "The approach to thermal equilibrium in quantized chaotic systems". In: *Journal of Physics A: Mathematical and General* 32.7 (1999), pp. 1163–1175. DOI: 10.1088/0305-4470/32/7/007. URL: https://doi.org/10.1088%2F0305-4470%2F32%2F7%2F007.

[8] Julian Sonner and Manuel Vielma. "Eigenstate thermalization in the Sachdev-Ye-Kitaev model". In: *Journal of High Energy Physics* 2017.11 (2017), p. 149. ISSN: 1029-8479. DOI: 10.1007/JHEP11(2017)149. URL: https://doi.org/10.1007/JHEP11(2017)149.

[9] A. Larkin and Y. N. Ovchinnikov. "Quasiclassical method in the theory of superconductivity". In: *Sov. Phys. JETP* 28 (1969), pp. 1200–1205. URL: https://doi.org/10.1038/s41567-018-0295-5.

[10] A. Kitaev. "A simple model of quantum holography, Part 1 and Part 2". In: *talks at KITP, Santa Barbara* (2015). URL: http://online.kitp.ucsb.edu/online/entangled15/kitaev/.

[11] Nima Lashkari et al. "Towards the fast scrambling conjecture". In: *Journal of High Energy Physics* 2013.4 (2013), p. 22. ISSN: 1029-8479. DOI: 10.1007/JHEP04(2013)022. URL: https://doi.org/10.1007/JHEP04(2013)022.

[12] Stephen H. Shenker and Douglas Stanford. "Black holes and the butterfly effect". In: *JHEP* 03 (2014), p. 067. DOI: 10.1007/JHEP03(2014)067. arXiv: 1306.0622 [hep-th].

[13] Stephen H. Shenker and Douglas Stanford. "Multiple Shocks". In: *JHEP* 12 (2014), p. 046. DOI: 10.1007/JHEP12(2014)046. arXiv: 1312.3296 [hep-th].

[14] Stephen H. Shenker and Douglas Stanford. "Stringy effects in scrambling". In: *Journal of High Energy Physics* 2015.5 (2015), p. 132. ISSN: 1029-8479. DOI: 10.1007/JHEP05(2015)132. URL: https://doi.org/10.1007/JHEP05(2015)132.

[15] Daniel A. Roberts, Douglas Stanford, and Leonard Susskind. "Localized shocks". In: *JHEP* 03 (2015), p. 051. DOI: 10.1007/JHEP03(2015)051. arXiv: 1409.8180 [hep-th].

[16] Juan Maldacena, Stephen H. Shenker, and Douglas Stanford. "A bound on chaos". In: *JHEP* 08 (2016), p. 106. DOI: 10.1007/JHEP08(2016)106. arXiv: 1503.01409 [hep-th].

[17] Subir Sachdev and Jinwu Ye. "Gapless spin-fluid ground state in a random quantum Heisenberg magnet". In: *Phys. Rev. Lett.* 70 (21 1993), pp. 3339–3342. DOI: 10.1103/PhysRevLett.70.3339. URL: https://link.aps.org/doi/10.1103/PhysRevLett.70.3339.

[18] Juan Maldacena and Douglas Stanford. "Comments on the Sachdev-Ye-Kitaev model". In: (2016). arXiv: 1604.07818. URL: http://arxiv.org/abs/1604.07818.

[19] Brian Swingle et al. "Measuring the scrambling of quantum information". In: *Phys. Rev. A* 94 (4 2016), p. 040302. DOI: 10.1103/PhysRevA.94.040302. URL: https://link.aps.org/doi/10.1103/PhysRevA.94.040302.

[20] Guanyu Zhu, Mohammad Hafezi, and Tarun Grover. "Measurement of many-body chaos using a quantum clock". In: *Phys. Rev. A* 94 (6 2016), p. 062329. DOI: 10.1103/PhysRevA.94.062329. URL: https://link.aps.org/doi/10.1103/PhysRevA.94.062329.

[21] Norman Y. Yao et al. "Interferometric Approach to Probing Fast Scrambling". In: (2016). arXiv: 1607.01801 [quant-ph].

[22] Nicole Yunger Halpern. "Jarzynski-like equality for the out-of-time-ordered correlator". In: *Phys. Rev. A* 95 (1 2017), p. 012120. DOI: 10.1103/PhysRevA.95.012120. URL: https://link.aps.org/doi/10.1103/PhysRevA.95.012120.

[23] Nicole Yunger Halpern, Brian Swingle, and Justin Dressel. "Quasiprobability behind the out-of-time-ordered correlator". In: *Phys. Rev. A* 97 (4 2018), p. 042105. DOI: 10.1103/PhysRevA.97.042105. URL: https://link.aps.org/doi/10.1103/PhysRevA.97.042105.

[24] Michele Campisi and John Goold. "Thermodynamics of quantum information scrambling". In: *Phys. Rev. E* 95 (6 2017), p. 062127. DOI: 10.1103/PhysRevE.95.062127. URL: https://link.aps.org/doi/10.1103/PhysRevE.95.062127.

[25] Beni Yoshida and Alexei Kitaev. "Efficient decoding for the Hayden-Preskill protocol". In: (2017). arXiv: 1710.03363 [hep-th].

[26] Martin Gärttner et al. "Measuring out-of-time-order correlations and multiple quantum spectra in a trapped ion quantum magnet". In: *Nature Phys.* 13 (2017), p. 781. DOI: 10.1038/nphys4119. arXiv: 1608.08938 [quant-ph].

[27] Ken Xuan Wei, Chandrasekhar Ramanathan, and Paola Cappellaro. "Exploring Localization in Nuclear Spin Chains". In: *Phys. Rev. Lett.* 120 (7 2018), p. 070501. DOI: 10.1103/PhysRevLett.120.070501. URL: https://link.aps.org/doi/10.1103/PhysRevLett.120.070501.

[28] Jun Li et al. "Measuring Out-of-Time-Order Correlators on a Nuclear Magnetic Resonance Quantum Simulator". In: *Phys. Rev. X* 7 (3 2017), p. 031011. DOI: 10.1103/PhysRevX.7.031011. URL: https://link.aps.org/doi/10.1103/PhysRevX.7.031011.

[29] Eric J. Meier et al. "Exploring quantum signatures of chaos on a Floquet synthetic lattice". In: *arXiv e-prints*, arXiv:1705.06714 (May 2017), arXiv:1705.06714. arXiv: 1705.06714 [cond-mat.quant-gas].

[30] Adam Nahum et al. "Quantum Entanglement Growth under Random Unitary Dynamics". In: *Phys. Rev. X* 7 (3 2017), p. 031016. DOI: 10.1103/PhysRevX.7.031016. URL: https://link.aps.org/doi/10.1103/PhysRevX.7.031016.

[31] C. W. von Keyserlingk et al. "Operator Hydrodynamics, OTOCs, and Entanglement Growth in Systems without Conservation Laws". In: *Phys. Rev. X* 8 (2 2018), p. 021013. DOI: 10.1103/PhysRevX.8.021013. URL: https://link.aps.org/doi/10.1103/PhysRevX.8.021013.

[32] Shenglong Xu and Brian Swingle. "Accessing scrambling using matrix product operators". In: (2018). arXiv: 1802.00801 [quant-ph].

[33] Yingfei Gu, Xiao-Liang Qi, and Douglas Stanford. "Local criticality, diffusion and chaos in generalized Sachdev-Ye-Kitaev models". In: *Journal of High Energy Physics* 2017.5 (2017), p. 125. ISSN: 1029-8479. DOI: 10.1007/JHEP05(2017)125. URL: https://doi.org/10.1007/JHEP05(2017)125.

[34] David J. Luitz and Yevgeny Bar Lev. "Information propagation in isolated quantum systems". In: *Phys. Rev. B* 96 (2 2017), p. 020406. DOI: 10.1103/PhysRevB.96.020406. URL: https://link.aps.org/doi/10.1103/PhysRevB.96.020406.

[35] A Bohrdt et al. "Scrambling and thermalization in a diffusive quantum many-body system". In: *New Journal of Physics* 19.6 (2017), p. 063001. DOI: 10.1088/1367-2630/aa719b. URL: https://doi.org/10.1088%2F1367-2630%2Faa719b.

[36] Markus Heyl, Frank Pollmann, and Balázs Dóra. "Detecting Equilibrium and Dynamical Quantum Phase Transitions in Ising Chains via Out-of-Time-Ordered Correlators". In: *Phys. Rev. Lett.* 121 (1 2018), p. 016801. DOI: 10.1103/PhysRevLett.121.016801. URL: https://link.aps.org/doi/10.1103/PhysRevLett.121.016801.

[37] Cheng-Ju Lin and Olexei I. Motrunich. "Out-of-time-ordered correlators in a quantum Ising chain". In: *Phys. Rev. B* 97 (14 2018), p. 144304. DOI: 10.1103/PhysRevB.97.144304. URL: https://link.aps.org/doi/10.1103/PhysRevB.97.144304.

[38] Adam Nahum, Sagar Vijay, and Jeongwan Haah. "Operator Spreading in Random Unitary Circuits". In: *Phys. Rev. X* 8 (2 2018), p. 021014. DOI: 10.1103/PhysRevX.8.021014. URL: https://link.aps.org/doi/10.1103/PhysRevX.8.021014.

[39] Tibor Rakovszky, Frank Pollmann, and C. W. von Keyserlingk. "Diffusive Hydrodynamics of Out-of-Time-Ordered Correlators with Charge Conservation". In: *Phys. Rev. X* 8 (3 2018), p. 031058. DOI: 10.1103/PhysRevX.8.031058. URL: https://link.aps.org/doi/10.1103/PhysRevX.8.031058.

[40] Vedika Khemani, David A. Huse, and Adam Nahum. "Velocity-dependent Lyapunov exponents in many-body quantum, semiclassical, and classical chaos". In: *Phys. Rev. B* 98 (14 2018), p. 144304. DOI: 10.1103/PhysRevB.98.144304. URL: https://link.aps.org/doi/10.1103/PhysRevB.98.144304.

[41] Vedika Khemani, Ashvin Vishwanath, and David A. Huse. "Operator Spreading and the Emergence of Dissipative Hydrodynamics under Unitary Evolution with Conservation Laws". In: *Phys. Rev. X* 8 (3 2018), p. 031057. DOI: 10.1103/PhysRevX.8.031057. URL: https://link.aps.org/doi/10.1103/PhysRevX.8.031057.

[42] Igor L. Aleiner, Lara Faoro, and Lev B. Ioffe. "Microscopic model of quantum butterfly effect: Out-of-time-order correlators and traveling combustion waves". In: *Annals of Physics* 375 (2016), pp. 378 –406. ISSN: 0003-4916. DOI: https://doi.org/10.1016/j.aop.2016.09.006. URL: http://www.sciencedirect.com/science/article/pii/S0003491616301919.

[43] Brian Swingle and Debanjan Chowdhury. "Slow scrambling in disordered quantum systems". In: *Phys. Rev. B* 95 (6 2017), p. 060201. DOI: 10.1103/PhysRevB.95.060201. URL: https://link.aps.org/doi/10.1103/PhysRevB.95.060201.

[44] Sašo Grozdanov, Koenraad Schalm, and Vincenzo Scopelliti. "Kinetic theory for classical and quantum many-body chaos". In: *Phys. Rev. E* 99 (1 2019), p. 012206. DOI: 10.1103/PhysRevE.99.012206. URL: https://link.aps.org/doi/10.1103/PhysRevE.99.012206.

[45] Aavishkar A. Patel et al. "Quantum Butterfly Effect in Weakly Interacting Diffusive Metals". In: *Phys. Rev. X* 7 (3 2017), p. 031047. DOI: 10.1103/PhysRevX.7.031047. URL: https://link.aps.org/doi/10.1103/PhysRevX.7.031047.

[46] Brian Swingle and Nicole Yunger Halpern. "Resilience of scrambling measurements". In: *Phys. Rev. A* 97 (6 2018), p. 062113. DOI: 10.1103/PhysRevA.97.062113. URL: https://link.aps.org/doi/10.1103/PhysRevA.97.062113.

[47] Justin Dressel et al. "Strengthening weak measurements of qubit out-of-time-order correlators". In: *Phys. Rev. A* 98 (1 2018), p. 012132. DOI: 10.1103/PhysRevA.98.012132. URL: https://link.aps.org/doi/10.1103/PhysRevA.98.012132.

[48] G. Menezes and J. Marino. "Slow scrambling in sonic black holes". In: *EPL (Europhysics Letters)* 121.6 (2018), p. 60002. DOI: 10.1209/0295-5075/121/60002. URL: https://doi.org/10.1209%2F0295-5075%2F121%2F60002.

[49] Thomas Scaffidi and Ehud Altman. "Semiclassical Theory of Many-Body Quantum Chaos and its Bound". In: (2017). arXiv: 1711.04768 [cond-mat.stat-mech].

[50] Márk Mezei. "Membrane theory of entanglement dynamics from holography". In: *Phys. Rev. D* 98 (10 2018), p. 106025. DOI: 10.1103/PhysRevD.98.106025. URL: https://link.aps.org/doi/10.1103/PhysRevD.98.106025.

[51] Daniel A. Roberts, Douglas Stanford, and Alexandre Streicher. "Operator growth in the SYK model". In: *Journal of High Energy Physics* 2018.6 (2018), p. 122. ISSN: 1029-8479. DOI: 10.1007/JHEP06(2018)122. URL: https://doi.org/10.1007/JHEP06(2018)122.

[52] Xiao Chen and Tianci Zhou. "Operator scrambling and quantum chaos". In: (2018). arXiv: 1804.08655 [cond-mat.str-el].

[53] Cheryne Jonay, David A. Huse, and Adam Nahum. "Coarse-grained dynamics of operator and state entanglement". In: (2018). arXiv: 1803.00089 [cond-mat.stat-mech].

[54] Yi-Zhuang You and Yingfei Gu. "Entanglement features of random Hamiltonian dynamics". In: *Phys. Rev. B* 98 (1 2018), p. 014309. DOI: 10.1103/PhysRevB.98.014309. URL: https://link.aps.org/doi/10.1103/PhysRevB.98.014309.

[55] Brian Swingle. "Unscrambling the physics of out-of-time-order correlators". In: *Nature Physics* 14.10 (2018), pp. 988–990. ISSN: 1745-2481. DOI: 10.1038/s41567-018-0295-5. URL: https://doi.org/10.1038/s41567-018-0295-5.

[56] Mike Blake, Hyunseok Lee, and Hong Liu. "A quantum hydrodynamical description for scrambling and many-body chaos". In: *JHEP* 10 (2018), p. 127. DOI: 10.1007/JHEP10(2018)127. arXiv: 1801.00010 [hep-th].

[57] L. D. Landau. "The theory of a Fermi liquid". In: *Soviet Physics JETP* 3 (1957), pp. 920–925.

[58] J. A. N. Bruin et al. "Similarity of Scattering Rates in Metals Showing T-Linear Resistivity". In: *Science* 339.6121 (2013), pp. 804–807. ISSN: 0036-8075. DOI: 10.1126/science.1227612. eprint: http://science.sciencemag.org/content/339/6121/804.full.pdf. URL: http://science.sciencemag.org/content/339/6121/804.

[59] A Legros et al. "Universal T-linear resistivity and Planckian dissipation in overdoped cuprates". In: *Nature Physics* 15.2 (2019), pp. 142–147. ISSN: 1745-2481. DOI: 10.1038/s41567-018-0334-2. URL: https://doi.org/10.1038/s41567-018-0334-2.

[60] Jan Zaanen. "Why the temperature is high". In: *Nature* 430 (2004), p. 512. URL: https://doi.org/10.1038/430512ahttp://10.0.4.14/430512a.

[61] S. Sachdev. *Quantum Phase Transitions*. Cambridge University Press, 2011. ISBN: 9781139500210.

[62] Jan Zaanen. "Planckian dissipation, minimal viscosity and the transport in cuprate strange metals". In: (2018). arXiv: 1807.10951 [cond-mat.str-el].

[63] J. C. Zhang et al. "Anomalous Thermal Diffusivity in Underdoped $YBa_2Cu_3O_{6+x}$". In: *Proc. Nat. Acad. Sci.* 114 (2017), pp. 5378–5383. DOI: 10.1073/pnas.1703416114. arXiv: 1610.05845 [cond-mat.supr-con].

[64] Mike Blake. "Universal Charge Diffusion and the Butterfly Effect in Holographic Theories". In: *Phys. Rev. Lett.* 117.9 (2016), p. 091601. DOI: 10.1103/PhysRevLett.117.091601. arXiv: 1603.08510 [hep-th].

[65] Mike Blake. "Universal Diffusion in Incoherent Black Holes". In: *Phys. Rev.* D94.8 (2016), p. 086014. DOI: 10.1103/PhysRevD.94.086014. arXiv: 1604.01754 [hep-th].

[66] Mike Blake, Richard A. Davison, and Subir Sachdev. "Thermal diffusivity and chaos in metals without quasiparticles". In: *Phys. Rev.* D96.10 (2017), p. 106008. DOI: 10.1103/PhysRevD.96.106008. arXiv: 1705.07896 [hep-th].

[67] Mike Blake and Aristomenis Donos. "Diffusion and Chaos from near AdS_2 horizons". In: *JHEP* 02 (2017), p. 013. DOI: 10.1007/JHEP02(2017)013. arXiv: 1611.09380 [hep-th].

[68] Mike Blake, Richard A. Davison, and Subir Sachdev. "Thermal diffusivity and chaos in metals without quasiparticles". In: *Phys. Rev. D* 96 (10 2017), p. 106008. DOI: 10.1103/PhysRevD.96.106008. URL: https://link.aps.org/doi/10.1103/PhysRevD.96.106008.

[69] Aavishkar A. Patel and Subir Sachdev. "Quantum chaos on a critical Fermi surface". In: *Proc. Nat. Acad. Sci.* 114 (2017), pp. 1844–1849. DOI: 10.1073/pnas.1618185114. arXiv: 1611.00003 [cond-mat.str-el].

[70] Juan Martin Maldacena. "The Large N limit of superconformal field theories and supergravity". In: *Int. J. Theor. Phys.* 38 (1999). [Adv. Theor. Math. Phys.2,231(1998)], pp. 1113–1133. DOI: 10.1023/A:1026654312961, 10.4310/ATMP.1998.v2.n2.a1. arXiv: hep-th/9711200 [hep-th].

[71] Ofer Aharony et al. "Large N field theories, string theory and gravity". In: *Phys. Rept.* 323 (2000), pp. 183–386. DOI: 10.1016/S0370-1573(99)00083-6. arXiv: hep-th/9905111 [hep-th].

[72] Martin Ammon and Johanna Erdmenger. *Gauge/gravity duality*. Cambridge: Cambridge University Press, 2015. ISBN: 9781107010345, 9781316235942. URL: http://www.cambridge.org/de/academic/subjects/physics/theoretical-physics-and-mathematical-physics/gaugegravity-duality-foundations-and-applications.

[73] Jan Zaanen et al. *Holographic Duality in Condensed Matter Physics*. Cambridge Univ. Press, 2015. ISBN: 9781107080089. URL: http://www.cambridge.org/mw/academic/subjects/physics/condensed-matter-physics-nanoscience-and-mesoscopic-physics/holographic-duality-condensed-matter-physics?format=HB.

[74] Sean A. Hartnoll, Andrew Lucas, and Subir Sachdev. "Holographic quantum matter". In: (2016). arXiv: 1612.07324 [hep-th].

[75] G.'t Hooft. "A planar diagram theory for strong interactions". In: *Nuclear Physics B* 72.3 (1974), pp. 461 –473. ISSN: 0550-3213. DOI: https://doi.org/10.1016/0550-3213(74)90154-0. URL: http://www.sciencedirect.com/science/article/pii/0550321374901540.

[76] Jacob D. Bekenstein. "Black Holes and Entropy". In: *Phys. Rev. D* 7 (8 1973), pp. 2333–2346. DOI: 10.1103/PhysRevD.7.2333. URL: https://link.aps.org/doi/10.1103/PhysRevD.7.2333.

[77] Gerard 't Hooft. "Dimensional reduction in quantum gravity". In: *Conf. Proc.* C930308 (1993), pp. 284–296. arXiv: gr-qc/9310026 [gr-qc].

[78] Leonard Susskind. "The World as a hologram". In: *J. Math. Phys.* 36 (1995), pp. 6377–6396. DOI: 10.1063/1.531249. arXiv: hep-th/9409089 [hep-th].

[79] Kenneth G. Wilson. "The renormalization group: Critical phenomena and the Kondo problem". In: *Rev. Mod. Phys.* 47 (4 1975), pp. 773–840. DOI: 10.1103/RevModPhys.47.773. URL: https://link.aps.org/doi/10.1103/RevModPhys.47.773.

[80] John McGreevy. "Holographic duality with a view toward many-body physics". In: *Adv. High Energy Phys.* 2010 (2010), p. 723105. DOI: 10.1155/2010/723105. arXiv: 0909.0518 [hep-th].

[81] S. S. Gubser, Igor R. Klebanov, and Alexander M. Polyakov. "Gauge theory correlators from noncritical string theory". In: *Phys. Lett.* B428 (1998), pp. 105–114. DOI: 10.1016/S0370-2693(98)00377-3. arXiv: hep-th/9802109 [hep-th].

[82] Edward Witten. "Anti-de Sitter space and holography". In: *Adv. Theor. Math. Phys.* 2 (1998), pp. 253–291. DOI: 10.4310/ATMP.1998.v2.n2.a2. arXiv: hep-th/9802150 [hep-th].

[83] Sayantani Bhattacharyya et al. "Nonlinear Fluid Dynamics from Gravity". In: *JHEP* 02 (2008), p. 045. DOI: 10.1088/1126-6708/2008/02/045. arXiv: 0712.2456 [hep-th].

[84] Veronika E. Hubeny, Shiraz Minwalla, and Mukund Rangamani. "The fluid/gravity correspondence". In: *Black holes in higher dimensions*. [,817(2011)]. 2012, pp. 348–383. arXiv: 1107.5780 [hep-th].

[85] K. S. Thorne, R. H. Price, and D. A. MacDonald. *Black holes: The membrane paradigm*. 1986.

[86] Hong Liu and Paolo Glorioso. "Lectures on non-equilibrium effective field theories and fluctuating hydrodynamics". In: *PoS* TASI2017 (2018), p. 008. DOI: 10.22323/1.305.0008. arXiv: 1805.09331 [hep-th].

[87] Sašo Grozdanov and Janos Polonyi. "Viscosity and dissipative hydrodynamics from effective field theory". In: *Phys. Rev.* D91.10 (2015), p. 105031. DOI: 10.1103/PhysRevD.91.105031. arXiv: 1305.3670 [hep-th].

[88] Michael Crossley, Paolo Glorioso, and Hong Liu. "Effective field theory of dissipative fluids". In: *JHEP* 09 (2017), p. 095. DOI: 10.1007/JHEP09(2017)095. arXiv: 1511.03646 [hep-th].

[89] Paolo Glorioso, Michael Crossley, and Hong Liu. "Effective field theory of dissipative fluids (II): classical limit, dynamical KMS symmetry and entropy current". In: *JHEP* 09 (2017), p. 096. DOI: 10.1007/JHEP09(2017)096. arXiv: 1701.07817 [hep-th].

[90] Paolo Glorioso, Hong Liu, and Srivatsan Rajagopal. "Global Anomalies, Discrete Symmetries, and Hydrodynamic Effective Actions". In: *JHEP* 01 (2019), p. 043. DOI: 10.1007/JHEP01(2019)043. arXiv: 1710.03768 [hep-th].

[91] Ping Gao, Paolo Glorioso, and Hong Liu. "Ghostbusters: Unitarity and Causality of Non-equilibrium Effective Field Theories". In: (2018). arXiv: 1803.10778 [hep-th].

[92] Ping Gao and Hong Liu. "Emergent Supersymmetry in Local Equilibrium Systems". In: *JHEP* 01 (2018), p. 040. DOI: 10.1007/JHEP01(2018)040. arXiv: 1701.07445 [hep-th].

[93] Paolo Glorioso and Hong Liu. "The second law of thermodynamics from symmetry and unitarity". In: (2016). arXiv: 1612.07705 [hep-th].

[94] Felix M. Haehl, R. Loganayagam, and Mukund Rangamani. "The eightfold way to dissipation". In: *Phys. Rev. Lett.* 114 (2015), p. 201601. DOI: 10.1103/PhysRevLett.114.201601. arXiv: 1412.1090 [hep-th].

[95] Felix M. Haehl, R. Loganayagam, and Mukund Rangamani. "Adiabatic hydrodynamics: The eightfold way to dissipation". In: *JHEP* 05 (2015), p. 060. DOI: 10.1007/JHEP05(2015)060. arXiv: 1502.00636 [hep-th].

[96] Kristan Jensen, Natalia Pinzani-Fokeeva, and Amos Yarom. "Dissipative hydrodynamics in superspace". In: *JHEP* 09 (2018), p. 127. DOI: 10.1007/JHEP09(2018)127. arXiv: 1701.07436 [hep-th].

[97] Felix M. Haehl, R. Loganayagam, and Mukund Rangamani. "The Fluid Manifesto: Emergent symmetries, hydrodynamics, and black holes". In: *JHEP* 01 (2016), p. 184. DOI: 10.1007/JHEP01(2016)184. arXiv: 1510.02494 [hep-th].

[98] Felix M. Haehl, R. Loganayagam, and M. Rangamani. "Topological sigma models & dissipative hydrodynamics". In: *JHEP* 04 (2016), p. 039. DOI: 10.1007/JHEP04(2016)039. arXiv: 1511.07809 [hep-th].

[99] Dam T. Son and Andrei O. Starinets. "Viscosity, Black Holes, and Quantum Field Theory". In: *Ann. Rev. Nucl. Part. Sci.* 57 (2007), pp. 95–118. DOI: 10.1146/annurev.nucl.57.090506.123120. arXiv: 0704.0240 [hep-th].

[100] Giuseppe Policastro, Dam T. Son, and Andrei O. Starinets. "From AdS / CFT correspondence to hydrodynamics". In: *JHEP* 09 (2002), p. 043. DOI: 10.1088/1126-6708/2002/09/043. arXiv: hep-th/0205052 [hep-th].

[101] Sangyong Jeon. "Hydrodynamic transport coefficients in relativistic scalar field theory". In: *Physical Review D* 52.6 (1995), pp. 3591–3642. ISSN: 05562821. DOI: 10.1103/PhysRevD.52.3591. arXiv: 9409250 [hep-ph].

[102] Peter Brockway Arnold, Guy D. Moore, and Laurence G. Yaffe. "Transport coefficients in high temperature gauge theories. 1. Leading log results". In: *JHEP* 11 (2000), p. 001. DOI: 10.1088/1126-6708/2000/11/001. arXiv: hep-ph/0010177 [hep-ph].

[103] Peter Brockway Arnold, Guy D. Moore, and Laurence G. Yaffe. "Effective kinetic theory for high temperature gauge theories". In: *JHEP* 01 (2003), p. 030. DOI: 10.1088/1126-6708/2003/01/030. arXiv: hep-ph/0209353 [hep-ph].

[104] Peter Brockway Arnold, Guy D Moore, and Laurence G. Yaffe. "Transport coefficients in high temperature gauge theories. 2. Beyond leading log". In: *JHEP* 05 (2003), p. 051. DOI: 10.1088/1126-6708/2003/05/051. arXiv: hep-ph/0302165 [hep-ph].

[105] Mark Abraao York and Guy D. Moore. "Second order hydrodynamic coefficients from kinetic theory". In: *Phys. Rev.* D79 (2009), p. 054011. DOI: 10.1103/PhysRevD.79.054011. arXiv: 0811.0729 [hep-ph].

[106] G. S. Denicol, T. Koide, and D. H. Rischke. "Dissipative relativistic fluid dynamics: a new way to derive the equations of motion from kinetic theory". In: *Phys. Rev. Lett.* 105 (2010), p. 162501. DOI: 10.1103/PhysRevLett.105.162501. arXiv: 1004.5013 [nucl-th].

[107] G. S. Denicol et al. "Derivation of transient relativistic fluid dynamics from the Boltzmann equation". In: *Phys. Rev.* D85 (2012). [Erratum: Phys. Rev.D91,no.3,039902(2015)], p. 114047. DOI: 10.1103/PhysRevD.85.114047,10.1103/PhysRevD.91.039902. arXiv: 1202.4551 [nucl-th].

[108] G. S. Denicol, S. Jeon, and C. Gale. "Transport Coefficients of Bulk Viscous Pressure in the 14-moment approximation". In: *Phys. Rev.* C90.2 (2014), p. 024912. DOI: 10.1103/PhysRevC.90.024912. arXiv: 1403.0962 [nucl-th].

[109] Guy D. Moore and Kiyoumars A. Sohrabi. "Kubo Formulae for Second-Order Hydrodynamic Coefficients". In: *Phys. Rev. Lett.* 106 (2011), p. 122302. DOI: 10.1103/PhysRevLett.106.122302. arXiv: 1007.5333 [hep-ph].

[110] Guy D. Moore and Kiyoumars A. Sohrabi. "Thermodynamical second-order hydrodynamic coefficients". In: *JHEP* 11 (2012), p. 148. DOI: 10.1007/JHEP11(2012)148. arXiv: 1210.3340 [hep-ph].

[111] D. N. Zubarev. *Nonequilibrium Statistical Thermodynamics*. New York: Consultants Bureau–Plenum, 1974.

[112] Sangyong Jeon. "Computing spectral densities in Finite temperature field theory". In: *PHYSICAL REVIEW D* 47.10 (1993).

[113] Enke Wang and Ulrich Heinz. "Nonperturbative calculation of the shear viscosity in hot ϕ^4 theory in real time". In: *Physics Letters, Section B: Nuclear, Elementary Particle and High-Energy Physics* 471.2-3 (1999), pp. 208–213. ISSN: 03702693. DOI: 10.1016/S0370-2693(99)01324-6. arXiv: 9910367 [hep-ph].

[114] Enke Wang and Ulrich Heinz. "Shear viscosity of hot scalar field theory in the real-time formalism". In: *Phys. Rev. D* 67 (2 2003), p. 025022. DOI: 10.1103/PhysRevD.67.025022. URL: https://link.aps.org/doi/10.1103/PhysRevD.67.025022.

[115] Manuel A. Valle Basagoiti. "Transport coefficients and ladder summation in hot gauge theories". In: *Phys. Rev. D* 66 (4 2002), p. 045005. DOI: 10.1103/PhysRevD.66.045005. URL: https://link.aps.org/doi/10.1103/PhysRevD.66.045005.

[116] Gert Aarts and J. M. Martinez Resco. "Ward identity and electrical conductivity in hot QED". In: *JHEP* 11 (2002), p. 022. DOI: 10.1088/1126-6708/2002/11/022. arXiv: hep-ph/0209048 [hep-ph].

[117] Gert Aarts and Jose M. Martínez Resco. "Transport coefficients from the two particle irreducible effective action". In: *Phys. Rev. D* 68 (8 2003), p. 085009. DOI: 10.1103/PhysRevD.68.085009. URL: https://link.aps.org/doi/10.1103/PhysRevD.68.085009.

[118] G. Policastro, Dan T. Son, and Andrei O. Starinets. "The Shear viscosity of strongly coupled N=4 supersymmetric Yang-Mills plasma". In: *Phys. Rev. Lett.* 87 (2001), p. 081601. DOI: 10.1103/PhysRevLett.87.081601. arXiv: hep-th/0104066 [hep-th].

[119] Pavel Kovtun, Dam T. Son, and Andrei O. Starinets. "Holography and hydrodynamics: Diffusion on stretched horizons". In: *JHEP* 10 (2003), p. 064. DOI: 10.1088/1126-6708/2003/10/064. arXiv: hep-th/0309213 [hep-th].

[120] Pavel K. Kovtun and Andrei O. Starinets. "Quasinormal modes and holography". In: *Phys. Rev.* D72 (2005), p. 086009. DOI: 10.1103/PhysRevD.72.086009. arXiv: hep-th/0506184 [hep-th].

[121] Paul Romatschke. "Retarded correlators in kinetic theory: branch cuts, poles and hydrodynamic onset transitions". In: *Eur. Phys. J.* C76.6 (2016), p. 352. DOI: 10.1140/epjc/s10052-016-4169-7. arXiv: 1512.02641 [hep-th].

[122] Aleksi Kurkela and Urs Achim Wiedemann. "Analytic structure of nonhydrodynamic modes in kinetic theory". In: (2017). arXiv: 1712.04376 [hep-ph].

[123] Kristan Jensen. "Chaos in AdS_2 Holography". In: *Phys. Rev. Lett.* 117.11 (2016), p. 111601. DOI: 10.1103/PhysRevLett.117.111601. arXiv: 1605.06098 [hep-th].

[124] Kedar Damle and Subir Sachdev. "Nonzero-temperature transport near quantum critical points". In: *Phys. Rev. B* 56 (14 1997), pp. 8714–8733. DOI: 10.1103/PhysRevB.56.8714. URL: https://link.aps.org/doi/10.1103/PhysRevB.56.8714.

[125] Alexander Altland and Ben Simons. *Condensed matter field theory; 2nd ed.* Cambridge: Cambridge Univ. Press, 2010. URL: https://cds.cern.ch/record/1257155.

[126] Sangyong Jeon and Laurence G. Yaffe. "From quantum field theory to hydrodynamics: Transport coefficients and effective kinetic theory". In: *Phys. Rev. D* 53 (10 1996), pp. 5799–5809. DOI: 10.1103/PhysRevD.53.5799. URL: https://link.aps.org/doi/10.1103/PhysRevD.53.5799.

[127] E. Gross and E. Jackson. "Kinetic Models and the Linearized Boltzmann Equation". In: *Phys. Fluids* 2 (1959), p. 432.

[128] Sašo Grozdanov, Koenraad Schalm, and Vincenzo Scopelliti. "Black Hole Scrambling from Hydrodynamics". In: *Phys. Rev. Lett.* 120 (23 2018), p. 231601. DOI: 10.1103/PhysRevLett.120.231601. URL: https://link.aps.org/doi/10.1103/PhysRevLett.120.231601.

[129] Mike Blake et al. "Many-body chaos and energy dynamics in holography". In: *JHEP* 10 (2018), p. 035. DOI: 10.1007/JHEP10(2018)035. arXiv: 1809.01169 [hep-th].

[130] Sašo Grozdanov et al. "The complex life of hydrodynamic modes". In: (2019). arXiv: 1904.12862 [hep-th].

[131] Sašo Grozdanov. "On the connection between hydrodynamics and quantum chaos in holographic theories with stringy corrections". In: *JHEP* 01 (2019), p. 048. DOI: 10.1007/JHEP01(2019)048. arXiv: 1811.09641 [hep-th].

[132] Mike Blake, Richard A. Davison, and David Vegh. "Horizon constraints on holographic Green's functions". In: (2019). arXiv: 1904.12883 [hep-th].

[133] Sašo Grozdanov, Koenraad Schalm, and Vincenzo Scopelliti. *In preparation.*

[134] Gert Aarts and Jose M. Martinez Resco. "Transport coefficients and the 2pi effective action in the large N limit". In: *Proceedings, 6th International Conference on Strong and Electroweak Matter (SEWM 2004): Helsinki, Finland, June 16-19, 2004*. 2005, pp. 231–240. DOI: 10.1142/9789812702159_0030. arXiv: hep-ph/0409090 [hep-ph].

[135] Gert Aarts and Jose M. Martinez Resco. "Shear viscosity in the O(N) model". In: *JHEP* 02 (2004), p. 061. DOI: 10.1088/1126-6708/2004/02/061. arXiv: hep-ph/0402192 [hep-ph].

[136] Debanjan Chowdhury and Brian Swingle. "Onset of many-body chaos in the $O(N)$ model". In: *Phys. Rev.* D96.6 (2017), p. 065005. DOI: 10.1103/PhysRevD.96.065005. arXiv: 1703.02545 [cond-mat.str-el].

[137] Shao-Kai Jian and Hong Yao. "Universal properties of many-body quantum chaos at Gross-Neveu criticality". In: (2018). arXiv: 1805.12299 [cond-mat.str-el].

[138] Aurelio Romero-Bermúdez, Koenraad Schalm, and Vincenzo Scopelliti. "Regularization dependence of the OTOC. Which Lyapunov spectrum is the physical one?" In: *Journal of High Energy Physics* 2019.7 (2019), p. 107. ISSN: 1029-8479. DOI: 10.1007/JHEP07(2019)107. URL: https://doi.org/10.1007/JHEP07(2019)107.

[139] S. Chapman and T.G. Cowling. *The mathematical theory of non-uniform gases*. 3rd ed. Cambridge, UK: Cambridge University Press, 1970.

[140] Iridii A Kvasnikov. *Thermodynamics and statistical physics: A theory of non-equilibrium systems (in Russian)*. Moscow, USSR: Moscow University Press, 1987.

[141] Laure Saint-Raymond. *Hydrodynamic Limits of the Boltzmann Equation*. Berlin, FRG: Springer-Verlag, 2009.

[142] J.H. Ferziger and H.G. Kaper. *Mathematical theory of transport processes in gases*. Amsterdam, Netherlands: North-Holland Publishing Company, 1972.

[143] G.E. Uhlenbeck and G.W. Ford. *Lectures in Statistical Mechanics*. Providence, R.I., USA: American Mathematical Society, 1963.

[144] S. R. De Groot. *Relativistic Kinetic Theory. Principles and Applications*. Ed. by W. A. Van Leeuwen and C. G. Van Weert. 1980.

[145] V.P. Silin. *Introduction to Kinetic Theory of Gases (in Russian)*. 3rd ed. Moscow, USSR: Nauka, 1971.

[146] H. Grad. "Asymptotic Theory of the Boltzmann Equation". In: *Phys. Fluids* 6 (1963), p. 0147.

[147] H. van Beijeren, R. van Zon, and J. R. Dorfman. "Kinetic Theory Estimates for the Kolmogorov-Sinai Entropy and the Largest Lyapunov Exponents for Dilute, Hard-Ball Gases and for Dilute, Random Lorentz Gases". In: *In: Szász D. (eds)* Hard Ball Systems and the Lorentz Gas*, (Springer Berlin, 2000)* (Sept. 1999). arXiv: chao-dyn/9909034 [chao-dyn].

[148] I. L. Aleiner and A. I. Larkin. "Role of divergence of classical trajectories in quantum chaos". In: *pre* 55 (Feb. 1997), R1243–R1246. DOI: 10.1103/PhysRevE.55.R1243. eprint: cond-mat/9610034.

[149] I. L. Aleiner and A. I. Larkin. "Divergence of classical trajectories and weak localization". In: *prb* 54 (Nov. 1996), pp. 14423–14444. DOI: 10.1103/PhysRevB.54.14423. eprint: cond-mat/9603121.

[150] A. I. Larkin and Y. N. Ovchinnikov. "Quasiclassical Method in the Theory of Superconductivity". In: *Soviet Journal of Experimental and Theoretical Physics* 28 (June 1969), p. 1200.

[151] Joseph Polchinski. "Chaos in the black hole S-matrix". In: (2015). arXiv: 1505.08108 [hep-th].

[152] Douglas Stanford. "Many-body chaos at weak coupling". In: *JHEP* 10 (2016), p. 009. DOI: 10.1007/JHEP10(2016)009. arXiv: 1512.07687 [hep-th].

[153] Igor L. Aleiner, Lara Faoro, and Lev B. Ioffe. "Microscopic model of quantum butterfly effect: out-of-time-order correlators and traveling combustion waves". In: *Annals Phys.* 375 (2016), pp. 378–406. DOI: 10.1016/j.aop.2016.09.006. arXiv: 1609.01251 [cond-mat.stat-mech].

[154] Aavishkar A. Patel et al. "Quantum butterfly effect in weakly interacting diffusive metals". In: *Phys. Rev.* X7.3 (2017), p. 031047. DOI: 10.1103/PhysRevX.7.031047. arXiv: 1703.07353 [cond-mat.str-el].

[155] Daniel A. Roberts and Brian Swingle. "Lieb-Robinson Bound and the Butterfly Effect in Quantum Field Theories". In: *Phys. Rev. Lett.* 117.9 (2016), p. 091602. DOI: 10.1103/PhysRevLett.117.091602. arXiv: 1603.09298 [hep-th].

[156] Ivan Kukuljan, Sašo Grozdanov, and Tomaž Prosen. "Weak Quantum Chaos". In: *Phys. Rev.* B96.6 (2017), p. 060301. DOI: 10.1103/PhysRevB.96.060301. arXiv: 1701.09147 [cond-mat.stat-mech].

[157] Efim B. Rozenbaum, Sriram Ganeshan, and Victor Galitski. "Lyapunov Exponent and Out-of-Time-Ordered Correlator's Growth Rate in a Chaotic System". In: *Phys. Rev. Lett.* 118 (8 2017), p. 086801. DOI: 10.1103/PhysRevLett.118.086801. URL: https://link.aps.org/doi/10.1103/PhysRevLett.118.086801.

[158] Tibor Rakovszky, Frank Pollmann, and C. W. von Keyserlingk. "Diffusive hydrodynamics of out-of-time-ordered correlators with charge conservation". In: (2017). arXiv: 1710.09827 [cond-mat.stat-mech].

[159] Vedika Khemani, Ashvin Vishwanath, and D. A. Huse. "Operator spreading and the emergence of dissipation in unitary dynamics with conservation laws". In: (2017). arXiv: 1710.09835 [cond-mat.stat-mech].

[160] Andrew Lucas. "Constraints on hydrodynamics from many-body quantum chaos". In: (2017). arXiv: 1710.01005 [hep-th].

[161] R. van Zon, H. van Beijeren, and Ch. Dellago. "Largest Lyapunov Exponent for Many Particle Systems at Low Densities". In: *Phys. Rev. Lett.* 80 (10 1998), pp. 2035–2038. DOI: 10.1103/PhysRevLett.80.2035. URL: https://link.aps.org/doi/10.1103/PhysRevLett.80.2035.

[162] Henrik Smith and Hojgaard H Jensen. *Transport phenomena*. Oxford: Clarendon Press, 1989.

[163] R. Balescu. *Equilibrium and nonequilibrium statistical mechanics*. New York: Wiley, 1975.

[164] H. Haug and A.-P. Jauho. *Quantum Kinetics in Transport and Optics of Semiconductors*. Berlin Heidelberg: Springer-Verlag, 2008. DOI: 10.1007/978-3-540-73564-9.

[165] Sašo Grozdanov, Nikolaos Kaplis, and Andrei O. Starinets. "From strong to weak coupling in holographic models of thermalization". In: *JHEP* 07 (2016), p. 151. DOI: 10.1007/JHEP07(2016)151. arXiv: 1605.02173 [hep-th].

[166] A. Altland and B.D. Simons. *Condensed Matter Field Theory*. Cambridge books online. Cambridge University Press, 2010. ISBN: 9780521769754. URL: https://books.google.rs/books?id=GpF0Pgo8CqAC.

[167] A. H. Mueller and D. T. Son. "On the Equivalence between the Boltzmann equation and classical field theory at large occupation numbers". In: *Phys. Lett.* B582 (2004), pp. 279–287. DOI: 10.1016/j.physletb.2003.12.047. arXiv: hep-ph/0212198 [hep-ph].

[168] Enke Wang and Ulrich W. Heinz. "Shear viscosity of hot scalar field theory in the real time formalism". In: *Phys. Rev.* D67 (2003), p. 025022. DOI: 10.1103/PhysRevD.67.025022. arXiv: hep-th/0201116 [hep-th].

[169] Alina Czajka and Sangyong Jeon. "Kubo formulas for the shear and bulk viscosity relaxation times and the scalar field theory shear τ_π calculation". In: *Phys. Rev.* C95.6 (2017), p. 064906. DOI: 10.1103/PhysRevC.95.064906. arXiv: 1701.07580 [nucl-th].

[170] Guy D. Moore. "Stress-stress correlator in ϕ^4 theory: poles or a cut?" In: *JHEP* 05 (2018), p. 084. DOI: 10.1007/JHEP05(2018)084. arXiv: 1803.00736 [hep-ph].

[171] Jorge Casalderrey Solana, Sašo Grozdanov, and Andrei O. Starinets. "Transport peak in thermal spectral function of $\mathcal{N} = 4$ supersymmetric Yang-Mills plasma at intermediate coupling". In: (2018). arXiv: 1806.10997 [hep-th].

[172] W. van Saarloos. "Front propagation into unstable states". In: *Phys.Rep.* 386 (Nov. 2003), pp. 29–222. DOI: 10.1016/j.physrep.2003.08.001. eprint: cond-mat/0308540.

[173] Julian S. Schwinger. "Brownian motion of a quantum oscillator". In: *J. Math. Phys.* 2 (1961), pp. 407–432. DOI: 10.1063/1.1703727.

[174] Pradip M. Bakshi and Kalyana T. Mahanthappa. "Expectation value formalism in quantum field theory. 1." In: *J. Math. Phys.* 4 (1963), pp. 1–11. DOI: 10.1063/1.1703883.

[175] Pradip M. Bakshi and Kalyana T. Mahanthappa. "Expectation value formalism in quantum field theory. 2." In: *J. Math. Phys.* 4 (1963), pp. 12–16. DOI: 10.1063/1.1703879.

[176] L. V. Keldysh. "Diagram technique for nonequilibrium processes". In: *Zh. Eksp. Teor. Fiz.* 47 (1964). [Sov. Phys. JETP20,1018(1965)], pp. 1515–1527.

[177] Matthew P. A. Fisher et al. "Boson localization and the superfluid-insulator transition". In: *Phys. Rev. B* 40 (1 1989), pp. 546–570. DOI: 10.1103/PhysRevB.40.546. URL: https://link.aps.org/doi/10.1103/PhysRevB.40.546.

[178] Sudip Chakravarty, Bertrand I. Halperin, and David R. Nelson. "Two-dimensional quantum Heisenberg antiferromagnet at low temperatures". In: *Phys. Rev. B* 39 (4 1989), pp. 2344–2371. DOI: 10.1103/PhysRevB.39.2344. URL: https://link.aps.org/doi/10.1103/PhysRevB.39.2344.

[179] Andrey V. Chubukov, Subir Sachdev, and Jinwu Ye. "Theory of two-dimensional quantum Heisenberg antiferromagnets with a nearly critical ground state". In: *Phys. Rev. B* 49 (17 1994), pp. 11919–11961. DOI: 10.1103/PhysRevB.49.11919. URL: https://link.aps.org/doi/10.1103/PhysRevB.49.11919.

[180] G. Aarts and J. M. Martinez Resco. "Transport coefficients from the 2PI effective action: Weak coupling and large N analysis". In: *J. Phys. Conf. Ser.* 35 (2006), pp. 414–419. DOI: 10.1088/1742-6596/35/1/039.

[181] Gert Aarts and Jose M. Martinez Resco. "Transport coefficients in large N(f) gauge theories with massive fermions". In: *JHEP* 03 (2005), p. 074. DOI: 10.1088/1126-6708/2005/03/074. arXiv: hep-ph/0503161 [hep-ph].

[182] John M. Cornwall, R. Jackiw, and E. Tomboulis. "Effective action for composite operators". In: *Phys. Rev. D* 10 (8 1974), pp. 2428–2445. DOI: 10.1103/PhysRevD.10.2428. URL: https://link.aps.org/doi/10.1103/PhysRevD.10.2428.

[183] T. Holstein. "Theory of transport phenomena in an electron-phonon gas". In: *Annals of Physics* 29 (Oct. 1964), pp. 410–535. DOI: 10.1016/0003-4916(64)90008-9.

[184] S Sorella and E Tosatti. "Semi-Metal-Insulator Transition of the Hubbard Model in the Honeycomb Lattice". In: *Europhysics Letters (EPL)* 19.8 (1992), pp. 699–704. DOI: 10.1209/0295-5075/19/8/007. URL: https://doi.org/10.1209%2F0295-5075%2F19%2F8%2F007.

[185] Carsten Honerkamp. "Density Waves and Cooper Pairing on the Honeycomb Lattice". In: *Phys. Rev. Lett.* 100 (14 2008), p. 146404. DOI: 10.1103/PhysRevLett.100.146404. URL: https://link.aps.org/doi/10.1103/PhysRevLett.100.146404.

[186] Sandro Sorella, Yuichi Otsuka, and Seiji Yunoki. "Absence of a Spin Liquid Phase in the Hubbard Model on the Honeycomb Lattice". In: *Scientific Reports* 2 (2012), p. 992. URL: https://doi.org/10.1038/srep00992http://10.0.4.14/srep00992https://www.nature.com/articles/srep00992{\#}supplementary-information.

[187] Igor F. Herbut. "Interactions and Phase Transitions on Graphene's Honeycomb Lattice". In: *Phys. Rev. Lett.* 97 (14 2006), p. 146401. DOI: 10.1103/PhysRevLett.97.146401. URL: https://link.aps.org/doi/10.1103/PhysRevLett.97.146401.

[188] Tarun Grover, D. N. Sheng, and Ashvin Vishwanath. "Emergent Space-Time Supersymmetry at the Boundary of a Topological Phase". In: *Science* 344.6181 (2014), pp. 280–283. DOI: 10.1126/science.1248253. arXiv: 1301.7449 [cond-mat.str-el].

[189] Sung-Sik Lee. "Emergence of supersymmetry at a critical point of a lattice model". In: *Phys. Rev. B* 76 (7 2007), p. 075103. DOI: 10.1103/PhysRevB.76.075103. URL: https://link.aps.org/doi/10.1103/PhysRevB.76.075103.

[190] Igor F. Herbut, and Bitan Roy. "Theory of interacting electrons on the honeycomb lattice". In: *Phys. Rev. B* 79 (8 2009), p. 085116. DOI: 10.1103/PhysRevB.79.085116. URL: https://link.aps.org/doi/10.1103/PhysRevB.79.085116.

[191] Rahul Nandkishore et al. "Superconductivity of disordered Dirac fermions". In: *Phys. Rev. B* 87 (17 2013), p. 174511. DOI: 10.1103/PhysRevB.87.174511. URL: https://link.aps.org/doi/10.1103/PhysRevB.87.174511.

[192] Pedro Ponte and Sung-Sik Lee. "Emergence of supersymmetry on the surface of three dimensional topological insulators". In: *New J. Phys.* 16.1 (2014), p. 013044. DOI: 10.1088/1367-2630/16/1/013044. arXiv: 1206.2340 [cond-mat.str-el].

[193] Zhichao Zhou et al. "Mott insulating states and quantum phase transitions of correlated SU($2N$) Dirac fermions". In: *Phys. Rev. B* 93 (24 2016), p. 245157. DOI: 10.1103/PhysRevB.93.245157. URL: https://link.aps.org/doi/10.1103/PhysRevB.93.245157.

[194] Laura Classen, Igor F. Herbut, and Michael M. Scherer. "Fluctuation-induced continuous transition and quantum criticality in Dirac semimetals". In: *Phys. Rev. B* 96 (11 2017), p. 115132. DOI: 10.1103/PhysRevB.96.115132. URL: https://link.aps.org/doi/10.1103/PhysRevB.96.115132.

[195] Zi-Xiang Li et al. "Fermion-induced quantum critical points". In: *Nature Communications* 8.1 (2017), p. 314. ISSN: 2041-1723. DOI: 10.1038/s41467-017-00167-6. URL: https://doi.org/10.1038/s41467-017-00167-6.

[196] David J. Gross and André Neveu. "Dynamical symmetry breaking in asymptotically free field theories". In: *Phys. Rev. D* 10 (10 1974), pp. 3235–3253. DOI: 10.1103/PhysRevD.10.3235. URL: https://link.aps.org/doi/10.1103/PhysRevD.10.3235.

[197] J. Zinn-Justin. "Four-fermion interaction near four dimensions". In: *Nuclear Physics B* 367.1 (1991), pp. 105 –122. ISSN: 0550-3213. DOI: https://doi.org/10.1016/0550-3213(91)90043-W. URL: http://www.sciencedirect.com/science/article/pii/055032139190043W.

[198] K S Novoselov et al. "Two-dimensional gas of massless Dirac fermions in graphene". In: *Nature* 438.7065 (2005), pp. 197–200. ISSN: 1476-4687. DOI: 10.1038/nature04233. URL: https://doi.org/10.1038/nature04233.

[199] A. H. Castro Neto et al. "The electronic properties of graphene". In: *Rev. Mod. Phys.* 81 (1 2009), pp. 109–162. DOI: 10.1103/RevModPhys.81.109. URL: https://link.aps.org/doi/10.1103/RevModPhys.81.109.

[200] Daniel Greif et al. "Short-Range Quantum Magnetism of Ultracold Fermions in an Optical Lattice". In: *Science* 340.6138 (2013), pp. 1307–1310. ISSN: 0036-8075. DOI: 10.1126/science.1236362. eprint: http://science.sciencemag.org/content/340/6138/1307.full.pdf. URL: http://science.sciencemag.org/content/340/6138/1307.

[201] Daniel Greif et al. "Formation and Dynamics of Antiferromagnetic Correlations in Tunable Optical Lattices". In: *Phys. Rev. Lett.* 115 (26 2015), p. 260401. DOI: 10.1103/PhysRevLett.115.260401. URL: https://link.aps.org/doi/10.1103/PhysRevLett.115.260401.

[202] Anton Mazurenko et al. "A cold-atom Fermi-Hubbard antiferromagnet". In: *Nature* 545 (2017), p. 462. URL: https://doi.org/10.1038/nature22362http://10.0.4.14/nature22362.

[203] Moshe Moshe and Jean Zinn-Justin. "Quantum field theory in the large N limit: A Review". In: *Phys. Rept.* 385 (2003), pp. 69–228. DOI: 10.1016/S0370-1573(03)00263-1. arXiv: hep-th/0306133 [hep-th].

[204] B. Rosenstein, Hoi-Lai Yu, and A. Kovner. "Critical exponents of new universality classes". In: *Physics Letters B* 314.3 (1993), pp. 381 –386. ISSN: 0370-2693. DOI: https://doi.org/10.1016/0370-2693(93)91253-J. URL: http://www.sciencedirect.com/science/article/pii/037026939391253J.

[205] Mark Pollicott. "On the rate of mixing of Axiom A flows". In: *Invent. Math.* 81.3 (1985), pp. 413–426.

[206] David Ruelle. "Resonances of chaotic dynamical systems". In: *Phys. Rev. Lett.* 56.5 (1986), p. 405.

[207] Patrick Hayden and John Preskill. "Black holes as mirrors: Quantum information in random subsystems". In: *JHEP* 09 (2007), p. 120. DOI: 10.1088/1126-6708/2007/09/120. arXiv: 0708.4025 [hep-th].

[208] Yasuhiro Sekino and Leonard Susskind. "Fast Scramblers". In: *JHEP* 10 (2008), p. 065. DOI: 10.1088/1126-6708/2008/10/065. arXiv: 0808.2096 [hep-th].

[209] Yi Ling, Peng Liu, and Jian-Pin Wu. "Holographic Butterfly Effect at Quantum Critical Points". In: (2016). arXiv: 1610.02669 [hep-th].

[210] Kedar S. Kolekar, Debangshu Mukherjee, and K. Narayan. "Notes on hyperscaling violating Lifshitz and shear diffusion". In: (2016). arXiv: 1612.05950 [hep-th].

[211] Andrew Lucas and Julia Steinberg. "Charge diffusion and the butterfly effect in striped holographic matter". In: *JHEP* 10 (2016), p. 143. DOI: 10.1007/JHEP10(2016)143. arXiv: 1608.03286 [hep-th].

[212] Richard A. Davison et al. "Thermoelectric transport in disordered metals without quasiparticles: The Sachdev-Ye-Kitaev models and holography". In: *Phys. Rev.* B95.15 (2017), p. 155131. DOI: 10.1103/PhysRevB.95.155131. arXiv: 1612.00849 [cond-mat.str-el].

[213] Pavel Kovtun. "Lectures on hydrodynamic fluctuations in relativistic theories". In: *J. Phys.* A45 (2012), p. 473001. DOI: 10.1088/1751-8113/45/47/473001. arXiv: 1205.5040 [hep-th].

[214] Dam T. Son and Andrei O. Starinets. "Minkowski space correlators in AdS / CFT correspondence: Recipe and applications". In: *JHEP* 09 (2002), p. 042. DOI: 10.1088/1126-6708/2002/09/042. arXiv: hep-th/0205051 [hep-th].

[215] C. P. Herzog and D. T. Son. "Schwinger-Keldysh propagators from AdS/CFT correspondence". In: *JHEP* 03 (2003), p. 046. DOI: 10.1088/1126-6708/2003/03/046. arXiv: hep-th/0212072 [hep-th].

[216] Steven S. Gubser, Igor R. Klebanov, and Arkady A. Tseytlin. "Coupling constant dependence in the thermodynamics of N=4 supersymmetric Yang-Mills theory". In: *Nucl. Phys.* B534 (1998), pp. 202–222. DOI: 10.1016/S0550-3213(98)00514-8. arXiv: hep-th/9805156 [hep-th].

[217] Yevgeny Kats and Pavel Petrov. "Effect of curvature squared corrections in AdS on the viscosity of the dual gauge theory". In: *JHEP* 01 (2009), p. 044. DOI: 10.1088/1126-6708/2009/01/044. arXiv: 0712.0743 [hep-th].

[218] Mauro Brigante et al. "Viscosity Bound Violation in Higher Derivative Gravity". In: *Phys. Rev.* D77 (2008), p. 126006. DOI: 10.1103/PhysRevD.77.126006. arXiv: 0712.0805 [hep-th].

[219] Sašo Grozdanov and Andrei O. Starinets. "On the universal identity in second order hydrodynamics". In: *JHEP* 03 (2015), p. 007. DOI: 10.1007/JHEP03(2015)007. arXiv: 1412.5685 [hep-th].

[220] Stefan A. Stricker. "Holographic thermalization in N=4 Super Yang-Mills theory at finite coupling". In: *Eur. Phys. J.* C74.2 (2014), p. 2727. DOI: 10.1140/epjc/s10052-014-2727-4. arXiv: 1307.2736 [hep-th].

[221] Sebastian Waeber et al. "Finite coupling corrections to holographic predictions for hot QCD". In: *JHEP* 11 (2015), p. 087. DOI: 10.1007/JHEP11(2015)087. arXiv: 1509.02983 [hep-th].

[222] Sašo Grozdanov and Wilke van der Schee. "Coupling constant corrections in holographic heavy ion collisions". In: (2016). arXiv: 1610.08976 [hep-th].

[223] Sašo Grozdanov and Andrei O. Starinets. "Second-order transport, quasinormal modes and zero-viscosity limit in the Gauss-Bonnet holographic fluid". In: *JHEP* 03 (2017), p. 166. DOI: 10.1007/JHEP03(2017)166. arXiv: 1611.07053 [hep-th].

[224] Konstadinos Sfetsos. "On gravitational shock waves in curved space-times". In: *Nucl. Phys.* B436 (1995), pp. 721–745. DOI: 10.1016/0550-3213(94)00573-W. arXiv: hep-th/9408169 [hep-th].

[225] Giuseppe Policastro, Dam T. Son, and Andrei O. Starinets. "From AdS / CFT correspondence to hydrodynamics. 2. Sound waves". In: *JHEP* 12 (2002), p. 054. DOI: 10.1088/1126-6708/2002/12/054. arXiv: hep-th/0210220 [hep-th].

[226] Sašo Grozdanov and Nikolaos Kaplis. "Constructing higher-order hydrodynamics: The third order". In: *Phys. Rev.* D93.6 (2016), p. 066012. DOI: 10.1103/PhysRevD.93.066012. arXiv: 1507.02461 [hep-th].

[227] Paul M. Chesler and Laurence G. Yaffe. "Holography and colliding gravitational shock waves in asymptotically AdS_5 spacetime". In: *Phys. Rev. Lett.* 106 (2011), p. 021601. DOI: 10.1103/PhysRevLett.106.021601. arXiv: 1011.3562 [hep-th].

[228] Yingfei Gu, Andrew Lucas, and Xiao-Liang Qi. "Energy diffusion and the butterfly effect in inhomogeneous Sachdev-Ye-Kitaev chains". In: *SciPost Phys.* 2.3 (2017), p. 018. DOI: 10.21468/SciPostPhys.2.3.018. arXiv: 1702.08462 [hep-th].

[229] Thomas Hartman, Sean A. Hartnoll, and Raghu Mahajan. "An upper bound on transport". In: *Phys. Rev. Lett.* 119.14 (2017), p. 141601. DOI: 10.1103/PhysRevLett.119.141601. arXiv: 1706.00019 [hep-th].

[230] Wilke van der Schee. "Equilibration and hydrodynamics at strong and weak coupling". In: *26th International Conference on Ultrarelativistic Nucleus-Nucleus Collisions (Quark Matter 2017) Chicago,Illinois, USA, February 6-11, 2017*. 2017. arXiv: 1705.01556 [nucl-th]. URL: https://inspirehep.net/record/1598155/files/arXiv:1705.01556.pdf.

[231] Brandon S. DiNunno et al. "Holographic constraints on Bjorken hydrodynamics at finite coupling". In: (2017). arXiv: 1707.08812 [hep-th].

[232] Sean A. Hartnoll. "Theory of universal incoherent metallic transport". In: *Nature Phys.* 11 (2015), p. 54. DOI: 10.1038/nphys3174. arXiv: 1405.3651 [cond-mat.str-el].

[233] Tomaž Prosen. "Lower bounds on high-temperature diffusion constants from quadratically extensive almost-conserved operators". In: *Phys. Rev. E* 89 (1 2014), p. 012142. DOI: 10.1103/PhysRevE.89.012142. URL: https://link.aps.org/doi/10.1103/PhysRevE.89.012142.

[234] Sašo Grozdanov et al. "Absence of disorder-driven metal-insulator transitions in simple holographic models". In: *Phys. Rev. Lett.* 115.22 (2015), p. 221601. DOI: 10.1103/PhysRevLett.115.221601. arXiv: 1507.00003 [hep-th].

[235] Sašo Grozdanov, Andrew Lucas, and Koenraad Schalm. "Incoherent thermal transport from dirty black holes". In: *Phys. Rev.* D93.6 (2016), p. 061901. DOI: 10.1103/PhysRevD.93.061901. arXiv: 1511.05970 [hep-th].

[236] P. Kovtun, Dan T. Son, and Andrei O. Starinets. "Viscosity in strongly interacting quantum field theories from black hole physics". In: *Phys. Rev. Lett.* 94 (2005), p. 111601. DOI: 10.1103/PhysRevLett.94.111601. arXiv: hep-th/0405231 [hep-th].

[237] Stephen H. Shenker and Douglas Stanford. "Black holes and the butterfly effect". In: *J. High Energy Phys.* 2014.3 (2014), pp. 0–30. ISSN: 10298479. DOI: 10.1007/JHEP03(2014)067. arXiv: 1306.0622.

[238] Stephen H. Shenker and Douglas Stanford. "Multiple shocks". In: *J. High Energy Phys.* 2014.12 (2014). ISSN: 10298479. DOI: 10.1007/JHEP12(2014)046. arXiv: 1312.3296.

[239] Debanjan Chowdhury and Brian Swingle. "Onset of many-body chaos in the $O(N)$ model". In: *Phys. Rev. D* 96 (2017), p. 065005. DOI: 10.1103/PhysRevD.96.065005. arXiv: 1703.02545. URL: http://arxiv.org/abs/1703.02545http://dx.doi.org/10.1103/PhysRevD.96.065005.

[240] Yunxiang Liao and Victor Galitski. "Nonlinear sigma model approach to many-body quantum chaos: Regularized and unregularized out-of-time-ordered correlators". In: *Phys. Rev.* B98.20 (2018), p. 205124. DOI: 10.1103/PhysRevB.98.205124. arXiv: 1807.09799 [cond-mat.dis-nn].

[241] H. Matsumoto et al. "Thermo Field Dynamics in Interaction Representation". In: *Prog. Theor. Phys.* 70.2 (1983), pp. 599–602. ISSN: 0033-068X. DOI: 10.1143/PTP.70.599. URL: https://academic.oup.com/ptp/article-lookup/doi/10.1143/PTP.70.599.

[242] H. Matsumoto, Y. Nakano, and H. Umezawa. "An equivalence class of quantum field theories at finite temperature". In: *J. Math. Phys.* 25.10 (1984), pp. 3076–3085. ISSN: 00222488. DOI: 10.1063/1.526023.

[243] Douglas Stanford. "Many-body chaos at weak coupling". In: *J. High Energy Phys.* 10 (2016), p. 009. ISSN: 10298479. DOI: 10.1007/JHEP10(2016)009. arXiv: 1512.07687.

[244] Avijit Das et al. "Light-Cone Spreading of Perturbations and the Butterfly Effect in a Classical Spin Chain". In: *Phys. Rev. Lett.* 121.2 (2018), p. 024101. ISSN: 0031-9007. DOI: 10.1103/PhysRevLett.121.024101. arXiv: 1711.07505. URL: https://link.aps.org/doi/10.1103/PhysRevLett.121.024101.

[245] Martin Gärttner et al. "Measuring out-of-time-order correlations and multiple quantum spectra in a trapped-ion quantum magnet". In: *Nat. Phys.* 13.8 (2017), pp. 781–786. ISSN: 1745-2473. DOI: 10.1038/nphys4119. URL: http://www.nature.com/doifinder/10.1038/nphys4119.

[246] R. van Zon, H. van Beijeren, and J. R. Dorfman. "Kinetic Theory Estimates for the Kolmogorov-Sinai Entropy, and the Largest Lyapunov Exponents for Dilute, Hard Ball Gases and for Dilute, Random Lorentz Gases". In: 2000, pp. 231–278. DOI: 10.1007/978-

3-662-04062-1_10. arXiv: 9909034 [chao-dyn]. URL: http://link.springer.com/10.1007/978-3-662-04062-1_10http://arxiv.org/abs/chao-dyn/9909034.

[247] Alexei Kitaev and S. Josephine Suh. "The soft mode in the Sachdev-Ye-Kitaev model and its gravity dual". In: (2017). arXiv: 1711.08467. URL: http://arxiv.org/abs/1711.08467.

[248] Mike Blake, Hyunseok Lee, and Hong Liu. "A quantum hydrodynamical description for scrambling and many-body chaos". In: (2017), pp. 1–53. arXiv: 1801.00010. URL: http://arxiv.org/abs/1801.00010.

[249] Yingfei Gu and Alexei Kitaev. "On the relation between the magnitude and exponent of OTOCs". In: (2018), pp. 1–20. arXiv: 1812.00120. URL: http://arxiv.org/abs/1812.00120.

[250] Yochai Werman, Steven A. Kivelson, and Erez Berg. "Quantum chaos in an electron-phonon bad metal". In: (2017). arXiv: 1705.07895 [cond-mat.str-el].

[251] Markus J. Klug, Mathias S. Scheurer, and Jörg Schmalian. "Hierarchy of information scrambling, thermalization, and hydrodynamic flow in graphene". In: *Phys. Rev.* B98.4 (2018), p. 045102. DOI: 10.1103/PhysRevB.98.045102. arXiv: 1712.08813 [cond-mat.str-el].

[252] Antonio M. García-García et al. "Chaotic-Integrable Transition in the Sachdev-Ye-Kitaev Model". In: *Phys. Rev. Lett.* 120.24 (2018), p. 241603. ISSN: 0031-9007. DOI: 10.1103/PhysRevLett.120.241603. arXiv: 1707.02197. URL: http://arxiv.org/abs/1707.02197http://dx.doi.org/10.1103/PhysRevLett.120.241603https://link.aps.org/doi/10.1103/PhysRevLett.120.241603.

[253] Horacio M Pastawski, Patricia R Levstein, and Gonzalo Usaj. "Quantum Dynamical Echoes in the Spin Diffusion in Mesoscopic Systems". In: *Phys. Rev. Lett.* 75.23 (1995), pp. 4310–4313. ISSN: 0031-9007. DOI: 10.1103/PhysRevLett.75.4310. URL: https://link.aps.org/doi/10.1103/PhysRevLett.75.4310.

[254] Rodolfo A. Jalabert and Horacio M. Pastawski. "Environment-independent decoherence rate in classically chaotic systems". In: *Phys. Rev. Lett.* 86.12 (2001), pp. 2490–2493. ISSN: 00319007. DOI: 10.1103/PhysRevLett.86.2490. arXiv: 0010094 [cond-mat].

[255] Tomaž Prosen. "General relation between quantum ergodicity and fidelity of quantum dynamics". In: *Phys. Rev. E* 65.3 (2002), p. 036208. ISSN: 1063-651X. DOI: 10.1103/PhysRevE.65.036208. arXiv: 0106149v2 [quant-ph]. URL: https://link.aps.org/doi/10.1103/PhysRevE.65.036208.

[256] Tomaž Prosen and Marko Znidaric. "Stability of quantum motion and correlation decay". In: *J. Phys. A. Math. Gen.* 35.6 (2002), pp. 1455–1481. ISSN: 0305-4470. DOI: 10.1088/0305-4470/35/6/309. arXiv: 0111014v2 [arXiv:nlin]. URL: http://stacks.iop.org/0305-4470/35/i=6/a=309?key=crossref.2ad33b3981f849499d451d6404c402fc.

[257] F. Haug et al. "Motional stability of the quantum kicked rotor: A fidelity approach". In: *Phys. Rev. A - At. Mol. Opt. Phys.* 71.4 (2005), pp. 1–11. ISSN: 10502947. DOI: 10.1103/PhysRevA.71.043803.

[258] Guanyu Zhu, Mohammad Hafezi, and Tarun Grover. "Measurement of many-body chaos using a quantum clock". In: *Phys. Rev. A* 94.6 (2016), p. 062329. ISSN: 2469-9926. DOI: 10.1103/PhysRevA.94.062329. arXiv: 1607.00079. URL: https://link.aps.org/doi/10.1103/PhysRevA.94.062329.

[259] Norman Y. Yao et al. "Interferometric Approach to Probing Fast Scrambling". In: (2016), pp. 1–6. arXiv: 1607.01801. URL: http://arxiv.org/abs/1607.01801.

[260] Brian Swingle et al. "Measuring the scrambling of quantum information". In: *Phys. Rev. A* 94.4 (2016), p. 040302. ISSN: 2469-9926. DOI: 10.1103/PhysRevA.94.040302. arXiv: 1602.06271. URL: http://arxiv.org/abs/1602.06271%0Ahttp://dx.doi.org/10.1103/PhysRevA.94.040302https://link.aps.org/doi/10.1103/PhysRevA.94.040302.

[261] Jorge Kurchan. "Quantum Bound to Chaos and the Semiclassical Limit". In: *Journal of Statistical Physics* 171.6 (2018), pp. 965–979. ISSN: 1572-9613. DOI: 10.1007/s10955-018-2052-7. URL: https://doi.org/10.1007/s10955-018-2052-7.

[262] Tomaž Prosen, Thomas H. Seligman, and Marko Znidaric. "Theory of Quantum Loschmidt Echoes". In: *Prog. Theor. Phys. Suppl.* 150 (2003), pp. 200–228. ISSN: 0375-9687. DOI: 10.1143/PTPS.150.200. arXiv: 0304104 [quant-ph]. URL: http://arxiv.org/abs/quant-ph/0304104%0Ahttp://dx.doi.org/10.1143/

PTPS.150.200https://academic.oup.com/ptps/article-lookup/doi/10.1143/PTPS.150.200.

[263] Charles H Bennett et al. "Teleporting an unknown quantum state via dual classical and Einstein-Podolsky-Rosen channels". In: *Phys. Rev. Lett.* 70.13 (1993), pp. 1895–1899. ISSN: 0031-9007. DOI: 10.1103/PhysRevLett.70.1895. URL: https://link.aps.org/doi/10.1103/PhysRevLett.70.1895.

[264] Charles H. Bennett et al. "Mixed-state entanglement and quantum error correction". In: *Phys. Rev. A* 54.5 (1996), pp. 3824–3851. ISSN: 1050-2947. DOI: 10.1103/PhysRevA.54.3824. URL: https://link.aps.org/doi/10.1103/PhysRevA.54.3824.

[265] A. Uhlmann. "The "transition probability" in the state space of a $*$-algebra". In: *Reports Math. Phys.* 9.2 (1976), pp. 273–279. ISSN: 00344877. DOI: 10.1016/0034-4877(76)90060-4. URL: http://linkinghub.elsevier.com/retrieve/pii/0034487776900604.

[266] Richard Jozsa. "Fidelity for Mixed Quantum States". In: *J. Mod. Opt.* 41.12 (1994), p. 2315. ISSN: 0950-0340. DOI: 10.1080/09500349414552171. URL: http://www.tandfonline.com/doi/abs/10.1080/09500349414552171.

[267] E. P. Wigner and M. M. Yanase. "Information contents of distributions". In: *Proc. Natl. Acad. Sci.* 49.6 (1963), pp. 910–918. ISSN: 0027-8424. DOI: 10.1073/pnas.49.6.910. URL: http://www.pnas.org/cgi/doi/10.1073/pnas.49.6.910.

[268] Felix M. Haehl and Moshe Rozali. "Effective Field Theory for Chaotic CFTs". In: *JHEP* 10 (2018), p. 118. DOI: 10.1007/JHEP10(2018)118. arXiv: 1808.02898 [hep-th].

[269] Jordan S. Cotler et al. "Black Holes and Random Matrices". In: (2016), pp. 1–71. arXiv: 1611.04650. URL: http://arxiv.org/abs/1611.04650.

[270] Antonio M. García-García and Jacobus J. M. Verbaarschot. "Spectral and thermodynamic properties of the Sachdev-Ye-Kitaev model". In: *Phys. Rev.* D94.12 (2016), p. 126010. DOI: 10.1103/PhysRevD.94.126010. arXiv: 1610.03816 [hep-th].

[271] Antonio M. García-García and Jacobus J. M. Verbaarschot. "Analytical Spectral Density of the Sachdev-Ye-Kitaev Model at finite N". In: *Phys. Rev.* D96.6 (2017), p. 066012. DOI: 10.1103/PhysRevD.96.066012. arXiv: 1701.06593 [hep-th].

[272] Bruno Bertini, Pavel Kos, and Tomaž Prosen. "Exact Spectral Form Factor in a Minimal Model of Many-Body Quantum Chaos". In: 2 (2018). DOI: arXiv:1805.00931v1. arXiv: 1805.00931. URL: http://arxiv.org/abs/1805.00931.

Samenvatting

Een van de spannende dingen van onderzoek is dat het nooit zeker is waar en wanneer de volgende belangrijke ontdekkingen plaats zullen vinden. We kunnen ons alleen laten leiden door onze nieuwsgierigheid en ons instinct. Dit proefschrift vat enkele antwoorden op de vele vragen die wij ons de afgelopen vier jaar hebben gesteld, samen. Sommige vragen kwamen tot stand met het oog op de technologische vooruitgang van (hopelijk) de aankomende jaren. Het begrip van hoge-temperatuur supergeleiders en van de mysteries van sterk-gekoppelde systemen, alsmede van de rol van kwantuminformatie, zou ons leven ingrijpend kunnen veranderen. Verder is de motivatie puur theoretisch.

Van een chaotisch systeem is bekend dat een een kleine verandering in de beginwaarden dramatische gevolgen kan hebben voor de evolutie van dat systeem (het *vlindereffect*). Deze gevoeligheid voor de beginwaarden is een eigenschap van het systeem op korte tijdsschalen en kleine afstanden. Om de chaos waar te nemen, moeten we daarom inzoomen. Daartegenover staat dat, als we eigenschappen op grote (tijd)schalen willen bestuderen (en dus uitzoomen), het systeem hydrodynamisch kunnen beschrijven. Dat twee eigenschappen die zich op verschillende tijdschalen afspelen aan elkaar gerelateerd zouden kunnen zijn, is een aantrekkelijk idee, wat een nieuwe vorm van symmetrie op zou kunnen leveren. Dit is een van de achterliggende motivaties van dit proefschrift: is het mogelijk dat chaos, die zich zeer vroeg in de ontwikkeling van een systeem manifesteert, invloed heeft op het hydrodynamisch transport in het systeem? Zelfs op klassiek niveau is dit een interessante vraag. Anderzijds is het begrijpen van chaos in veel-deeltjes kwantumsystemen nog intrigerender. Desalniettemin is er de afgelopen jaren op beide thema's vooruitgang geboekt, veelal door gebruik te maken van de AdS/CFT dualiteit.

In dit proefschrift hebben wij deze vragen vanuit twee tegenovergestelde richtingen bestudeerd, zowel vanuit zwakgekoppelde veldentheorieën, waarbij een combinatie van veldtheoretische technieken gebruikt is, als vanuit de AdS/CFT dualiteit. Daarnaast hebben wij een fermionisch en bosonisch kwantum kritisch punt bestudeerd, dit zijn "exotische" aggregatietoestanden waarin kwantuminformatie een belangrijke rol speelt.

De belangrijkste resultaten van dit proefschrift bestaan uit de formuler-

ing van een Boltzmann-achtige vergelijking voor veel-deeltijes chaos, de ontdekking van een nieuwe eigenschap van thermische correlatiefuncties (*pole-skipping*) en de analyse van wat de juiste en zinvolle observabele is om experimenteel kwantumchaos te bestuderen. De techniek die hiervoor gebruikt is, is een specifieke correlatiefunctie, welke uitgebreid bestudeerd is in dit proefschrift, de ongelijke-tijd correlatiefunctie (out-of-time ordered correlator, OTOC).

In hoofdstuk twee schrijven we de kinetische vergelijking voor veel-deeltijes chaos neer. Deze vergelijking, met een structuur à la Boltzmann, brengt een precies, microscopisch begrip met zich mee van wat kwantumchaos in verdunde systemen is, namelijk een bruto uitwisseling van energie. Kwalitatief kan men zich deze kinetische vergelijking zo voorstellen: denk aan een netwerk waar elke knoop in- en uitgaande verbindingen heeft. Het kan een energienetwerk zijn van een land waar de knopen overeenkomen met de plekken waar energie geproduceerd of verbruikt wordt, of een sociaal netwerk waar de knopen de gebruikers zijn en de verbindingen willekeurige, oriënteerbare connecties (tweet/retweet, like/dislike). In dit beeld telt de traditionele Boltzmann transportvergelijking voor transport de tijdsevolutie van de *netto toename* in een knoop (respectievelijk de energie productie ten opzichte van het verbruik, of het aantal tweets min het aantal retweets van één enkel account). De kinetische vergelijking voor kwantumchaos telt daarentegen het totaal van inkomende plus uitgaande bijdragen. Dit is geen constante, en voor kwantumsystemen is het typerend dat dit exponentieel groeit, een signaal van kwantumchaos. Er zijn limieten aan de snelheid van deze exponentiële groei. Onze interpretatie van kwantumchaos in termen van kinetische theorie geeft aan dat, voor sommige soorten netwerken, dit optellen een heel specifiek karakter heeft, namelijk een exponentiële groei. Hierbij is het de vraag waarom, microscopisch gezien, deze grootheid begrensd is en of dit soort resultaten uitgebreid kunnen worden naar generieke netwerken, weg van de kwantumsystemen.

In hoofdstuk drie proberen we de algemeenheid van deze kinetische theorie voor chaos te begrijpen. We onderzoeken wat er gebeurt in systemen waar kwantuminformatie en verstrengeling op lange afstanden een rol beginnen te spelen, wat bijvoorbeeld in de buurt van een kwantumkritisch punt gebeurt. We laten zien dat, voor twee paradigmatische theorieën, het bosonische $O(N)$ vector model en het Gross-Neveu model, in de buurt van het kwantumkritisch punt, chaos nog steeds kan worden beschreven met onze kinetische theorie. In hoofdstuk vier analyseren we sterk-gekoppelde systemen met behulp van de holografische dualiteit. We laten zien dat chaotische eigenschappen van zwarte gaten bestudeerd kunnen worden met een experiment ver uit evenwicht dat overeenkomt met diffusief gedrag in

de buurt van de horizon. Voor systemen die duaal zijn aan zwarte gaten, laat chaos een afdruk achter in de correlatiefuncties laat in de tijd, die het hydrodynamisch transport bepalen. Dit fenomeen is uitermate verrassend en heeft de naam *pole-skipping* gekregen.

In het laatste hoofdstuk stellen we een belangrijke vraag aan de orde met betrekking tot de OTOC. De afgelopen jaren is er veel belangstelling geweest om protocollen te bedenken voor experimenten om de OTOC te meten. De discussie is gebaseerd op de stelling, die vaak in de literatuur wordt aangehaald, dat de OTOC niet gevoelig is voor de manier waarop deze geregulariseerd wordt. Wij vechten deze stelling aan en laten zien dat zowel in sterk- als in zwakgekoppelde theorieën, de OTOC sterk afhankelijk is van diens regularisatie. We geven een indicatie van welke regularisatie de "fysische" is en interpreteren dit resultaat zowel in het kader van de kinetische theorie, die in de vorige hoofdstukken afgeleid is, als in het kader van het Loschmidt echo experiment.

Summary

One of the exciting things about research is that we never know in which topic and when the next important discovery will occur. We can only follow our curiosity and our instinct, maybe guided by the power of analogies. This thesis summarizes a few answers to the many questions we have been puzzled and fascinated by in the course of the last four years. Some of these questions arose by having in mind the technological development of the (hopefully) near future. The understanding of high-temperature superconductors and the mysterious behaviour of strongly coupled physics, together with the role of quantum information, might potentially have a big impact on our lives. Another motivation is purely theoretical.

We know that, if a system is chaotic, a small change of the initial condition can dramatically affect its time evolution (the *butterfly effect*). This sensitivity to the initial condition is a property of the early time and small scale of the system, *i.e.*, we need to zoom in to see it. On the other side, if we want to study the large scale properties and the collective behaviour at late times, *i.e.*, zooming out, we can likely apply a hydrodynamic description. The idea that two phenomena belonging to different time scales could be related is very charming, and can reveal the existence of a new symmetry. This is one of the theoretical motivations of this thesis: is it possible that chaos, which happens at a very early time, can affect hydrodynamic transport in a system? Even at the classical level, this question appears enigmatic. On the other side, for quantum systems, understanding many-body chaos is even more intriguing. Nevertheless, over the past few years some progress has been made on both topics, often by means of the AdS/CFT duality.

In this thesis we investigated these questions from two opposite directions, both from weakly coupled field theories, using a combination of field theory techniques, and from strongly-coupled field theories, using the AdS/CFT correspondence. Moreover, we studied a fermionic and bosonic quantum critical point, which are 'exotic' states of matter where quantum information plays an important role.

The main results of this thesis consist of the formulation of a Boltzmann-like equation for many-body chaos, the discovery of a new property of thermal correlation functions (*pole-skipping*), and the analysis of which is

the correct and meaningful observable to measure experimentally in order to probe quantum chaos. The tool for this investigation is a particular correlation function, extensively analysed in this thesis, the out-of-time ordered correlation function (OTOC).

In chapter two, we write the kinetic equation for many-body chaos. This equation, with a Boltzmamnn-like structure, gives a precise microscopic understanding of what quantum chaos represents in diluted systems, namely a gross energy exchange. A qualitative picture of this kinetic equation is the following: imagine a network where each node has ingoing and outgoing connections. It can be the power network of a country where the nodes correspond to the sites where electricity is generated/used or a social network where the nodes are the users and the links are any orientable connections (tweet/retweet, like/dislike). In this framework, the traditional Boltzmann equation for transport counts the time evolution of the net *gain* of the node (respectively how much electricity is generated with respect to the amount used, or the number of tweets minus the number of retweets of a single account). The kinetic equation for quantum chaos, on the other side, counts the sum of the ingoing and outgoing contributions. This quantity is not constant in time, and for quantum systems typically growths exponentially, a signature of quantum chaos. The rate of exponential growth can be shown to be bounded [16]. Our kinetic theory interpretation of quantum chaos indicates that, for some classes of networks, this counting has a specific behaviour, exponential in time. This raises several questions of why, microscopically, this quantity is bounded and whether similar results can be extended to general networks, beyond quantum systems.

In chapter three we try to understand the generality of this kinetic theory for chaos. We check what happens for systems where quantum information and long range entanglement begin to play a role, as for example in the proximity of a quantum critical point. We show that, for two paradigmatic theories, the bosonic $O(N)$ vector model and the Gross-Neveu model, close to the quantum critical point (QCP), chaos is still described by our kinetic theory.

In chapter four we analyse strongly coupled systems by means of the holographic duality. We show that the chaotic properties of black holes can be probed with a highly out-of-equilibrium experiment that corresponds to diffusive behaviour near the horizon. For systems dual to black holes, chaos leaves imprints in the late-time correlation functions that determine hydrodynamic transport. This phenomenon is highly surprising and has been named *pole-skipping* [56].

In the last chapter we address an important question regarding the

out-of-time correlation (OTOC) function. Over the last years there has been much interest in experimental protocols to measure the OTOC. The discussion has relied on the statement, often found in literature, that the OTOC is insensitive to the way it is regularized. We challenge this statement and show that both in weak and strongly coupled theories the OTOC strongly depends on the regularization. We indicate which regularization corresponds to the physical one and we interpret this result both in terms of the kinetic theory derived in the previous chapters and the Loschmidt echo experiment.

Curriculum Vitæ

I was born in Messina, Italy, on April 10, 1991. I grew up in Varapodio, a small village in Calabria, in the South of Italy, where I received my primary education. I attended high-school at the "Liceo Scientifico Nicola Pizi", with a scientific oriented program. In 2009 I moved to Rome to begin my studies at the Physics Department of "La Sapienza University of Rome". There, I was admitted to the honours program and I completed my BSc degree cum laude in 2012 with a thesis on "Peter-Weyl theorem and $SL(2,\mathbb{C})$ representations", supervised by Marco Bochicchio. Subsequently, I started the MSc program in theoretical physics at the same university, which, in 2014, I completed cum laude with a thesis on "Spin connection as Lorentz gauge field in Fairchild's action" (supervisor Giovanni Montani). During the MSc, I was part of the honours program and I undertook research projects in string theory under the supervision of Massimo Bianchi (Tor Vergata University). I have worked on these projects for the six subsequent months.

In September 2015, I started my PhD at Leiden University in the group of Koenraad Schalm on a project funded by the Netherlands Organisation for Scientific Research (NWO). I began studying the hydrodynamical transport properties of electrons in deformed graphene in collaboration with Adrew Lucas (Harvard University) and my supervisor. Intrigued by quantum chaos and the idea that it could affect hydrodynamic transport, I started to collaborate on this topic with Saso Grozdanov and Koenraad Schalm. Some of the results obtained during these years are presented in this thesis.

During my PhD I presented my research in seminars at the universities of Stanford, Harvard, Massachussets Institute of Technology (USA), at the conferences "Integrable and chaotic quantum dynamics" in Bled (SLO), "Physics at Veldhoven 2019" in Veldhoven (NL) and at a number of schools attended over these four years in France and The Netherlands. In the academic years 2015-2018, I served as a teaching assistant to the master courses "Effective Field theory" and "Quantum Field Theory".

I look forward to discover the new challenges and adventures that the (classical) butterfly effect will create in the coming years outside academia. I hope that, somehow, they will have something to do with hydrodynamics.

List of publications

- S. Grozdanov, K. Schalm and V. Scopelliti. *Many-body chaos and transport in large N (or weakly coupled) QFTs and close to the Quantum Critical Point.* In preparation . [Chapter 3]
- A. Romero-Bermúdez, K. Schalm and V. Scopelliti. *Regularization dependence of the OTOC. Which Lyapunov spectrum is the physical one?* JHEP **2019**, 107 (2019). [Chapter 5]
- S. Grozdanov, K. Schalm and V. Scopelliti. *Kinetic theory for classical and quantum many-body chaos.* Phys. Rev. E **99**, 012206, (2019). [Chapter 2]
- S. Grozdanov, K. Schalm and V. Scopelliti. *Black hole scrambling from hydrodynamics.* Phys. Rev. Lett. **120**, 231601 (2018). [Chapter 4]

Other publications by the author are:

- Y. Cheipesh, A. I. Pavlov, J. Tworzydlo, D. V. Efremov, V. Scopelliti, and N. V. Gnezdilov. *Planckian superconductor.* In preparation.
- V. Scopelliti, K. E. Schalm, A. Lucas. *Hydrodynamic charge and heat transport on inhomogeneous curved spaces.* Phys. Rev. B **96**, no.7, 075150, (2017).
- F. Cianfrani, G. Montani, V. Scopelliti. *Spin connections as Lorentz gauge field in Fairchild's action.* Mod. Phys. Lett. A **31**, 1650124, (2016).

Acknowledgements

The last four years have been a very enriching journey, both personally and professionally. And, as in all journeys, numerous people had an important role, from the ones I have spent time to have a drink or spend one day with, to the people I have had constantly around me. In the following, it is my pleasure to acknowledge some of the people who, academically, contributed to this thesis.

Firstly, I would like to thank Koenraad for his guidance, for the many hours spent discussing physics in his office and for stimulating me to follow ambitious intuitions. I will always remember the excitement I felt when ideas worked out, as well as the wonder of discovering totally unexpected results.

I would also like to thank Jan for the many thought-provoking conversations and for motivating the whole group to always keep the big picture of our research in mind.

Most of the work in this thesis was done in collaboration with Sašo: I feel lucky to have had the opportunity to work with him. I have learnt that "I don't understand what this means" can be the start of a full PhD program. I am very thankful for that.

I am grateful to Andy, for all the chats about physics, to Aurelio for his insights whenever I had a question, and to Nikolay, with whom I share the curiosity to find a way to experimentally check some of the ideas presented in this thesis.

I would like to thank all the people that have joined the group during these four years for creating a nice and stimulating atmosphere: Alex, Andrey, Bartek, Balazs, Christian, Emad, Floris, Jaakko, Josko, Ke, Miguel, Mohammad, Nick, Nikos, Petter, Philippe, Robert-Jan, Sasha, Simon, Tereza and Vladimir.

The Lorentz Institute is a great place to do, and to learn how to do research; I am thankful to everyone. I would also like to thank the secretaries, and Fran in particular, for all the help given during these years regarding administrative and practical problems.

A special thanks goes to Jorgos, with whom I have shared an office during the PhD.

There are many friends who contributed to make these years so vibrant. I am grateful to all of them, for the moments spent together and the ones to come.

Finally, I would like to thank my whole family for their constant and unconditioned support.